ALASKAN WAY VIADUCT

EVALUATION OF GRAY'S RETROFIT PROPOSAL

Prepared for the

Washington State Department of Transportation

By

T.Y. Lin International

July 31, 2006

TABLE OF CONTENTS

APPENDICIES

EXECUTIVE SUMMARY

Victor Gray et al. have proposed retrofitting the Alaskan Way Viaduct with a shoring system comprised of auxiliary structural steel frames and dampers. This report to the Washington State Department of Transportation (WSDOT) summarizes the results of an independent evaluation of the effectiveness of Gray's proposal. Gray's proposal did not include the dimensions of the structural steel frames, or the sizes of their component members. In order to conduct this review, the sizes of members were determined by successive trials to be reasonably effective in reducing the demands on the existing structure, without being extremely large. Additional amended proposals submitted by Gray are reviewed in Appendices to this report.

The evaluation focuses on a design earthquake with a return period of 500 years, and a maximum considered earthquake with a return period of 2500 years. Victor Gray has stated that his proposal is designed to deal with the 500 year event, which is considered the minimum seismic standard for design. To put these values in perspective, the Nisqually earthquake of February 28, 2001 has been estimated to correspond to a return period of about 150 years, so it was less intense than the design earthquake considered in this report. A return period of 500 years is the minimum hazard used by the WSDOT (and AASHTO) for the seismic retrofit of ordinary structures. A return period of the order of 2500 years is commonly used for the seismic retrofit of critical structures, and is the design standard for new lifeline structures, including any replacement for the current Viaduct.

The design standard in the rare 2500 year event is to prevent collapse and loss of life. This event corresponds to a 2% chance of being exceeded over a 50 year life of the structure. For the more modest 500 year design event, the standard is to limit the effects to a condition of repairable damage. Repairable damage will include major cracking and some spalling, which may require the Viaduct to be out of service for repairs, but closures should be brief and the structure should not approach collapse. The 500 year event corresponds to a 10% chance of being exceeded over a 50 year life of the structure. The classification of severe damage noted below is reserved for foundations, and represents a structural failure condition, but one which should not result in immediate collapse since the failure is in the foundation unit. The standard for repairable damaged does not extend to the foundation structures hidden below grade. Those elements are expected to survive the Design Earthquake without structural damage that would necessitate repairs.

With the auxiliary frames and dampers from the Gray proposal in place, the estimated damage to the structure in the two major earthquake events is summarized in the following table. (See Section 5 for other results.)

Element	**Earthquake Event**	
	Design (500 yr)	**Rare (2500 yr)**
Columns	Repairable	Failure
Floorbeams	Repairable	Significant
Joints	Repairable	Significant
Piles	Significant	Severe
Footings	Severe	Severe

The summary indicates that the foundations of the Viaduct would remain particularly vulnerable to earthquake damage even after the Gray retrofit for the lower minimum design event. In the case of the rare event, the Viaduct may still collapse without further retrofit. In the minimum design event piles would fail in cyclic tension and compression, and footings would fail in shear. While ground improvement could lessen the risk of an abrupt collapse of the structure, the foundation failures would either render the Viaduct unusable for an extended period of time, or require total replacement.

The practical conclusion is that major additional structural retrofit would be required beyond what is included in the Gray proposal in order to meet current minimum design standards for seismic safety.

Streetscape Rendering of Gray Proposal

Rendering of Gray Proposal Under Viaduct

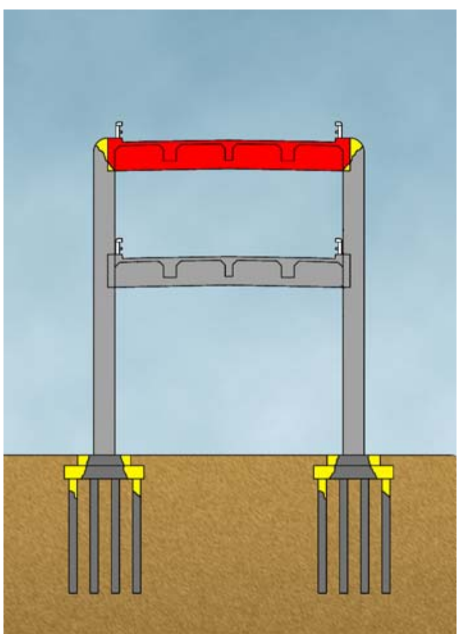

Expected Damage for Design (500 yr) EQ

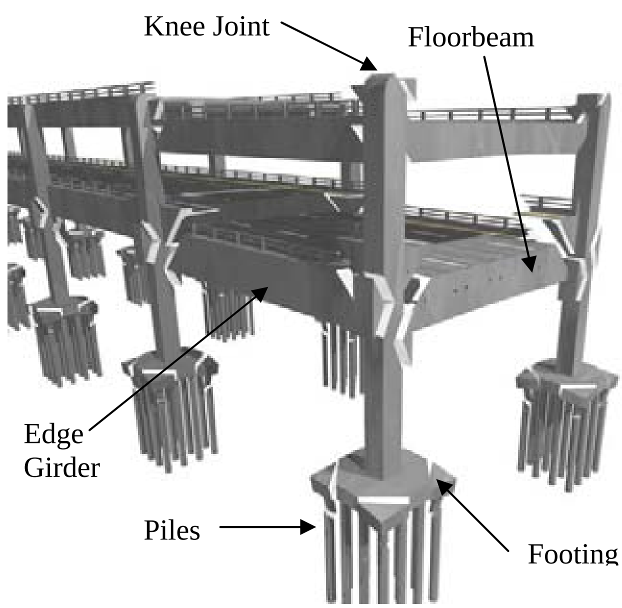

General Failure Modes – Design and Rare EQ

1. INTRODUCTION

Victor Gray et al. have proposed retrofitting the Alaskan Way Viaduct by shoring the structure with auxiliary structural steel frames and dampers. This report to the Washington State Department of Transportation (WSDOT) summarizes the results of an independent evaluation of the effectiveness of Gray's proposal. After initiating this evaluation, Gray el al submitted additional alternatives for retrofits. These were not analyzed in detail, but are evaluated in the appendices to this report.

1.1. THE ALASKAN WAY VIADUCT

The Alaskan Way Viaduct is an 2.2 mile long double-decked, reinforced concrete viaduct carrying State Route 99 along the shoreline of Elliot Bay and past downtown Seattle. It is an important part of Seattle's road system, carrying approximately 110,000 vehicles per day. The structure does not meet modern standards for earthquake resistant design. The viaduct is underlain by soft soils that are likely to liquefy during a major earthquake. The viaduct is shown in Figure 1.

The viaduct consists of independent structural units comprising three bays each. The plans of a typical structural unit[1] are shown in Appendix A. The unit consists of four transverse frames that support longitudinal edge girders and stringers on two levels. Transverse sub-floorbeams connect the girders and the stringers on each level. The reinforced concrete deck is monolithic with all these members, on each level. With respect to earthquakes, the viaduct has several critical structural deficiencies [5]:

- The reinforcing bar splices in the lower-level columns may fail in flexure.
- Both the upper and lower-level joints are vulnerable to degradation from high diagonal tensile stresses; they may fail before the adjacent members hinge. Reinforcing details in these regions also are brittle, and subject to sudden failure after cracking of the concrete.
- The shear strength of the lower-level columns is marginal; they might fail in shear before reaching their flexural capacity.
- Both the upper and lower-level columns have inadequate confining reinforcement.
- The footings could fail if the columns do not.

The Alaskan Way Viaduct was damaged in the Nisqually earthquake of February 28, 2001. The epicenter of this magnitude M_w=6.8 earthquake was located in the Nisqually Valley about 12 miles northeast of Olympia, WA and about 35 miles southwest of Seattle, WA [6]. The most severe damage to the viaduct during the Nisqually earthquake was to the structural unit comprising Bents 97-100, near S. Washington Street. The damage to the structure included cracking of the transverse floorbeams and joints within each bent, and of the longitudinal edge girders [13]. The cracking of the joints was the most severe damage. The upper, east knee joint of Bent 100 was badly cracked and spalled and the reinforcement within that joint was exposed. Some of the reinforcement was fractured.

The Alaskan Way Viaduct contains sections designed by the Washington State Department of Transportation (WSDOT) and other sections designed by the Seattle Engineering Department (SED). The overall configuration of the structures within these sections is similar, but they utilize different structural systems.

[1] One of those designed by the Washington State Department of Transportation.

The structures designed by the WSDOT contain relatively heavy sub-floorbeams that transmit vertical loads to the edge girders and hence to the columns. The structures designed by the SED contain relatively heavy stringers that transmit vertical loads to the floorbeams within each frame and hence to the columns. The overall vulnerabilities of the two types of structure are generally similar (as listed above), however design differences, such as edge girder and knee joint detailing, create different demands for a comprehensive retrofit design.

The unit comprising Bents 151-154 of the viaduct (see Appendix A) was used to evaluate Gray's proposal. This unit was designed by the WSDOT and contains details typical of other units designed by that agency. It is a straight unit, which simplified the modeling of the structure.

1.2. GRAY'S PROPOSAL

Gray's initial proposal is included in Appendix B of this report. The proposal includes two longitudinal structural steel frames and two transverse structural steel frames per three-bay unit of the structure. Both types of frame are illustrated in Figure 2.

The longitudinal frames are placed between Bents 152 and 153 on the east and west sides of the structure. The upper story of each frame engages the structure at the column/girder joints. The beam that runs parallel to the lower level edge girder engages diagonal braces through a pair of dampers. The transverse frames are placed to the "outsides" of Bents 152 and 153 and are independent of the longitudinal frames. Each frame engages the structure at the upper level column/floorbeam joints. The beam that runs underneath the lower deck of the viaduct engages the structure through a pair of dampers attached to the floorbeam. The frames are all supported on the existing footings of the viaduct.

Gray's proposal doesn't include the dimensions of the structural steel frames, or the sizes of their component members. For this evaluation we laid out the frames by scaling from the sketches shown in Appendix B, and to fit the existing structure. The sizes of members were determined by successive trials to be reasonably effective in reducing the demands on the existing structure, without being extremely large. We did not attempt to optimize the design of the frames, or even to very closely satisfy design allowables for the frames, since the proposal is a conceptual one.

Gray's proposal also includes steel jackets around the bases of the columns, presumably to prevent degradation of the splices of the main column reinforcing bars located immediately above the footings. Although Gray's proposal only shows jackets on the middle columns of the unit, we have assumed that similar jackets would be placed around the end columns, since they are subject to similar demands.

Gray's proposal also includes placement of dampers between adjacent units of the viaduct, presumably to minimize pounding between them during an earthquake. Since our evaluation of the proposal is based on analysis of a single unit only, we have not addressed the effectiveness of these dampers. It is unlikely that dampers placed between structural units would significantly reduce the forces within those units, however. This is because the dampers would have to be effectively "lock-up" devices in order to minimize the pounding between units. They would then tend to just synchronize the response of adjacent units, without dissipating much energy.

Gray's proposal also includes ground improvement. This has not been explicitly considered, since it isn't well defined. Account of the ground improvement has been included when evaluating the lateral capacity of the viaduct's foundations. Ground improvement will have a varying effect along the length of the viaduct, and may adversely effect motions at the base of the structure by tuning the foundations into resonance with the energy of the earthquake.

2. EVALUATION CRITERIA

2.1. GROUND MOTIONS

ATC/MCEER [3] defines two design events for the seismic design of bridges. These are an expected earthquake (EE) with a return period of 108 years (37% probability of exceeding in 50 years) and a maximum considered earthquake with a return period of 2500 years (2% probability of exceeding in 50 years). For the Alaskan Way Viaduct and Seawall Replacement Project, the seismic hazard and ground motions for these two events were determined by Shannon & Wilson [11]. The maximum considered earthquake is referred to as a "rare" earthquake (RE) in the Shannon & Wilson report and in this document. Both the EE and RE ground motions were used to determine the effectiveness of Gray's proposal. The Nisqually earthquake has been estimated to correspond to a return period of about 150 years [13]. It was thus slightly more intense than the expected earthquake considered in this report.

In addition to the rare and expected earthquakes, Gray's proposal was evaluated for a "design" earthquake with a return period of 500 years (10% probability of exceeding in 50 years). This level of seismic hazard has been used for the seismic retrofit of ordinary structures (e.g., highway overpasses) for reasons of economy. It is the *minimum* hazard used by the WSDOT for the seismic retrofit of structures. Retrofit to this level of seismic hazard provides lesser performance and reduced safety with respect to retrofit for a rare earthquake. This event has not been used for other phases of the Alaskan Way Viaduct and Seawall Replacement Project and the corresponding seismic hazard is not defined in reference [11].

Acceleration spectra for the horizontal components of the ground motions are shown in Figure 3a. Spectra are shown for both "Zone A" and "Zone B." Each of these zones corresponds to a range of soil profiles encountered along the alignment of the structure. Since Gray's proposal is intended as a generic retrofit for a large portion of the Alaskan Way Viaduct, ground motions corresponding to both zones were used in the evaluation. All three of the seed motions defined by Shannon & Wilson were used for time history analysis, for both the EE and RE events. Thus for each event, the structure was analyzed for six ground motions (two zones times three seed motions).

For the rare earthquake, Figure 3a shows spectra corresponding to both the fault normal and fault parallel components. This directivity effect reflects the proximity of the structure to the dominant source for the rare earthquake, the Seattle Fault Zone. Since the Seattle Fault is oriented generally east-west, and the structure is generally oriented north-south, the fault normal component was applied along the longitudinal axis of the structure (and the fault parallel component was applied transversely).

Response spectra for the design earthquake were computed by Shannon & Wilson [12] specifically for evaluation of Gray's proposal. Acceleration spectra corresponding to Zones A and B soil profiles are shown in Figure 3b. Ground motions for analysis of the design earthquake were obtained by scaling the motions for the rare earthquake so as to be compatible with the design event spectra.[2]

2.2. PERFORMANCE CRITERIA

For the expected event, only nominal damage should be allowed so that the structure may continue in service during and immediately after an earthquake. Minimal damage implies essentially elastic performance, and is characterized by:

---

[2] This frequency domain scaling was performed by T.Y. Lin International.

- Minor inelastic response
- Narrow, post-earthquake cracking in concrete, similar to that from a highway overload
- No apparent permanent deformations
- Inconsequential yielding of secondary steel members

For the rare event, significant damage may be allowed, although the risk of collapse should be minimal. Significant damage may require closure of the structure for repair, or complete replacement of the structure, and is characterized by:

- Yield of reinforcement, possibly requiring replacement
- Major spalling of cover concrete
- Yield of steel members, possibly requiring replacement
- Permanent offset of the structure

Performance criteria for the design event are not easily established because this level of seismic hazard is not often used for the retrofit of major structures.[3] Past design practice for the 500 year event allowed only "repairable" damage. This is damage that can be repaired without closing the structure to traffic for an extended period of time. Otherwise, the future expected economic costs are too high to justify a reduced design standard. Repairable damage is characterized by:

- Yield of reinforcement, although replacement should not be necessary
- Minor spalling of cover concrete
- Yield of steel members, although replacement should not be necessary
- Small permanent offsets, not interfering with functionality
- No significant damage to below-grade foundation elements, with no post-earthquake repair

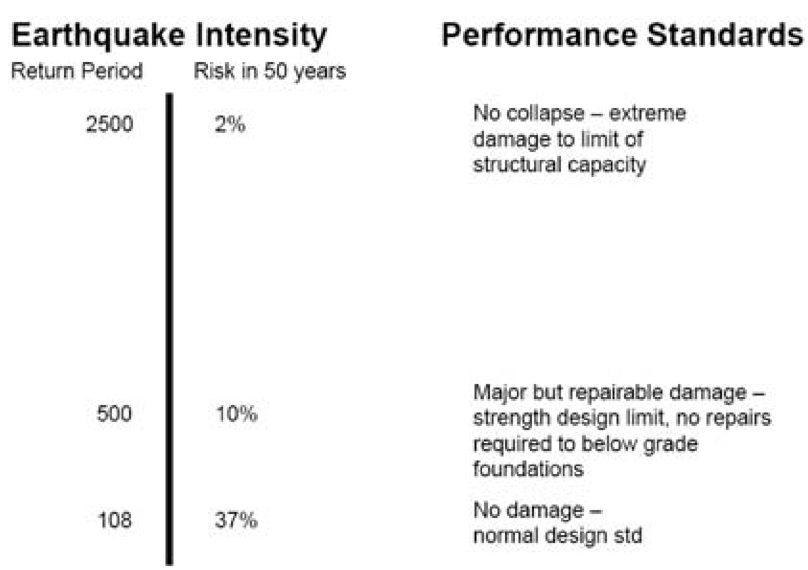

Earthquake Risk and Design Standards

[3] Lifeline structures are usually retrofitted for ground motions with return periods of 1500-2500 years.

2.3. TECHNICAL CRITERIA

The performance criteria given above are rendered into technical (seismic retrofit) criteria in this section. The technical criteria consist of limiting deformations, strains, stresses, etc. on the different structural systems and components, for the defined damage levels.

2.3.1. Reinforced Concrete

2.3.1.1. Material Properties

Material properties were taken from reference [5], are summarized in the following. The bulk of the structure was specified to be cast from Class A concrete, with a specified strength of 3000 psi. As recommended by Priestley [10], the actual strength was assumed to be 50% higher, or 4500 psi. Footings were specified to be Class B concrete, with a specified strength of 2200 psi.

Reinforcing steel was specified to be intermediate grade, with a nominal yield strength of 40 ksi. Also in accordance with Priestley [10], the actual strength was assumed to be 10% higher, or 44 ksi.

2.3.1.2. Allowable Strains

The allowable strains for reinforced concrete elements corresponding to the allowed levels of damage are given in Table 1.

Table 1, Allowable Strain Values for Reinforced Concrete

Component/Material	Strain		
	Minimal	**Design**	**Significant**
Main reinforcing bars	0.01	0.025	0.05
Concrete	0.004	0.004	0.005

The allowable strains for minimal and repairable damage are from reference [4]. The allowable strain for main reinforcing bars for significant damage is taken from reference [5], and is intended to minimize buckling of the bars when the spacing between transverse reinforcing hoops is large. The value ultimately derives from Priestley [9]. The allowable strain for concrete for significant damage is that recommended by Priestley [10], and is commonly used for unconfined concrete.

2.3.1.3. Shear Strength

The shear strength of beams and columns was computed in accordance with Section 7.4.8 of Priestley [10]. In Priestley's method, the shear strength of a member is the sum of three terms

$$V_n = V_c + V_s + V_p \qquad (1)$$

where

$$V_c = k\sqrt{f_c^{'}}A_e \qquad (2a)$$

$$V_s = \frac{A_v f_y D^{'} \cot\theta}{s} \qquad (2b)$$

$$V_p = P \tan \alpha \tag{2c}$$

are the contributions of concrete, reinforcing steel, and axial compression, respectively. The contribution of concrete was assumed to degrade with increasing curvature ductility as shown in Figure 7.12 of Priestley [10]. The angle θ will be taken as 30º.

Shear failure should not occur for any of the damage limit states.

2.3.1.4. Splices

The effects of lap-splice degradation on the strength and ductility of plastic hinges were evaluated in accordance with Section 7.4.6(b) of Priestley [10]. Degradation of flexural strength was assumed to begin at a curvature ductility μ_3 corresponding to a compressive strain $\varepsilon_c = 0.002$ on the extreme fiber of a section. The residual flexural strength corresponding to the dead load was taken to correspond to a curvature ductility of $\mu_3 + 8$.

The minimal damage limit state was taken to correspond to a curvature ductility of μ_3. The significant damage limit state was taken to correspond to a curvature ductility of $\mu_3 + 8$. Repairable splice damage is difficult to define so only qualitative evaluations were made.

2.3.1.5. Anchorage

The anchorage of reinforcing bars was evaluated following the recommendations of Priestley [9].

2.3.1.6. Knee and Tee Joints

Principal tensile stresses in knee and tee joints were limited to $3.5\sqrt{f_c^{'}}$ (psi units) for the minimal damage limit state. For the significant damage limit state, joint shear strains should be limited to 0.01 for closing of knee joints and to 0.04 for tee joints and opening of knee joints. Since the joints were modeled with elastic elements, damage to the joints was assessed based on the magnitude of the computed principal tensile stresses. Principal tensile stresses up to $5.0\sqrt{f_c^{'}}$ (psi units) may be sustained before joint degradation begins[4].

2.3.1.7. Footings

Footings were evaluated for flexure (positive and negative), beam shear, joint shear, and the effects of footing damage on the anchorage of column bars. The evaluations were in accordance with Priestley [10].

Footing failures should not occur for any of the damage limit states.

2.3.1.8. Piles

The WSDOT portion of the structure—and Bents 151-154 in particular—are supported on "composite" piles. The upper portion of these piles is concrete, and the lower portion is timber. Pile lengths vary from

---

[4] In the structures designed by the Seattle Engineering Department the top reinforcing bars in the upper level floorbeams are bent down within the knee joints and welded to the column bars. These bars are all 1-½ inch square bars. This detail is particularly vulnerable to joint shear stress, as evidenced by the fracture of some of these bars and welds at Bent 100 during the Nisqually earthquake. A more stringent criteria for joint shear stress would be appropriate for the SED portion of the viaduct.

52 to 81 feet. The piles were driven to blow counts varying from 34 to 45 blows/foot. No bearing values are reported, although the nominal resistance may be 40 tons as on other portions of the structure (SED section). On the SED section, most actual bearing values were around 65 tons.

Piles were modeled as elastic elements (pile failure was not explicitly modeled in the time history) for analysis of both the expected and rare events. Pile demands are reported with respect to an assumed capacity of 60 tons, or 120 kips.

2.3.1.9. Steel Jackets

The effects of steel jacketing on splice strength and column ductility were evaluated as described in Section 8.2 of Priestley [10].

2.3.2. Auxiliary Frame

The auxiliary frame was proportioned to remain elastic or nearly elastic for the rare event. The capacities of members were taken to be their nominal capacities with normal resistance factors.

3. MODELING AND SEISMIC ANALYSIS

3.1. MODELING

The evaluation was based on time history analysis of a three-dimensional model of Bents 151-154 of the viaduct (a typical WSDOT unit). The model used is shown in Figure 4, including both the viaduct and the auxiliary frames. Figure 4d shows the existing structure only, and Figure 4e shows the auxiliary frames only. The model was constructed using the ADINA [1] general-purpose finite element program. ADINA is well suited to the seismic analysis of bridges and similar structures. In addition to special purpose elements for the inelastic modeling of structural elements, the program has robust algorithms for time history analysis, and is the Caltrans standard for non-linear dynamic analysis.

The model was constructed from scratch from Drawings 7, 43, 44, & 45 (of 136) of Contract Number 5262 of the project (the drawings are included in Appendix A). Specific features of the model are as follows:

The columns, floorbeams, and edge girders were all modeled with inelastic moment-curvature elements. The moment-curvature response of sections was computed using the computer program XTRACT [7]. The moment-curvature response of the columns was modeled in both the longitudinal and transverse directions and considering a wide range of axial forces about the dead load axial force in each member. Moment-curvature calculations were performed for all variations in reinforcement of the columns and the various relationships were applied to different elements with due consideration of bar cut-offs and development lengths. Ten elements were used to model each column so that the strength of the columns could be reproduced with high fidelity.

The moment-curvature response of the floorbeams and edge girders was considered about horizontal axes only. In each case, an effective width of the adjacent deck, including reinforcement, was included with the beam. Since the floorbeams and girders are reinforced asymmetrically in each section, according to the dead load demands, asymmetric moment-curvature relationships were used. As for the columns, all variations in reinforcement were considered and appropriate moment-curvature relationships were assigned to different elements. Flexure of the floorbeams and girders about vertical axes is effectively prevented by composite action with the adjacent decks, so elastic moment-curvature relationships were used in this direction.

The membrane stiffness of the upper and lower decks was modeled with elastic shell elements. The composite flexural stiffness of the decks, floorbeams, and edge girders was included in the moment-curvature modeling of the later elements, as described above. All of the elements were modeled at a common elevation, near the centroid of both the deck/floorbeam and deck/girder members.

The tee and knee joints at the juncture of the columns, floorbeams, and edge girders were modeled with elastic beam elements between the geometric center of the joints and the faces of the respective members. Each joint element utilized the cross-section of the adjacent member—cracked section properties were used.

The piles supporting the structure were modeled with individual truss elements. This modeling may be seen in Figure 4. The axial stiffness of the piles was computed assuming that they are tip-supported. Because the piles are not connected to the footings to resist tensile forces, truss elements with gaps were used to allow separation of the footings from the piles. This nonlinear modeling allows the structure to rock during the analysis if the ground shaking is sufficiently intense. It also makes it straightforward to determine the peak axial forces in the piles. The lateral flexibility of the foundations was not considered. The mass of the footings was lumped at nodes located at the tops and the bottoms of the footings.

The auxiliary frames were modeled with elastic beam elements and nonlinear dampers. The sizes of the auxiliary frame members used in the analysis are shown in Figures 5a & b for the longitudinal and transverse frames, respectively. The members were determined by iterative analysis so as to obtain significant reductions in demand on the existing structure, without using unreasonably large sections. Nonlinear dampers were modeled with a force-velocity relationship

$$F = 250 \frac{\text{kip} \cdot \text{sec}^{1/3}}{\text{ft}^{1/3}} \cdot V^{1/3} , \qquad (3)$$

also determined by iteration. Low-exponent dampers are generally more effective than linear dampers. Two dampers are included with each auxiliary frame.

The general correctness of the model was verified by comparing results with those reported in reference [5]. This report is of a vulnerability study conducted by the University of Washington (UW) for the WSDOT. The study included evaluation of a typical unit designed by the WSDOT, evaluation of a typical unit designed by the SED, and a geotechnical evaluation of the site of the viaduct.

The dead load of the existing structure, from the model shown in Figure 4d is 4890 kip, excluding the footings. The weight of the existing structure reported in [5] is 4800 kip. The difference may be largely attributed to the higher density of concrete utilized in the current analysis, which is 155 pcf versus 150 pcf used in the UW study.

3.1.1. Modal Analysis

Further verification of the model was obtained through modal analysis. The periods of the first three modes of vibration are shown in Table 2:

Table 2, Modal Properties, Periods of Vibration, seconds

Model		Mode		
		Longitudinal	**Transverse**	**Torsional**
UW study		0.91	0.76	0.66
This study	Gross section properties	0.97	0.70	0.61
	Cracked section properties (50% of I_{gross})	1.26	0.97	0.83
	Moment-curvature elements	1.57	0.97	0.86

With gross section properties (and elastic elements), the modal properties of the model utilized in this study are similar to those reported in the UW study. More pertinent to the seismic response are the modal properties obtained utilizing cracked section properties for the columns, floorbeams, and edge girders. The periods of vibration of the structure are increased approximately by the $\sqrt{2}$ when the cracked moments of inertia are assumed to be 50% of the gross values. When moment-curvature elements are substituted for the elastic elements, the periods of vibration increase again. This reflects the fact that the column moments of inertia may be less than 50% of the gross values based on the axial force level and reinforcement details, and the direction considered.

Also of interest are the modal properties with the auxiliary frames in place; these are shown in Table 3. Two cases are shown. In the first, the dampers are ignored, since they have no stiffness (and little mass). In the second case, the dampers were modeled as rigid struts. This is meaningful for low exponent dampers (like those described by Equation 3) with large coefficients, which may transmit large forces with little relative displacement.

Table 3, Modal Properties of Retrofitted Structure, Periods of Vibration, seconds				
Model		**Mode**		
		Longitudinal	**Transverse**	**Torsional**
Existing structure		1.57	0.97	0.86
Retrofitted structure	Dampers absent	1.08	0.62	0.69
	Dampers modeled as struts	0.44	0.42	0.44

In any case, it is evident that the auxiliary frames significantly stiffen the structure. This is significant, because the auxiliary frames reduce the fundamental periods of vibration of the structure so that they fall within the period range of the most intense ground shaking for rare earthquakes and Zone A site conditions—see Figure 3.

3.2. SEISMIC ANALYSIS

The seismic analysis was performed by applying time histories of ground displacement directly to the foundations of the structure. Longitudinal, transverse, and vertical ground motions were applied simultaneously. Free-field, surface motions were used; soil-structure interaction was not performed. For the slender piles supporting the Alaskan Way Viaduct, it's likely that the effective motions that excite the structure are very similar to the free-field, surface motions.

The response of the structure was computed for six ground motions each for both the rare and expected earthquakes—considering two soil profiles and three seed motions each. For each quantity of interest, and for each event, the time histories of response were then scanned to determine the peak value occurring over the six time histories. Thus the controlling results are implicitly the largest response for structures located in both soil profile zones. Also, for each quantity of interest—e.g., the moment in a column—the corresponding forces—e.g., the axial force in the column—occurring at the same time were also tabulated.

3.2.1. Rayleigh Damping

Damping was modeled using Rayleigh damping. A damping ratio of 5% of critical was set at anchor periods of 0.25 and 2.5 seconds. The former period corresponds to the highest frequency component observed for forces within the structure. The later period corresponds to the highest observed period of relative displacement of the structure.

Care was taken not to overdamp elements subjected to inelastic demands. The stiffness proportional term of Rayleigh damping was set to a small value for moment-curvature elements subjected to inelastic ductility demands exceeding two. (Rayleigh damping parameters may be set for individual element groups in ADINA.) Also, the stiffness term was set to a small value for the piles, so as not to interfere with the observed uplift of the structure.

4. RESULTS

4.1. RESPONSE OF EXISTING STRUCTURE

The response of the existing structure is first summarized to provide a baseline against which to judge the effectiveness of the retrofit measures proposed by Gray et al. Only a few results are presented, since the focus of the report is the performance of the retrofitted structure.

4.1.1. Rare Earthquake

For the rare earthquake, the drift of the existing structure is summarized in Figure 6.[5] This shows the peak relative displacement of the lower level of the structure with respect to the foundation (denoted “lower” in the figure), the peak relative displacement of the upper level of the structure with respect to the lower level (denoted “upper” in the figure), and the peak relative displacement of the upper level of the structure with respect to the foundation (denoted “total” in the figure). The drift in the longitudinal direction is extremely large, which means that collapse is imminent. The near collapse—of the model—is due to excessive displacement in the longitudinal direction and P-Δ effects. This type of collapse might not occur in the actual structure because of interaction between adjacent units.

4.1.2. Expected Earthquake

For the expected earthquake, the drift of the existing structure is summarized in Figure 7. The corresponding column curvature ductility demands are summarized in Figure 8. The peak ductility demands are 2.5-3.0. The corresponding material strains were computed from a section analysis of the simultaneous axial force and curvature demands on the columns. They were found to be slightly less that the limiting values for minimal damage given in Section 2.3.1.2. The calculated ductility demands do imply degradation of the shear strength of the columns, however, which could be problematic.

Floorbeam curvature ductility demands are summarized in Figure 9. The peak ductility demands imply material strains exceeding the criteria for minimal damage given in Section 2.3.1.2. The calculated demands also imply significant degradation of the shear strength of the floorbeams.

4.2. RESPONSE OF RETROFITTED STRUCTURE

4.2.1. Rare Earthquake

For the rare earthquake, the drift of the retrofitted structure is summarized in Figure 10.[6] This shows the peak relative displacement of the lower level of the structure with respect to the foundation, the peak relative displacement of the upper level of the structure with respect to the lower level, and the peak relative displacement of the upper level of the structure with respect to the foundation. The drift in the longitudinal direction is concentrated into the lower level of the structure. The upper stories of the longitudinal auxiliary frames are braced, and they restrain the drift of the upper level of the structure.

The total drift in the transverse direction is divided between the upper and lower levels of the structure—very roughly in proportion to the story heights. The peak drifts are summarized in Table 4:

---

[5] Run existing.06

[6] Run gray.08

Table 4, Transverse Drift, Retrofitted Structure, feet			
Bent	**Level**		
	Lower	**Upper**	**Total**
End	0.80	0.29	1.14
Middle	0.71	0.27	1.02

These demands may be compared with the results of pushover analyses, which are described in the next section.

4.2.1.1. Pushover Analysis

For the retrofitted structure, pushover analyses were performed using the computer program CAPP [8]. In this frame analysis program members may be modeled with inelastic hinges at their ends. These concentrated hinges utilize moment-rotation relationships, which may be derived from moment-curvature relationships computed using XTRACT, for instance. A significant feature of the program is that degrading moment-rotation relationships may be used, a feature which is not available in ADINA.

Pushover analyses were performed for a typical end bent and a typical middle bent, in the transverse direction. The CAPP model of a typical end bent is shown in Figure 11. The columns and floorbeams were modeled with concentrated hinges at their ends. The model also included inelastic elements modeling the jacketed sections of the lower level columns, and the column splices immediately above the lower deck. A degrading moment-rotation relationship was used for the splice elements. The results of the pushover analyses are summarized in Table 5:

Table 5, Pushover Analysis Results, Displacement Capacities -Transverse Direction				
Bent	**Level**	**Capacity, feet**	**Failure**	**Note**
End	Upper	0.38	Splice	Push @ lower; restraint @ upper
		0.49	U. floorbeam	Push @ upper; restraint @ lower
	Total	1.32	L. floorbeam	Force split 60/40 @ upper/lower levels
Middle	Upper	0.33	Splice	Push @ lower; restraint @ upper
		0.38	U. floorbeam	Push @ upper; restraint @ lower
	Total	0.85	L. floorbeam	Force split 60/40 @ upper/lower levels

There is no definite result for the displacement capacity of the upper level of the structure (relative to the lower level) from the pushover analysis. This is because there are multiple ways in which to perform the pushover. Nevertheless, the results are indicative of the magnitude of the displacement capacity and possible failure modes.

Comparing the drift demands from the previous section—for the rare earthquake—with the calculated displacement capacity of the structure, it may be seen that the total demand exceeds the capacity of the middle bents; the demand capacity ratio is 1.02/0.85=1.20. This indicates that the lower floorbeams will fail during a rare event.

The pushover analysis described in this section has some limitations. As mentioned already, there is no definitive way to perform the pushover of a two level structure. Also, the pushover analysis assumed that the axial forces in the columns were constant, and equal to the dead load axial forces. These are significant limitations. The time history analyses described in subsequent sections do not suffer from these limitations.

4.2.2. Design and Expected Earthquakes

For the design and expected earthquakes, the drift of the retrofitted structure is summarized in Figures 12a & b and Figures 13a & b, respectively.

4.2.3. Columns

4.2.3.1. Rare Earthquake

For the rare earthquake, the curvature ductility demands on the columns are summarized in Figure 14. The plots show that plastic hinges form in the tops and bottoms of the columns, in both levels of the structure and in both directions. In the upper level columns of the end bents, the hinges don't form at the very tops of the columns because there is additional main reinforcement at this location. The hinges form at a weaker section a few feet from the tops of the columns.

To evaluate the ratio of demand to capacity of the columns it is more meaningful to refer to Figures 15 and 16, however. For the end and middle bents, respectively, these are plots of simultaneous curvature and axial force demands versus capacity curves. Plots are shown for each variation of reinforcing occurring in each type of bent, and for each direction of motion. The designation "Columns.End.B.16," for instance, refers to section B on the drawings, with 16 main reinforcing bars. As shown in Figures 15 and 16 the curvature capacity of a section is a function of the axial force acting on it. The capacity decreases with increasing axial force because the controlling failure criterion is the ultimate concrete strain.

Figure 15 shows that the flexural demands on the end columns slightly exceed the capacity in the transverse direction, for the section designated "Columns.End" (the typical section). Figure 16 shows that the flexural demands on the middle columns slightly exceed the capacity in the longitudinal direction, for the section designated "Columns.Middle" (the typical section). A closer look reveals a more insidious problem, however. The axial forces on the middle columns are very high, over 3500 kip, which is equivalent to a stress of about $0.4 f_c^{'}$. These forces are caused by rocking of the structure and impact of the columns and footings against the piles.

Rocking is possible because the piles are not anchored to the footings. The structure can lift off the piles if the excitation is sufficiently intense. Since the center of gravity of the structure is located about 40 feet above the bottoms of the footings, and the distance out-to-out of the footings is 59 feet, an acceleration of

$$a_{rock} = \frac{59\,feet}{2 \cdot 40\,feet} g = 0.74g \tag{4}$$

is sufficient to initiate rocking in the transverse direction. As discussed in Section 3.1.1, the addition of the auxiliary frames reduces the transverse period of vibration of the structure to between 0.42-0.62 seconds, depending on how the dampers are treated. As may be seen from Figure 3, this is within the range of peak spectral acceleration for Zone A soil profiles; the peak spectral acceleration is 1.7g.

This simple analysis indicates that rocking will occur with the auxiliary frames in place, and this was observed in the time history analysis. The high axial forces in the columns were found to be correlated with the rocking and due to impact of the structure against the piles.

The ductility of the existing columns is small at the axial force levels indicated by the analysis. The computer program used for the moment-curvature analysis (XTRACT) was not able to converge to a solution for axial loads exceeding 1000 kips, implying that the column response is ill-conditioned or unstable. Solutions were obtained for high axial load levels using a custom Mathcad program, however, and these results are shown in Figure 16. The Mathcad analysis also shows that the column response at high axial load levels is brittle. Catastrophic column—and viaduct—failure would ensue if the curvature capacity was even slightly exceeded. The results shown in Figure 16 indicate that the structure would collapse in a rare earthquake due to combined flexure and axial forces caused by rocking and impact.

Column shear demand/capacity ratios were computed using simultaneous axial force and shear demands, and considering the peak ductility demands on the members as described in Section 2.3.1.3. The controlling demand/capacity ratios for the rare earthquake are summarized in Table 6:

Table 6, Column Shear D/C, Retrofitted Structure, Rare Earthquake

Bent	Level	Direction	Demand/Capacity
End	Upper	Longitudinal	0.80
		Transverse	1.19
	Lower	Longitudinal	0.52
		Transverse	0.71
Middle	Upper	Longitudinal	0.61
		Transverse	0.84
	Lower	Longitudinal	1.16
		Transverse	0.90

There is no evident pattern to these demand/capacity ratios. Nevertheless, shear failure is indicated at two locations.

4.2.3.2. Design Earthquake

For the design earthquake, the curvature ductility demands on the columns are summarized in Figure 17. The largest values only slightly exceed unity, so damage should be repairable.

The controlling demand/capacity ratios for shear are summarized in Table 7:

Table 7, Column Shear D/C, Retrofitted Structure, Design Earthquake

Bent	Level	Direction	Demand/Capacity
End	Upper	Longitudinal	0.21
		Transverse	0.49
	Lower	Longitudinal	0.18
		Transverse	0.39
Middle	Upper	Longitudinal	0.20
		Transverse	0.55
	Lower	Longitudinal	0.35
		Transverse	0.35

These demand/capacity ratios are all less than unity, so shear failure would not be expected.

4.2.3.3. Expected Earthquake

For the expected earthquake, the curvature ductility demands on the columns are summarized in Figure 18. They are all less than unity, so damage would not be expected.

The controlling demand/capacity ratios for shear are summarized in Table 8:

Table 8, Column Shear D/C, Retrofitted Structure, Expected Earthquake			
Bent	**Level**	**Direction**	**Demand/Capacity**
End	Upper	Longitudinal	0.08
		Transverse	0.31
	Lower	Longitudinal	0.11
		Transverse	0.20
Middle	Upper	Longitudinal	0.11
		Transverse	0.38
	Lower	Longitudinal	0.20
		Transverse	0.17

These demand/capacity ratios are all less than unity, so shear failure would not be expected.

4.2.4. Column Splices

Gray's proposal includes steel jackets around the bases of the columns, which will prevent degradation of the splices of the main reinforcing bars located immediately above the footings. But similar splices are located in the upper level columns, immediately above the lower deck, and these splices remain unprotected in Gray's proposal. For the rare earthquake, the peak transverse drift demand shown in Figure 10b is 0.29 feet for the upper level of the structure. This is less than the displacement capacity—0.38 feet—corresponding to splice failure, according to the pushover analysis described in Section 4.2.1.1. Based on the curvature ductility demands shown in Figure 14 for the rare earthquake—5.0 at the bases of the upper level columns—modest degradation of the splices would be expected, but not failure.

Since the curvature ductility demands on the columns are all less than unity for the design and expected earthquakes—see Figures 17 and 18—damage to the splices would not be expected in those events.

4.2.5. Floorbeams

4.2.5.1. Rare Earthquake

For the rare earthquake, the curvature ductility demands on the floorbeams are summarized in Figure 19. There are separate plots for the upper and lower level floorbeams, and positive (∪) and negative (∩) demands are plotted separately. The plots show that plastic hinges form at the faces of the columns. The largest demands are for positive bending. The floorbeams are reinforced asymmetrically to resist primarily vertical loads and have little bottom reinforcement at the column faces. Evidently, the seismic moments exceed the dead load moments at the faces of the columns so that the total moments are positive. (In the units design by the WSDOT, the primary load path for dead loads is through the edge girders).

Plots of simultaneous curvature and axial force demands on the floorbeams are shown in Figure 20; there are separate plots for the upper and lower level floorbeams. The capacity curves are represented by clusters of points along the curvature axes (for axial forces of zero). This is because the capacities of the various floorbeams sections are nearly the same, and because the capacity was only calculated for an axial force of zero (because the axial forces in the floorbeams are modest).

Figure 20b indicates that the lower level floorbeams will fail in flexure—in negative bending near one of the columns. This same failure was predicted by the pushover analysis described in Section 4.2.1.1. A demand/capacity ratio of 1.20 was obtained for the middle bents from that analysis. A similar ratio may be inferred from Figure 20b.

Disregarding the predicted flexural failure of the lower level floorbeams, demand/capacity ratios for shear of the floorbeams were computed considering both the shears induced by plastic hinging and the reduction in the shear strength of concrete due to inelastic curvature ductility demand [10]. The computed demand/capacity ratios for shear are summarized in Table 9. They are all less than unity.

Table 9, Floorbeam Demand/Capacity Ratios for Shear

Bent	Level	Demand/Capacity
End	Upper	0.71
	Lower	0.71
Middle	Upper	0.60
	Lower	0.66

4.2.5.2. Design Earthquake
For the design earthquake, the curvature ductility demands on the floorbeams are summarized in Figure 21. The largest demands occur on the lower level floorbeams, and are up to 7.8 in positive bending and 5.2 in negative bending. These values are large enough to cause significant cracking and yielding of reinforcement, but within the limits for repairable damage provided that there is not major degradation in development of reinforcing details.

4.2.5.3. Expected Earthquake
For the expected earthquake, the curvature ductility demands on the floorbeams are summarized in Figure 22. They are all less than unity; normally, damage would not be expected. It is likely that any pre-existing flexural or shear cracks would be further widened by a seismic event, however.

4.2.6. Edge Girders

For the rare earthquake, the curvature ductility demands on the edge girders are summarized in Figure 23. There are separate plots for the upper and lower level girders; positive (∪) and negative (∩) demands are plotted together. Although yielding is indicated, the curvature ductility demands are modest and comfortably less than the capacity of the girders. The largest demand occurs in negative bending, at some distance from a column face, near a cut-off of top reinforcement. It may be that the demands on the girders are small because the longitudinal auxiliary frames prevent displacement of the upper level of the structure relative to the lower level.

For the design earthquake, the curvature ductility demands on the edge girders are summarized in Figure 24. They are all less than unity; normally, damage would not be expected. It is likely that any pre-existing flexural or shear cracks would be further widened by a seismic event, however. Peak curvature ductility demands for the expected earthquake are about 0.4. This behavior may differ for the units design by the SED. The edge girders in these units have lighter reinforcing, and will see higher D/C ratios than the WSDOT units.

4.2.7. Knee Joints

In the longitudinal direction, principal tensile stresses in the (upper level) knee joints were computed from the peak moments in the edge girders. In the transverse direction, they were computed from the peak moments in the floorbeams. The computed values of principal tensile stress are summarized in Table 10, where they have been normalized by $\sqrt{f_c'}$ (psi units).

Table 10, Knee Joint Principal Tensile Stresses, Normalized			
Event	**Bent**	**Direction**	**Normalized Stress**
Rare	End	Longitudinal	3.1
		Transverse	5.2
	Middle	Longitudinal	2.0
		Transverse	4.2
Expected	End	Longitudinal	0.1
		Transverse	1.6
	Middle	Longitudinal	0.1
		Transverse	1.6

Joint stresses are quite low for the longitudinal direction of excitation. As for the edge girders, it appears that the longitudinal auxiliary frames effectively restrain the upper level of the structure.

For the rare earthquake, the principal tensile stresses may be compared with $5.0\sqrt{f_c^{'}}$ (psi units), above which degradation of the joints may be expected. The calculated stresses are marginally acceptable.[7] For the expected earthquake, the principal tensile stresses are all less than $3.5\sqrt{f_c^{'}}$ (psi units), so joint damage should be minimal. Stresses for the design event are intermediate to those for the rare and expected earthquakes. In any event, existing cracks are likely to be widened. In SED designed units, the noted marginal reinforcing details (welded rebar laps) can be expected to fail at the design demand level.

4.2.8. Tee Joints

In the longitudinal direction, principal tensile stresses in the (lower level) tee joints were computed from the peak moments in the edge girders. In the transverse direction, they were computed from the peak moments in the columns. The computed values of principal tensile stress are summarized in Table 11, where then have been normalized by $\sqrt{f_c^{'}}$ (psi units).

Table 11, Tee Joint Principal Tensile Stresses, Normalized			
Event	**Bent**	**Direction**	**Normalized Stress**
Rare	End	Longitudinal	4.0
		Transverse	4.7
	Middle	Longitudinal	1.7
		Transverse	6.0
Expected	End	Longitudinal	0.4
		Transverse	2.0
	Middle	Longitudinal	0.1
		Transverse	2.1

[7] In the structures designed by the Seattle Engineering Department the top reinforcing bars in the upper level floorbeams are bent down within the knee joints and welded to the column bars. These bars are all 1-½ inch square bars. This detail is particularly vulnerable to joint shear stress, as evidenced by the fracture of some of these bars and welds at Bent 100 during the Nisqually earthquake. At the stress levels reported in Table 10 for the rare earthquake, splice failure is likely, with consequent degradation of joint strength and stiffness. This detail is a worrisome feature of the SED portion of the viaduct, even for the expected event.

Again, joint stresses are quite low for the longitudinal direction of excitation, and probably for the same reason: restraint of the structure by the upper level auxiliary frames.

For the rare earthquake, the principal tensile stresses may be compared with $5.0\sqrt{f_c^{'}}$ (psi units), above which degradation of the joints may be expected. The calculated stresses suggest moderate degradation of the joints—in the transverse direction. For the expected earthquake, the principal tensile stresses are all less than $3.5\sqrt{f_c^{'}}$ (psi units), so joint damage should be minimal. Stresses for the design event are intermediate to those for the rare and expected earthquakes. In any event, existing cracks are likely to be widened.

4.2.9. Reinforcing Bar Anchorage

The anchorage of the reinforcing bars was studied by the University of Washington and summarized in "Seismic Vulnerability of the Alaskan Way Viaduct: WSDOT Typical Unit"[5]. According to that report, the anchorage of the reinforcing bars is generally satisfactory. The bars which were reported to be most suspect are the bottom bars of the floorbeams, where they are anchored into the columns. These conditions were evaluated again, using Priestley's methodology [9].

At the end bents, the bottom reinforcement of both the upper and lower level floorbeams is 2 #13[8] bars. These are embedded 34 inches versus a development length of 22 inches. Since the curvature ductility demands on the columns are modest adjacent to the floorbeams—a maximum of 4.0 for the rare earthquake—degradation of the embedment does not seem likely. Using Priestley's methodology, the anchorage of the bars is satisfactory. Following the AASHTO LRFD code [2], however, the development length is 54 inches, and the embedment is only 63% of that required.

At the middle bents, the bottom reinforcement of both the upper and lower level floorbeams is 2 #17 bars. These are embedded 40 inches versus a development length of 29 inches. Again, since the curvature ductility demands on the columns are modest adjacent to the floorbeams—a maximum of 5.0—degradation of the embedment does not seem likely. Using Priestley's methodology, the anchorage of the bars is satisfactory. Following the AASHTO LRFD code, however, the development length is 68 inches, and the embedment is only 59% of that required.

4.2.10. Piles

There is little information available regarding the capacity of the piles supporting the structure. Based on the data summarized in Section 2.3.1.8, the piles were assumed to have a capacity of 120 kips for the purpose of tabulating demand/capacity ratios.

Since individual piles were included in the model it was straightforward to extract the peak forces in them from the analysis. The peak compressive forces are summarized in Table 12. The tensile forces were zero since the structure was allowed to uplift from the piles, which aren't anchored to the footings.

---

[8] These are an archaic bar size, but follow the same system as modern bars. A #13 bar has a nominal diameter of 13/8 inches.

Table 12, Pile Compressive Forces and Demand/Capacity Ratios			
Event	**Bent**	**Force, kip**	**D/C**
Rare	End	360	3.0
	Middle	770	6.4
Design	End	240	2.0
	Middle	450	3.7
Expected	End	130	1.1
	Middle	240	2.0

The demands on the end bents are less meaningful than the demands on the middle bents because the analysis was of a single unit only. Although the dead load of the adjacent units was included on the end footings, the dynamic effect of the adjacent units was missing in the analysis.

For the rare event, the computed demands are suggestive of severe damage to the foundations of the viaduct. This is damage exceeding the acceptable limits for significant damage, and possibly leading to collapse of the structure. The computed demands for the design event exceed the acceptable limits for repairable damage to the structure. The computed demands for the expected event are indicative of moderate damage, greater than the allowed minimal damage.

The lateral capacity of the foundations was estimated to be about 300 kips for the end bents and about 500 kips for the middle bents. These values are based on a passive pressure of 7.7 ksf on the footings (which assumes that the existing soils are improved) and a nominal lateral capacity of 10 kips/pile. For the middle bents only, the peak lateral forces on the foundations are summarized in Table 13; the corresponding demand/capacity ratios are based on the aforementioned capacity.

Table 13, Foundation Lateral and Demand/Capacity Ratios			
Event	**Direction**	**Force, kip**	**D/C**
Rare	Longitudinal	1610	3.2
	Transverse	1630	3.3
Design	Longitudinal	850	1.7
	Transverse	1020	2.0
Expected	Longitudinal	470	0.9
	Transverse	510	1.0

The demands for the rare event are suggestive of significant damage to the foundations. The demands for the design event indicate damage levels requiring repair, which for the design level event is not desirable for structure that is below grade. The demands for the expected event are comparable to the capacity, so no damage is predicted.

4.2.11. Footings

The middle footings of the structure were evaluated for shear, flexure, column bar anchorage, and joint shear using the pile forces reported in the previous section. The end footings were not evaluated because the pile forces at those footings don’t included the effects of the adjacent bents.

For the rare earthquake, the computed demand/capacity ratio for beam shear was 5.8. The computed demand/capacity ratio for flexure of the footings was 3.2. The column bars are adequately anchored if the footing remains intact. But, because significant footing damage is indicated, the anchorage of the bars was evaluated using the splitting strength methodology of Priestley [9]. The computed demand/capacity ratio was then 1.3. The peak principal tensile stress induced in the column/footing joints by flexure of the columns was estimated to be $7.8\sqrt{f_c^{'}}$ (psi units). In aggregate, these demand/capacity ratios indicate that the footings would be severely damaged in a rare earthquake, in excess of limits for significant damage.

For the design earthquake, the computed demand/capacity ratio for beam shear was 3.6. The computed demand/capacity ratio for flexure of the footings was 2.0. Based on the splitting strength, the demand/capacity ratio for anchorage of the column bars is 1.3, as for the rare earthquake. The peak principal tensile stress induced in the column/footing joints by flexure of the columns was estimated to be $4.6\sqrt{f_c^{'}}$ (psi units). In aggregate, these demand/capacity ratios imply severe damage to the footings in an expected earthquake, in excess of the limits for repairable damage.

For the expected earthquake, the computed demand/capacity ratio for beam shear was 2.1. The computed demand/capacity ratio for flexure of the footings was 1.2. Based on the splitting strength, the demand/capacity ratio for anchorage of the column bars is 1.3, as for the rare earthquake. The peak principal tensile stress induced in the column/footing joints by flexure of the columns was estimated to be $2.4\sqrt{f_c^{'}}$ (psi units). In aggregate, these demand/capacity ratios imply significant damage to the footings in an expected earthquake, in excess of the limits for minimal damage.

4.2.12. Auxiliary Frames

For the rare earthquake, the tensile and compressive forces in the members of the auxiliary frame are tabulated in Figure 25. Also shown in the figure are demand/capacity ratios based on axial forces only and demand/capacity ratios computed using the AASHTO LRFD code [2] formulas for combined axial force and flexure. The members of the auxiliary frame were sized to achieve demand/capacity ratios around 1.0 or less in the rare earthquake. (Gray's proposal does not include the sizes of the members.) Figure 25 shows that this goal was largely achieved. No attempt was made to optimize the members since design of the auxiliary frames was not the goal of the study. Some columns have demand/capacity ratios up to about 1.5. Ratios like this might be acceptable in a final design, since a portion of the demand is minor axis bending. And, limited inelastic bending might not severely compromise the effectiveness of the auxiliary frames. The force and stroke demands on the auxiliary frame dampers are summarized in Figures 26 and 27, respectively.

For the expected earthquake, the auxiliary frame forces and damper forces and strokes are tabulated in Figures 28, 29, and 30, respectively. The demands are modest.

5. SUMMARY & CONCLUSIONS

Victor Gray et al. have proposed retrofitting the Alaskan Way Viaduct by shoring the structure with auxiliary structural steel frames and dampers. This report to the Washington State Department of Transportation (WSDOT) summarizes the results of an independent evaluation of the effectiveness of Gray's proposal. The unit comprising Bents 151-154 of the viaduct (see Appendix A) was used to evaluate Gray's proposal. This unit was designed by the WSDOT and contains details typical of other units designed by that agency. It is a straight unit, which simplified the modeling of the structure.

Gray's proposal doesn't include the dimensions of the structural steel frames, or the sizes of their component members. The sizes of members were determined by repeated trials to be reasonably effective in reducing the demands on the existing structure, without being extremely large. Gray has submitted two additional retrofit concepts subsequent to initiation of this review that are similarly general in nature, and lack specific dimensions and details. These are addressed in Appendices C and D of this report.

The evaluation was made with respect to an expected earthquake with a return period of 108 years, a design earthquake with a return period of 500 years, and a maximum considered (or "rare") earthquake with a return period of 2500 years. Minimal damage was allowed for the expected event, repairable damage was allowed for the design event, and significant damage was allowed for the rare event. Repairable damage is damage that can be repaired without prolonged closing the structure to traffic. Significant damage may require extended closure for repair, but the risk of collapse should be minimal. The evaluation was based on time history analysis of a three-dimensional model created using the ADINA computer program.

For the rare earthquake, the structure has several vulnerable elements, in spite of the retrofit with auxiliary frames and dampers. These include:

- The columns are subjected to high compressive forces due to rocking of the structure and impact against the piles. In combination with the flexural demands, it's likely that the columns—and the viaduct—will fail.
- The floorbeams are subjected to flexural demands in negative bending (adjacent to the columns and opposite to the dead load bending) that exceed the limits for significant damage.
- Large principal tensile stresses occur in the knee and tee joints. Moderate degradation of the joints can be expected.
- The piles are subjected to very high compressive forces, up to 750 kip each. Severe damage is likely.
- The footings are subjected to excessive shear and flexural demands, and high joint shears. Severe damage is likely.
- The foundations are overloaded laterally, with a demand/capacity ratio of approximately three.

The severity of the demands may be partly attributed to the fact that the auxiliary frames stiffen the structure so that is fundamental periods of vibration coincide with the frequency range of strongest shaking for Zone A soil profiles.

The damage in the design and expected events is summarized in Table 14.

Table 14, Damage Summary			
Element	**Earthquake Event**		
	Expected(108)	**Design(500)**	**Rare(2500)**
Columns	Cracking	Repairable	*Failure*
Floorbeams	Cracking	Repairable	Significant
Joints	Cracking	Repairable	Significant
Piles	*Moderate*	*Significant*	*Severe*
Footings	*Significant*	*Severe*	*Severe*
Criteria	Minimal	Repairable	Significant

The last line of the table indicates the general criterion for each event. Italic font indicates element damage exceeding the criteria for a particular event. Additional detail can be found in the body of the report.

In the design and expected events, the foundations of the viaduct that are most vulnerable. For the design event, demand/capacity ratios are about four. For the expected event, demand/capacity ratios are about two. The vulnerability of the foundations makes the value of the retrofit questionable even for the design and expected earthquakes. Substantial additional retrofit measures would be necessary in order to meet design standards for seismic resistance.

6. REFERENCES

1. ADINA R&D, Inc., ADINA Theory and Modeling Guide, www.adina.com.

2. American Association of State Highway and Transportation Officials, "AASHTO LRFD Bridge Design Specifications," 2004.

3. ATC/MCEER, "Recommended LRFD Guidelines for the Seismic Design of Highway Bridges," MCEER/ATC-49, Multidisciplinary Center for Earthquake Engineering Research, 2003.

4. Applied Technology Council, "Improved Seismic Design Criteria for California Bridges: Provisional Recommendations," ATC-32, June, 1996.

5. Eberhard, M.O., De la Colina, J., & Ryter, S., "Seismic Vulnerability of the Alaskan Way Viaduct: WSDOT Typical Unit, Washington State Transportation Center, June, 1995.

6. Filiatrault, A., et. al., "Reconnaissance Report of the February 28, 2001 Nisqually (Seattle-Olympia) Earthquake," Report No. SSRP-2001/02, UCSD, La Jolla, CA.

7. Imbsen & Associates, cross-sectional X sTRuctural Analysis of ComponenTs (XTRACT), www.imbsen.com/xtract.htm.

8. Imbsen & Associates, Capacity Analysis Pushover Program (CAPP), www.imbsen.com/capp.htm.

9. Priestley, M.J.N., Seible, F. & Chai, Y.H., Design Guidelines for Assessment, Retrofit and Repair of Bridges for Seismic Performance," Report No. SSRP-92/01, Department of Applied Mechanics and Engineering Sciences. University of California, San Diego, August, 1992.

10. Priestley, M.J.N., Seible, F. & Calvi, G.M., Seismic Design and Retrofit of Bridges, John Wiley & Sons, 1996.

11. Shannon & Wilson, "Alaskan Way Viaduct and Seawall Replacement Project, Ground Motion Study Report," October, 2004.

12. Shannon & Wilson, email to Washington State Department of Transportation, July, 2006.

13. T.Y. Lin International, "Alaskan Way Viaduct—Independent Review of Frame 100," April 14, 2001.

LIST OF FIGURES

List of Figures

List of Figures

FIGURES

Figure 1 Alaskan Way Viaduct

SAP2000 6/29/06 15:27:06

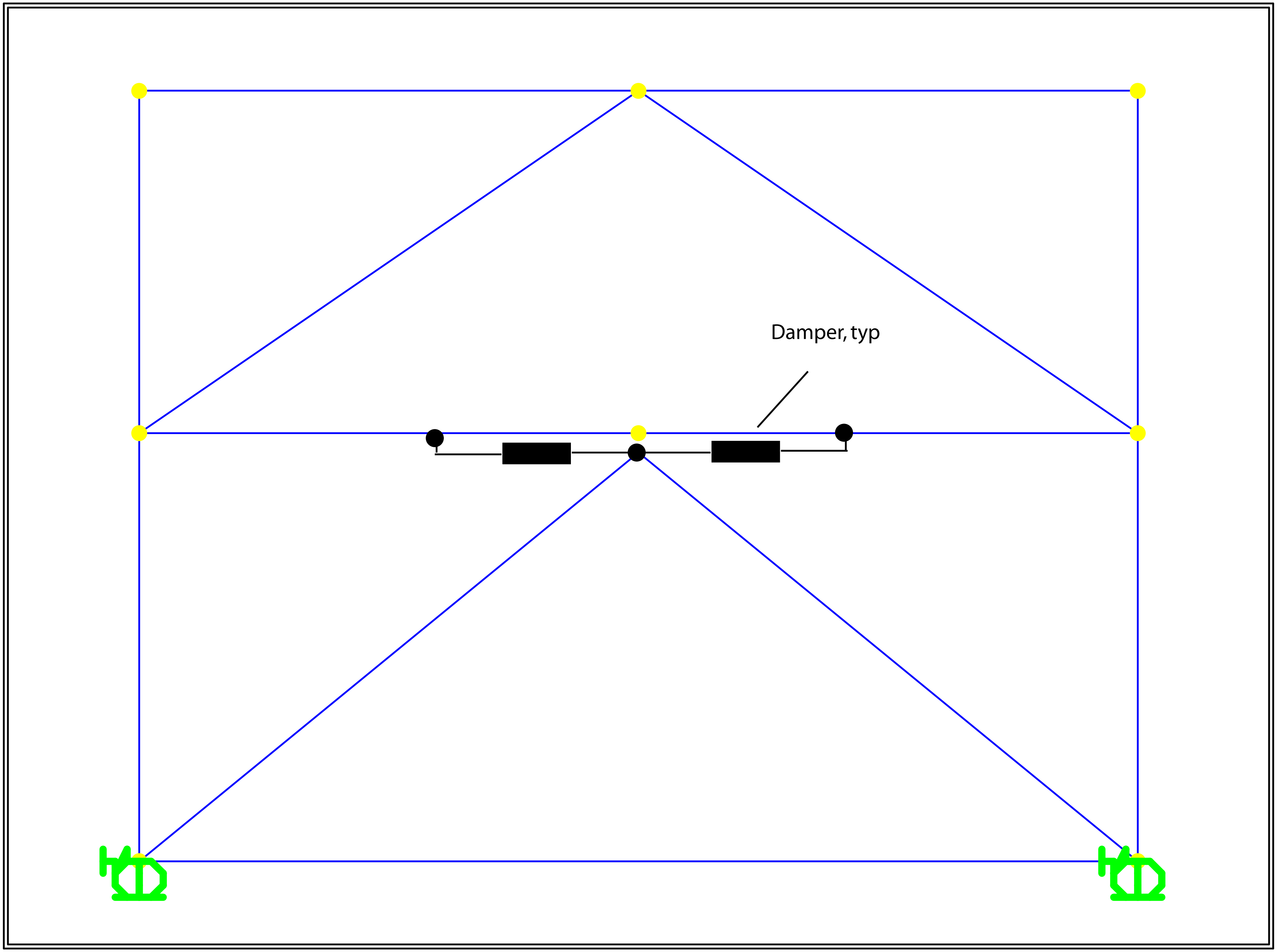

Figure 2a, Longitudinal auxiliary frame per Gray's proposal

SAP2000

6/29/06 16:21:35

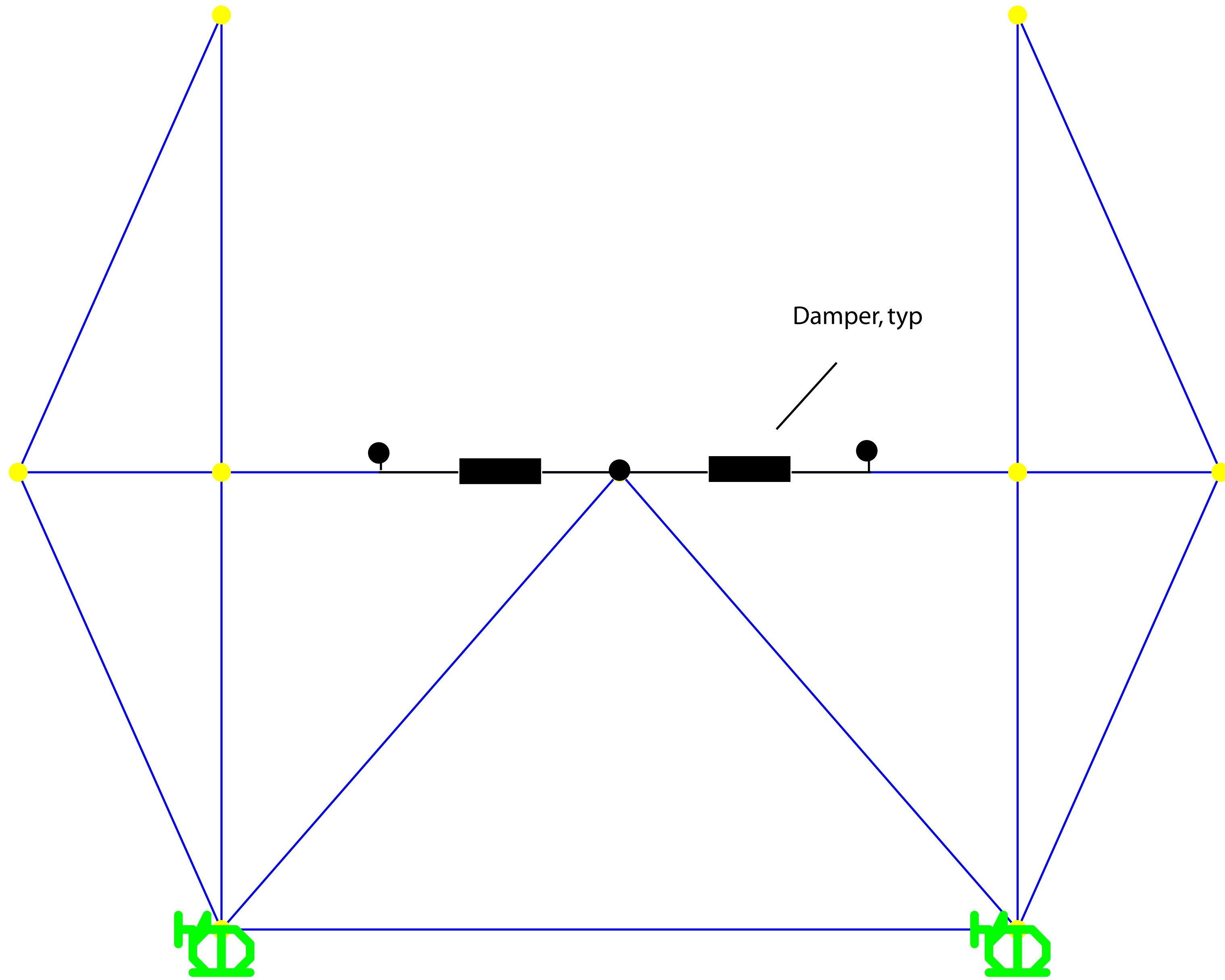

Figure 2b, Transverse auxiliary frame per Gray’s proposal

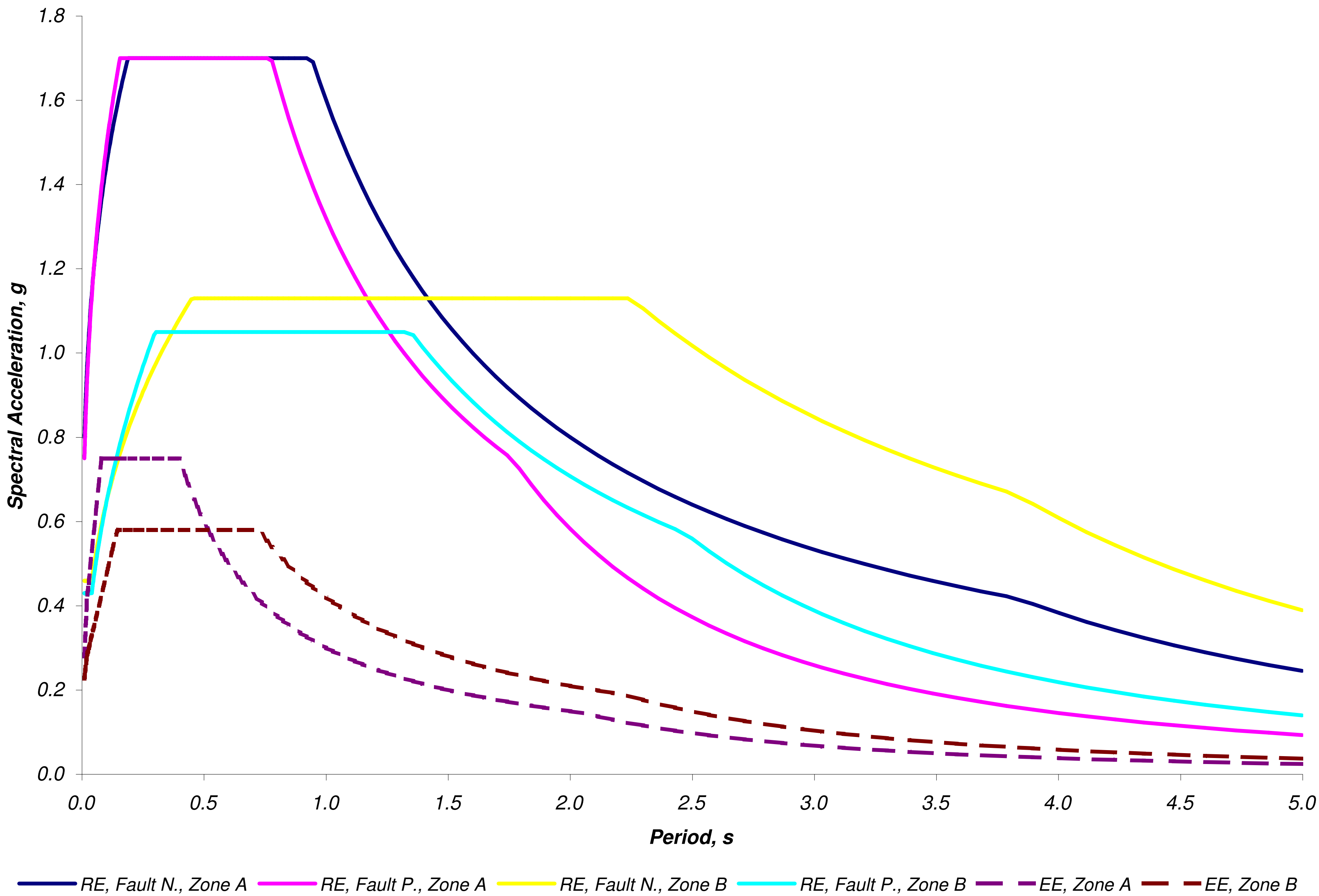

Figure 3a, Acceleration spectra for horizontal motions, rare and expected earthquakes

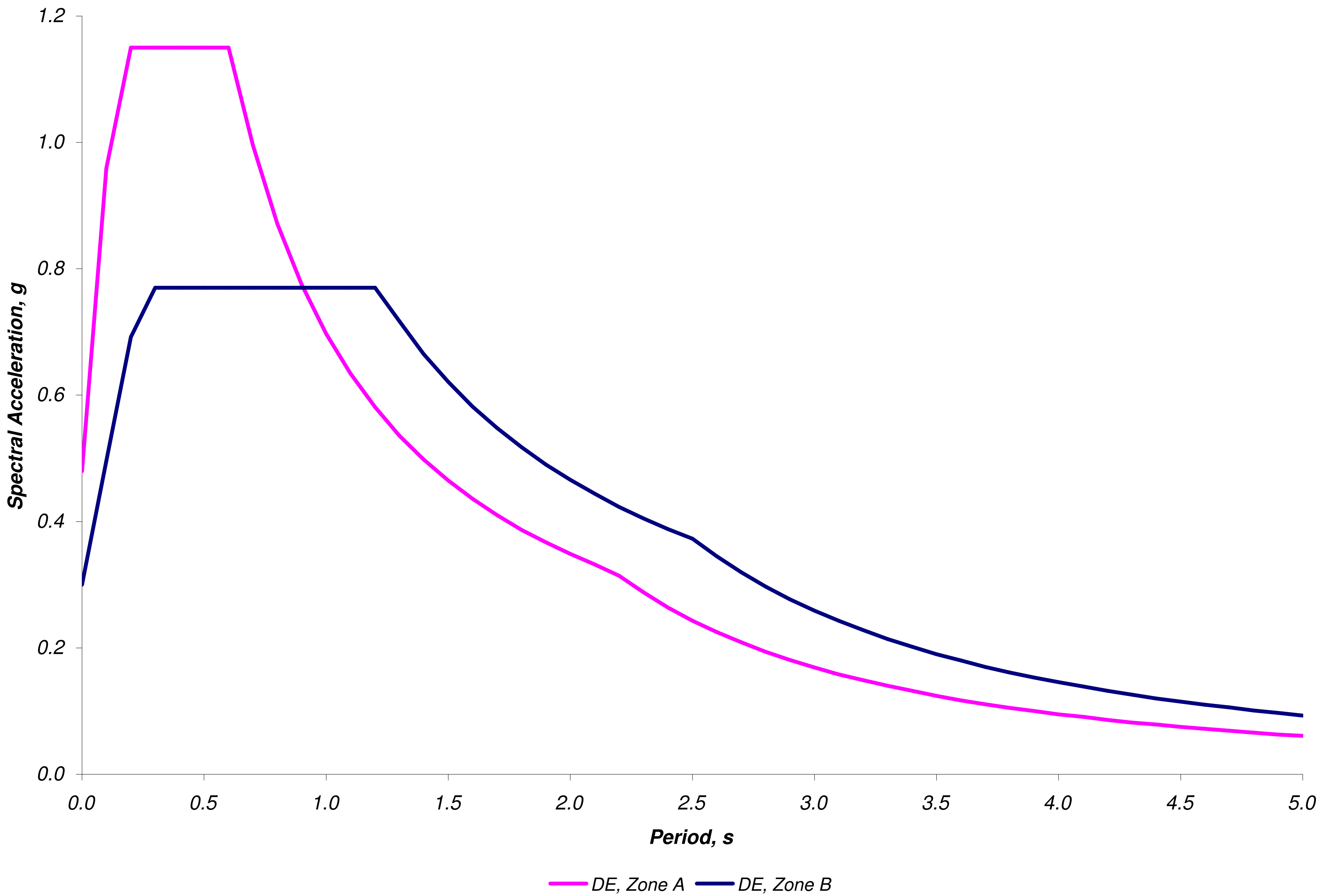

Figure 3b, Acceleration spectra for horizontal motions, design earthquake

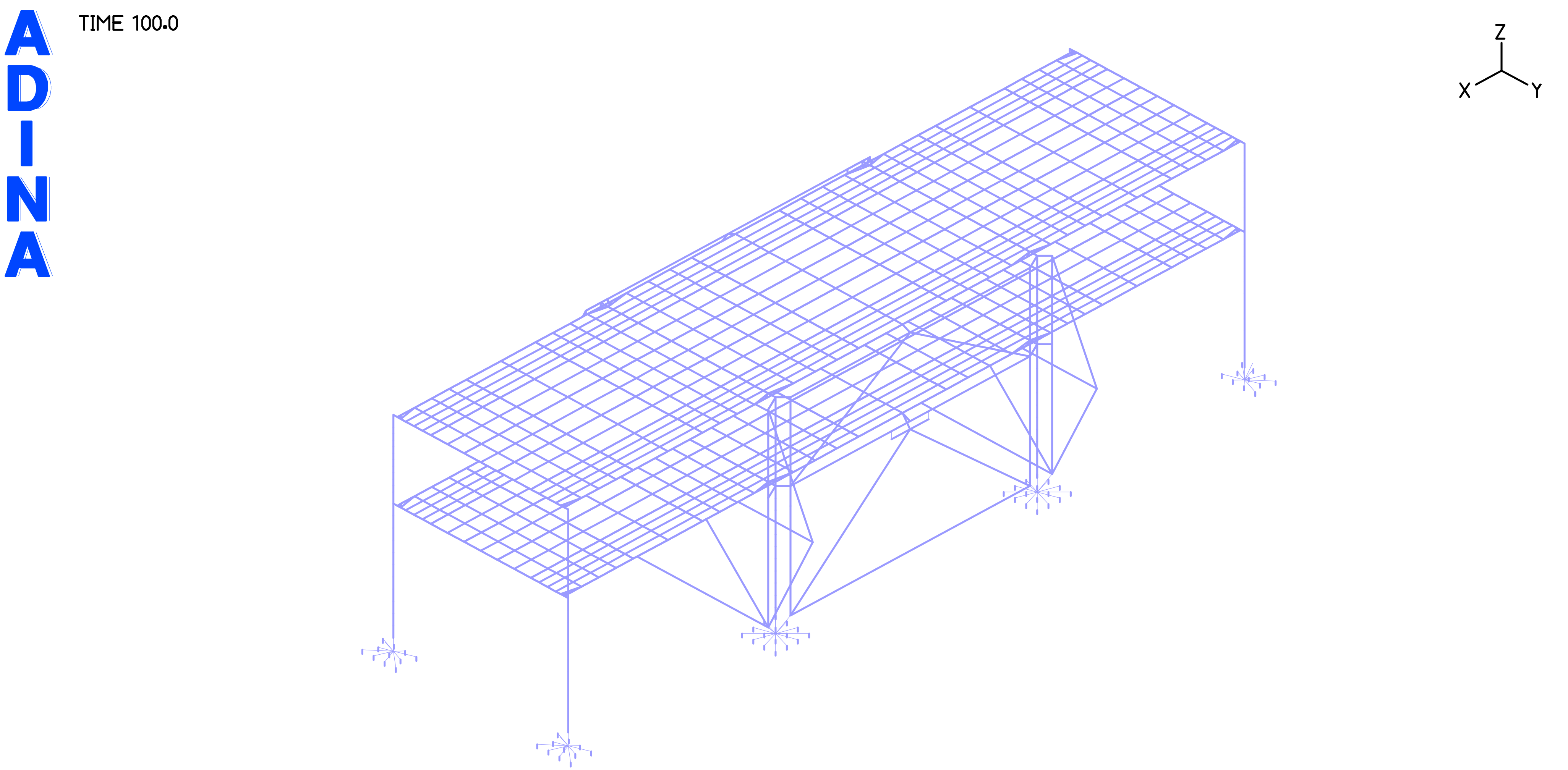

Figure 4a, Analytical model, three-dimensional view

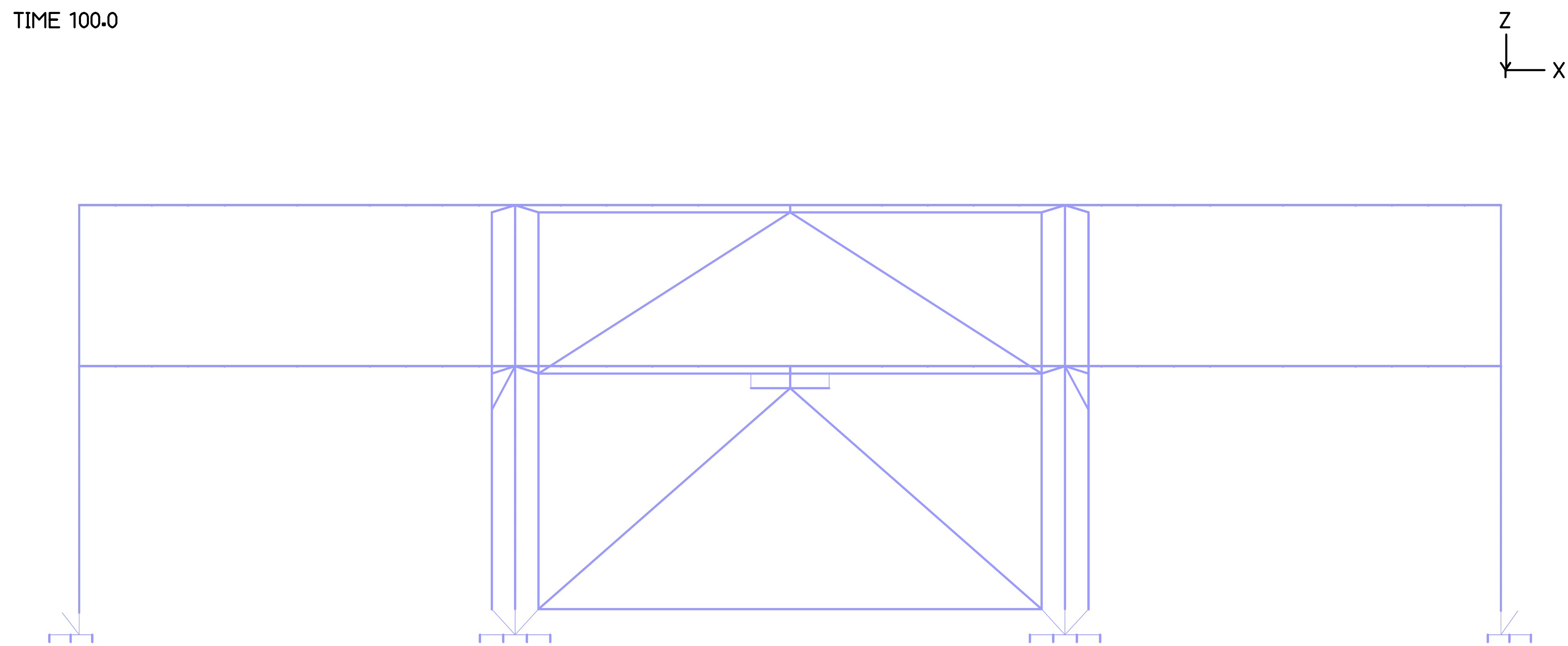

Figure 4b, Analytical model, longitudinal elevation

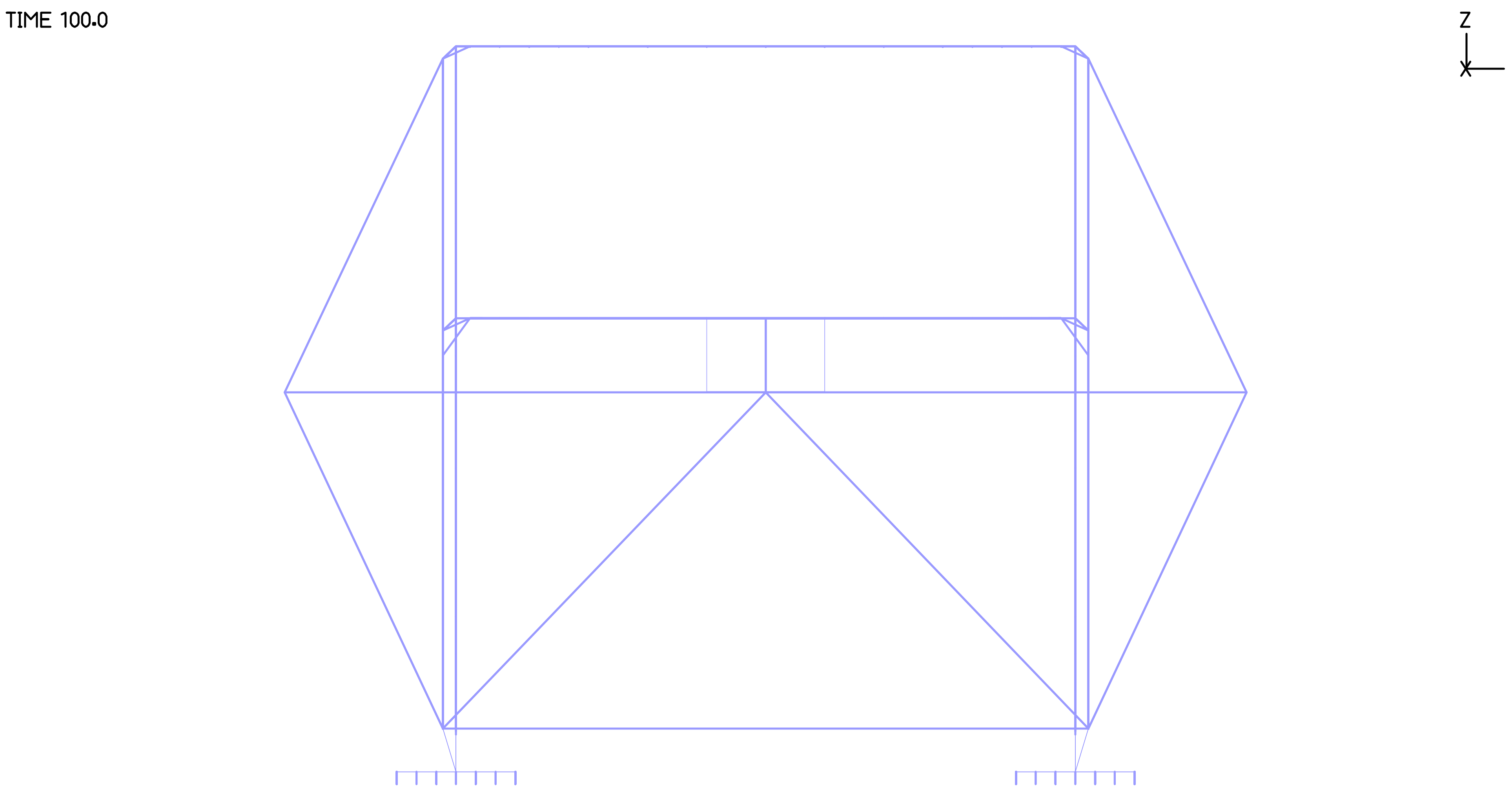

Figure 4c, Analytical model, transverse elevation

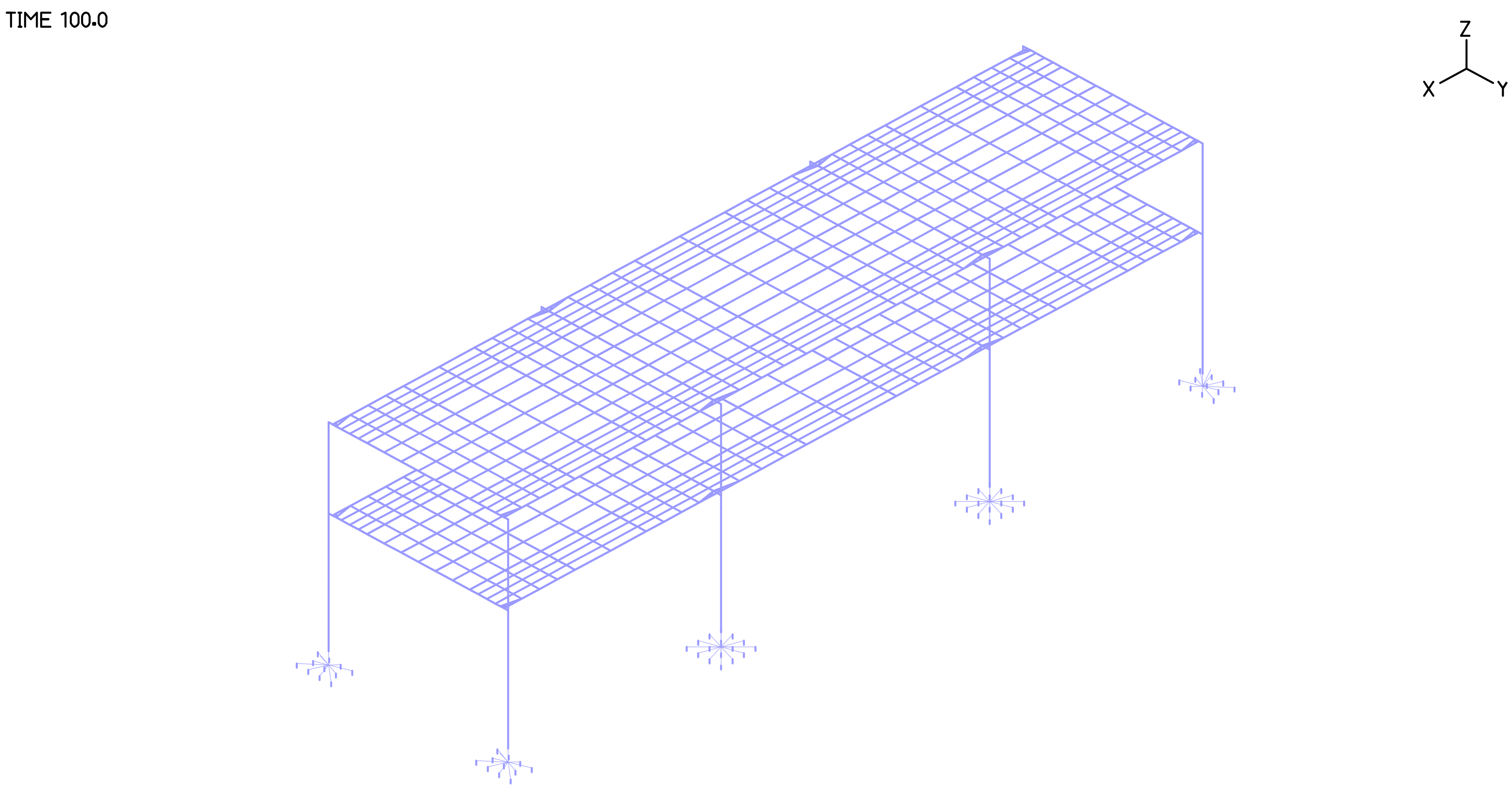

Figure 4d, Analytical model, existing structure only

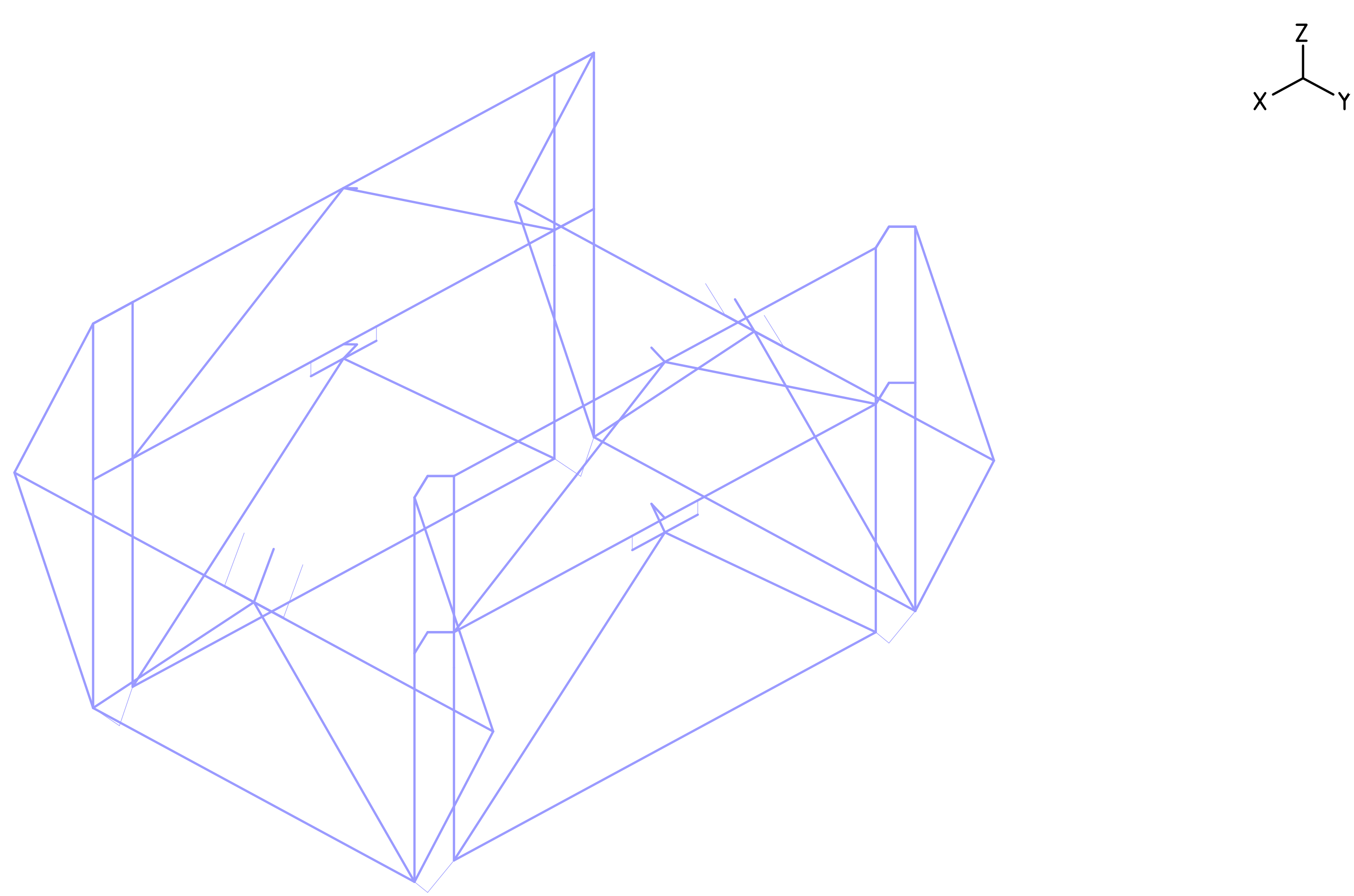

Figure 4e, Analytical model, auxiliary frames only

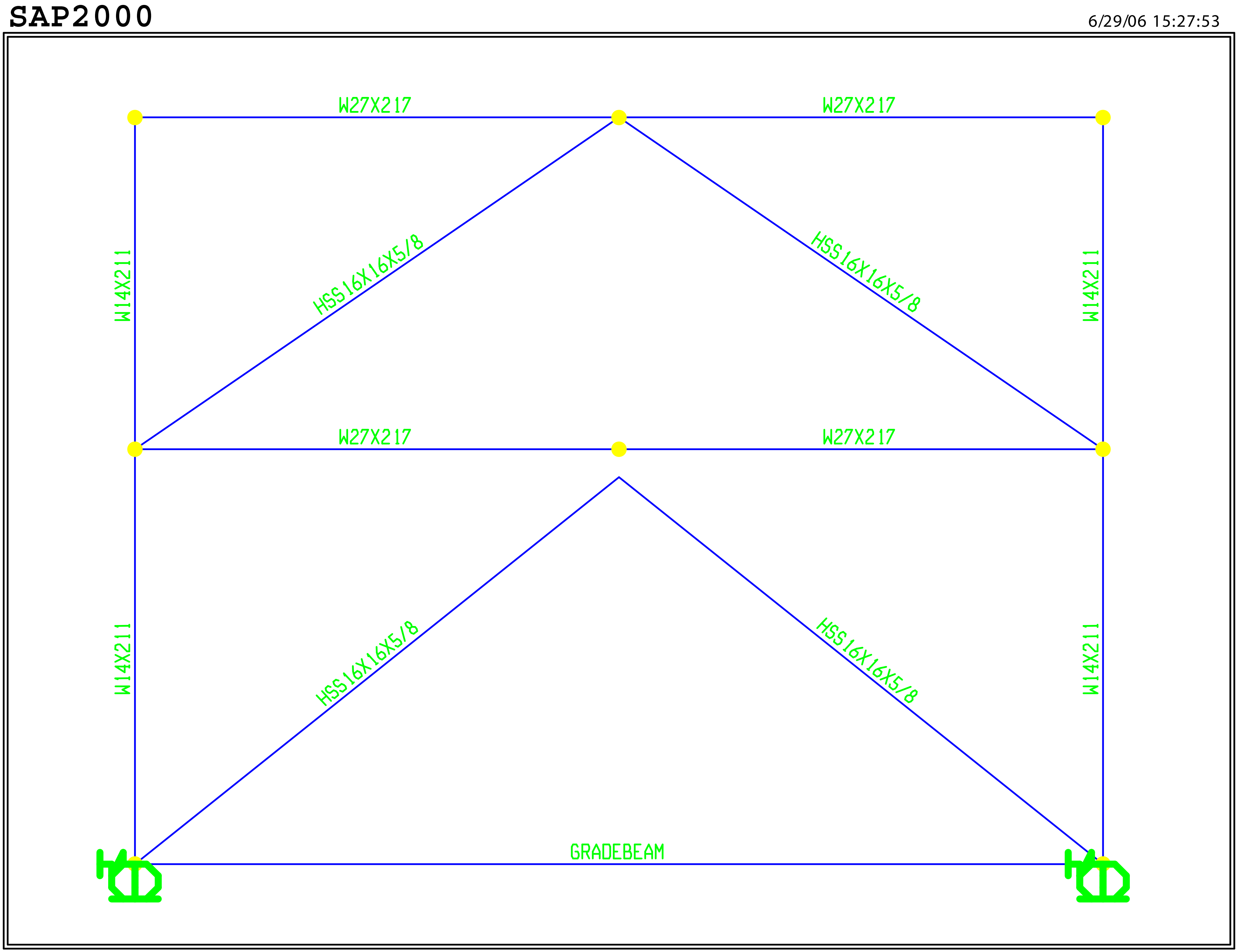

Figure 5a, Auxiliary frame member sizes, longitudinal frames

SAP2000

6/29/06 16:14:03

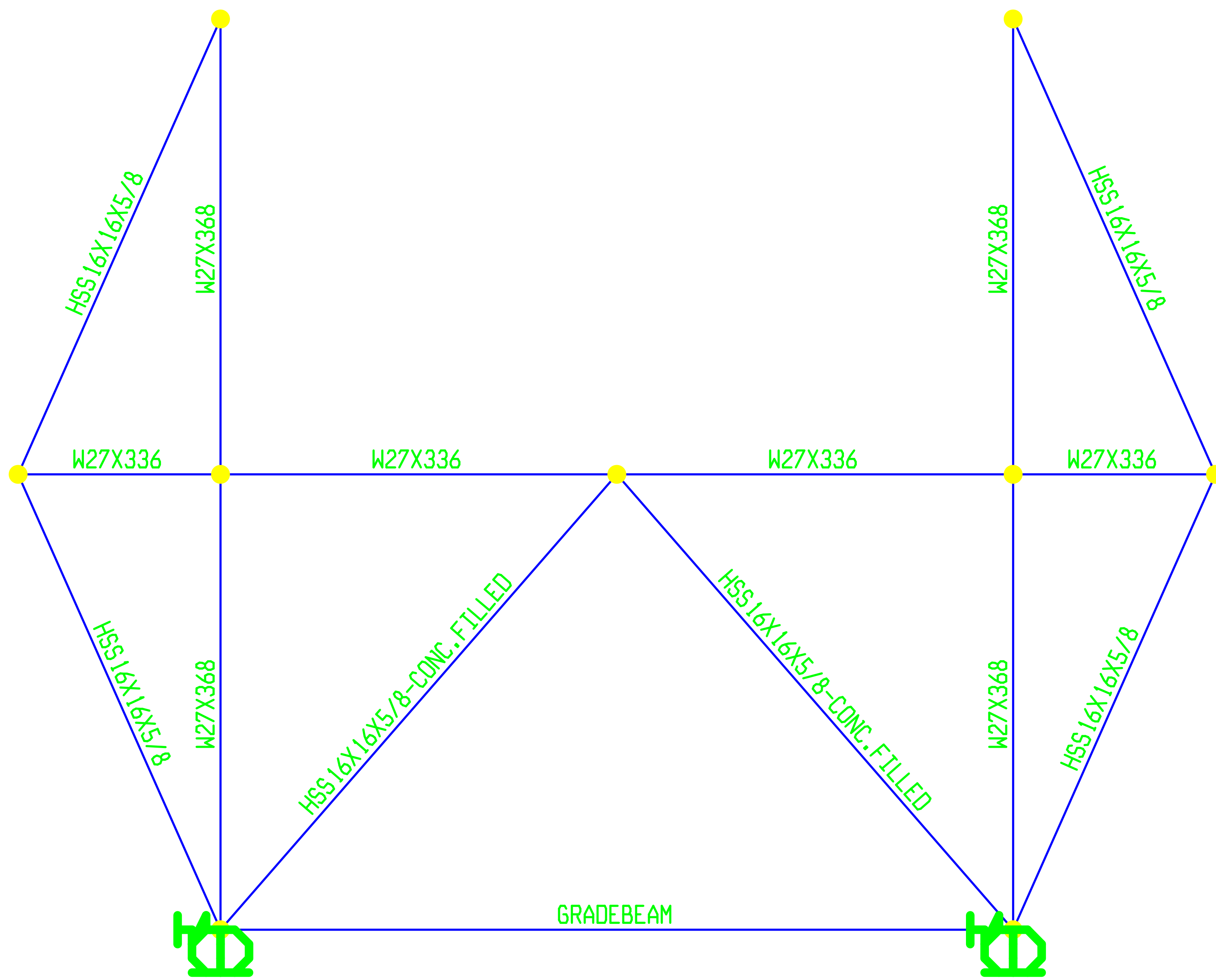

Figure 5b, Auxiliary frame member sizes, transverse frames

Model Name:	existing.06	**Absolute Drifts**
Model Description:	Alaska Way Viaduct, Evaluation of Grays Proposal	
Model Variation:	rare earthquake	29 Jun 06 1:51 PM

Longitudinal

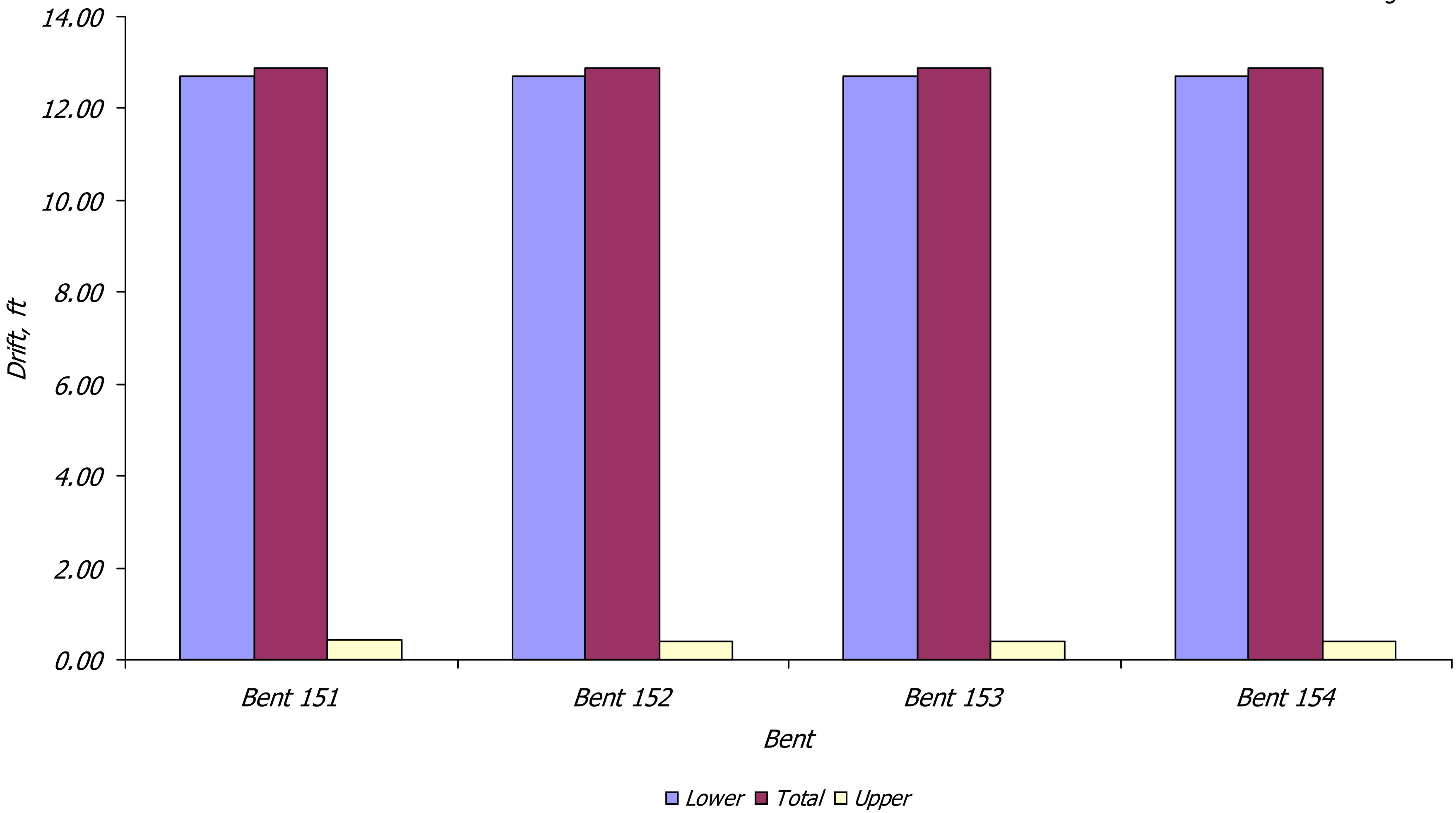

Figure 6a Drift of existing structure, rare earthquake, longitudinal direction

Model Name: existing.06

Absolute Drifts

Model Description: Alaska Way Viaduct, Evaluation of Grays Proposal

Model Variation: rare earthquake

29 Jun 06 1:51 PM

Transverse

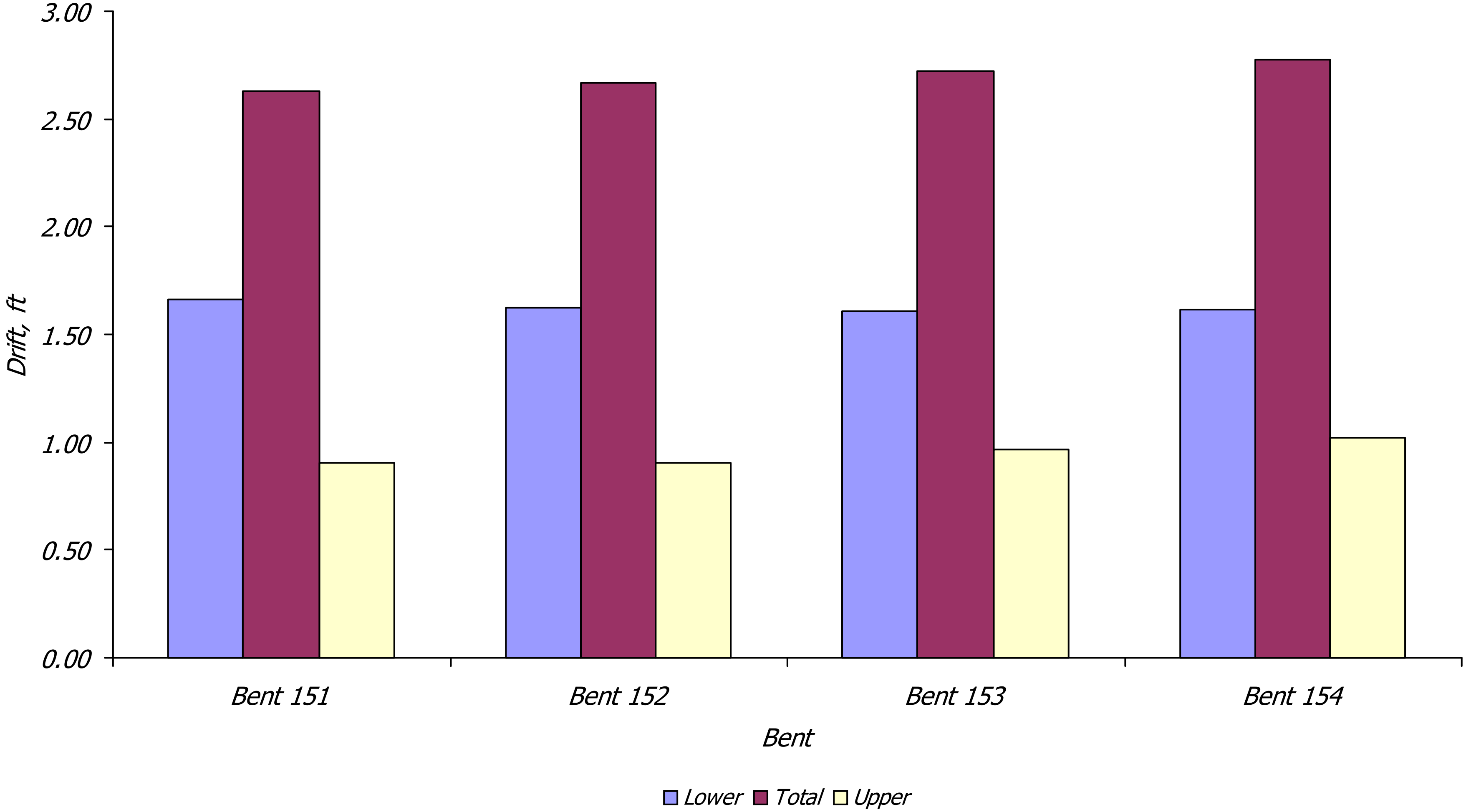

Figure 6b Drift of existing structure, rare earthquake, transverse direction

Model Name: existing.06

Absolute Drifts

Model Description: Alaska Way Viaduct, Evaluation of Grays Proposal

Model Variation: expected earthquake

25 Jul 06 2:30 PM

Longitudinal

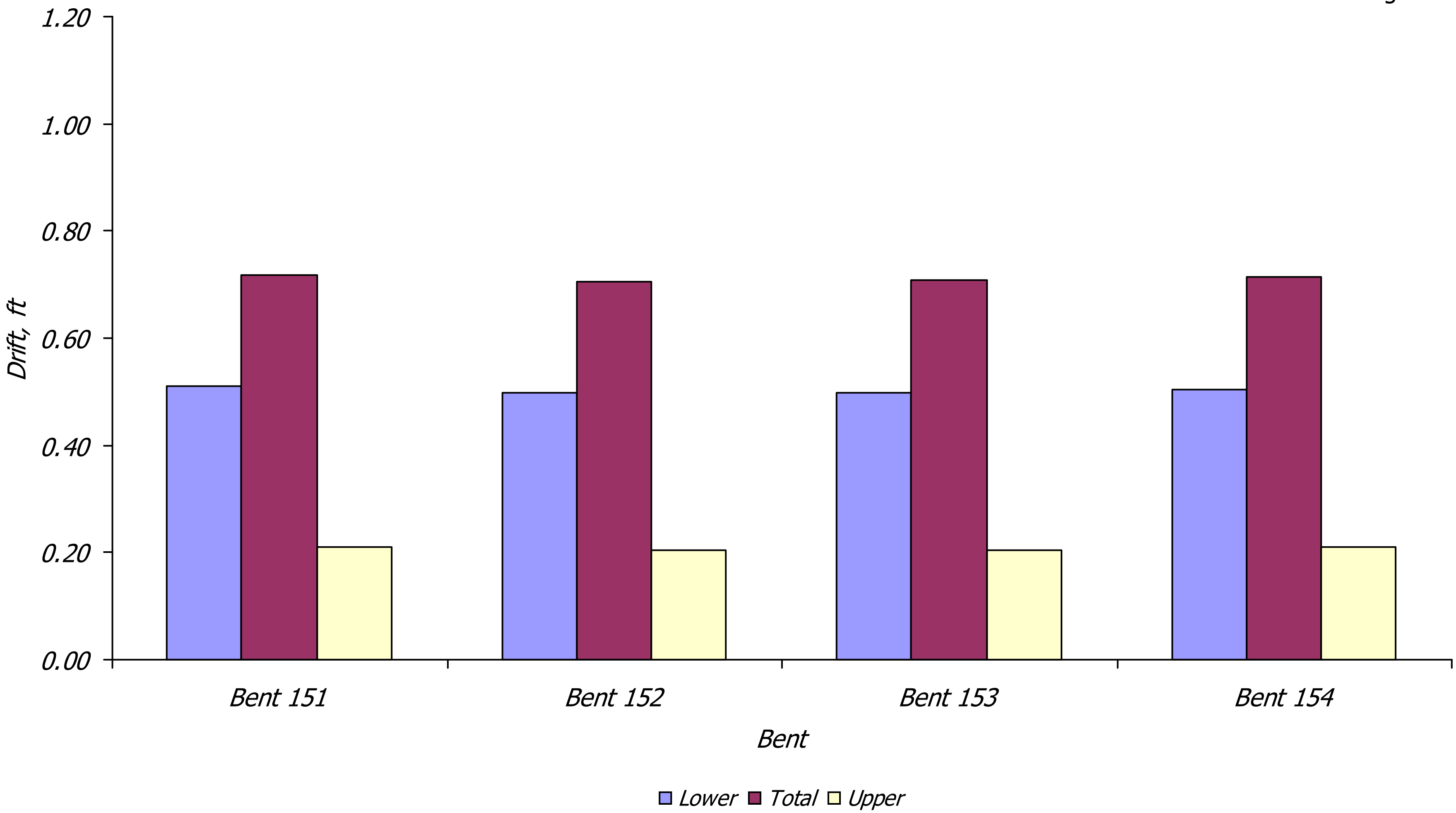

Figure 7a Drift of existing structure, expected earthquake, longitudinal direction

Model Name: existing.06

Absolute Drifts

Model Description: Alaska Way Viaduct, Evaluation of Grays Proposal

Model Variation: expected earthquake 25 Jul 06 2:30 PM

Transverse

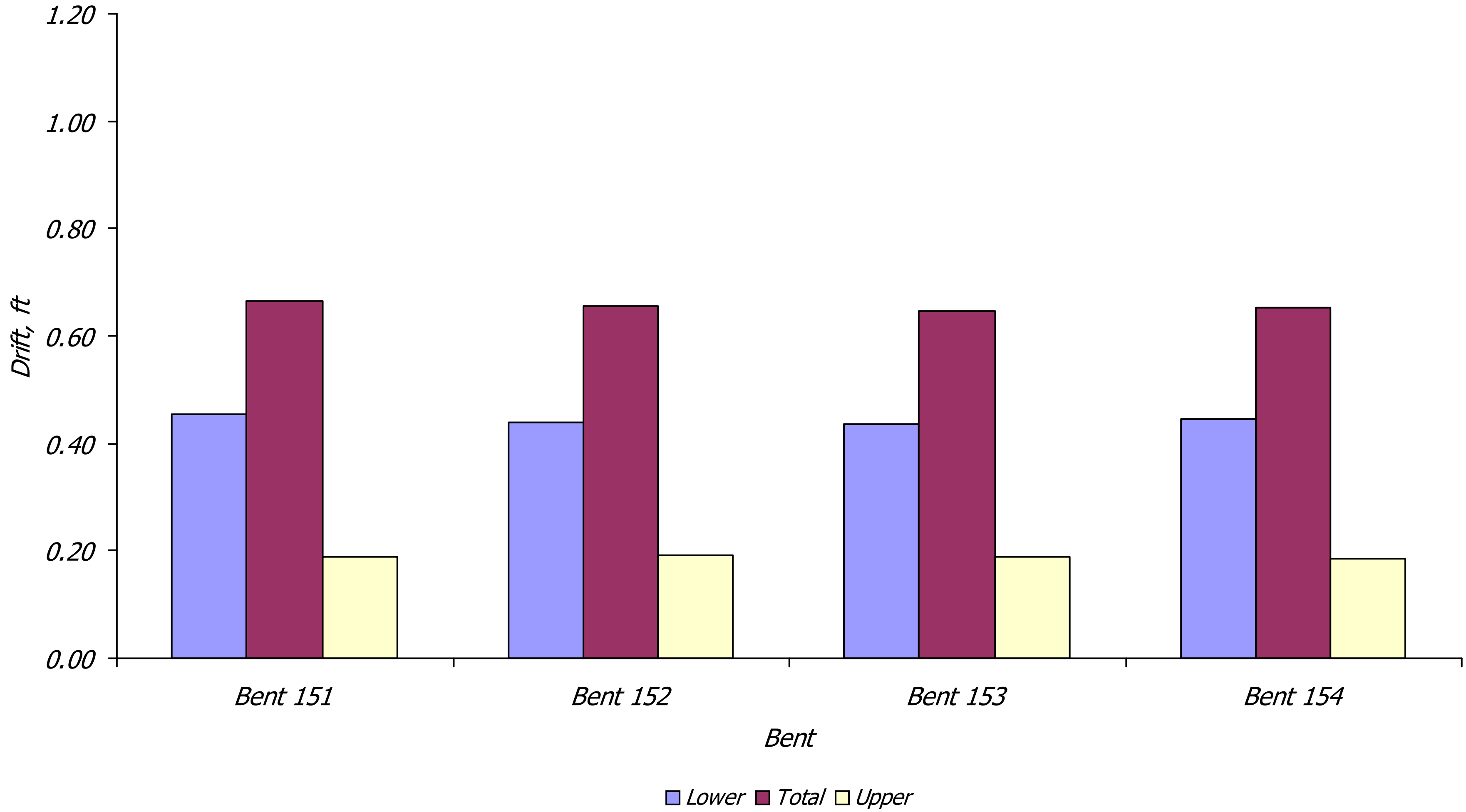

Figure 7b Drift of existing structure, expected earthquake, transverse direction

Model Name: existing.06

Column Curvature Ductility Demand

Model Description: Alaska Way Viaduct, Evaluation of Grays Proposal

Model Variation: expected earthquake

25 Jul 06 2:41 PM

Longitudinal Direction

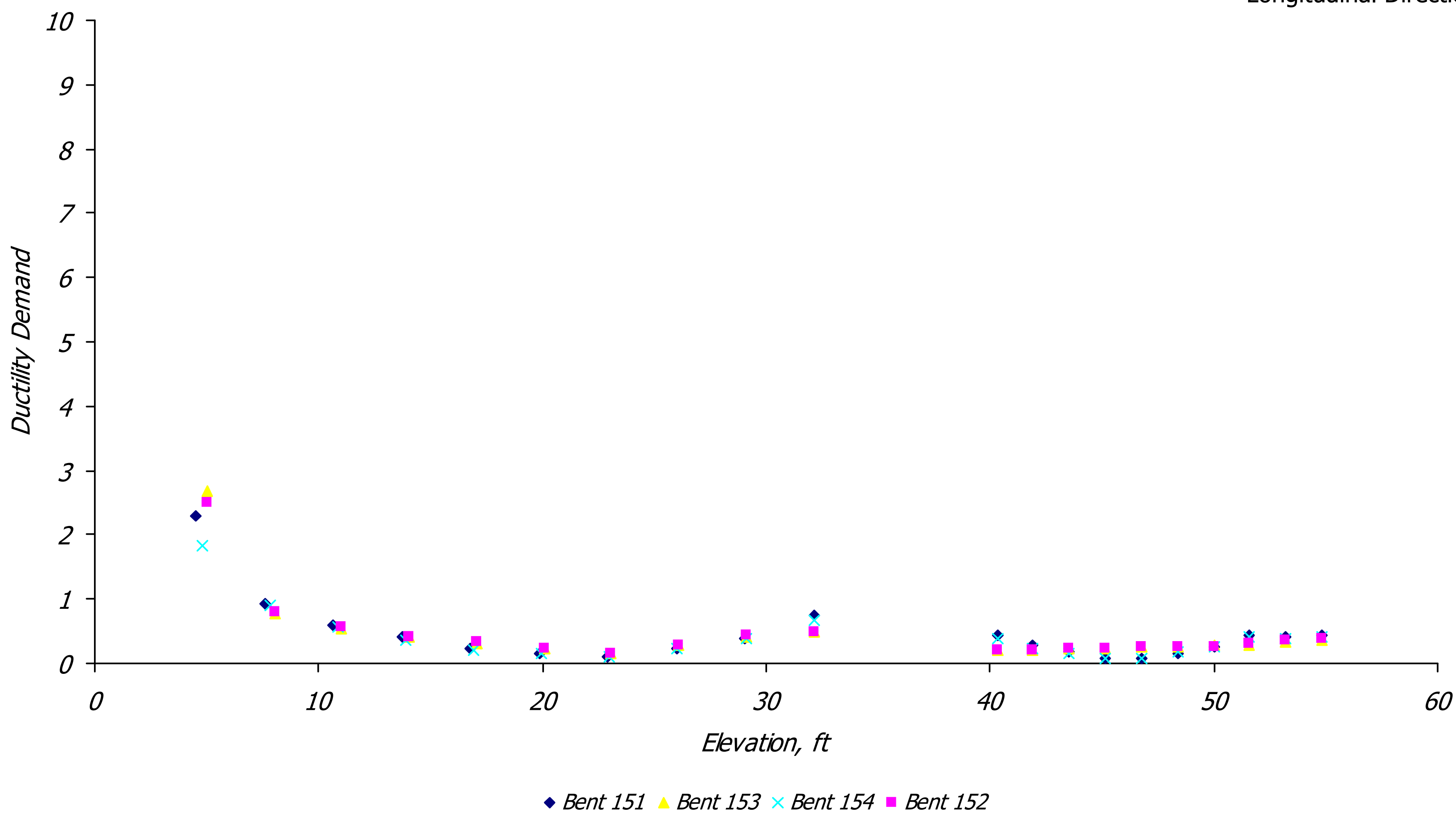

Figure 8a Column curvature ductility demand, existing structure, expected earthquake, longitudinal direction

Model Name: existing.06

Column Curvature Ductility Demand

Model Description: Alaska Way Viaduct, Evaluation of Grays Proposal

Model Variation: expected earthquake

25 Jul 06 2:41 PM

Transverse Direction

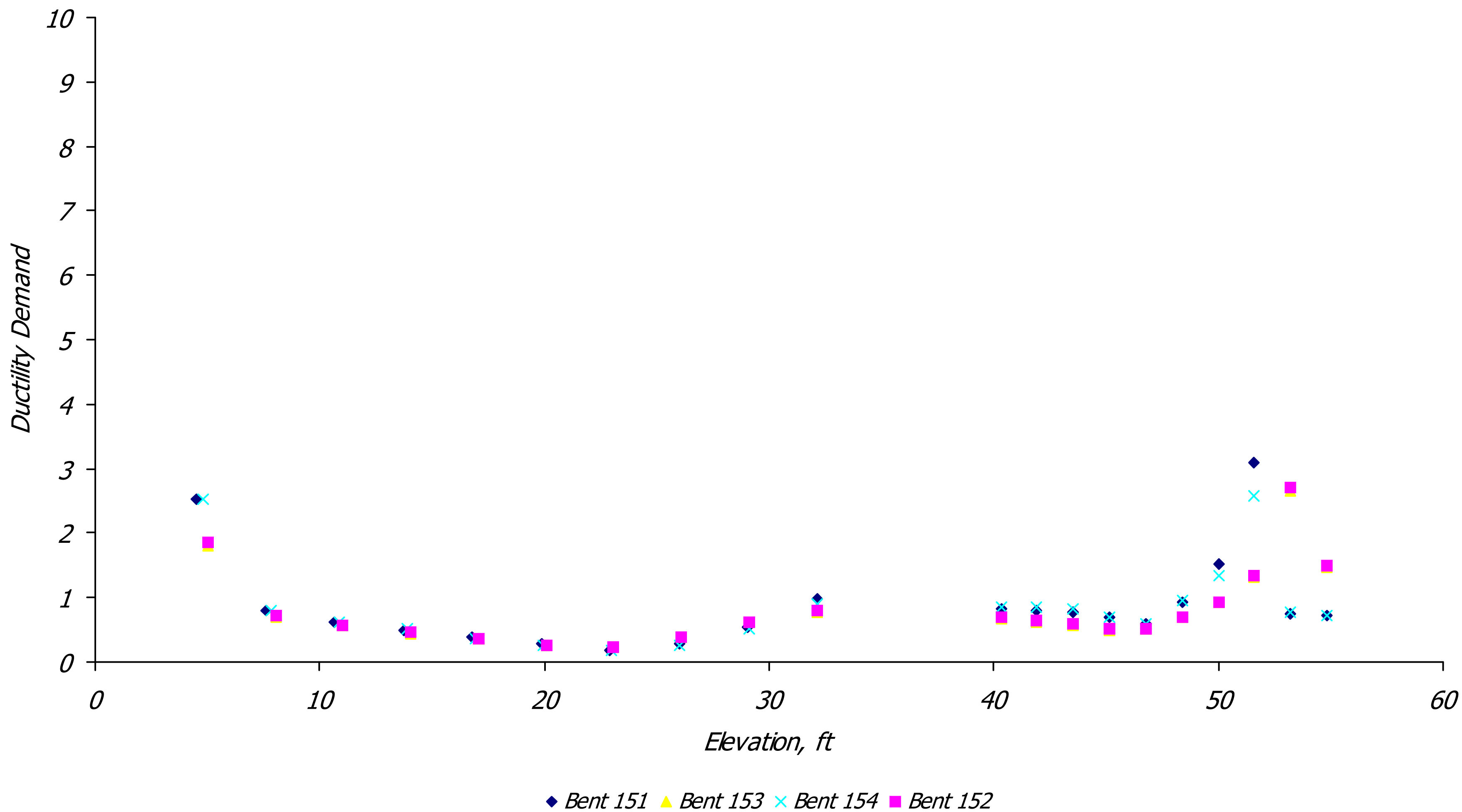

Figure 8b Column curvature ductility demand, existing structure, expected earthquake, transverse direction

Model Name: existing.06

Floorbeam Curvature Ductility Demand

Model Description: Alaska Way Viaduct, Evaluation of Grays Proposal

Model Variation: expected earthquake 25 Jul 06 2:56 PM

Upper Level

Positive Curvature

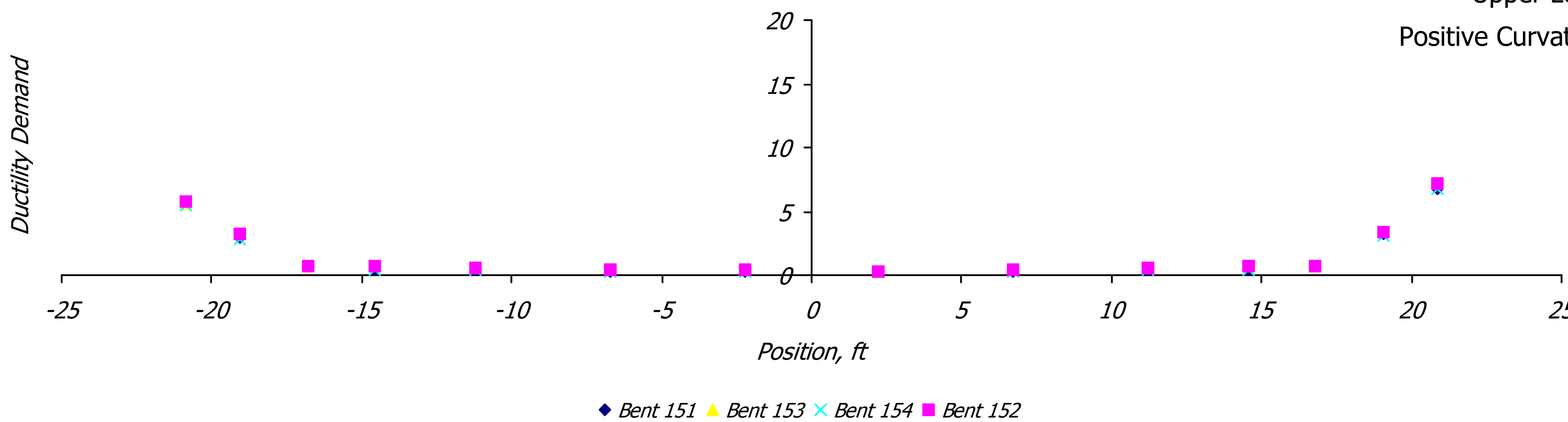

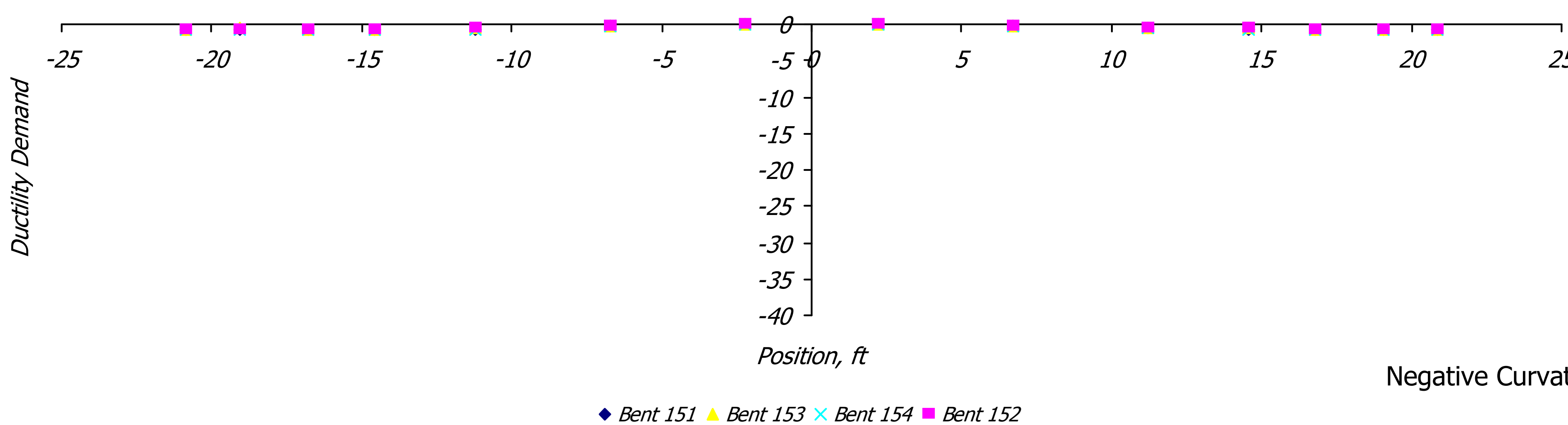

Negative Curvature

Figure 9a Floorbeam curvature ductility demand, existing structure, expected earthquake, upper level

Model Name: existing.06

Floorbeam Curvature Ductility Demand

Model Description: Alaska Way Viaduct, Evaluation of Grays Proposal

Model Variation: expected earthquake

25 Jul 06 2:56 PM

Lower Level

Positive Curvature

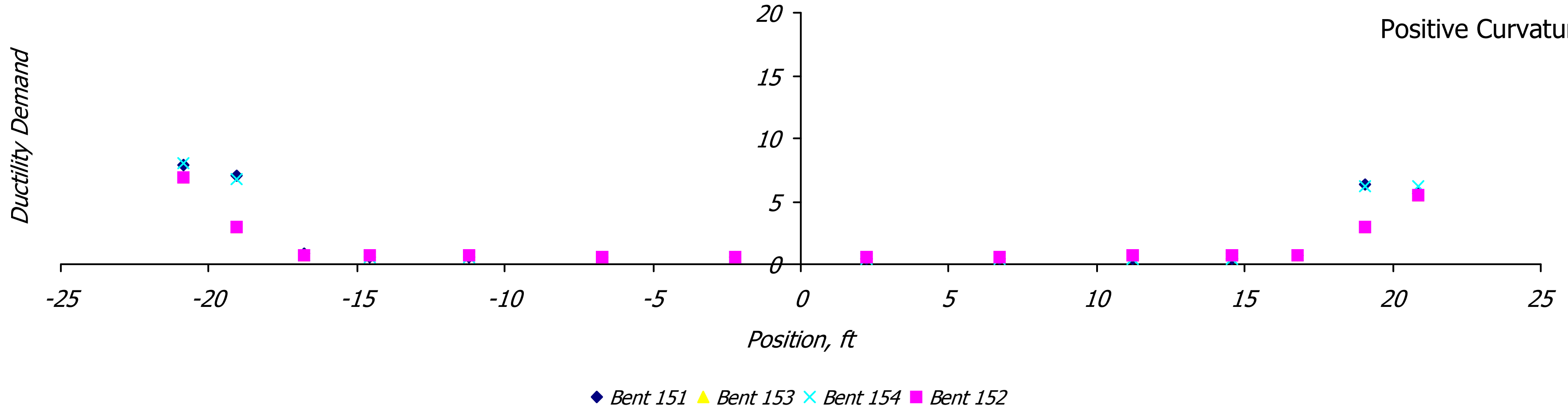

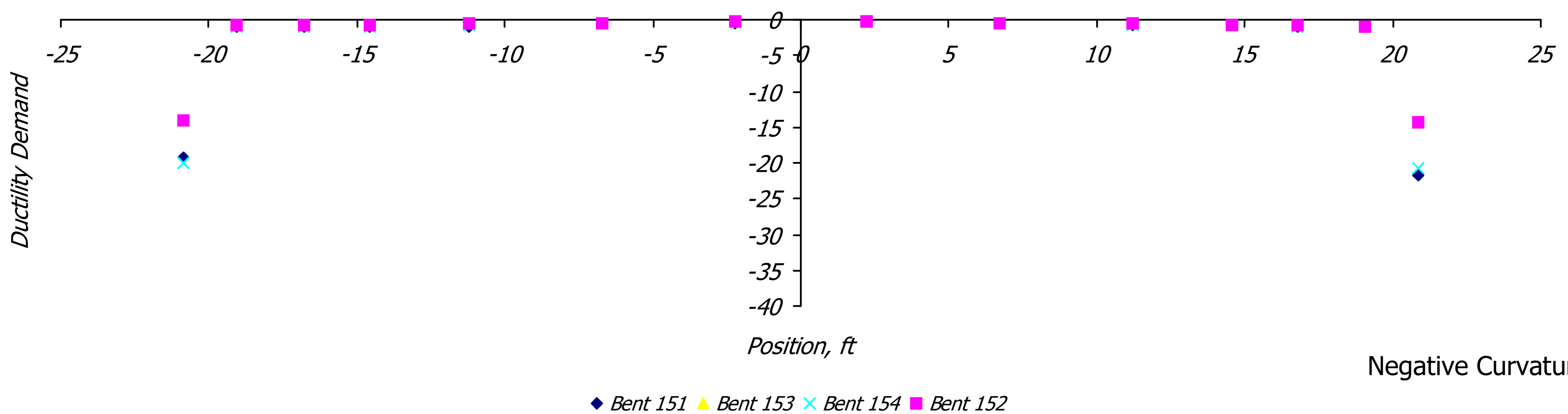

Negative Curvature

Figure 9b Floorbeam curvature ductility demand, existing structure, expected earthquake, lower level

Model Name:	gray.08	**Absolute Drifts**
Model Description:	Alaska Way Viaduct, Evaluation of Grays Proposal	
Model Variation:	rare earthquake	25 Jul 06 2:32 PM

Longitudinal

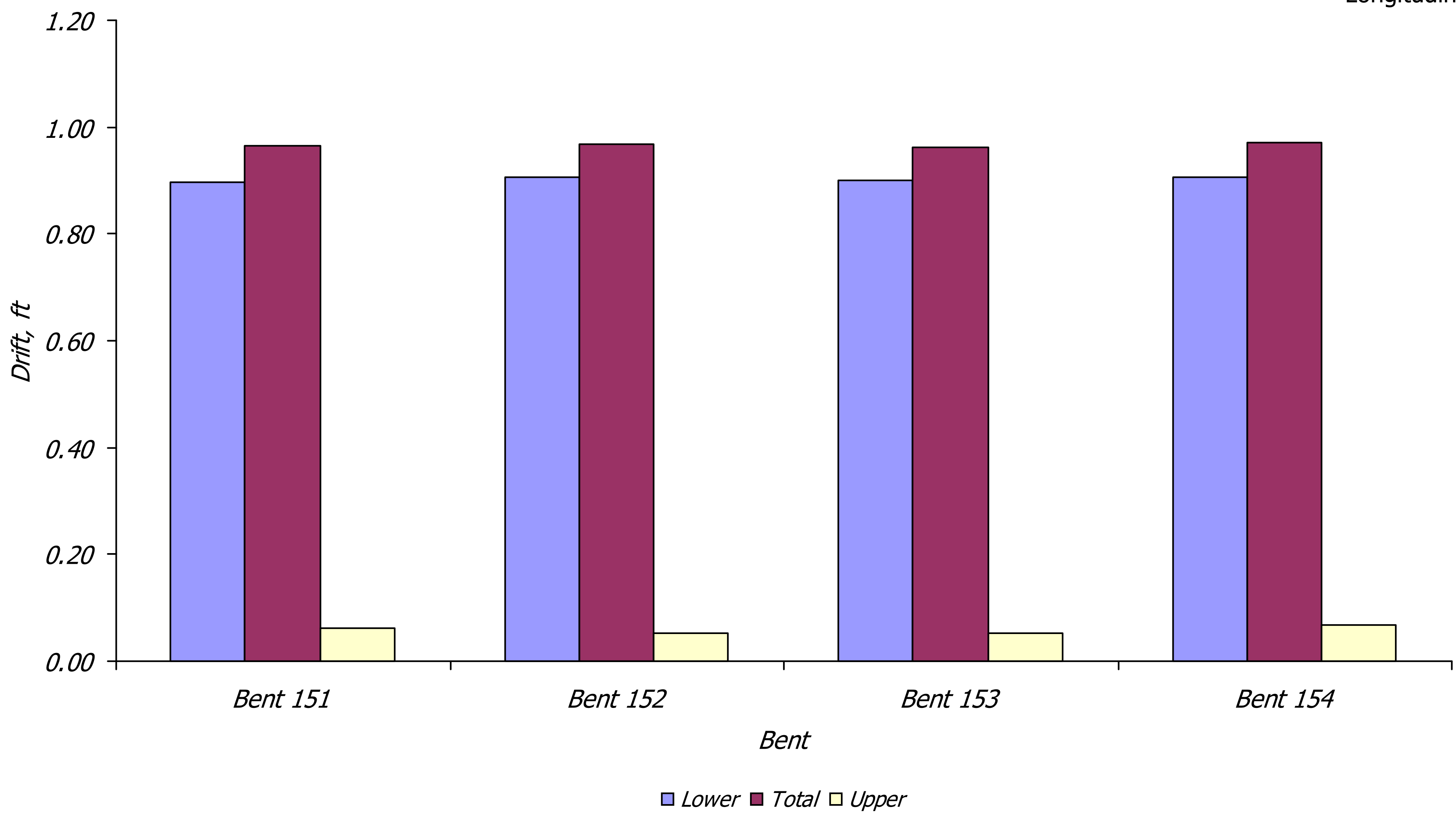

Figure 10a Drift of retrofitted structure, rare earthquake, longitudinal direction

Model Name:	gray.08	**Absolute Drifts**
Model Description:	Alaska Way Viaduct, Evaluation of Grays Proposal	
Model Variation:	rare earthquake	25 Jul 06 2:32 PM

Transverse

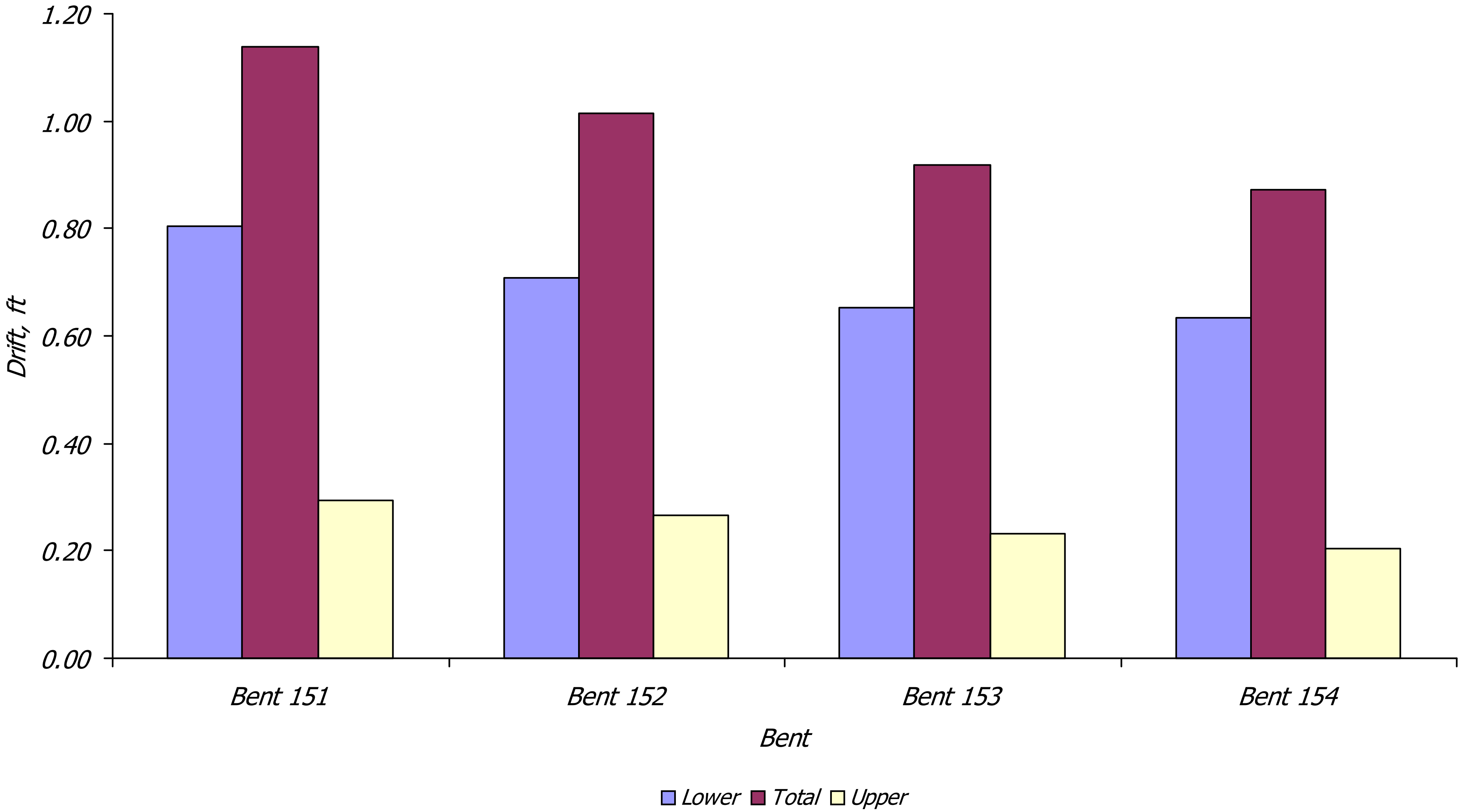

Figure 10b Drift of retrofitted structure, rare earthquake, transverse direction

CAPP Project Report

Loading Name: Combo1

Report Type: Deformed Shape - Units: ft

Comments: End Bent Push Over (case 1)

J.Chan
T.Y.Lin International
6/29/2006
Alaskan Way Viaduct
490031.00
Page __ of __

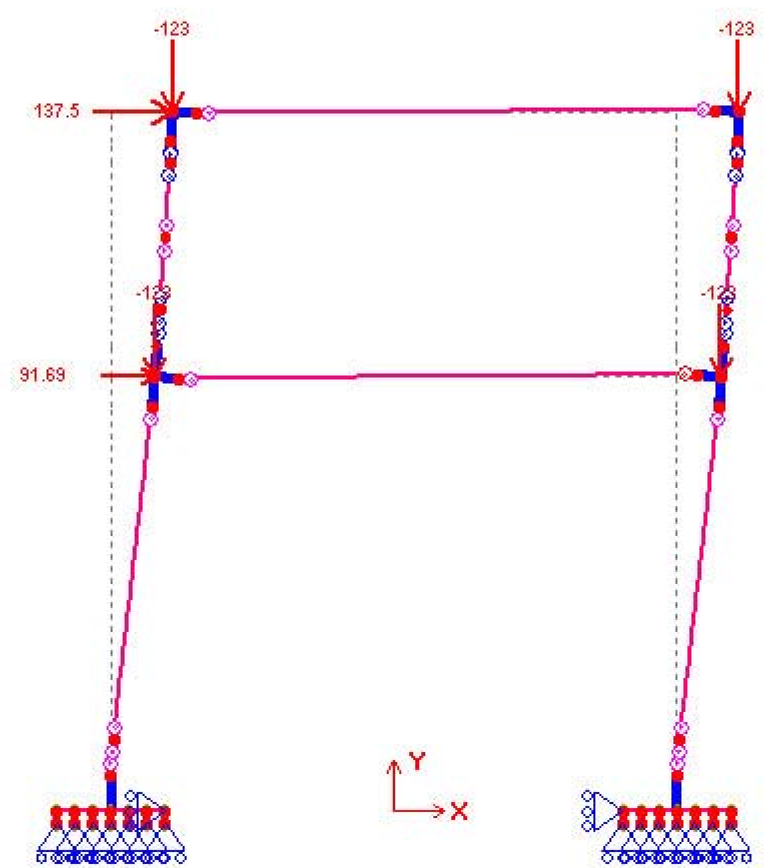

Figure 11, CAPP model for pushover analyses, typical end bent

Model Name:	gray.08	**Absolute Drifts**
Model Description:	Alaska Way Viaduct, Evaluation of Grays Proposal	
Model Variation:	design earthquake	25 Jul 06 2:33 PM

Longitudinal

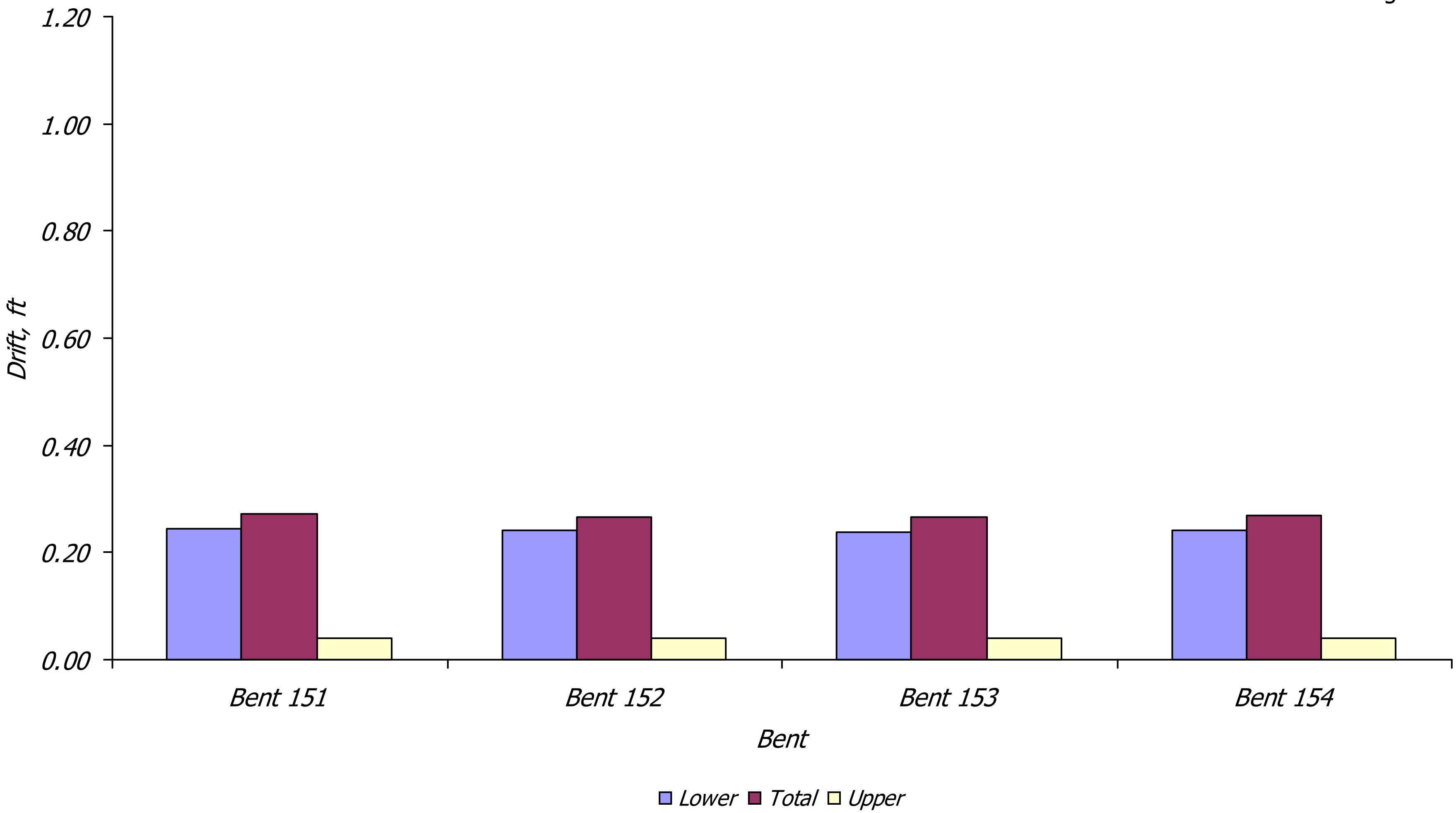

Figure 12a Drift of retrofitted structure, design earthquake, longitudinal direction

Model Name:	gray.08	**Absolute Drifts**
Model Description:	Alaska Way Viaduct, Evaluation of Grays Proposal	
Model Variation:	design earthquake	25 Jul 06 2:33 PM

Transverse

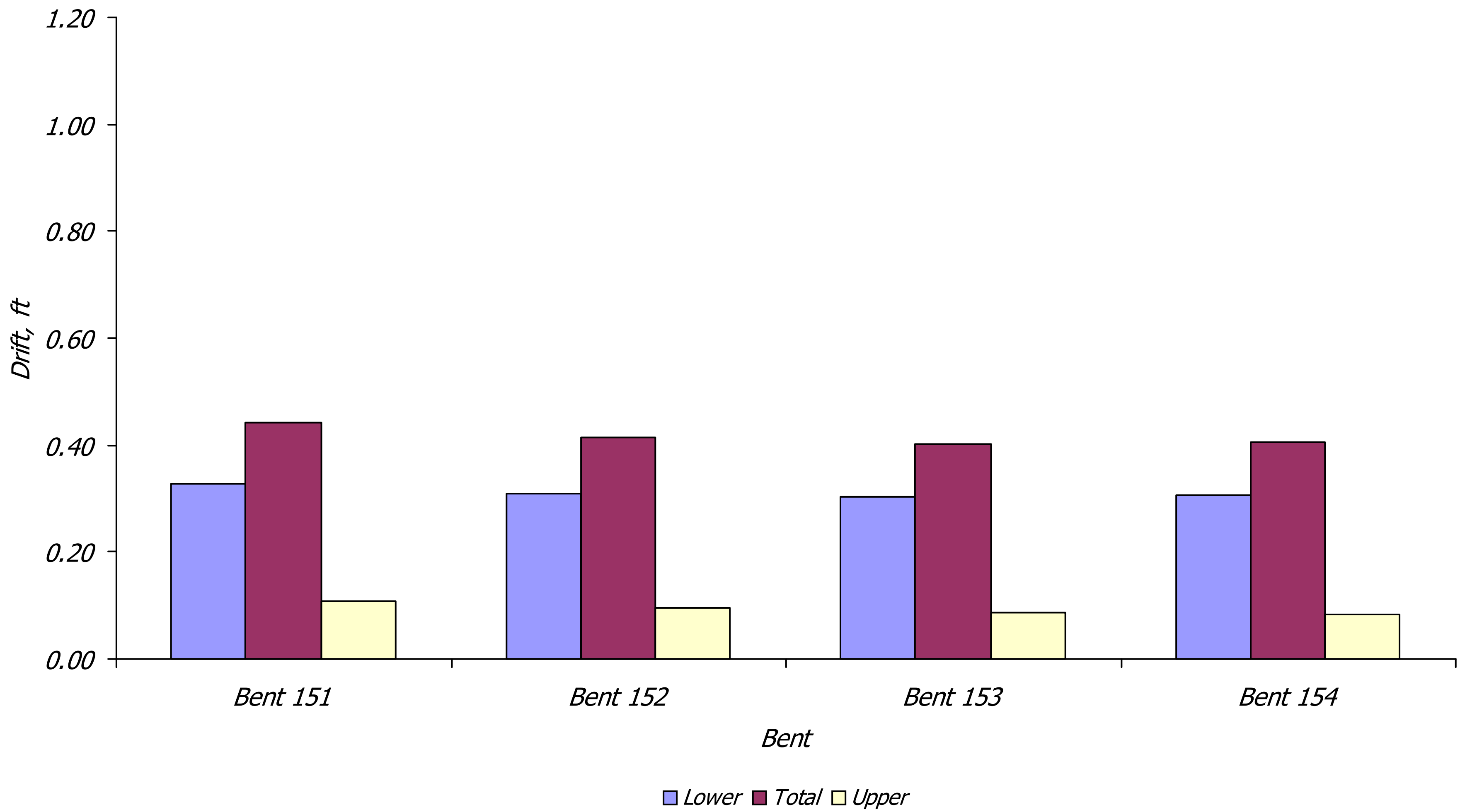

Figure 12b Drift of retrofitted structure, design earthquake, transverse direction

Model Name:	gray.08
Model Description:	Alaska Way Viaduct, Evaluation of Grays Proposal
Model Variation:	expected earthquake

Absolute Drifts

25 Jul 06 2:35 PM

Longitudinal

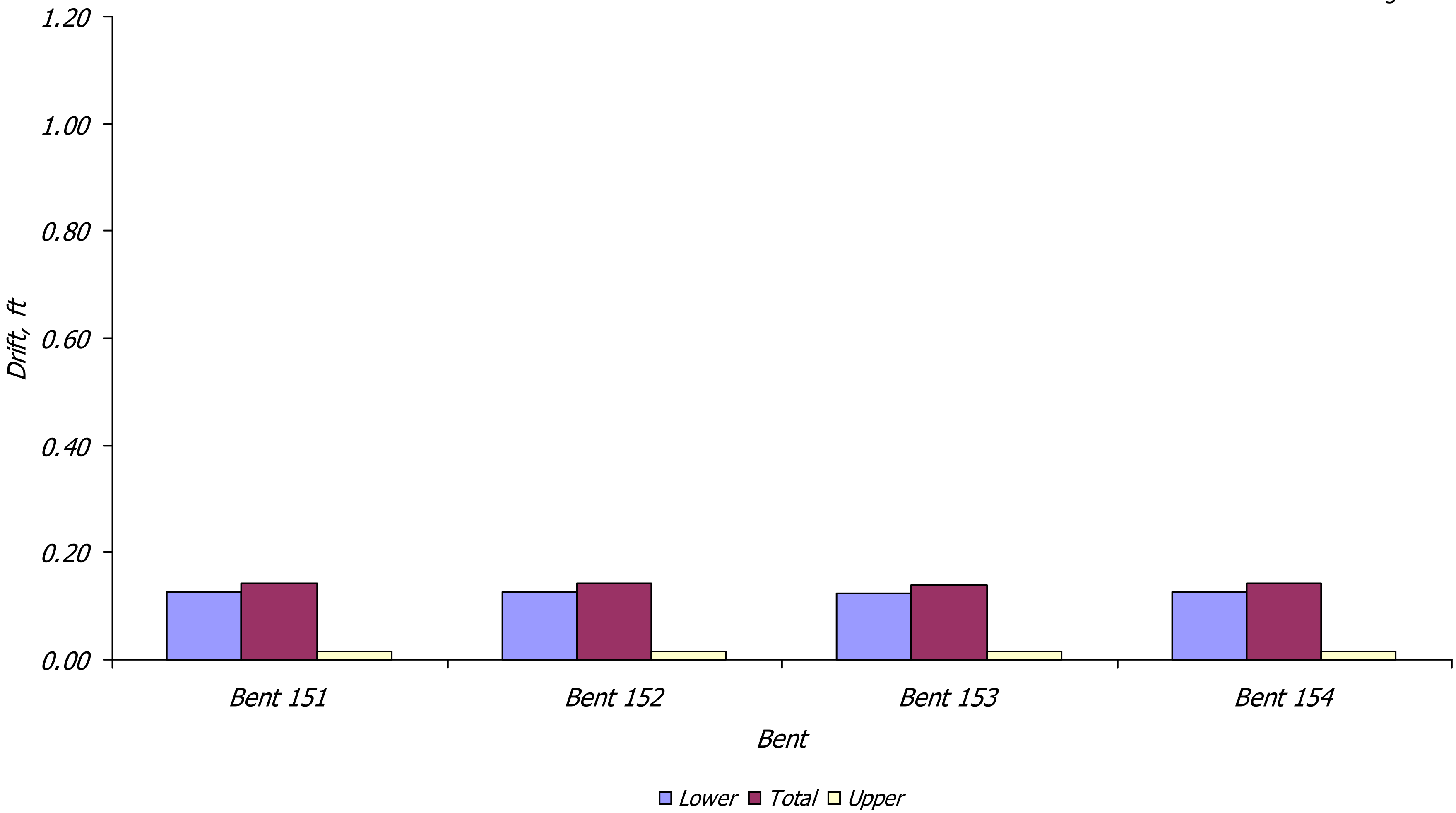

Figure 13a Drift of retrofitted structure, expected earthquake, longitudinal direction

Model Name:	gray.08	**Absolute Drifts**
Model Description:	Alaska Way Viaduct, Evaluation of Grays Proposal	
Model Variation:	expected earthquake	25 Jul 06 2:35 PM

Transverse

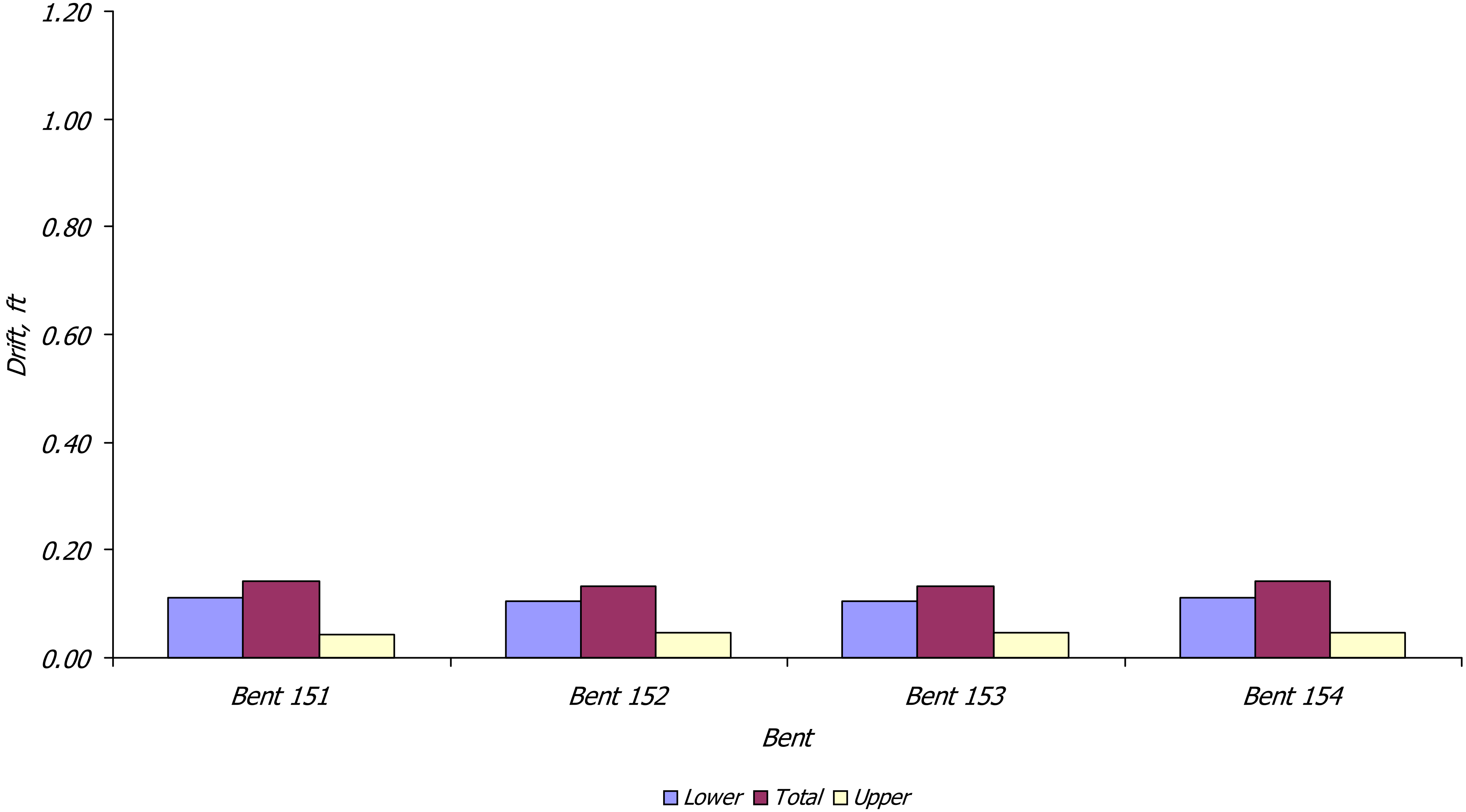

Figure 13b Drift of retrofitted structure, expected earthquake, transverse direction

Model Name:	gray.08	**Column Curvature Ductility Demand**
Model Description:	Alaska Way Viaduct, Evaluation of Grays Proposal	
Model Variation:	rare earthquake	25 Jul 06 2:44 PM

Longitudinal Direction

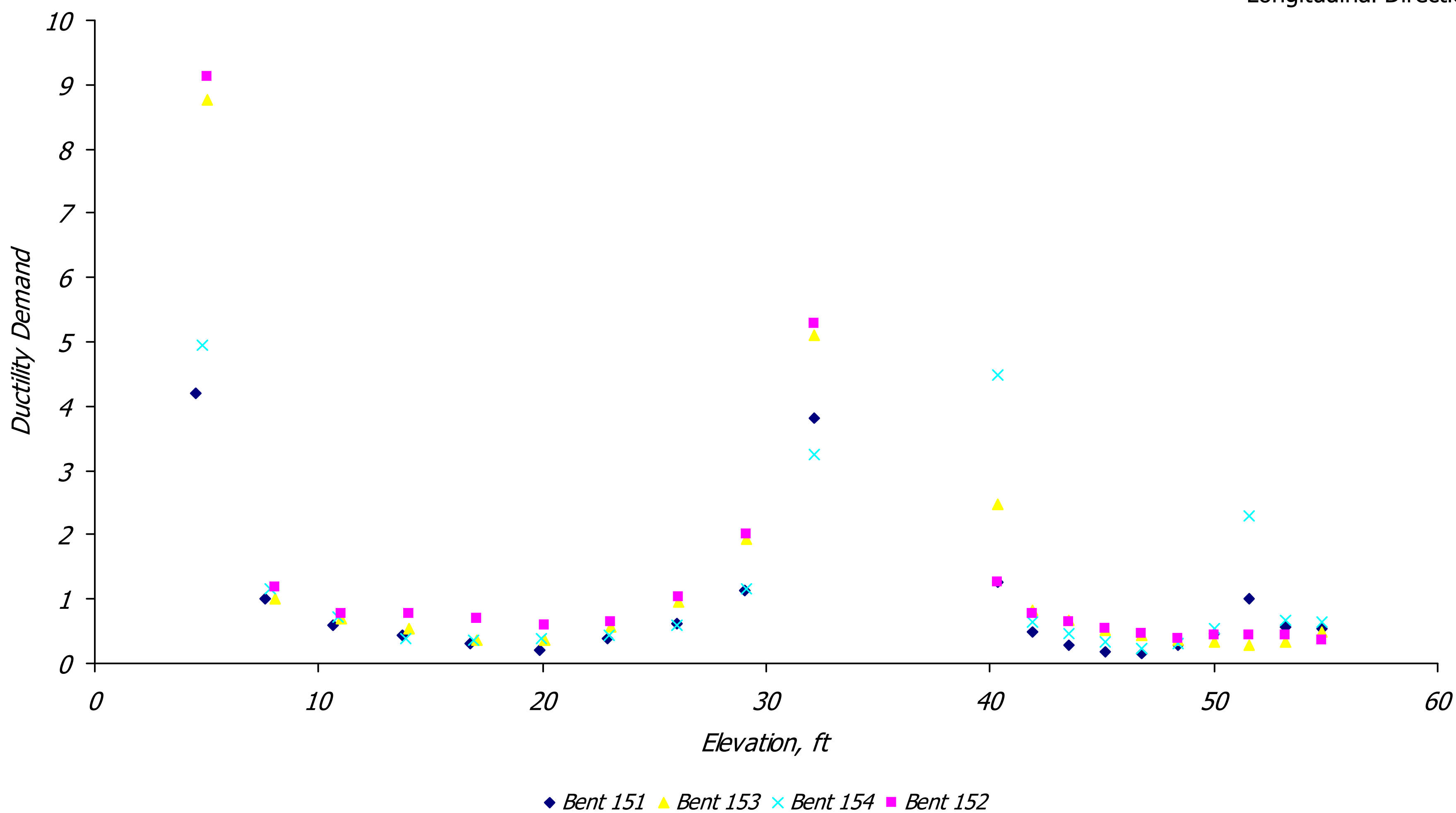

Figure 14a Column curvature ductility demand, retrofitted structure, rare earthquake, longitudinal direction

Model Name: gray.08

Column Curvature Ductility Demand

Model Description: Alaska Way Viaduct, Evaluation of Grays Proposal

Model Variation: rare earthquake 25 Jul 06 2:44 PM

Transverse Direction

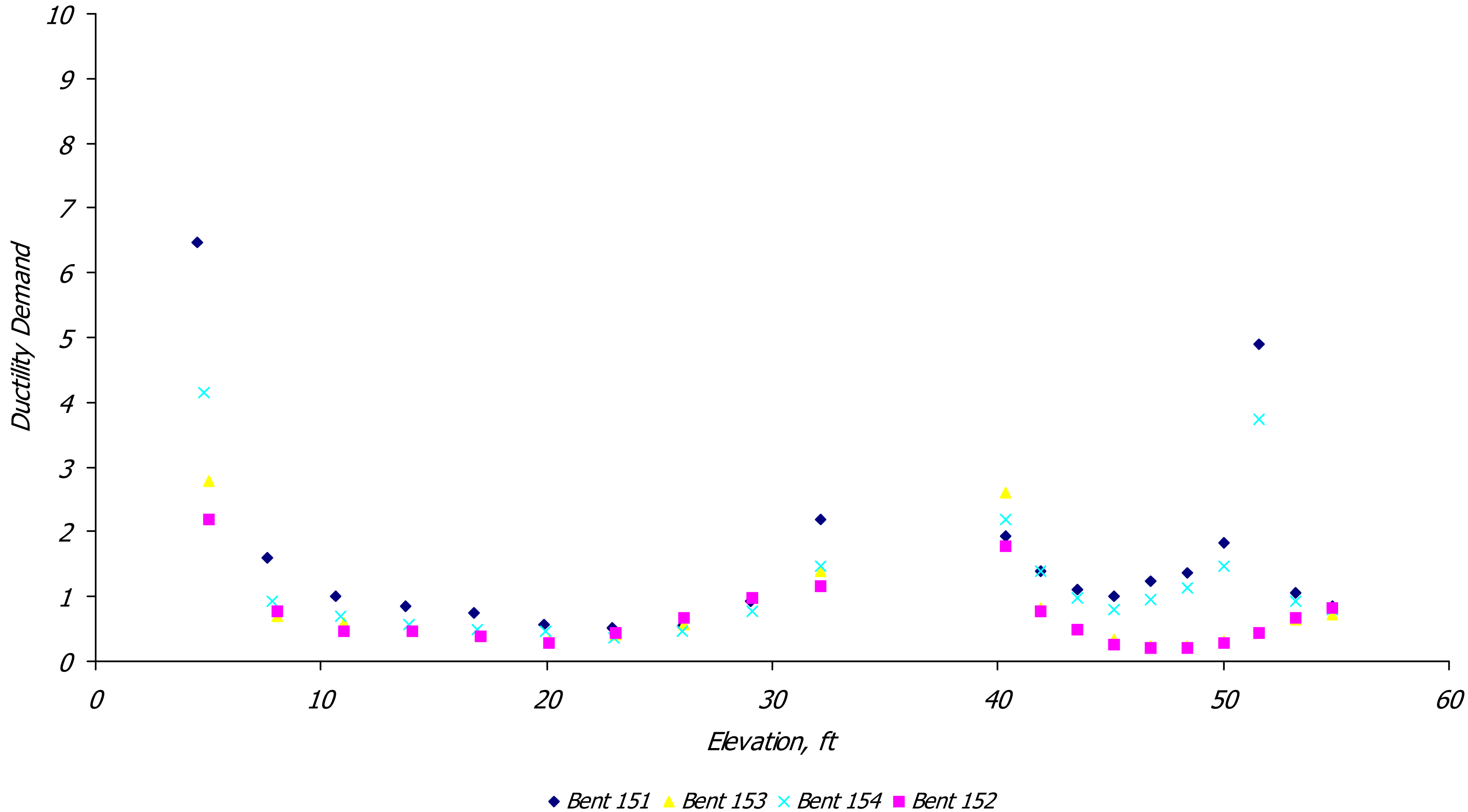

Figure 14b Column curvature ductility demand, retrofitted structure, rare earthquake, transverse direction

Model Name: gray.08

Model Description: Alaska Way Viaduct, Evaluation of Grays Proposal

Model Variation: rare earthquake

End Column Curvature

25 Jul 06 3:42 PM

Section: Columns.End

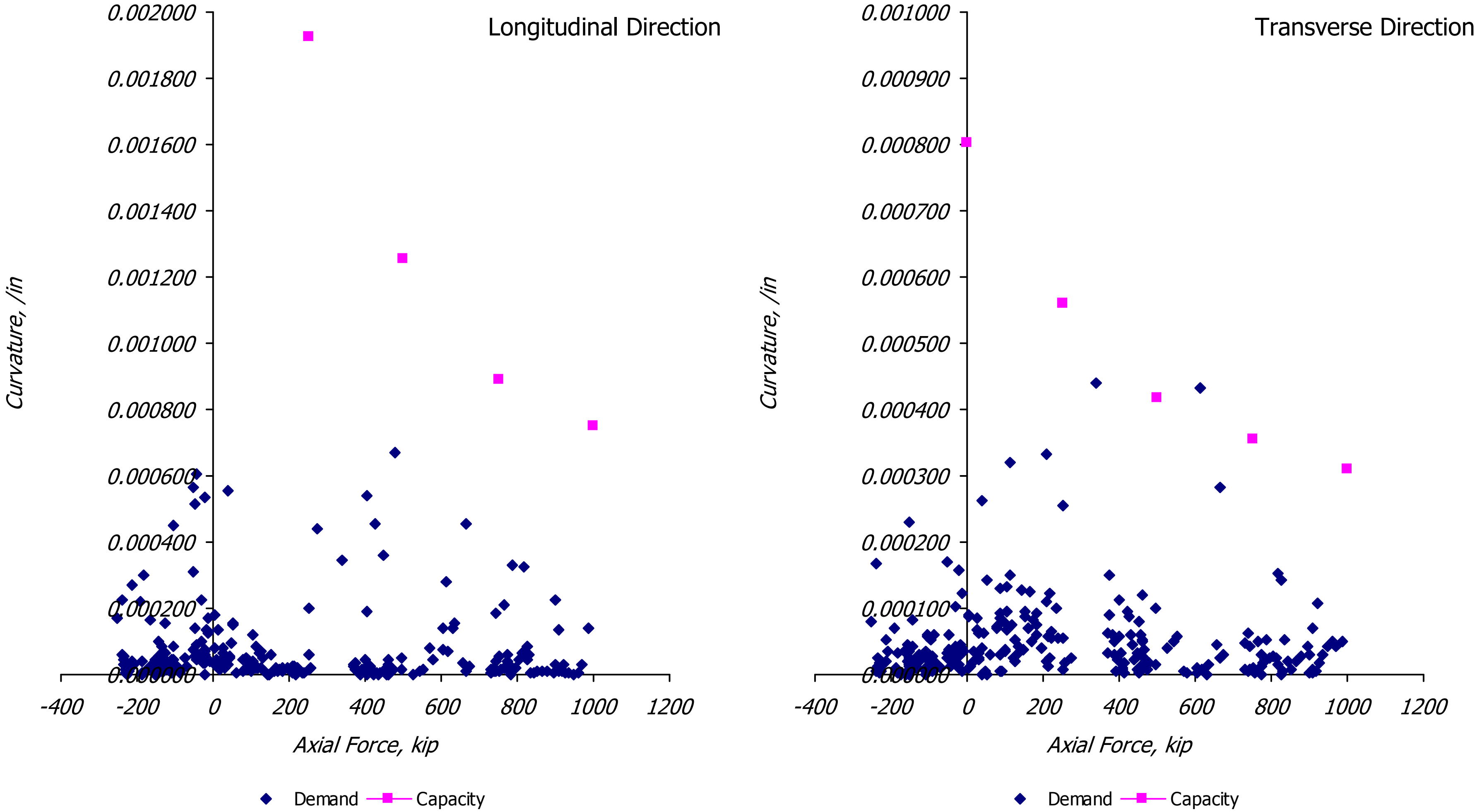

Figure 15 Column curvature versus axial force, retrofitted structure, rare earthquake, end bents

Model Name: gray.08

End Column Curvature

Model Description: Alaska Way Viaduct, Evaluation of Grays Proposal

Model Variation: rare earthquake

25 Jul 06 3:42 PM

Section: Columns.End.B.16

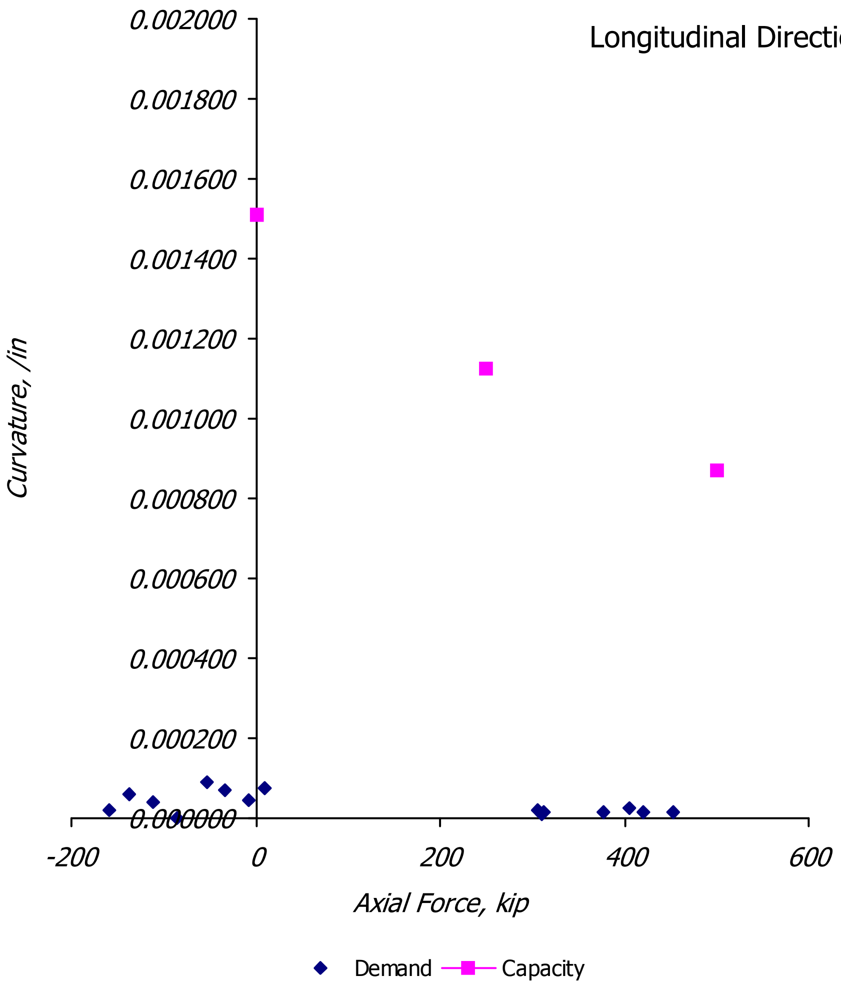

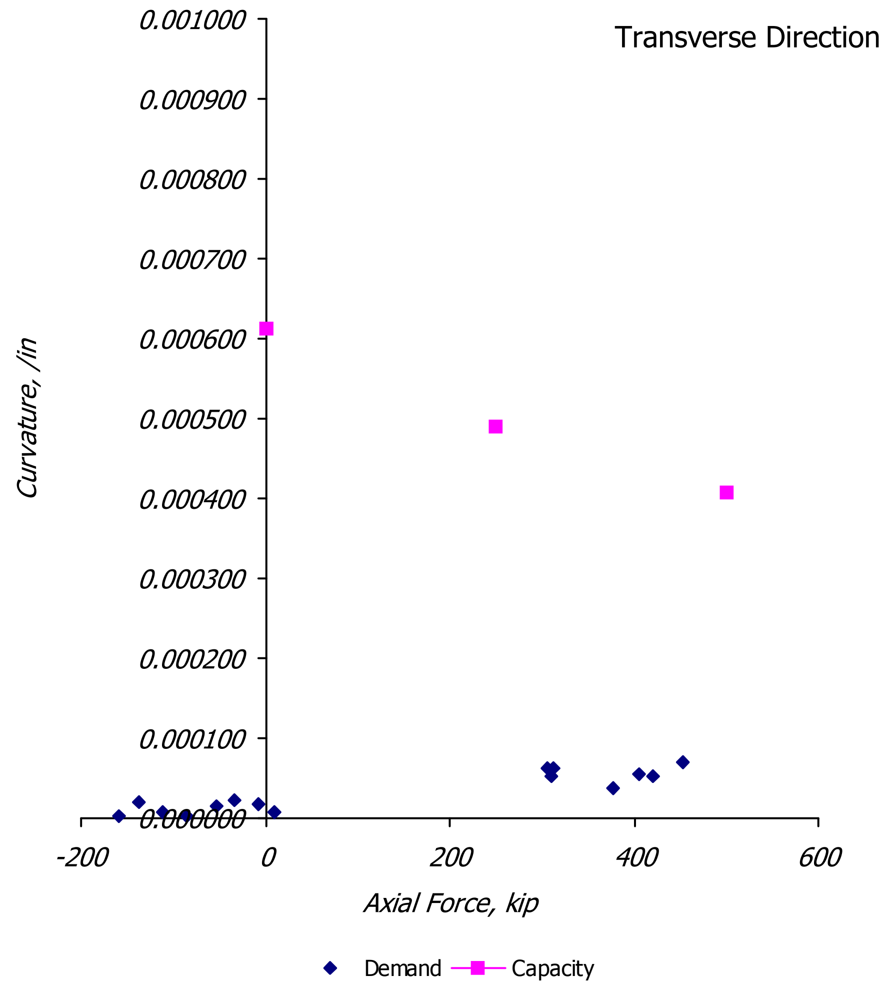

Figure 15 (cont.) Column curvature versus axial force, retrofitted structure, rare earthquake, end bents

Model Name: gray.08

Model Description: Alaska Way Viaduct, Evaluation of Grays Proposal

Model Variation: rare earthquake

End Column Curvature

25 Jul 06 3:42 PM

Section: Columns.End.B.20

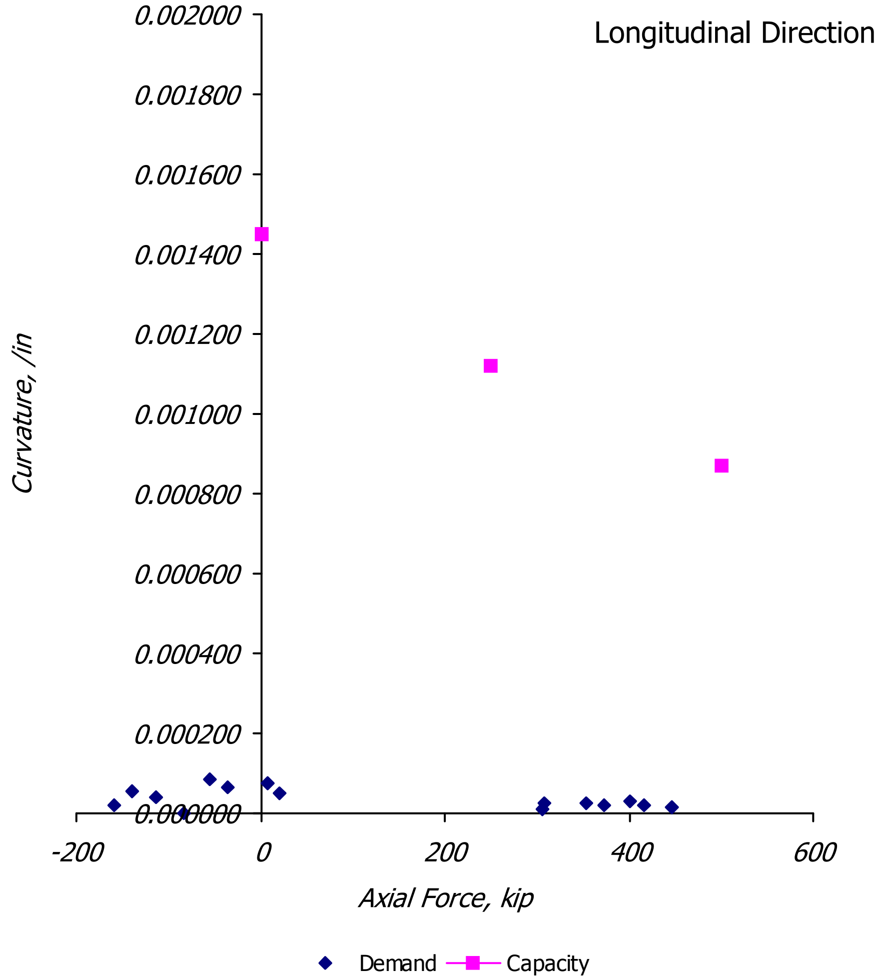

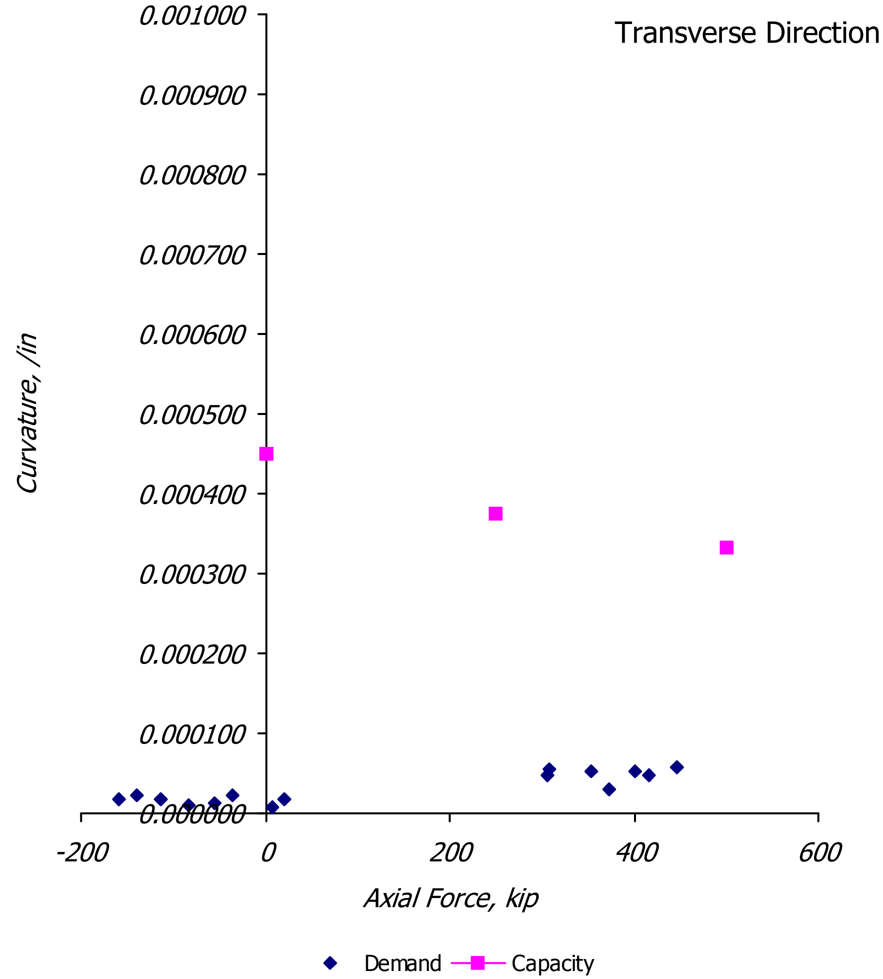

Figure 15 (cont.) Column curvature versus axial force, retrofitted structure, rare earthquake, end bents

Model Name: gray.08

Middle Column Curvature

Model Description: Alaska Way Viaduct, Evaluation of Grays Proposal

Model Variation: rare earthquake

25 Jul 06 3:45 PM

Section: Columns.Middle

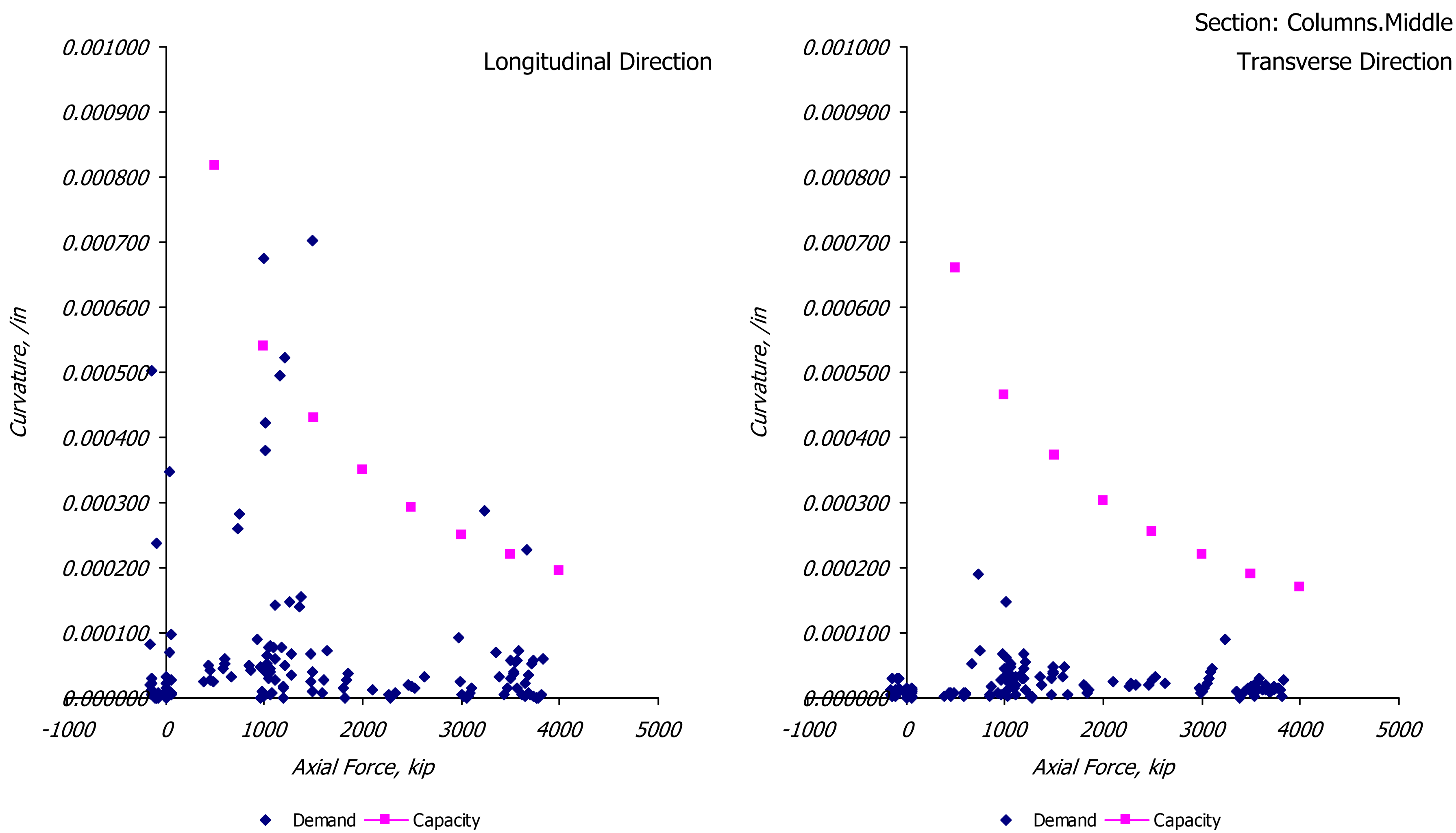

Figure 16 Column curvature versus axial force, retrofitted structure, rare earthquake, middle bents

Model Name:	gray.08	**Middle Column Curvature**
Model Description:	Alaska Way Viaduct, Evaluation of Grays Proposal	
Model Variation:	rare earthquake	25 Jul 06 3:45 PM

Section: Columns.Middle.A

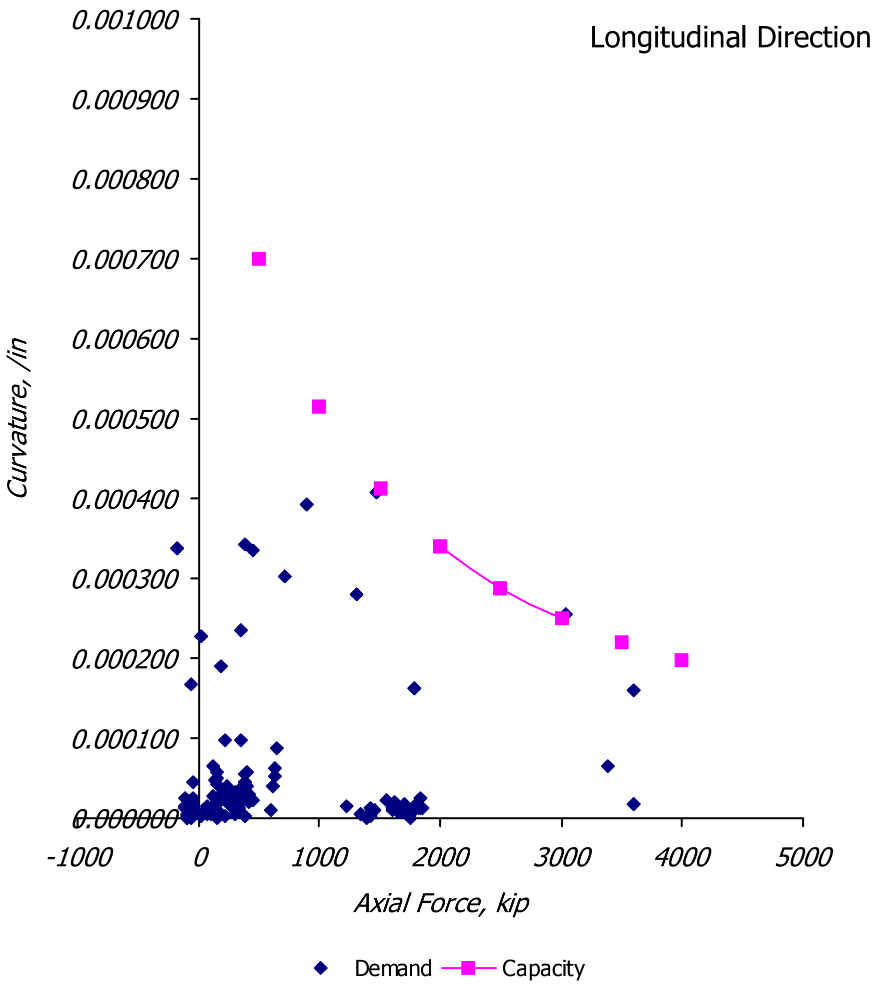

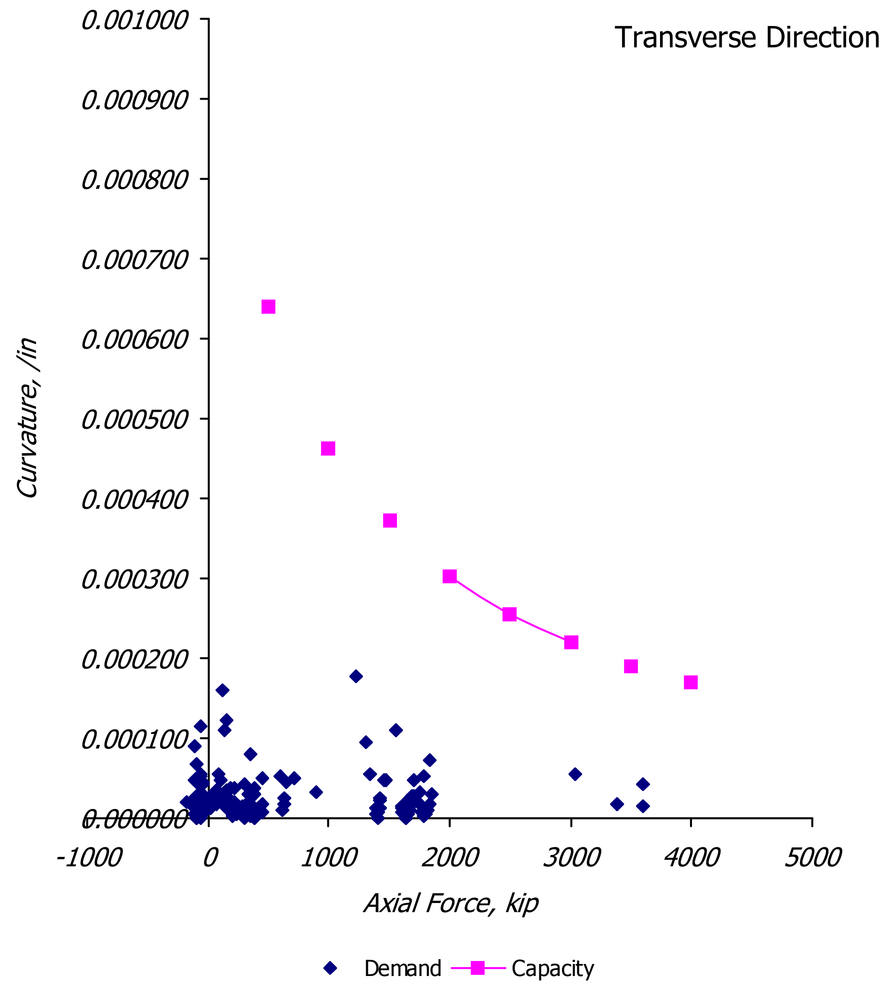

Figure 16 (cont.) Column curvature versus axial force, retrofitted structure, rare earthquake, middle bents

Model Name: gray.08

Middle Column Curvature

Model Description: Alaska Way Viaduct, Evaluation of Grays Proposal

Model Variation: rare earthquake

25 Jul 06 3:45 PM

Section: Columns.Middle.F

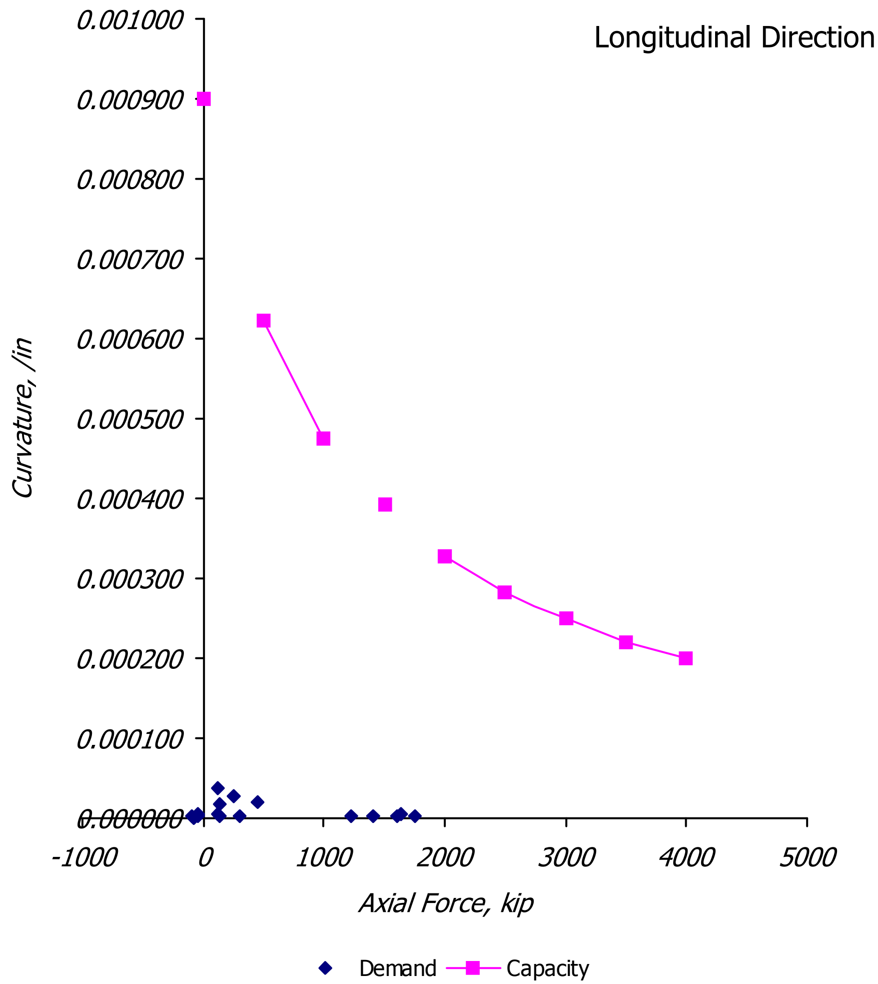

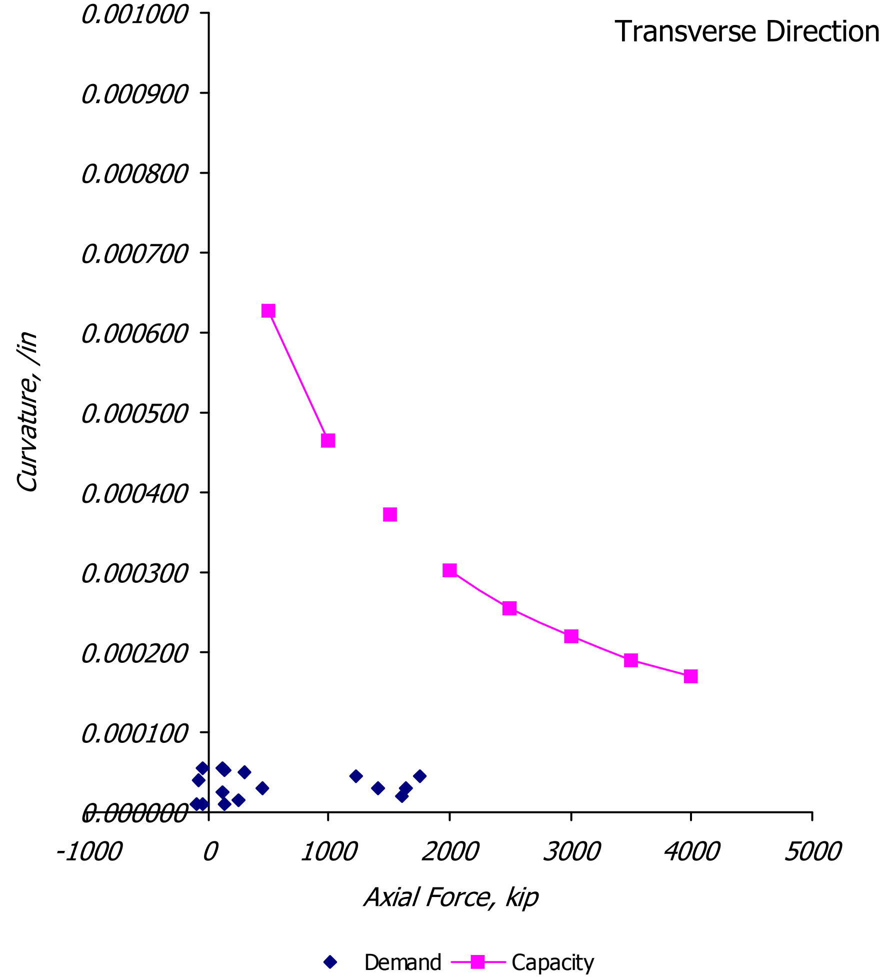

Figure 16 (cont.) Column curvature versus axial force, retrofitted structure, rare earthquake, middle bents

Model Name: gray.08

Column Curvature Ductility Demand

Model Description: Alaska Way Viaduct, Evaluation of Grays Proposal

Model Variation: design earthquake

25 Jul 06 2:46 PM

Longitudinal Direction

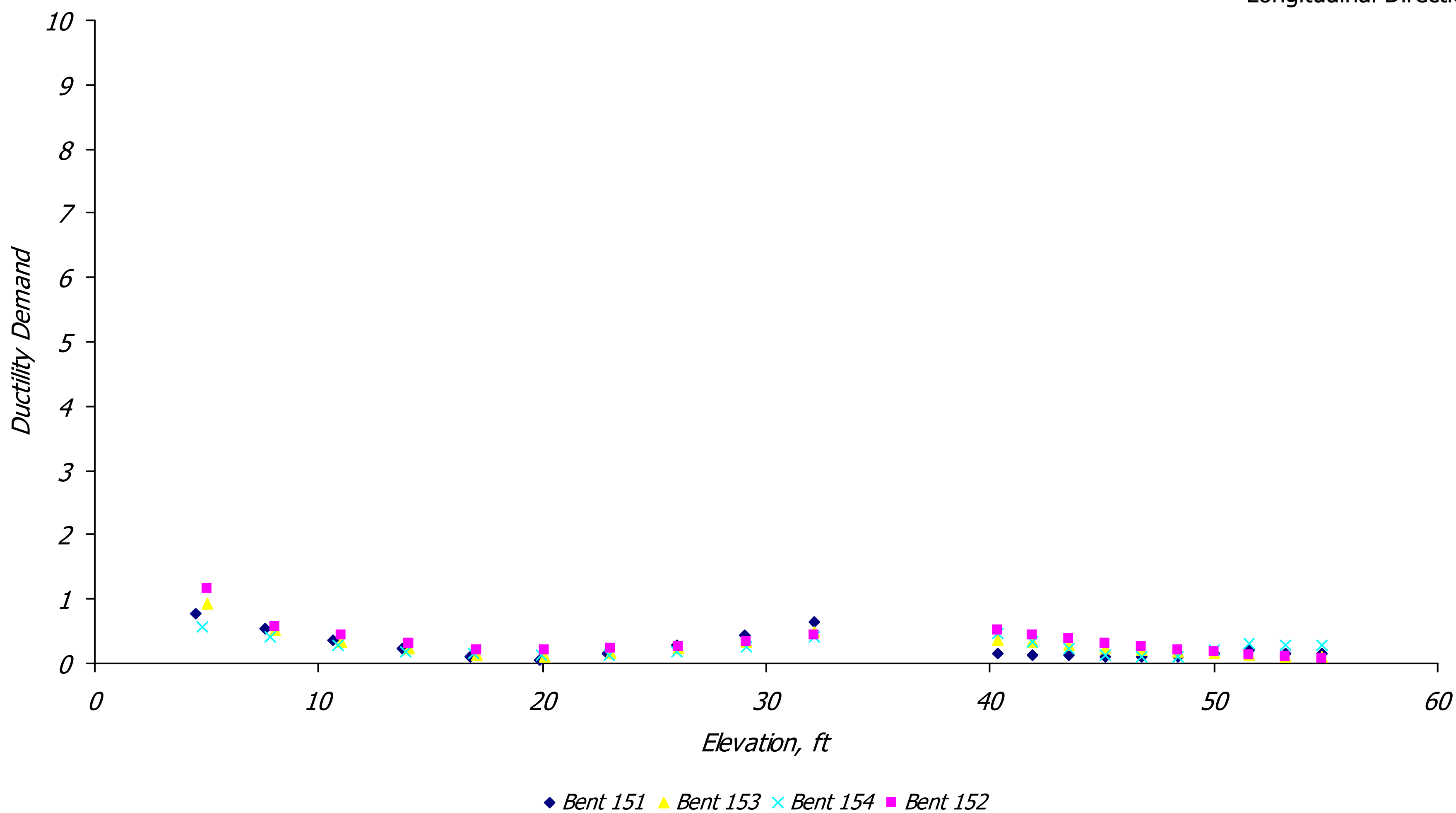

Figure 17a Column curvature ductility demand, retrofitted structure, design earthquake, longitudinal direction

Model Name: gray.08

Column Curvature Ductility Demand

Model Description: Alaska Way Viaduct, Evaluation of Grays Proposal

Model Variation: design earthquake 25 Jul 06 2:46 PM

Transverse Direction

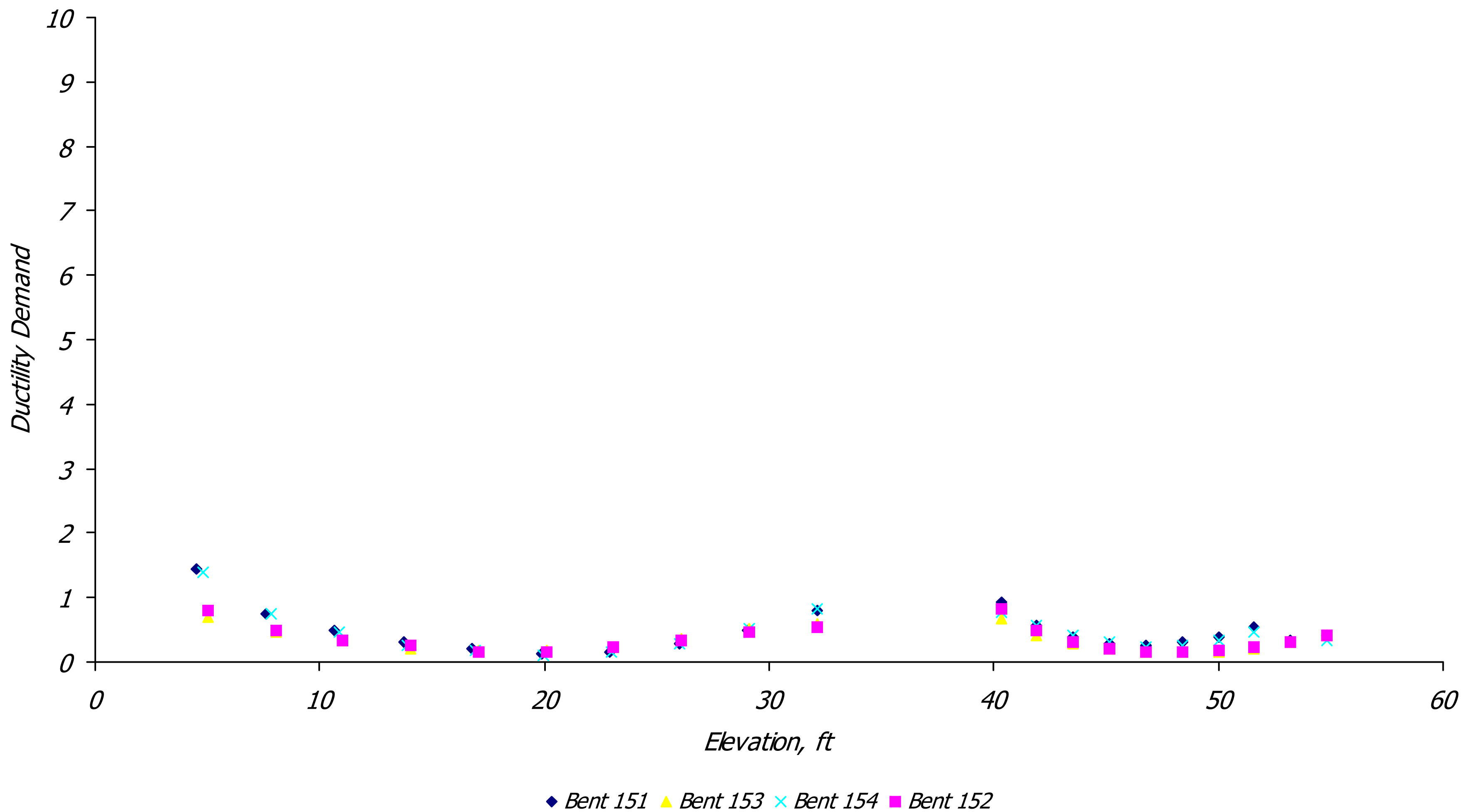

Figure 17b Column curvature ductility demand, retrofitted structure, design earthquake, transverse direction

Model Name: gray.08

Column Curvature Ductility Demand

Model Description: Alaska Way Viaduct, Evaluation of Grays Proposal

Model Variation: expected earthquake 25 Jul 06 2:47 PM

Longitudinal Direction

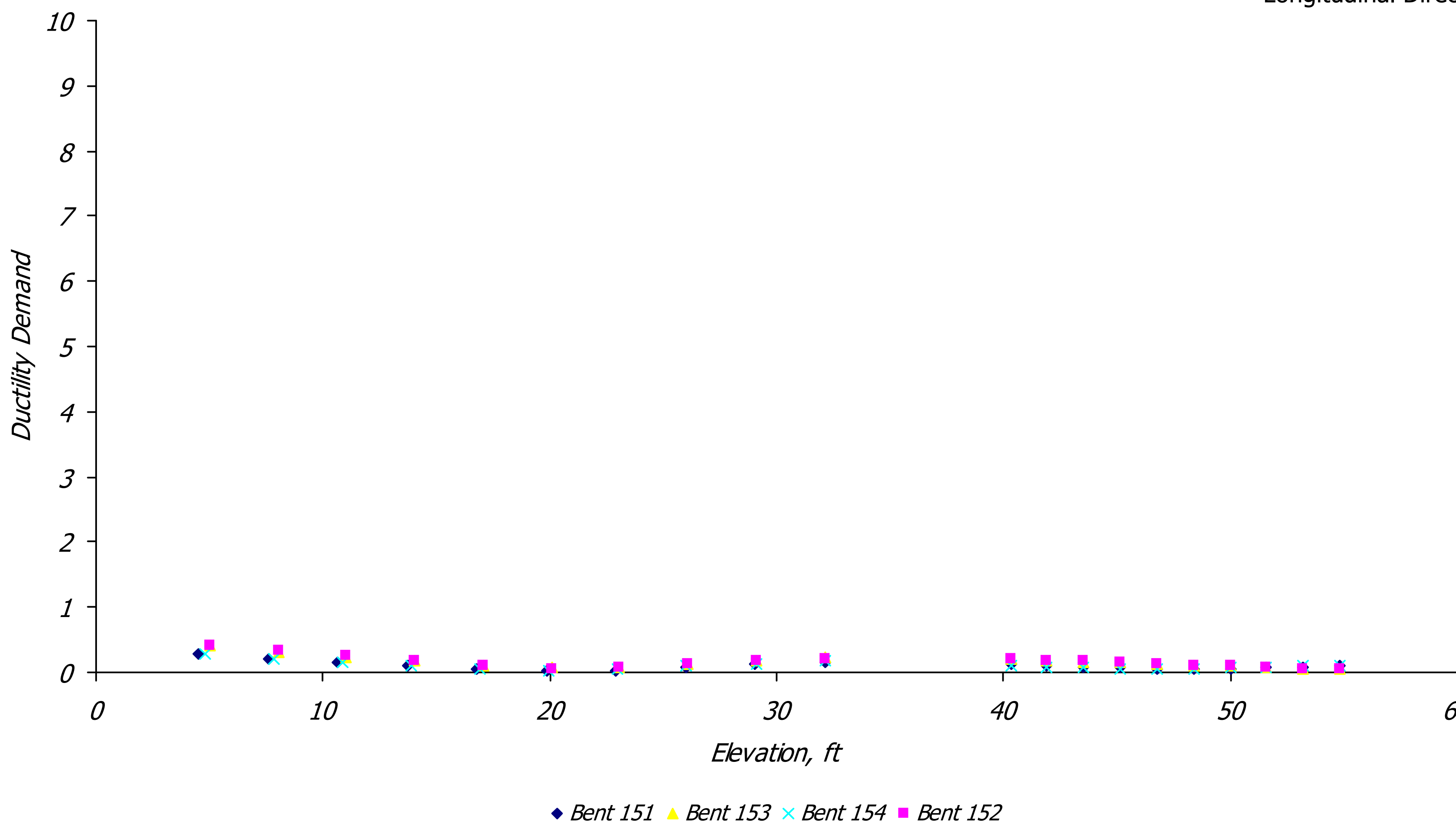

Figure 18a Column curvature ductility demand, retrofitted structure, expected earthquake, longitudinal direction

Model Name:	gray.08	**Column Curvature Ductility Demand**
Model Description:	Alaska Way Viaduct, Evaluation of Grays Proposal	
Model Variation:	expected earthquake	25 Jul 06 2:47 PM

Transverse Direction

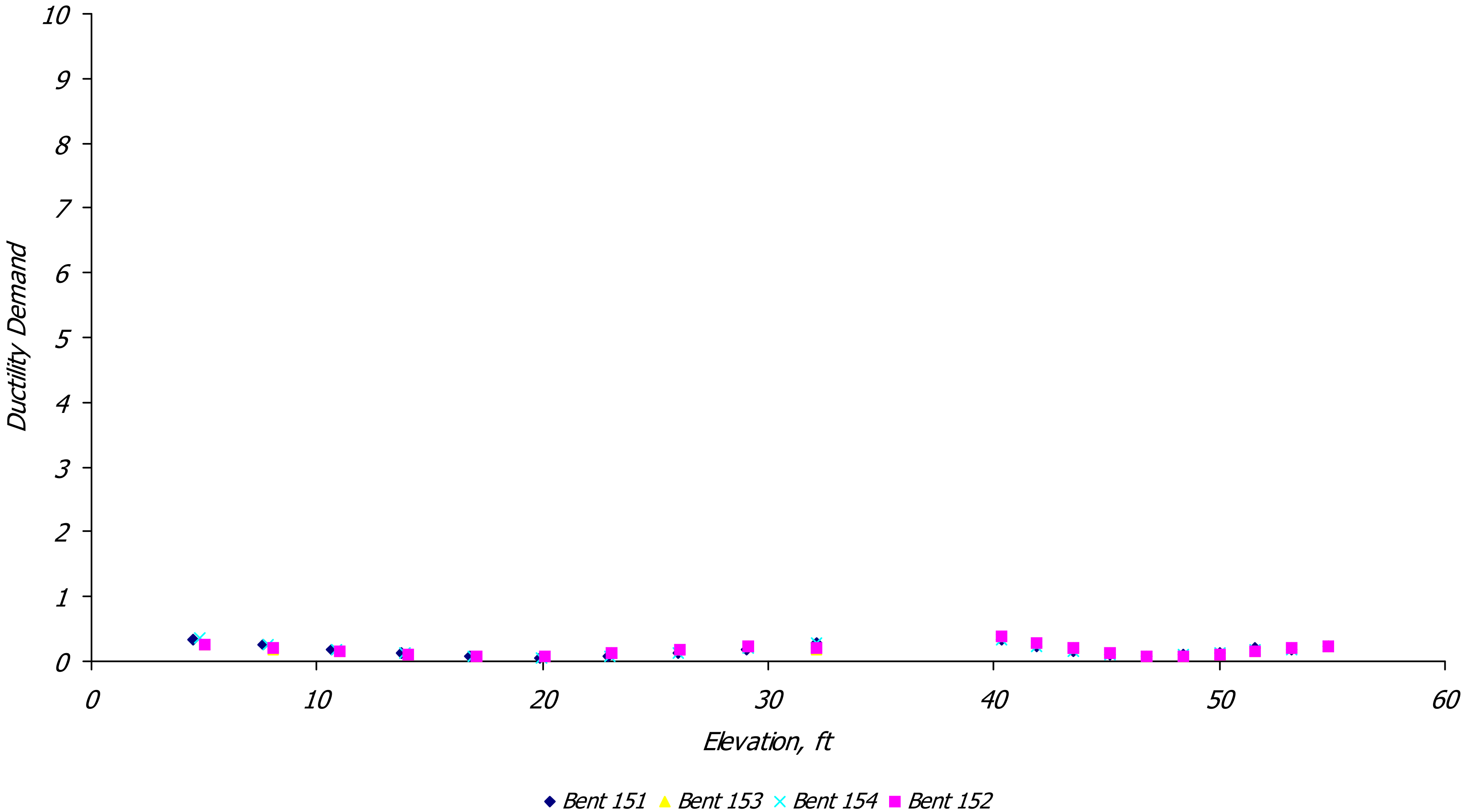

Figure 18b Column curvature ductility demand, retrofitted structure, expected earthquake, transverse direction

Model Name: gray.08

Floorbeam Curvature Ductility Demand

Model Description: Alaska Way Viaduct, Evaluation of Grays Proposal

Model Variation: rare earthquake

25 Jul 06 3:00 PM

Upper Level

Positive Curvature

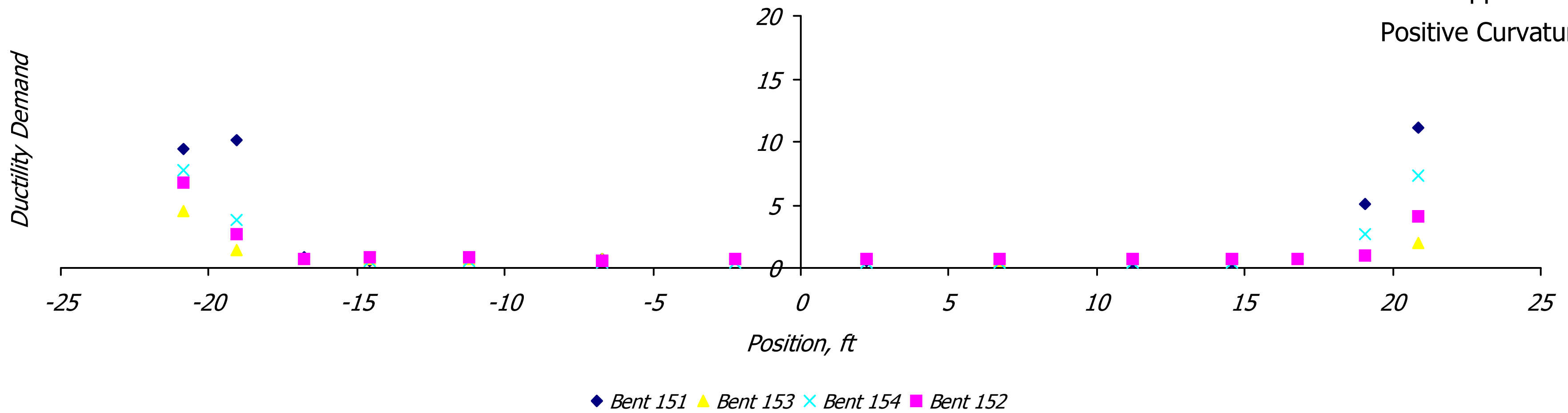

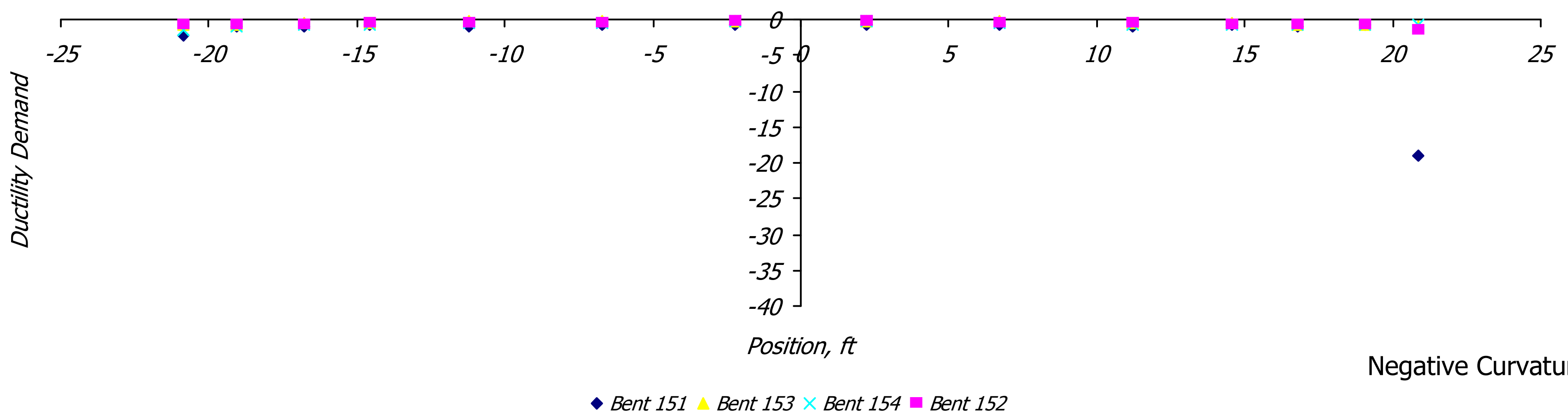

Negative Curvature

Figure 19a Floorbeam curvature ductility demand, retrofitted structure, rare earthquake, upper level

Model Name:	gray.08	**Floorbeam Curvature Ductility Demand**
Model Description:	Alaska Way Viaduct, Evaluation of Grays Proposal	
Model Variation:	rare earthquake	25 Jul 06 3:00 PM

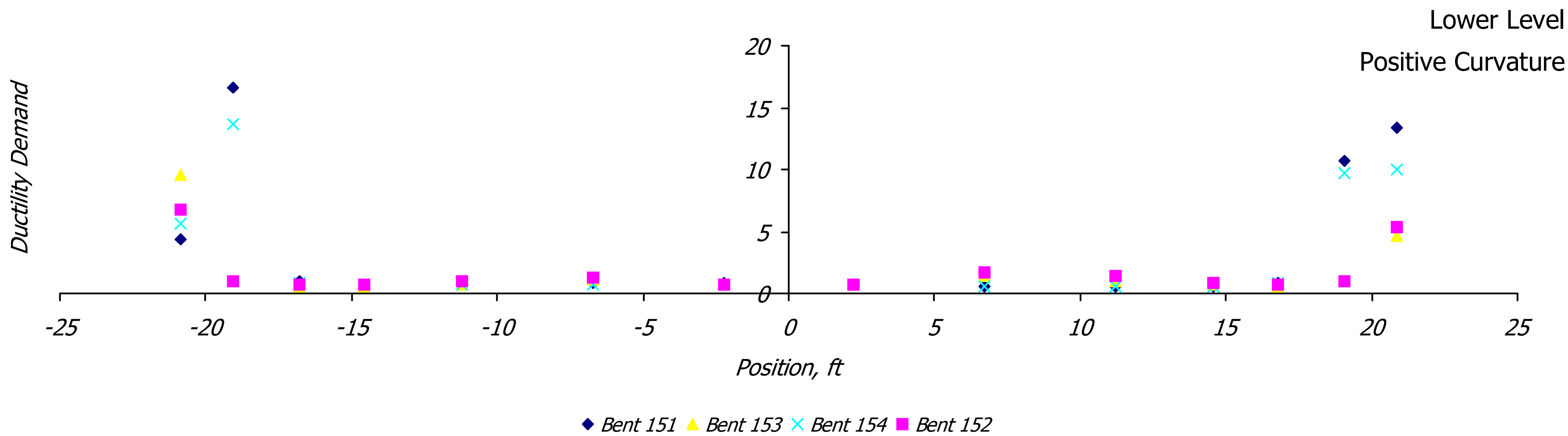

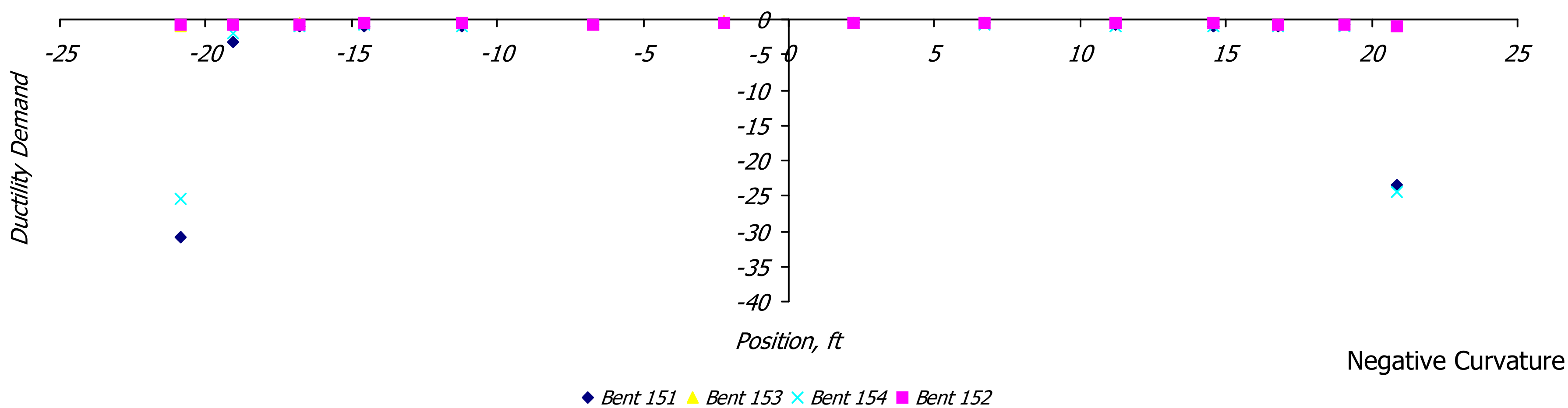

Figure 19b Floorbeam curvature ductility demand, retrofitted structure, rare earthquake, lower level

Model Name: gray.08

Floorbeam Curvature

Model Description: Alaska Way Viaduct, Evaluation of Grays Proposal

Model Variation: rare earthquake

25 Jul 06 3:39 PM

Upper Level

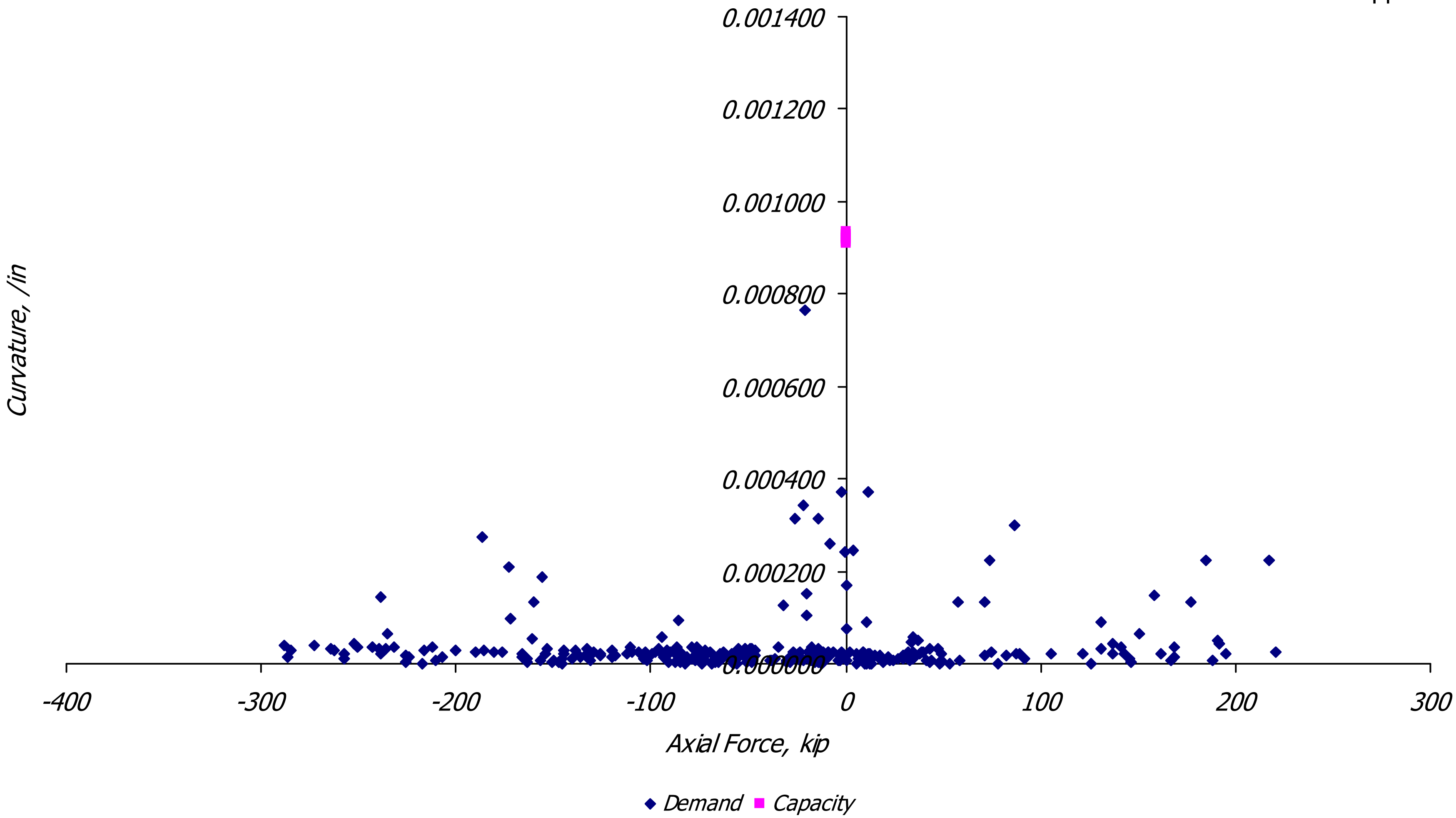

Figure 20a Floorbeam curvature versus axial force, retrofitted structure, rare earthquake, upper level

Model Name:	gray.08	**Floorbeam Curvature**
Model Description:	Alaska Way Viaduct, Evaluation of Grays Proposal	
Model Variation:	rare earthquake	25 Jul 06 3:39 PM

Lower Level

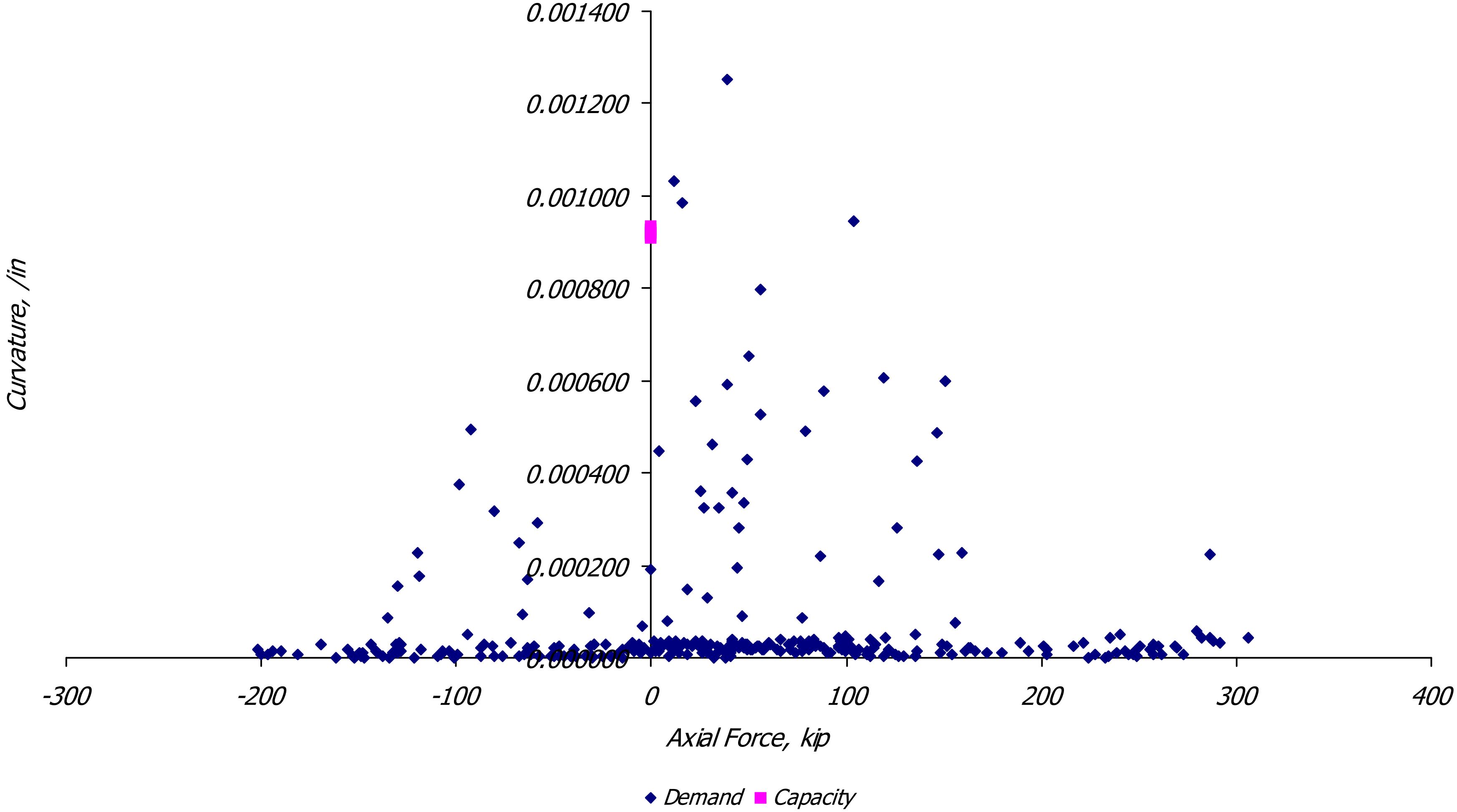

Figure 20b Floorbeam curvature versus axial force, retrofitted structure, rare earthquake, lower level

Model Name: gray.08

Floorbeam Curvature Ductility Demand

Model Description: Alaska Way Viaduct, Evaluation of Grays Proposal

Model Variation: design earthquake

25 Jul 06 3:03 PM

Upper Level

Positive Curvature

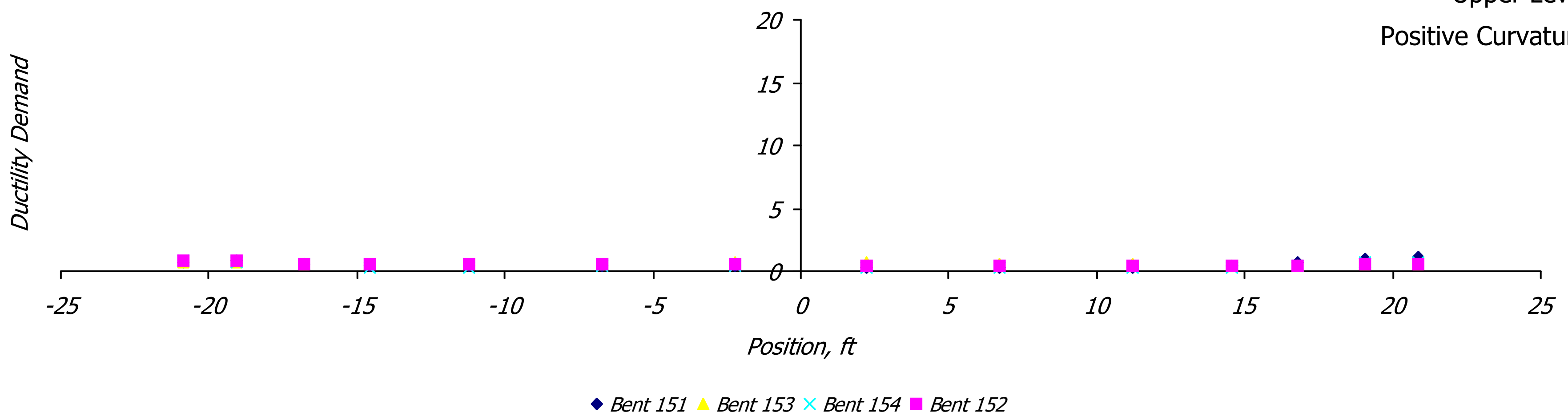

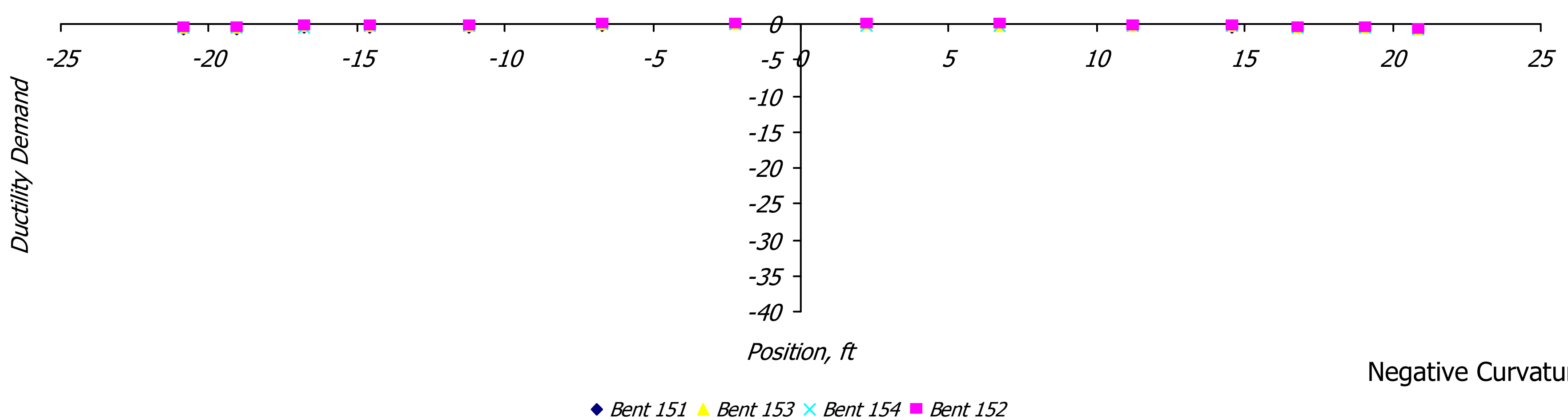

Negative Curvature

Figure 21a Floorbeam curvature ductility demand, retrofitted structure, design earthquake, upper level

Model Name: gray.08

Model Description: Alaska Way Viaduct, Evaluation of Grays Proposal

Model Variation: design earthquake

Floorbeam Curvature Ductility Demand

25 Jul 06 3:03 PM

Lower Level

Positive Curvature

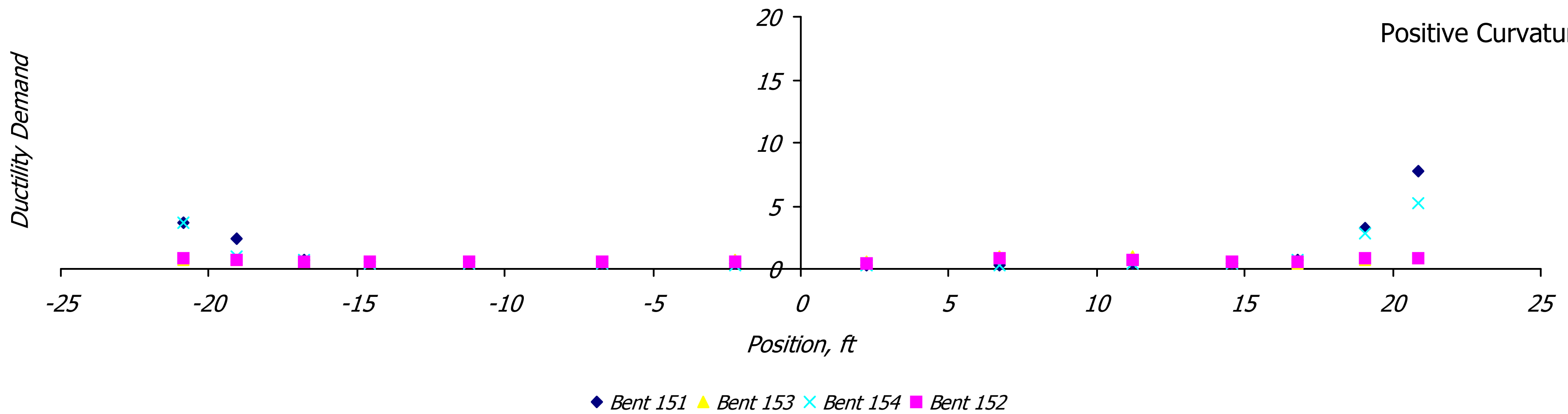

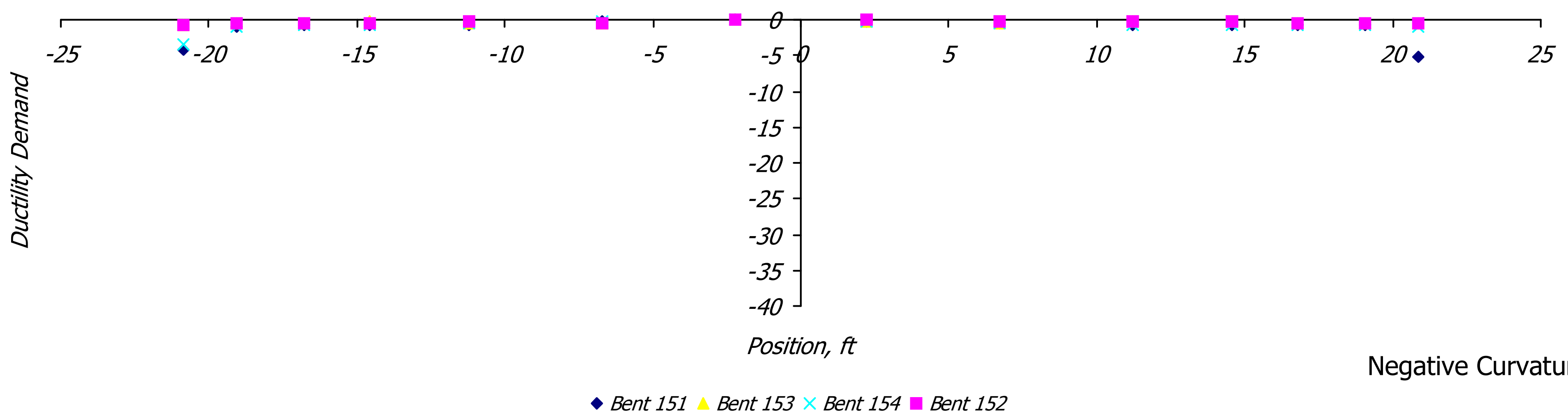

Negative Curvature

Figure 21b Floorbeam curvature ductility demand, retrofitted structure, design earthquake, lower level

Model Name: gray.08

Floorbeam Curvature Ductility Demand

Model Description: Alaska Way Viaduct, Evaluation of Grays Proposal

Model Variation: expected earthquake 25 Jul 06 3:05 PM

Upper Level

Positive Curvature

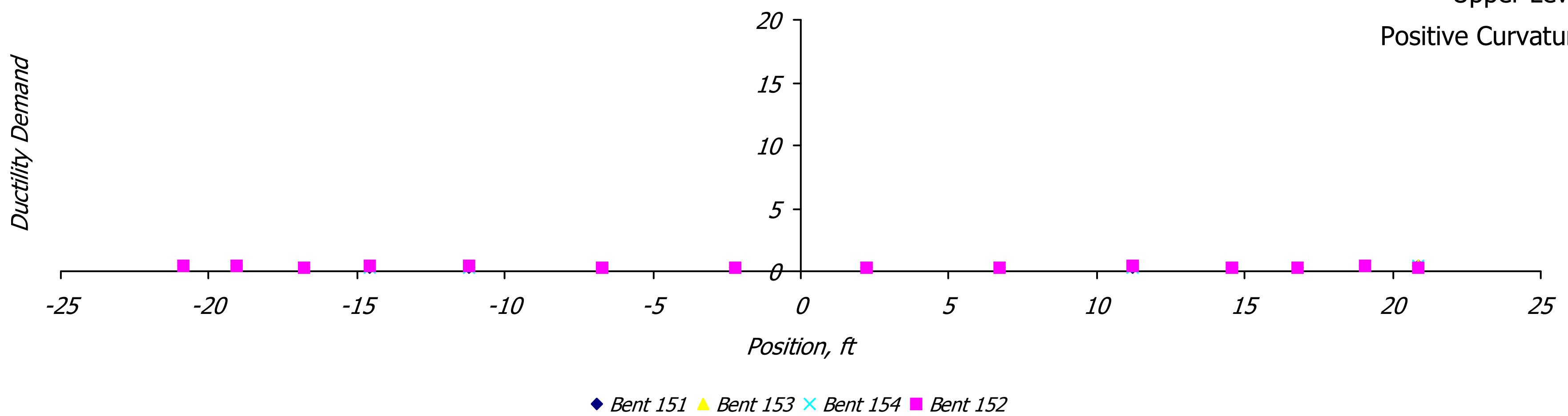

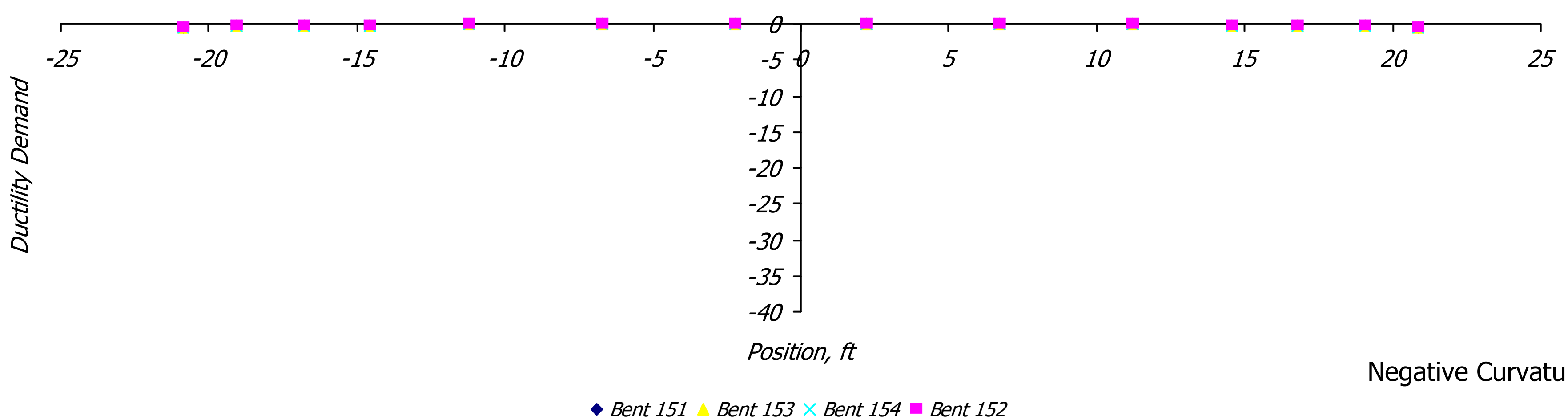

Negative Curvature

Figure 22a Floorbeam curvature ductility demand, retrofitted structure, expected earthquake, upper level

Model Name: gray.08

Floorbeam Curvature Ductility Demand

Model Description: Alaska Way Viaduct, Evaluation of Grays Proposal

Model Variation: expected earthquake

25 Jul 06 3:05 PM

Lower Level

Positive Curvature

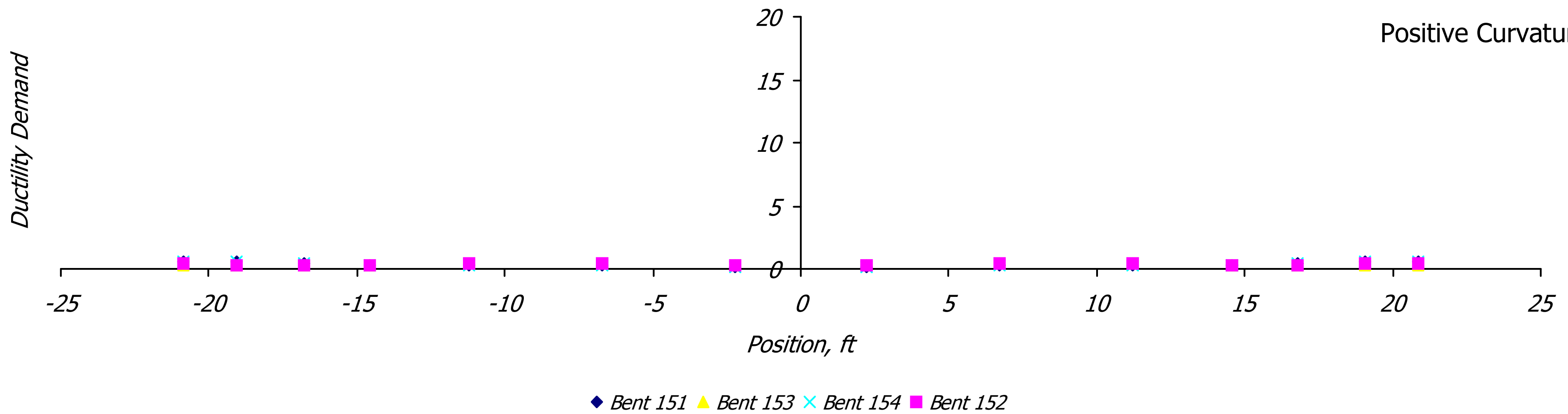

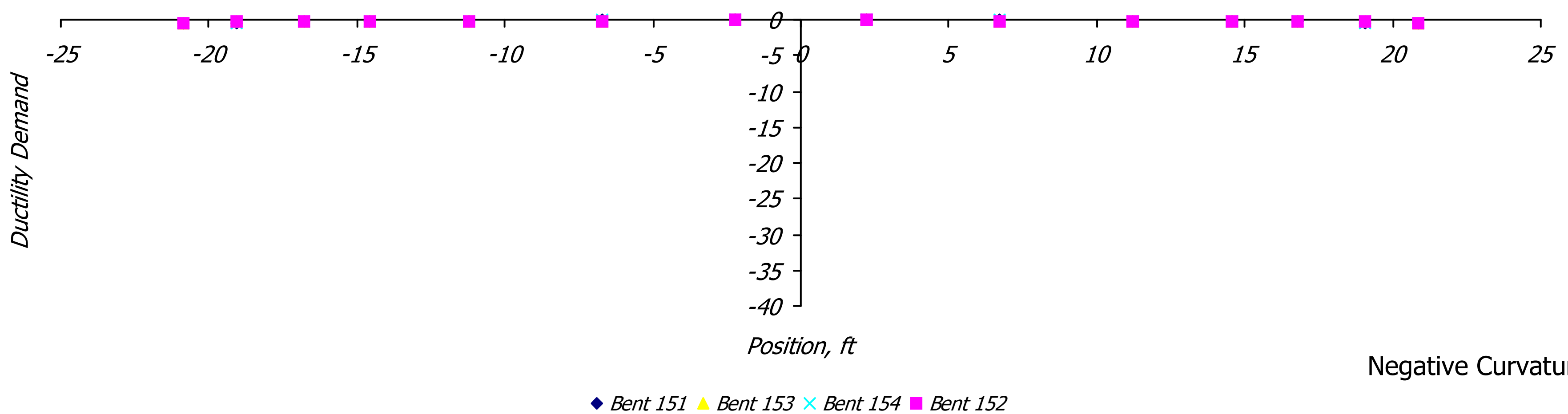

Negative Curvature

Figure 22b Floorbeam curvature ductility demand, retrofitted structure, expected earthquake, lower level

Model Name: gray.08

Girder Curvature Ductility Demand

Model Description: Alaska Way Viaduct, Evaluation of Grays Proposal

Model Variation: rare earthquake

25 Jul 06 3:32 PM

Upper Level

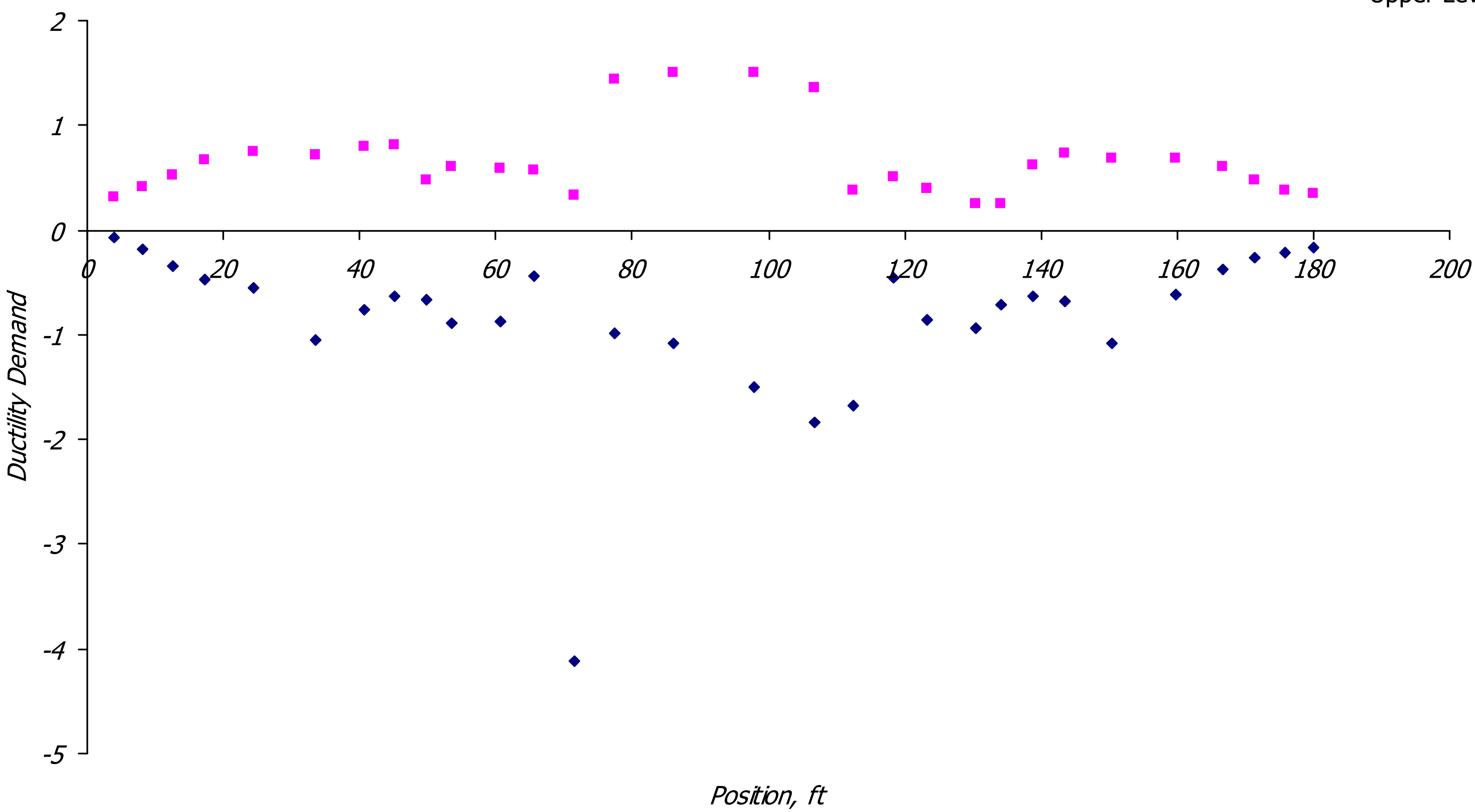

Figure 23a Girder curvature ductility demand, retrofitted structure, rare earthquake, upper level

Model Name: gray.08

Girder Curvature Ductility Demand

Model Description: Alaska Way Viaduct, Evaluation of Grays Proposal

Model Variation: rare earthquake

25 Jul 06 3:32 PM

Lower Level

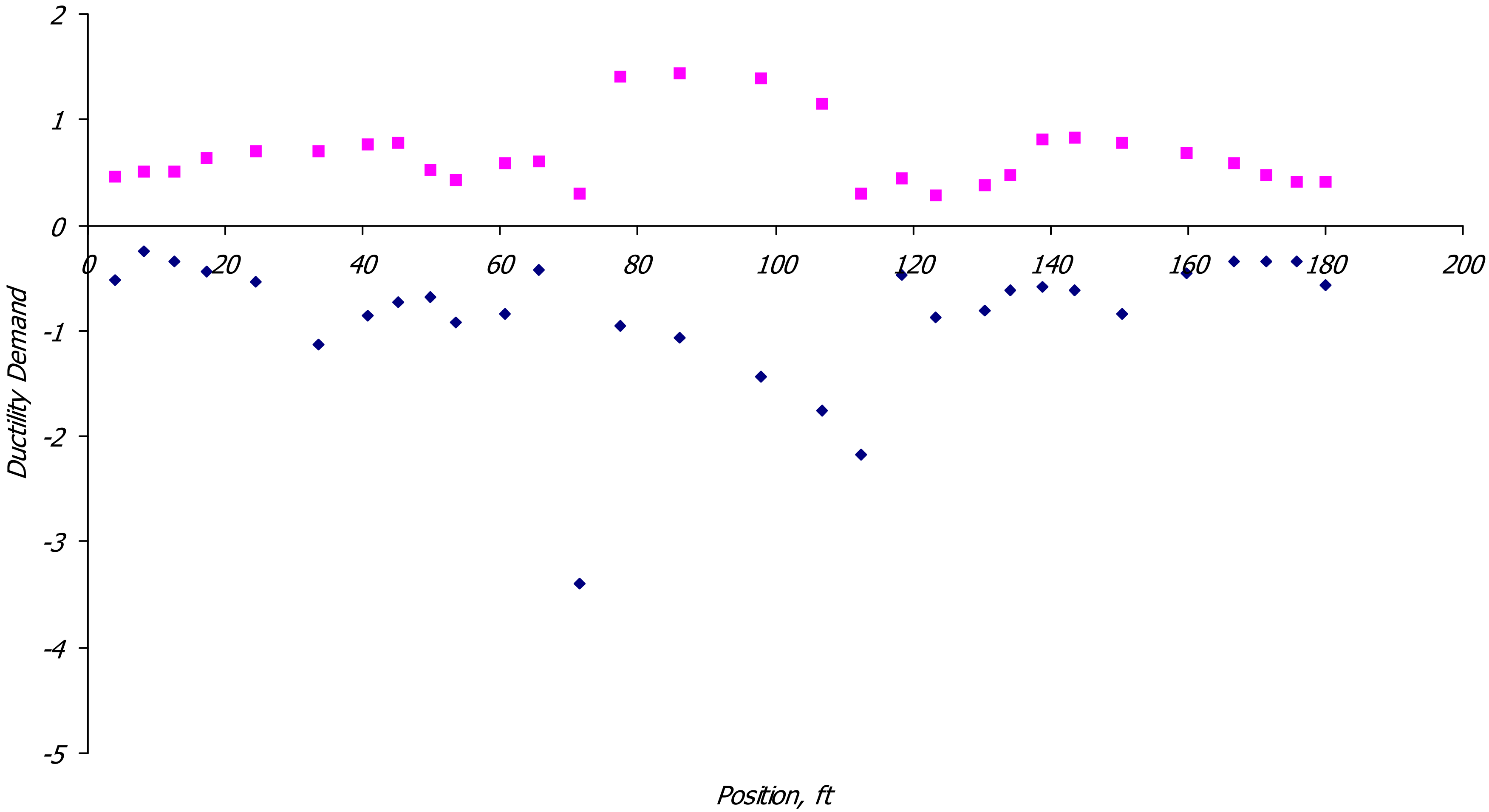

Figure 23b Girder curvature ductility demand, retrofitted structure, rare earthquake, lower level

Model Name:	gray.08	**Girder Curvature Ductility Demand**
Model Description:	Alaska Way Viaduct, Evaluation of Grays Proposal	
Model Variation:	design earthquake	25 Jul 06 3:34 PM

Upper Level

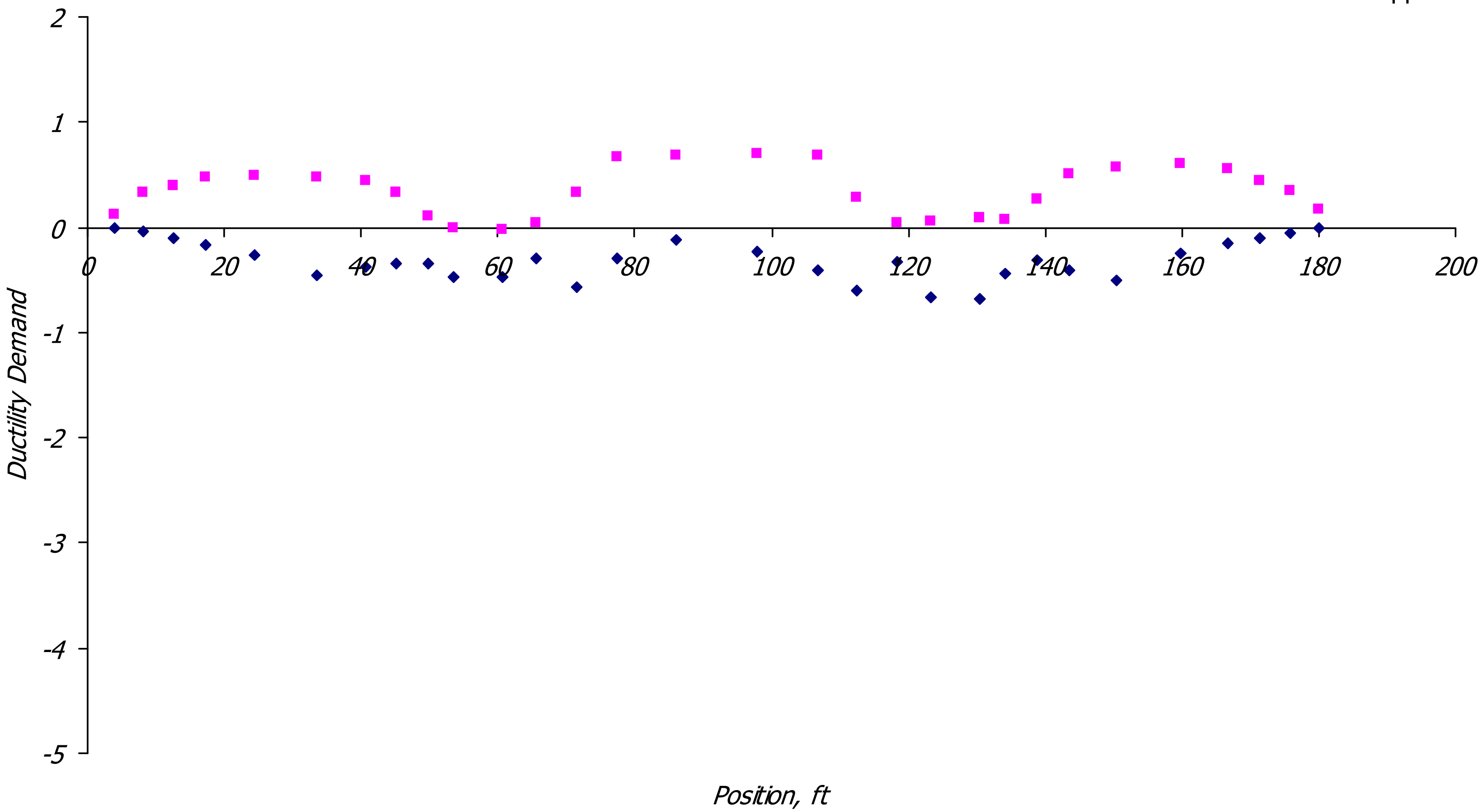

Figure 24a Girder curvature ductility demand, retrofitted structure, design earthquake, upper level

Model Name:	gray.08	**Girder Curvature Ductility Demand**
Model Description:	Alaska Way Viaduct, Evaluation of Grays Proposal	
Model Variation:	design earthquake	25 Jul 06 3:34 PM

Lower Level

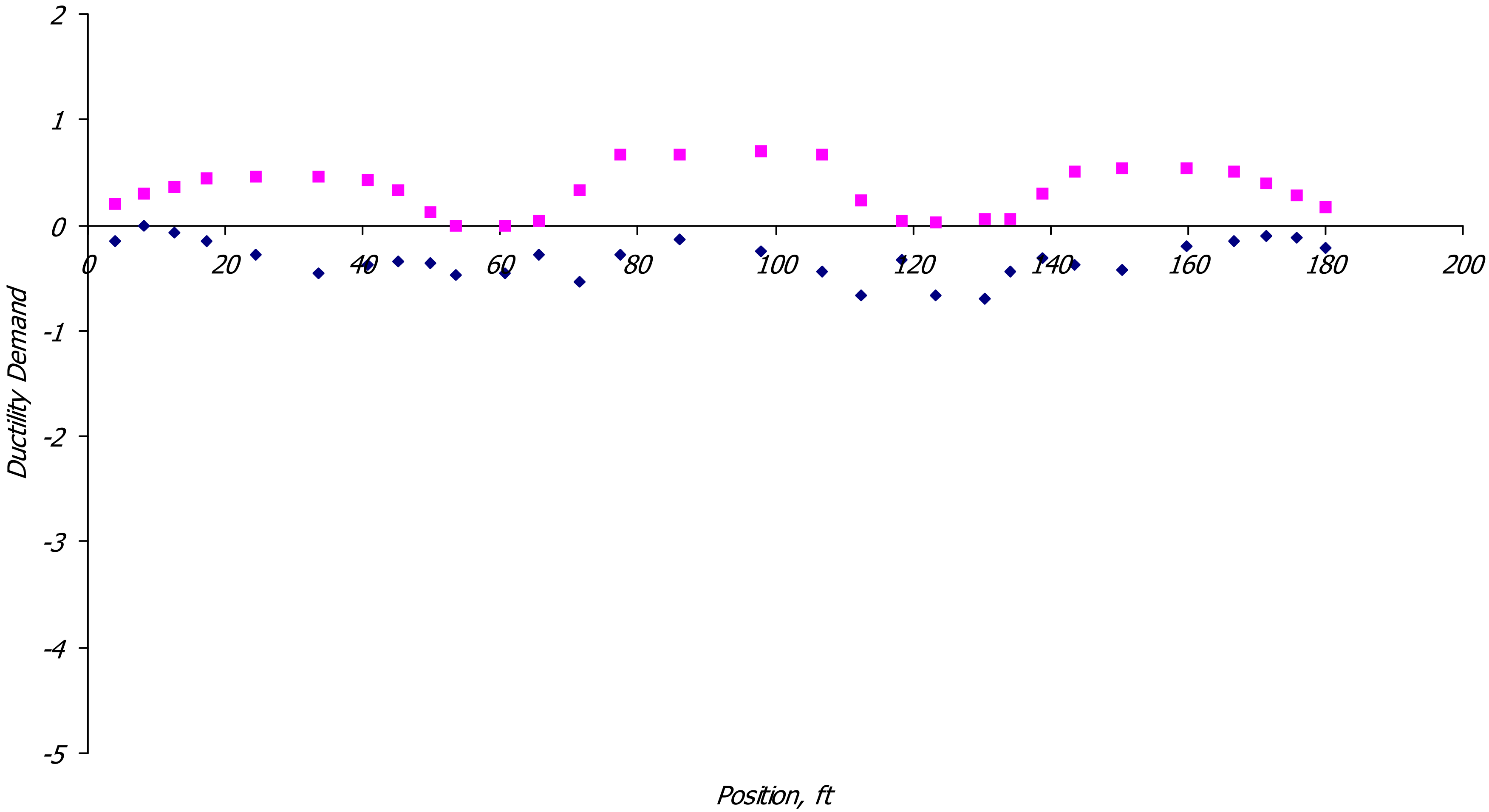

Figure 24b Girder curvature ductility demand, retrofitted structure, design earthquake, lower level

Model Name: gray.08

Auxiliary Frame Forces

Model Description: Alaska Way Viaduct, Evaluation of Grays Proposal

Model Variation: rare earthquake 24 Jul 06 6:59 PM

Frame	Position	Level	Tension	Compression	AxialD/C	D/C
Type	Beams					
Frame a	Beam	1	636	-763	0.19	0.47
Frame a	Beam	2	772	-939	0.36	0.76
Frame a	Beam	3	828	-855	0.32	0.63
Frame a	Beam	4	715	-664	0.17	0.41
Frame a	Gradebeam	0	97	-479	0.21	0.42
Frame d	Beam	1	769	-1051	0.27	0.78
Frame d	Beam	2	893	-1328	0.50	1.07
Frame d	Beam	3	1148	-1001	0.38	0.85
Frame d	Beam	4	968	-800	0.20	0.64
Frame d	Gradebeam	0	108	-548	0.25	0.61
Frame e	Gradebeam	0	419	-881	0.40	1.10
Frame e	Lower	1	479	-546	0.38	0.80
Frame e	Lower	2	63	-85	0.03	0.23
Frame e	Lower	3	62	-84	0.03	0.17
Frame e	Lower	4	609	-437	0.31	0.69
Frame e	Upper	2	495	-857	0.80	0.82
Frame e	Upper	3	786	-507	0.47	0.48
Frame f	Gradebeam	0	423	-1033	0.47	1.08
Frame f	Lower	1	436	-686	0.48	0.81
Frame f	Lower	2	50	-97	0.03	0.18
Frame f	Lower	3	50	-97	0.03	0.16
Frame f	Lower	4	614	-482	0.34	0.58
Frame f	Upper	2	619	-667	0.62	0.64
Frame f	Upper	3	671	-658	0.61	0.67

Figure 25 Auxiliary frame forces, rare earthquake

Model Name:	gray.08
Model Description:	Alaska Way Viaduct, Evaluation of Grays Proposal
Model Variation:	rare earthquake

Auxiliary Frame Forces

24 Jul 06 6:59 PM

Frame	Position	Level	Tension	Compression	AxialD/C	D/C
Type	Braces					
Frame a	Lower	1	1528	-1514	0.82	0.82
Frame a	Lower	2	1482	-1551	0.84	0.84
Frame a	Outrigger	1	888	-867	0.74	0.74
Frame a	Outrigger	2	981	-908	0.78	0.78
Frame d	Lower	1	2166	-1776	0.96	0.96
Frame d	Lower	2	1766	-2183	1.18	1.18
Frame d	Outrigger	1	1201	-1172	1.00	1.00
Frame d	Outrigger	2	1345	-1247	1.07	1.07
Frame e	Lower	1	767	-612	0.68	0.69
Frame e	Lower	2	606	-777	0.86	0.87
Frame e	Upper	1	995	-618	0.62	0.62
Frame e	Upper	2	602	-1011	1.01	1.01
Frame f	Lower	1	875	-596	0.66	0.66
Frame f	Lower	2	594	-881	0.98	0.99
Frame f	Upper	1	806	-788	0.79	0.79
Frame f	Upper	2	767	-826	0.83	0.83

Figure 25 (cont.) Auxiliary frame forces, rare earthquake

Model Name: gray.08

Auxiliary Frame Forces

Model Description: Alaska Way Viaduct, Evaluation of Grays Proposal

Model Variation: rare earthquake 24 Jul 06 6:59 PM

Frame	Position	Level	Tension	Compression	AxialD/C	D/C
Type	Columns					
Frame a	East	1	615	-801	0.31	0.70
Frame a	East	2	738	-904	0.19	0.57
Frame a	East	3	744	-904	0.28	0.68
Frame a	West	1	702	-695	0.27	0.67
Frame a	West	2	810	-800	0.17	0.55
Frame a	West	3	817	-791	0.25	0.50
Frame b	East	1	606	-417	0.24	1.46
Frame b	East	2	609	-418	0.20	1.44
Frame b	East	3	14	-47	0.02	0.45
Frame b	West	1	535	-511	0.29	1.07
Frame b	West	2	528	-506	0.18	1.08
Frame b	West	3	9	-45	0.02	0.41
Frame c	East	1	376	-666	0.38	1.53
Frame c	East	2	375	-663	0.24	1.36
Frame c	East	3	13	-44	0.02	0.38
Frame c	West	1	439	-542	0.31	1.12
Frame c	West	2	444	-548	0.20	1.10
Frame c	West	3	17	-33	0.02	0.33
Frame d	East	1	785	-1061	0.41	1.06
Frame d	East	2	903	-1225	0.26	0.85
Frame d	East	3	903	-1213	0.38	0.94
Frame d	West	1	970	-823	0.32	0.83
Frame d	West	2	1149	-949	0.21	0.84
Frame d	West	3	1156	-948	0.30	0.75

Figure 25 (cont.) Auxiliary frame forces, rare earthquake

Model Name:	gray.08
Model Description:	Alaska Way Viaduct, Evaluation of Grays Proposal
Model Variation:	rare earthquake

Damper Forces

24 Jul 06 7:00 PM

Frame	Force
Direction	**Longitudinal**
Frame e	377
Frame f	406
Direction	**Transverse**
Frame a	354
Frame d	363

Figure 26 Auxiliary frame damper forces, rare earthquake

Model Name:	gray.08
Model Description:	Alaska Way Viaduct, Evaluation of Grays Proposal
Model Variation:	rare earthquake

Damper Strokes

24 Jul 06 7:00 PM

Frame	Stroke
Direction	**Longitudinal**
Frame e	0.904
Frame f	0.742
Direction	**Transverse**
Frame a	0.208
Frame d	0.278

The damper strokes tabulated are in a single direction (plus or minus), the total strokes are twice the tabulated values.

Figure 27 Auxiliary frame damper strokes, rare earthquake

Model Name:	gray.08	**Auxiliary Frame Forces**
Model Description:	Alaska Way Viaduct, Evaluation of Grays Proposal	
Model Variation:	expected earthquake	24 Jul 06 6:57 PM

Frame	Position	Level	Tension	Compression	AxialD/C	D/C
Type	Beams					
Frame a	Beam	1	275	-281	0.07	0.12
Frame a	Beam	2	331	-336	0.13	0.18
Frame a	Beam	3	347	-341	0.13	0.17
Frame a	Beam	4	286	-275	0.07	0.12
Frame a	Gradebeam	0	44	-59	0.03	0.11
Frame d	Beam	1	280	-256	0.07	0.12
Frame d	Beam	2	341	-320	0.12	0.16
Frame d	Beam	3	309	-326	0.12	0.17
Frame d	Beam	4	258	-273	0.07	0.11
Frame d	Gradebeam	0	46	-95	0.04	0.14
Frame e	Gradebeam	0	117	-156	0.07	0.08
Frame e	Lower	1	274	-289	0.20	0.31
Frame e	Lower	2	27	-25	0.01	0.07
Frame e	Lower	3	26	-26	0.01	0.06
Frame e	Lower	4	267	-274	0.19	0.23
Frame e	Upper	2	185	-213	0.20	0.11
Frame e	Upper	3	196	-190	0.18	0.10
Frame f	Gradebeam	0	118	-184	0.08	0.14
Frame f	Lower	1	278	-262	0.18	0.22
Frame f	Lower	2	31	-22	0.01	0.07
Frame f	Lower	3	30	-23	0.01	0.06
Frame f	Lower	4	290	-270	0.19	0.23
Frame f	Upper	2	185	-184	0.17	0.10
Frame f	Upper	3	194	-186	0.17	0.10

Figure 28 Auxiliary frame forces, expected earthquake

Model Name:	gray.08
Model Description:	Alaska Way Viaduct, Evaluation of Grays Proposal
Model Variation:	expected earthquake

Auxiliary Frame Forces

24 Jul 06 6:57 PM

Frame	Position	Level	Tension	Compression	AxialD/C	D/C
Type	Braces					
Frame a	Lower	1	746	-748	0.40	0.40
Frame a	Lower	2	726	-769	0.41	0.41
Frame a	Outrigger	1	328	-342	0.29	0.29
Frame a	Outrigger	2	361	-365	0.31	0.31
Frame d	Lower	1	694	-685	0.37	0.37
Frame d	Lower	2	665	-717	0.39	0.39
Frame d	Outrigger	1	319	-335	0.29	0.29
Frame d	Outrigger	2	352	-357	0.31	0.31
Frame e	Lower	1	374	-358	0.40	0.40
Frame e	Lower	2	350	-382	0.42	0.43
Frame e	Upper	1	241	-238	0.24	0.24
Frame e	Upper	2	220	-259	0.26	0.26
Frame f	Lower	1	373	-356	0.40	0.40
Frame f	Lower	2	349	-380	0.42	0.42
Frame f	Upper	1	222	-236	0.24	0.24
Frame f	Upper	2	217	-240	0.24	0.24

Figure 28 (cont.) Auxiliary frame forces, expected earthquake

Model Name: gray.08

Auxiliary Frame Forces

Model Description: Alaska Way Viaduct, Evaluation of Grays Proposal

Model Variation: expected earthquake 24 Jul 06 6:57 PM

Frame	Position	Level	Tension	Compression	AxialD/C	D/C
Type	Columns					
Frame a	East	1	255	-315	0.12	0.18
Frame a	East	2	309	-341	0.07	0.16
Frame a	East	3	314	-336	0.10	0.15
Frame a	West	1	266	-301	0.12	0.20
Frame a	West	2	322	-333	0.07	0.17
Frame a	West	3	327	-329	0.10	0.17
Frame b	East	1	136	-177	0.10	0.19
Frame b	East	2	139	-174	0.06	0.19
Frame b	East	3	-3	-9	0.00	0.10
Frame b	West	1	126	-176	0.10	0.18
Frame b	West	2	129	-173	0.06	0.17
Frame b	West	3	-3	-9	0.00	0.11
Frame c	East	1	123	-188	0.11	0.19
Frame c	East	2	126	-185	0.07	0.21
Frame c	East	3	-3	-9	0.00	0.10
Frame c	West	1	120	-178	0.10	0.22
Frame c	West	2	124	-175	0.06	0.21
Frame c	West	3	-3	-9	0.00	0.10
Frame d	East	1	256	-287	0.11	0.22
Frame d	East	2	315	-311	0.07	0.16
Frame d	East	3	320	-307	0.10	0.14
Frame d	West	1	237	-306	0.12	0.21
Frame d	West	2	289	-334	0.07	0.16
Frame d	West	3	294	-328	0.10	0.17

Figure 28 (cont.) Auxiliary frame forces, expected earthquake

Model Name:	gray.08	**Damper Forces**
Model Description:	Alaska Way Viaduct, Evaluation of Grays Proposal	
Model Variation:	expected earthquake	24 Jul 06 6:58 PM

Frame	Force
Direction	**Longitudinal**
Frame e	233
Frame f	232
Direction	**Transverse**
Frame a	217
Frame d	224

Figure 29 Auxiliary frame damper forces, expected earthquake

Model Name:	gray.08
Model Description:	Alaska Way Viaduct, Evaluation of Grays Proposal
Model Variation:	expected earthquake

Damper Strokes

24 Jul 06 6:58 PM

Frame	Stroke
Direction	**Longitudinal**
Frame e	0.116
Frame f	0.111
Direction	**Transverse**
Frame a	0.073
Frame d	0.071

The damper strokes tabulated are in a single direction (plus or minus), the total strokes are twice the tabulated values.

Figure 30 Auxiliary frame damper strokes, expected earthquake

APPENDIX A

ALASKAN WAY VIADUCT—TYPICAL UNIT

FED. ROAD DIST. NO.	STATE	FED. AID PROJ. NO.	FISCAL YEAR	SHEET NO.	TOTAL SHEETS
8	WASH.	U-001-3(12)		8	146

Note: All Grade Elevations are finished grades along ℄ of Viaduct

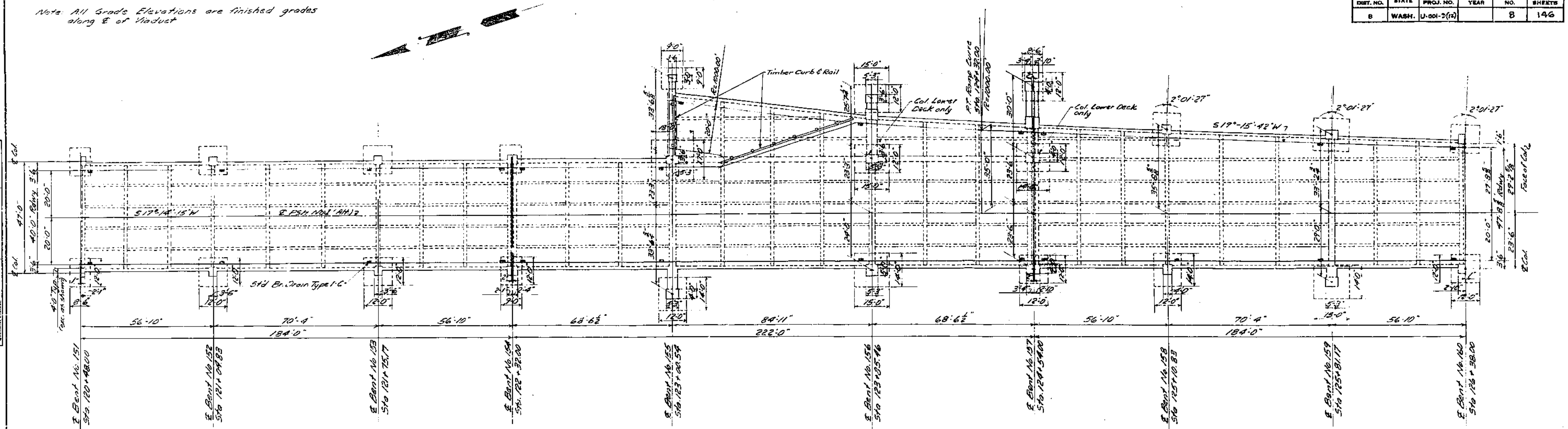

PLAN BENT NO. 151 TO BENT NO. 160

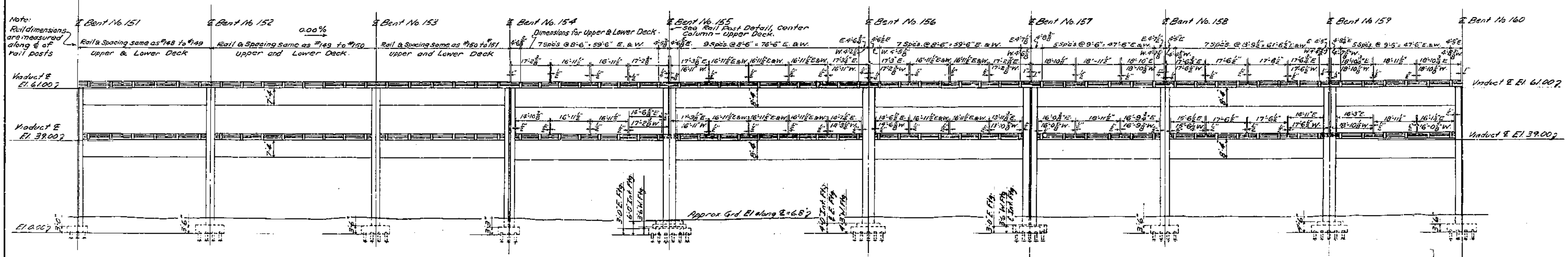

ELEVATION

PRIMARY STATE HIGHWAY NO. 1
ALASKAN WAY VIADUCT IN SEATTLE
HOLGATE ST. NORTH
KING COUNTY

LAYOUT-BENT 151 to 160

WASHINGTON STATE HIGHWAY COMMISSION
DEPARTMENT OF HIGHWAYS
OLYMPIA, WASHINGTON
E. C. HUNTLEY, Chairman
R. E. BANGEL, Member
H. E. MORGAN, Member
OSCAR E. STONE, Member
R. A. MOISIO, Member

APPROVED: March 27, 1956
ASST. DIRECTOR OF HIGHWAYS
CONTRACT NUMBER 5262

APPROVED:
BRIDGE ENGINEER

SHEET 7 OF 136 SHEETS

DATE	REVISION	BY	CHK'D.	APPR'D.
4/5/56	Added Timber Guard Rail @ Ramp	WBH	MJN	W.A.R.

T281

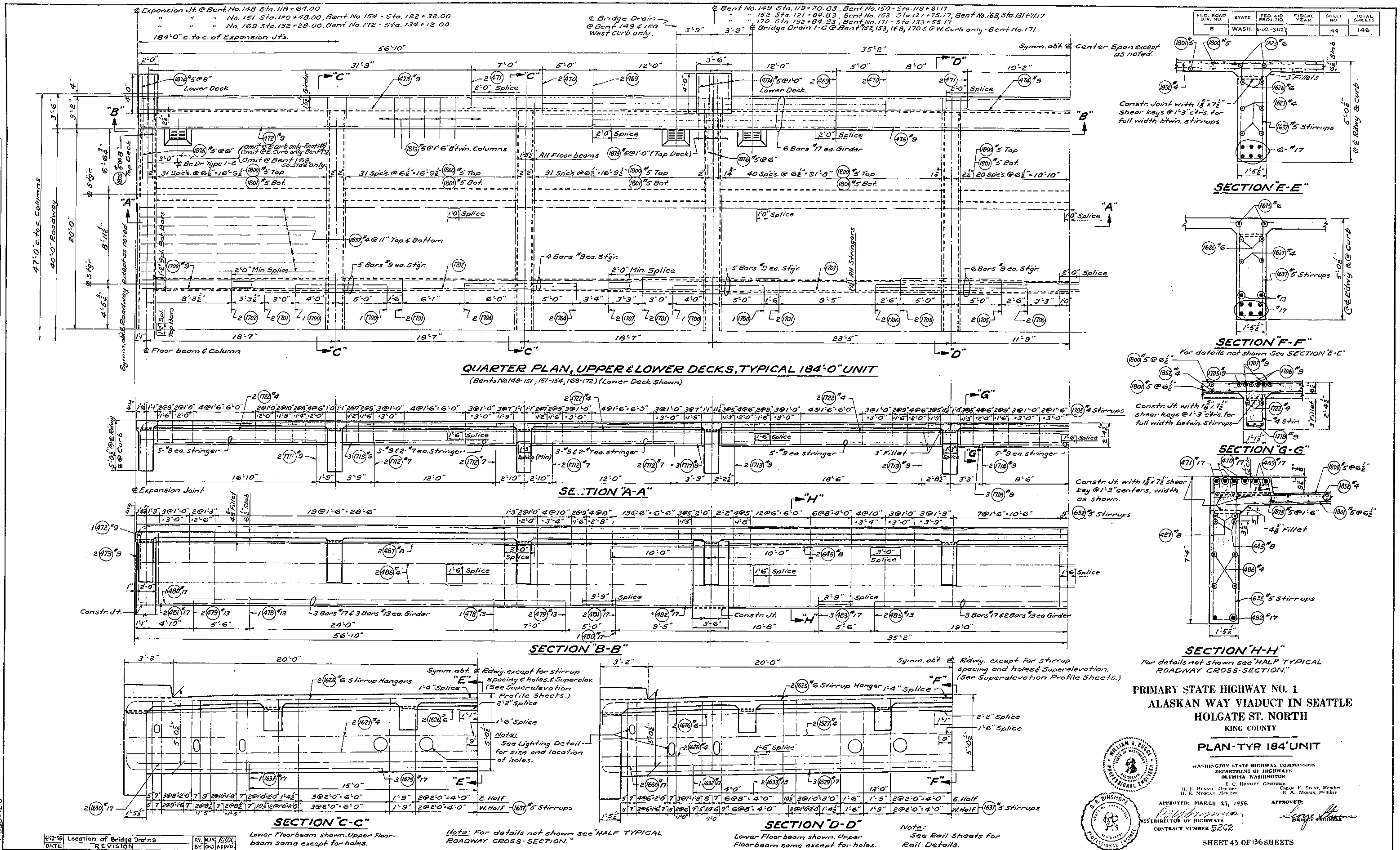
QUARTER PLAN, UPPER & LOWER DECKS, TYPICAL 184'-0" UNIT
(Bents No.148-151, 151-154, 169-172) (Lower Deck Shown)
184'-0" c. to c. of Expansion Jt's.
SECTION "A-A"
SECTION "B-B"
SECTION "C-C"
Lower Floorbeam shown. Upper Floorbeam same except for holes.
Note: For details not shown see "HALF TYPICAL ROADWAY CROSS-SECTION."
SECTION "D-D"
Lower Floorbeam shown. Upper Floorbeam same except for holes.
Note: See Rail Sheets for Rail Details.
SECTION "E-E"
SECTION "F-F"
For details not shown See SECTION "E-E"
SECTION "G-G"
SECTION "H-H"
For details not shown see "HALF TYPICAL ROADWAY CROSS-SECTION."
FED. ROAD DIV. NO. 8 | STATE WASH. | SHEET NO. 44 | TOTAL SHEETS 146
4-13-56 Location of Bridge Drains
DATE REVISION
PRIMARY STATE HIGHWAY NO. 1
ALASKAN WAY VIADUCT IN SEATTLE
HOLGATE ST. NORTH
KING COUNTY
PLAN-TYP 184' UNIT
WASHINGTON STATE HIGHWAY COMMISSION
DEPARTMENT OF HIGHWAYS
OLYMPIA, WASHINGTON
APPROVED: MARCH 27, 1956
ASST. DIRECTOR OF HIGHWAYS
CONTRACT NUMBER 5262
APPROVED: BRIDGE ENGINEER
SHEET 43 OF 136 SHEETS

FED. ROAD DIV. NO.	STATE	FED. AID PROJ. NO.	FISCAL YEAR	SHEET NO.	TOTAL SHEETS
8	WASH.	U-001-3(12)		45	146

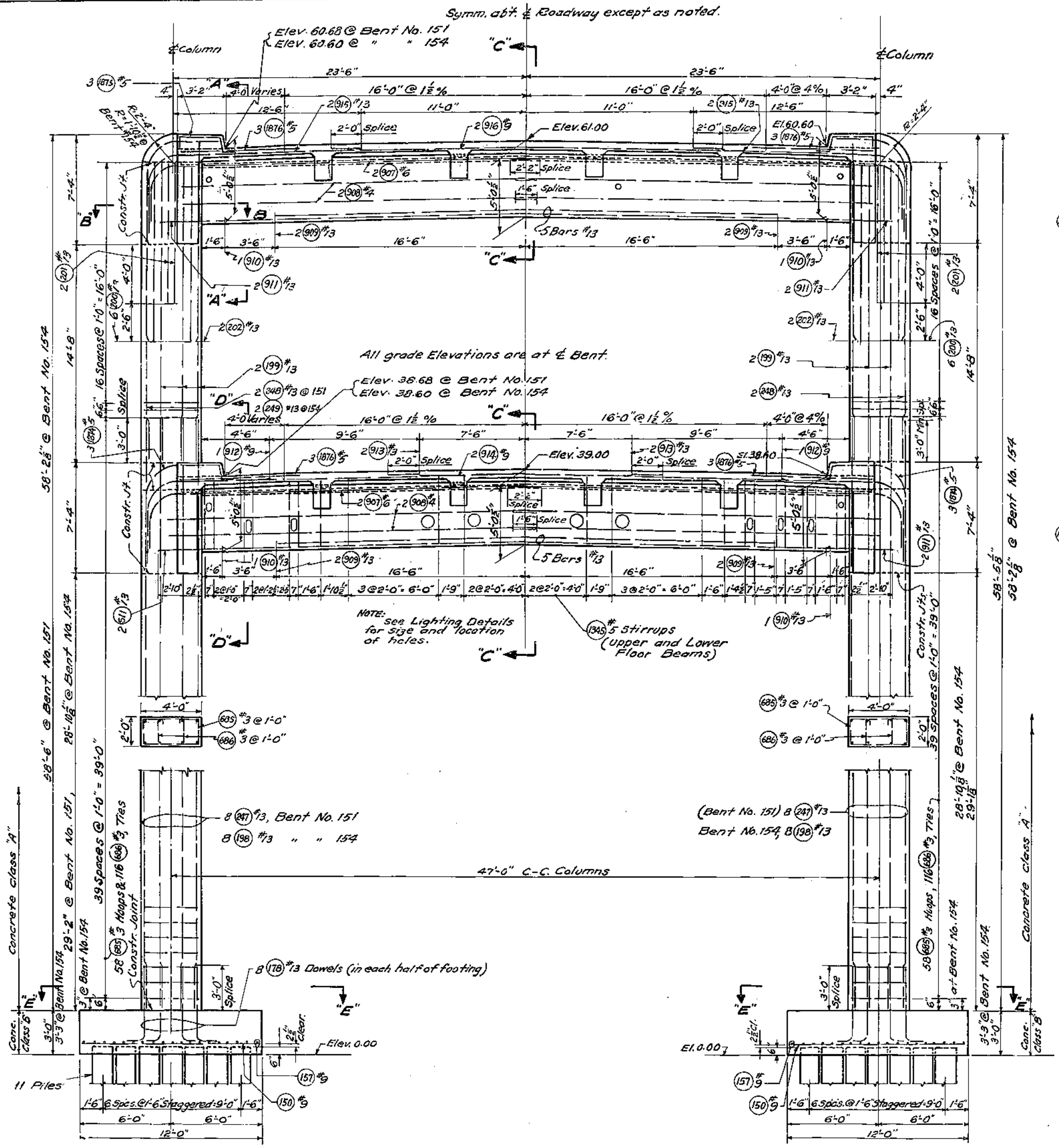

ELEVATION - END BENT NO. 151

(Typical End Bent - 184' Unit)
North ½ Bent No. 151 Shown, South ½ similar.
North ½ Bent No. 154 similar except as noted.
See "Elevation of South-half of End Bent No. 154" for footing details @ Bent No. 154.

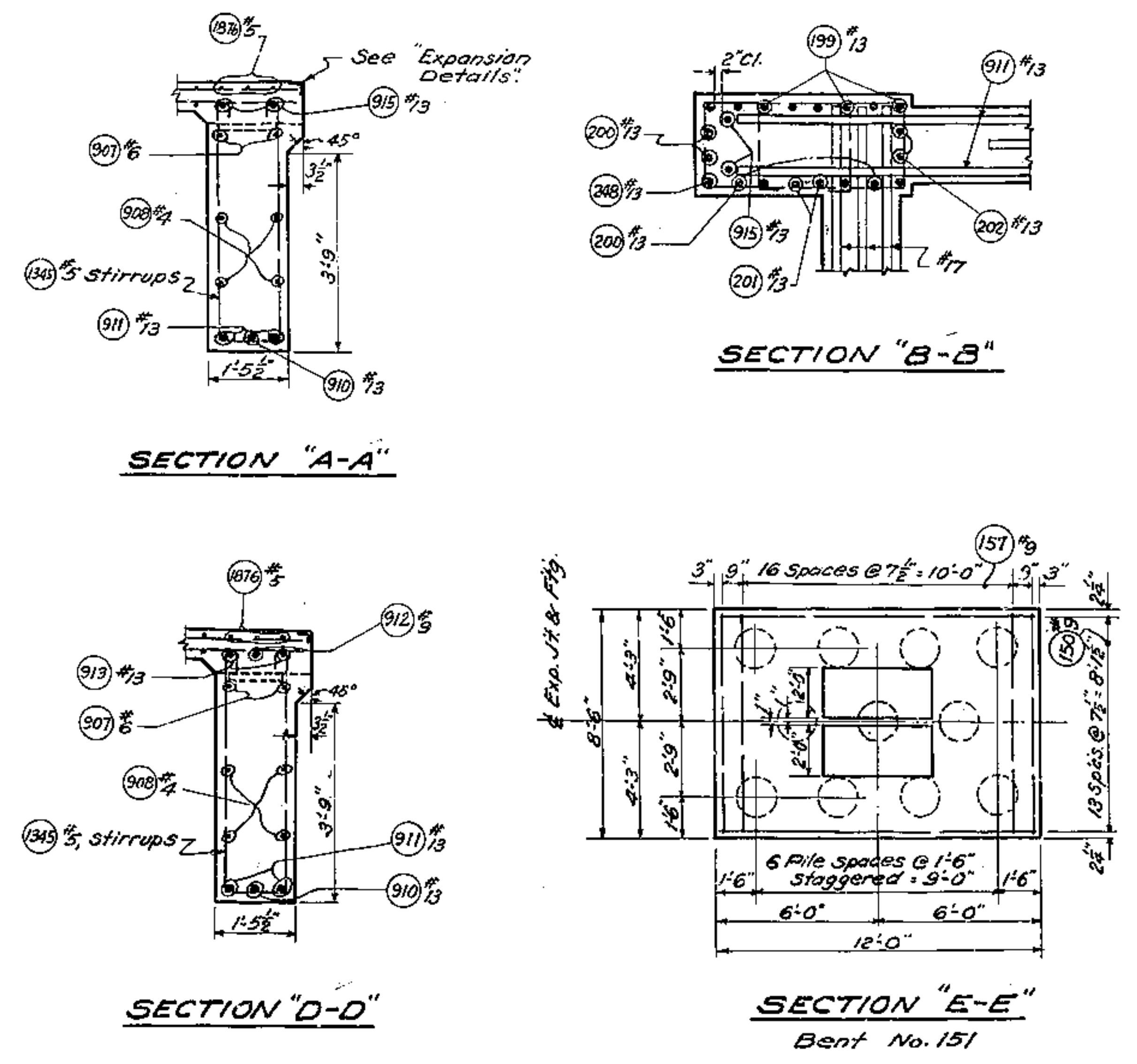

SECTION "A-A"

SECTION "B-B"

SECTION "C-C"

SECTION "D-D"

SECTION "E-E"
Bent No. 151

Note:
See Drain Sheets for location of drain pipe anchor bolts.

PRIMARY STATE HIGHWAY NO. 1
ALASKAN WAY VIADUCT IN SEATTLE
HOLGATE ST. NORTH
KING COUNTY

ELEVATION - BENT 151

WASHINGTON STATE HIGHWAY COMMISSION
DEPARTMENT OF HIGHWAYS
OLYMPIA, WASHINGTON
E. C. HUNTLEY, Chairman
R. E. JENSEN, Member — OSCAR E. STONE, Member
R. E. MORGAN, Member — R. A. MURPHY, Member

APPROVED: MARCH 27, 1956 — APPROVED:
ASS'T. DIRECTOR OF HIGHWAYS — BRIDGE ENGINEER
CONTRACT NUMBER 5262

SHEET 44 OF 136 SHEETS

DATE	REVISIONS	BY	CHKD	APPVD.
4-23-56	Elevations Bent No. 151	P.Y.	W.J.N.	

1-390-12(8)

P
1281

FED. ROAD DIV. NO.	STATE	FED. AID PROJ. NO.	FISCAL YEAR	SHEET NO.	TOTAL SHEETS
8	WASH.	U-001-3(12)		46	146

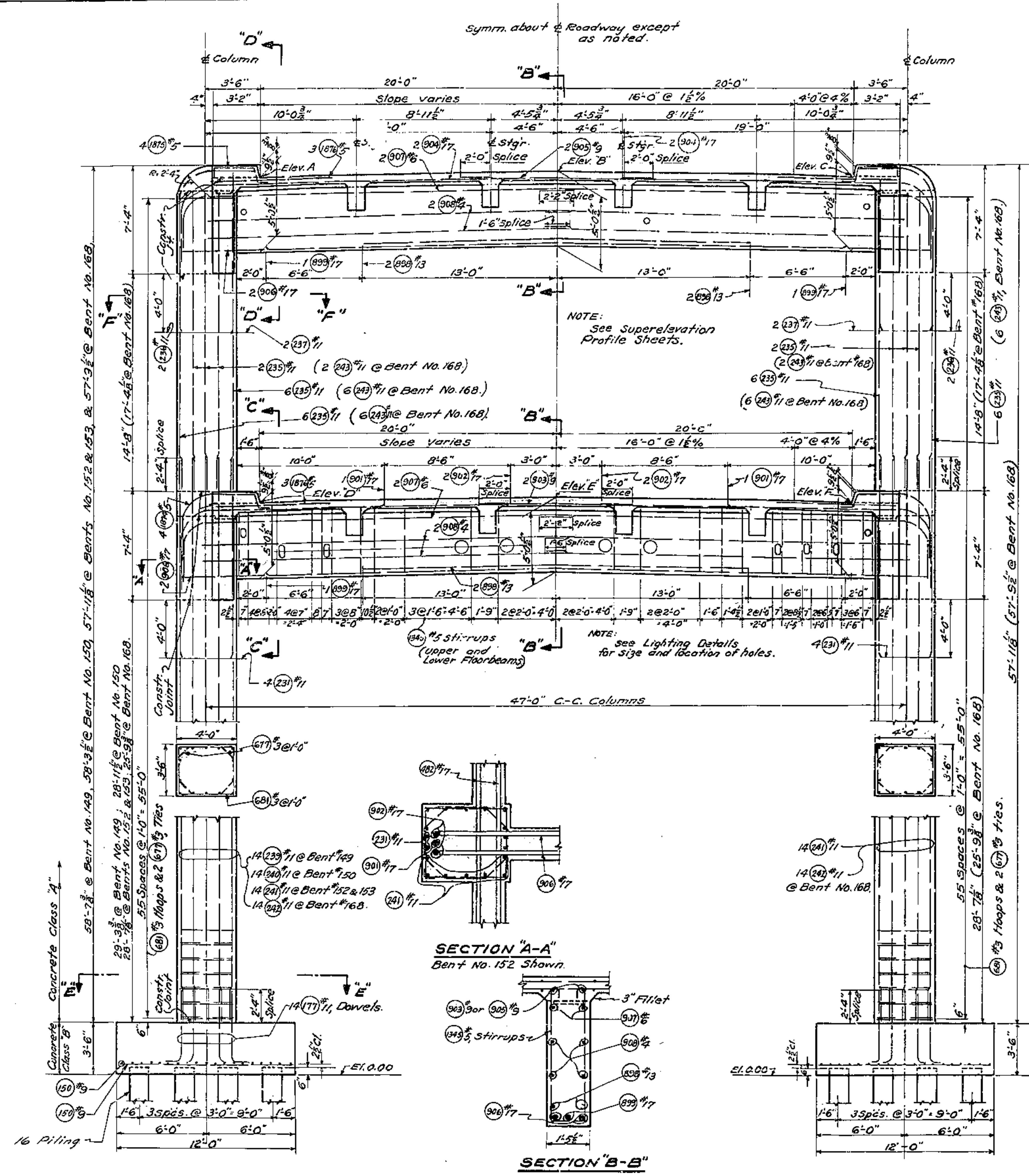

ELEVATION AT INTERMEDIATE BENT NO. 152

(TYPICAL INTERMEDIATE BENT - 184'-0" UNIT)

Bent Nos. 149, 150, 153 and 168 similar except as noted.

SECTION "A-A"
Bent No. 152 Shown.

SECTION "B-B"

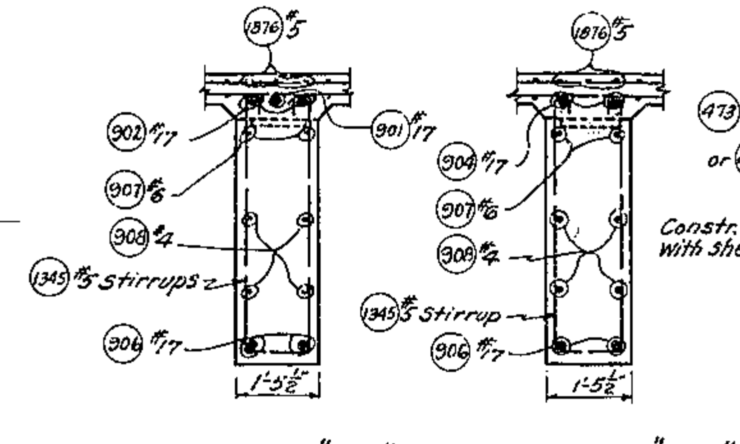

SECTION "C-C"   SECTION "D-D"

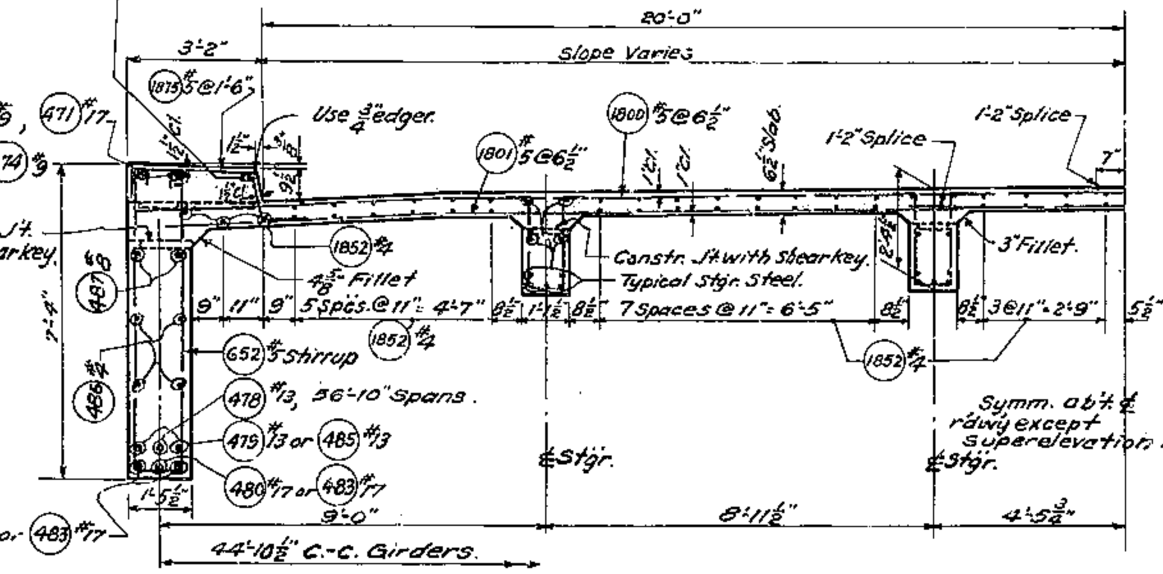

HALF ROADWAY SECTION NEAR ℄ SPANS.

(TYPICAL 184'-0" UNIT)

NOTE: See Superelevation Profile Sheets.

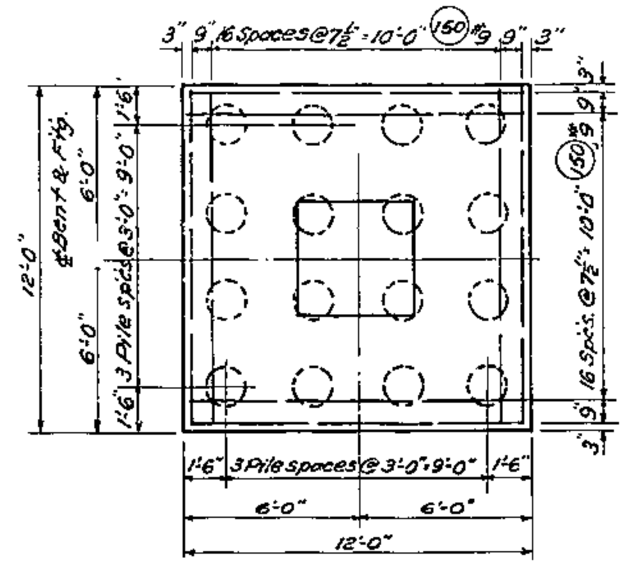

SECTION "E-E"

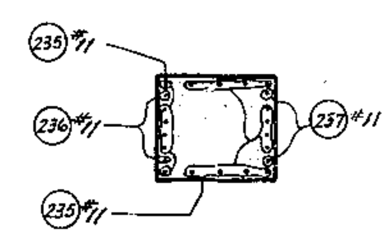

SECTION "F-F"
(Bent No. 152 shown)

BENT NO.	ELEVATION					
	A	B	C	D	E	F
149	61.29	61.00	60.60	39.29	39.00	38.60
150	60.96	61.00	60.60	38.96	39.00	38.60
152	60.60	61.00	60.60	38.60	39.00	38.60
153	60.60	61.00	60.60	38.60	39.00	38.60
168	60.47	60.87	60.47	35.80	36.20	35.80

Note: See Drain Sheets for location of drain pipe anchor bolts.

4-23-56	Slope of Rdwy Cross-Section	F.Y.	M.J.N.	
DATE	REVISION	BY	CH'D	APP'D

PRIMARY STATE HIGHWAY NO. 1
ALASKAN WAY VIADUCT IN SEATTLE
HOLGATE ST. NORTH

KING COUNTY

ELEVATION - BENT 152

WASHINGTON STATE HIGHWAY COMMISSION
DEPARTMENT OF HIGHWAYS
OLYMPIA, WASHINGTON

E. C. HUNTLEY, Chairman
R. E. HESSEL, Member   OSCAR E. STONE, Member
H. E. MORGAN, Member   R. A. MOISIO, Member

APPROVED: MARCH 27, 1956   APPROVED:

ASST. DIRECTOR OF HIGHWAYS   BRIDGE ENGINEER

CONTRACT NUMBER 5262

SHEET 45 OF 136 SHEETS

P / 1287   5 / 103

I-390-12A

APPENDIX B

PROPOSAL BY VICTOR GRAY ET AL.

ALASKAN WAY VIADUCT

ELEVATION - 3 SPAN UNIT

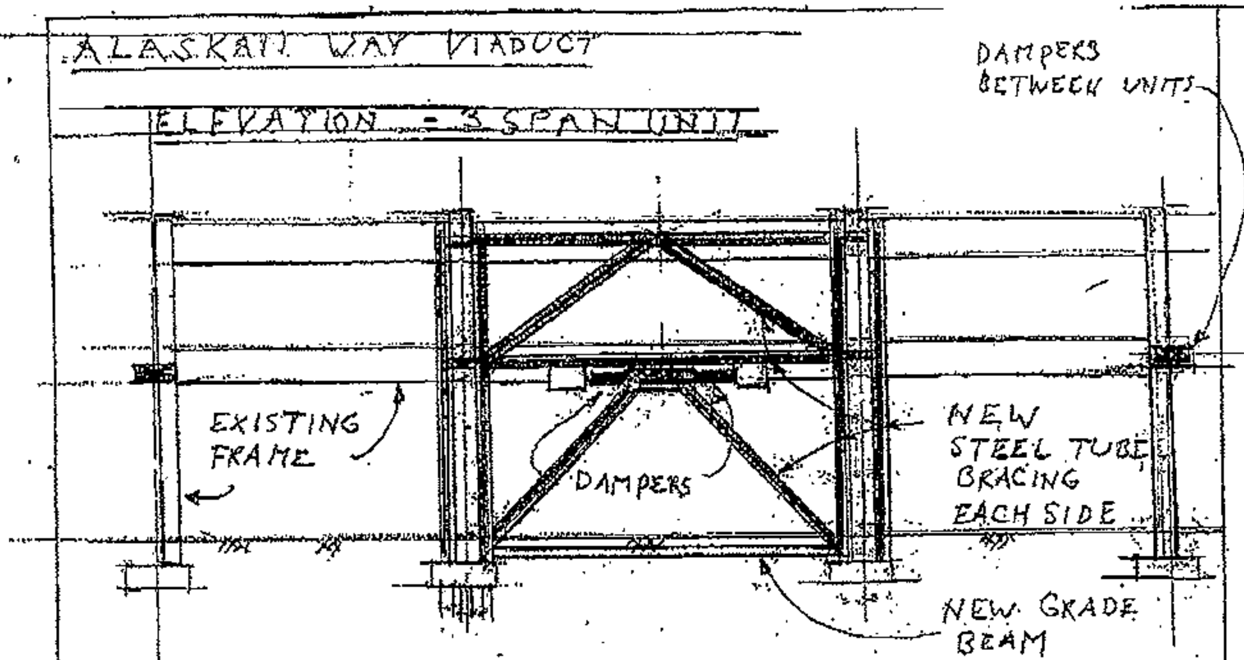

CROSS SECTION

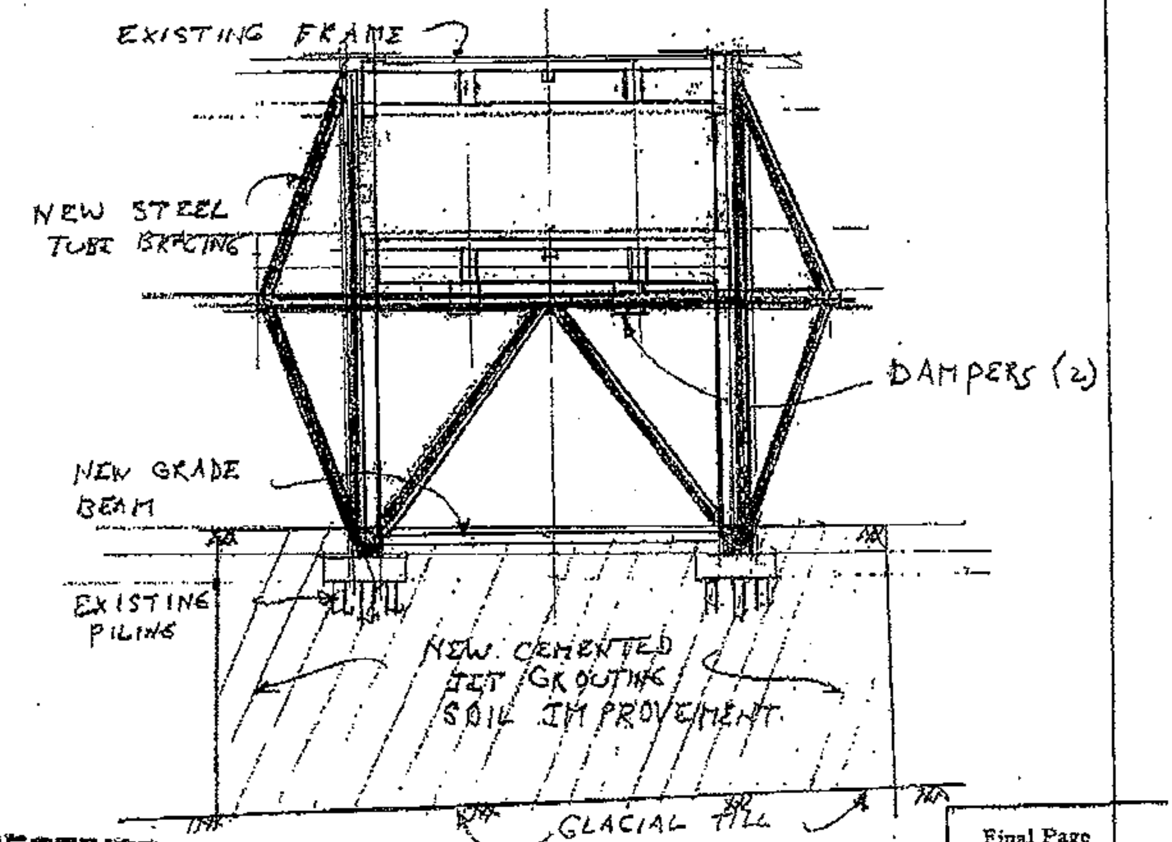

Final Page

RECEIVED
DEC 10 2004
AWVSP Team Office

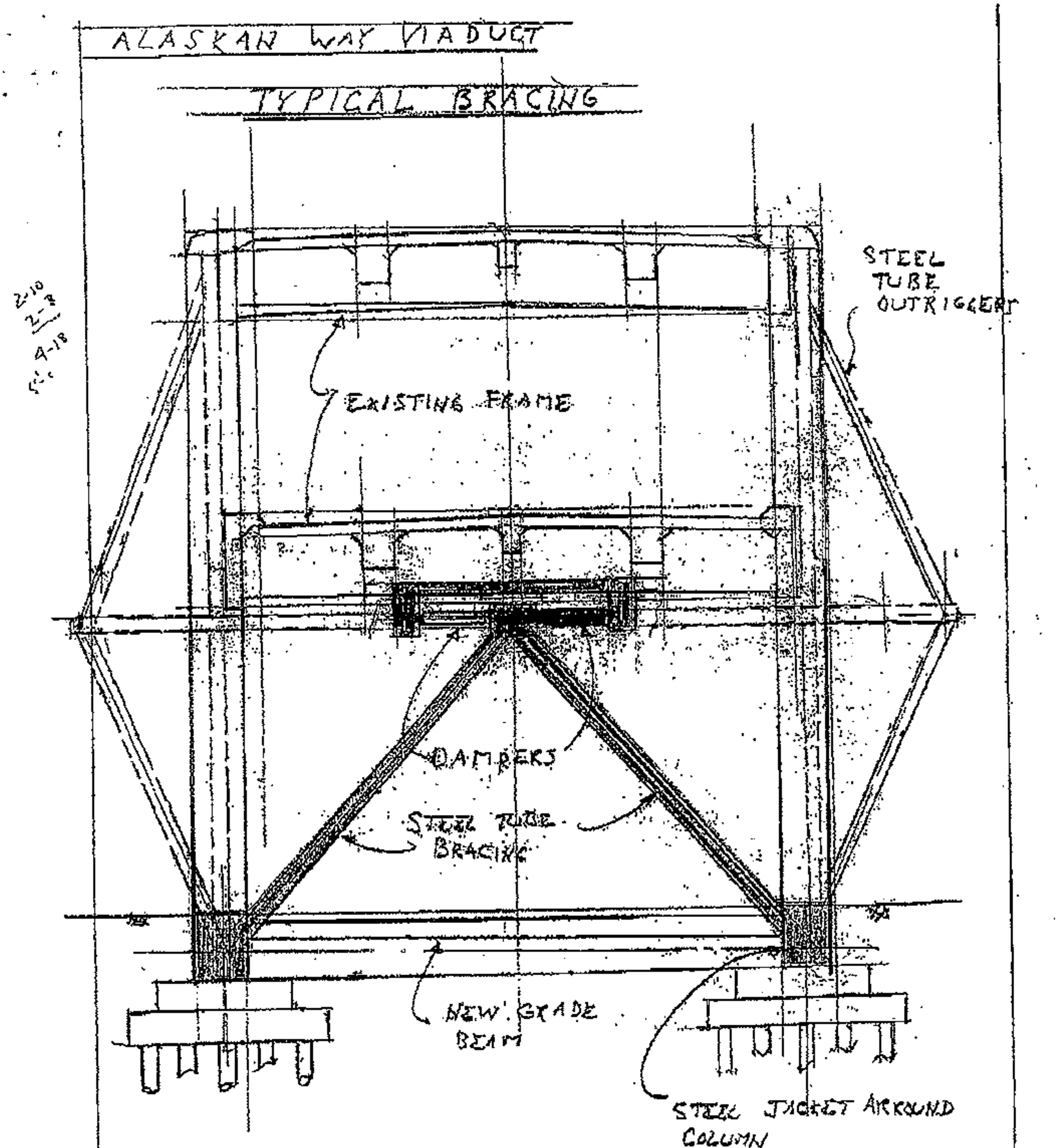

RECEIVED
DEC 10 2004
AWVSP Team Office

Final Page

ALASKAN WAY VIADUCT

SECTION @ RELIEVING PLATFORM (NEAR SENECA) BENT 75

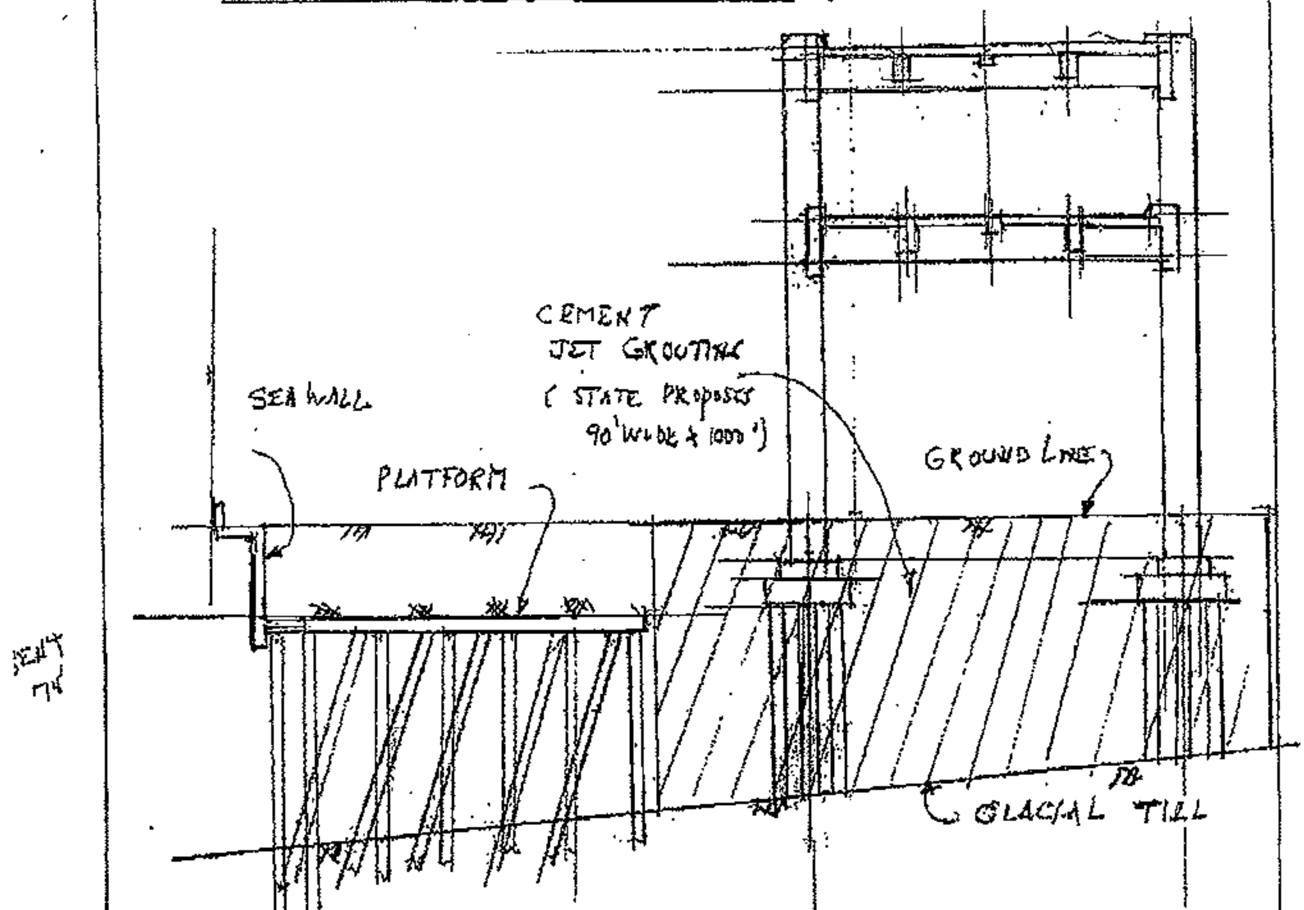

SECTION @ GRAVITY SEA WALL (NEAR YESLER) BENT 96

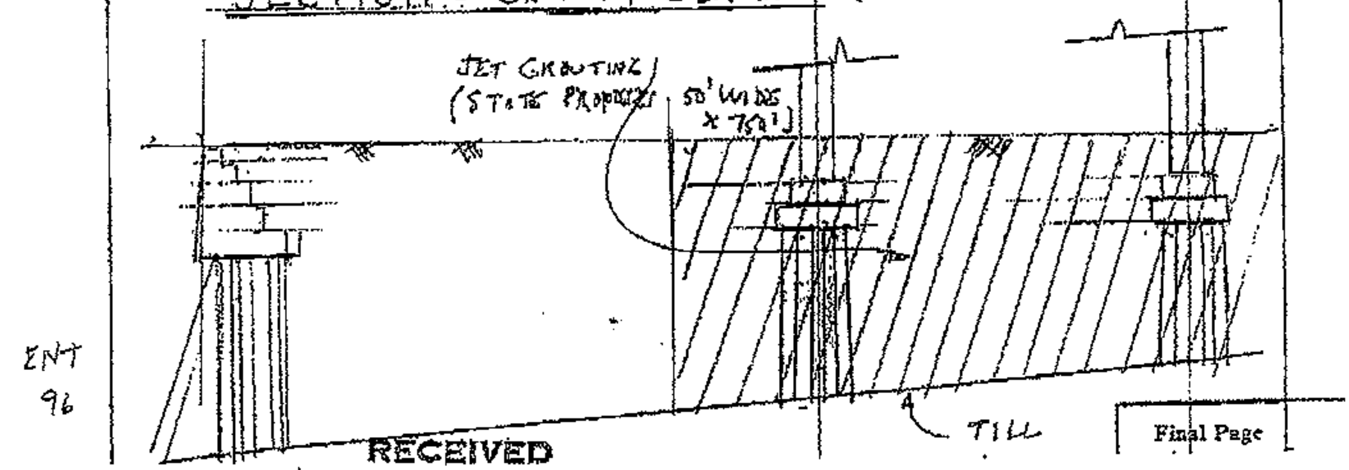

Final Page

RECEIVED
DEC 10 2004
AWVSP Team Office

ALASKAN WAY VIADUCT

CROSS SECTION @ SINGLE DECKS @ BENT 36

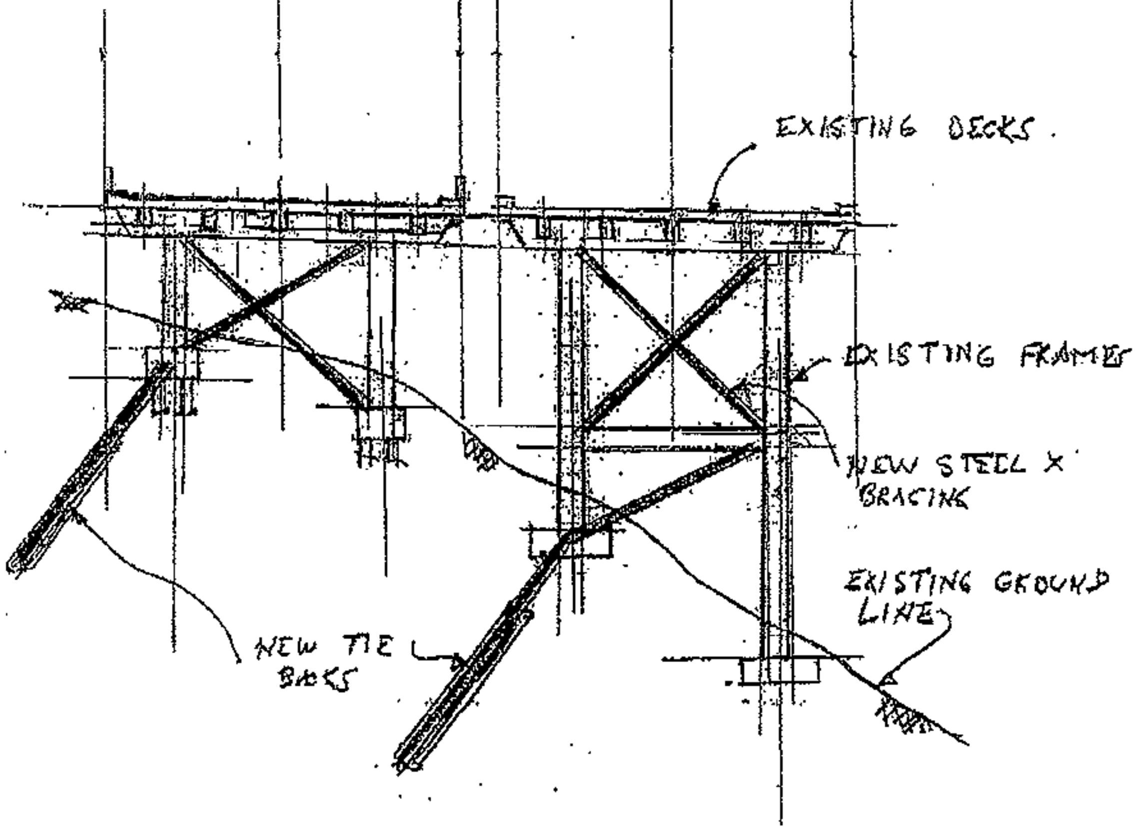

BENT 36

RECEIVED
DEC 10 2004
AWVSP Team Office

Final Page

ALASKAN WAY VIADUCT

CROSS SECTION @ BENT # 143

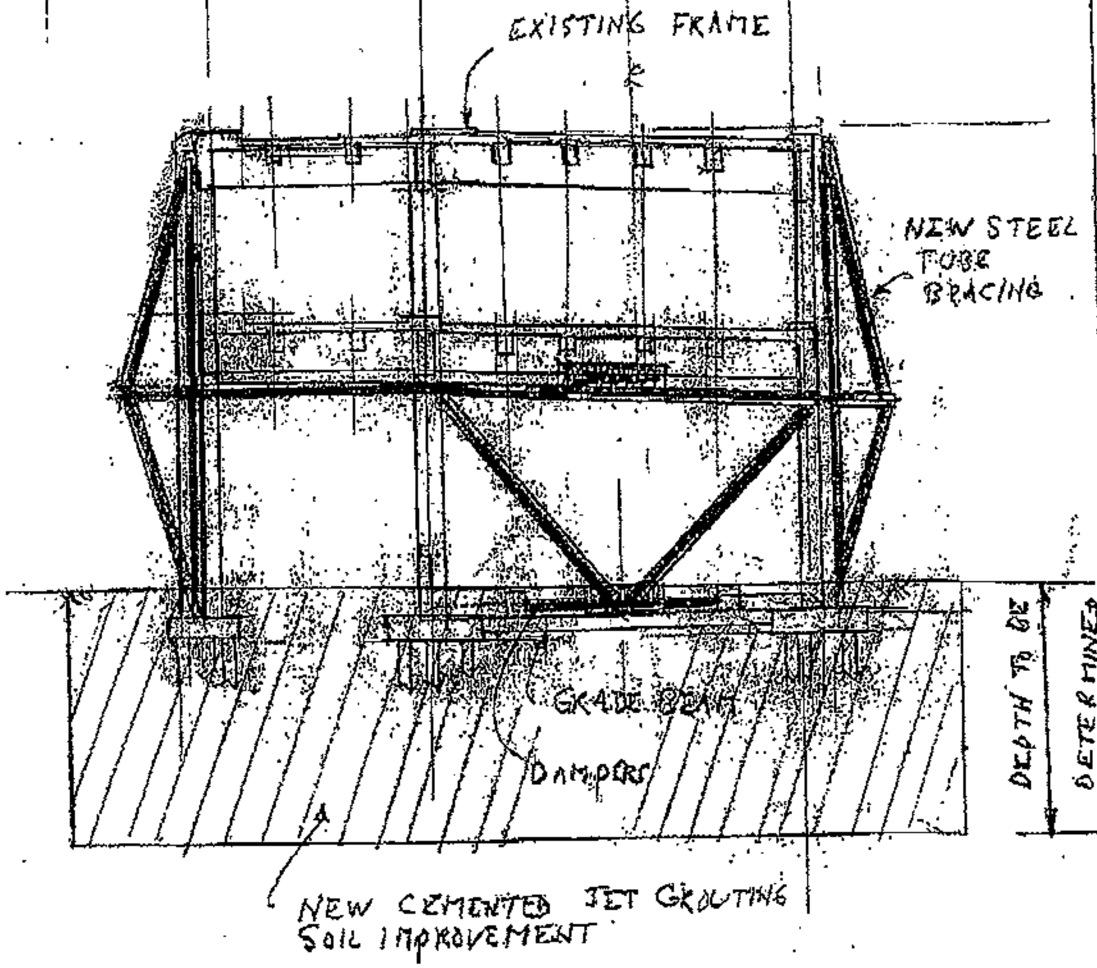

RECEIVED
DEC 10 2004
AWVSP Team Office

Final Page

APPENDIX C

EVALUATION OF MODIFIED PROPOSAL BY VICTOR GRAY ET AL.

DESCRIPTION OF MODIFICATIONS

Modifications to the original Gray proposal include the following (see following sketches):

1. Elimination of the external outrigger frames and K bracing that extended the shoring steel to the upper deck level.

2. Possible elimination of dampers in the lateral K brace support system (this is conflicting in two sketches – one shows dampers, the other does not) and/or replacement of K bracing with Buckling-Restrained braces.

3. Elimination of the along station framing support for the damper connection to the edge girder, in favor of direct connection to the edge girders. (This also is not clear from the various sketches – one appears to remove additional framing, the other does not.)

4. A general indication of additional retrofit to columns through the use of steel jackets.

EVALUATION OF REVISIONS

While the number of revisions seems substantial, the character of the revisions will not significantly change the performance and reliability of the proposed concept as a seismic retrofit. Based on the analyses conducted for the base concept, removal of upper level bracing will likely increase demand on the edge girders, which could be critical for the SED designed region of the Viaduct.

One obvious point of departure with the prior concept is the addition of retrofit elements for beams and columns that was not previously included. In so much as this extends the scope of retrofit, these changes are indicative of the need for a more comprehensive retrofit design than that initially proposed. However, in terms of the overall earthquake response of the structure, the proposed changes do not address the fundamental limitations of the proposed concept. The framing systems—in whichever of the forms proposed—do not address the fundamental strength deficiencies of the foundation elements. The stiffness of the transverse framing produces a greater rocking motion that adds to the demand on the piles and footings. The Gray proposal focuses on the deficiencies of the upper framing system – beams and columns – but in doing so, aggravates the deficiencies in the foundation elements. In addition, the deficiencies in the upper knee joints are not addressed in this new bracing arrangement.

In the event that this new Gray proposal does remove the supplemental framing for dampers along the edge girders, the SED units would show a need for substantial additional retrofit of the edge girder members. They have only marginally acceptable strength for their current function. In the event that this new Gray proposal removes dampers from the transverse K brace system in favor of only the buckling restrained braces, additional overturning may increase demand on already overloaded foundation elements.

In summary, the deficiencies of the existing Viaduct are so pervasive that partial retrofit schemes are not sufficient for seismic design standards. A limited retrofit, such as proposed by Gray, serves only to reassign the location of critical failure from one deficiency to another. Any retrofit scheme that purports to meet current engineering design standards will have to be comprehensive, and include all of the major structural members and foundation elements of the bridge. Soil improvement is not a substitute for foundation retrofit. Soil modification only addresses (to some extent) the concern for lateral spreading and loss of the sea wall. Structural failures within the foundation elements are not mitigated by the proposed soil modification, and may, in some locations, be aggravated by changes in effective ground motion due to the stiffened soils.

A revised numerical analysis for this subsequent Gray concept may result in slightly different demands. However we do not expect that conclusions regarding the sufficiency of the retrofit would change with further analysis.

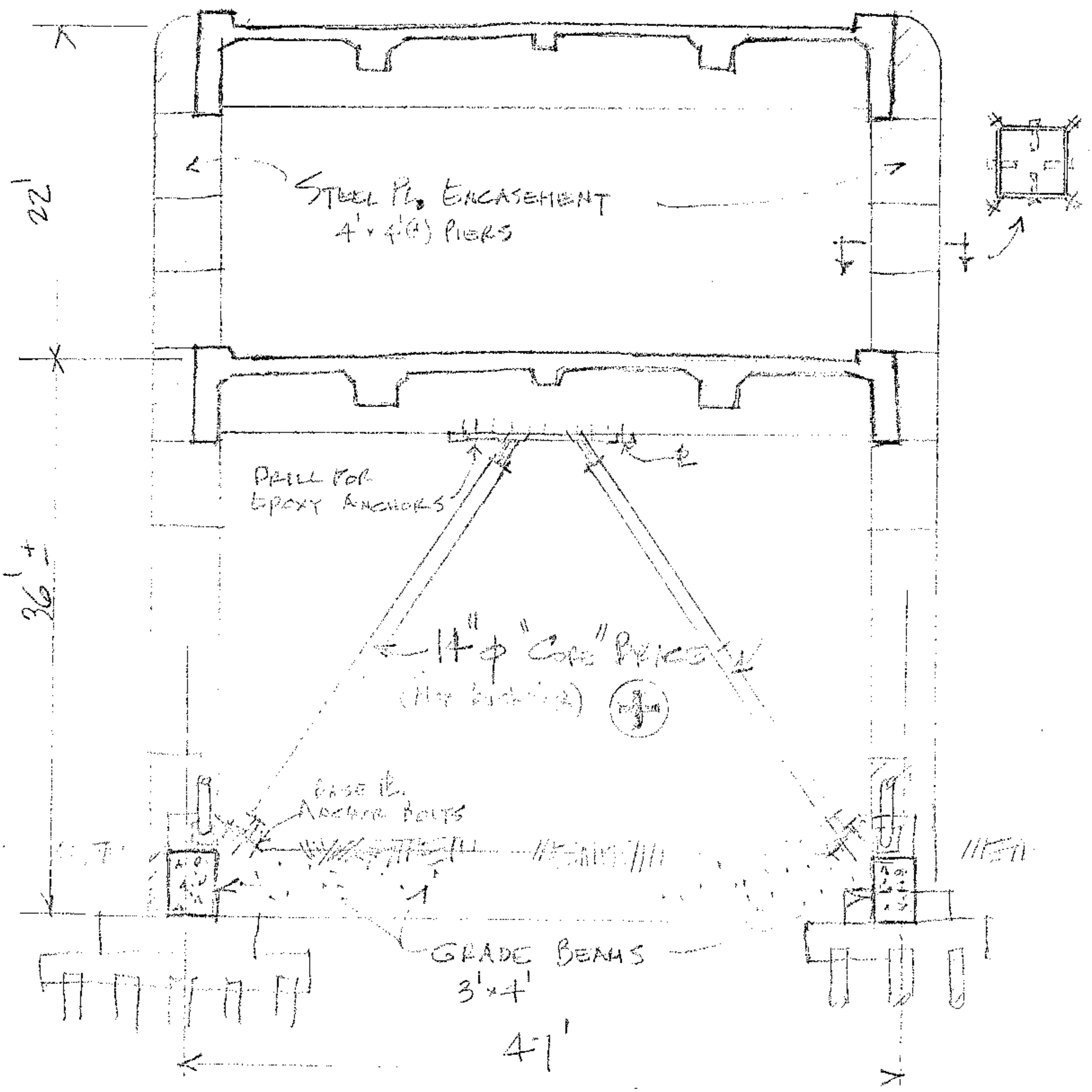

TYPICAL CROSS SECTION X

S1

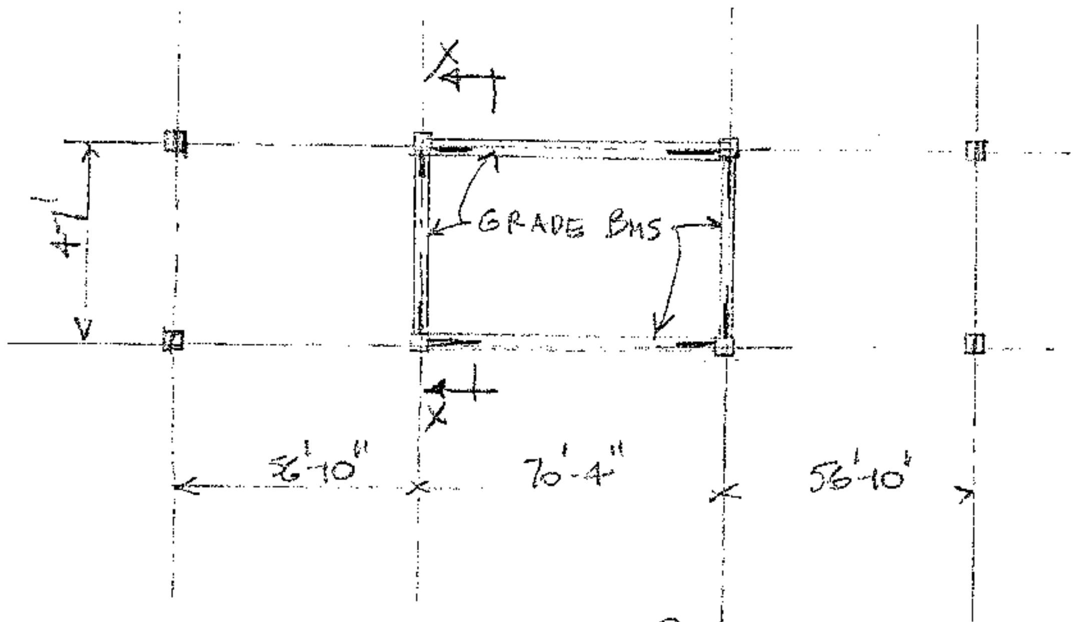

GROUND PLAN

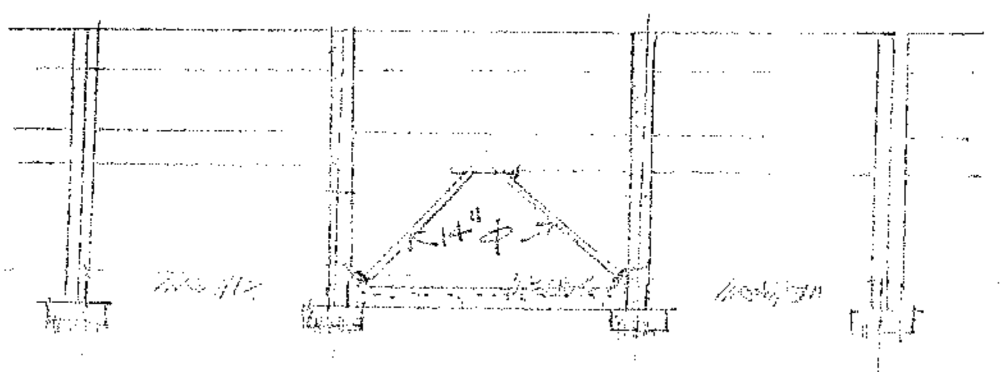

TYPICAL ELEVATION

BUCKLING-RESTRAINED BRACES

The Unbonded Brace is one type of buckling-restrained brace, and is a simple but yet remarkably effective configuration of steel and concrete producing a tension-compression load-carrying brace element capable of stable yielding behavior without buckling. The basic concept of the Unbonded Brace is the prevention of compression buckling of a central steel core by encasing it over its length in a steel tube filled with concrete or mortar. A slip interface, or "unbonding" layer, between the steel core and the surrounding concrete is provided to ensure that compression and tension loads are carried only by the steel core. The materials and geometry of the slip layer must be carefully designed and constructed to allow relative movement between the steel core and the concrete due to shearing and Poisson's effect, while simultaneously inhibiting local buckling of the core as it yields in compression.

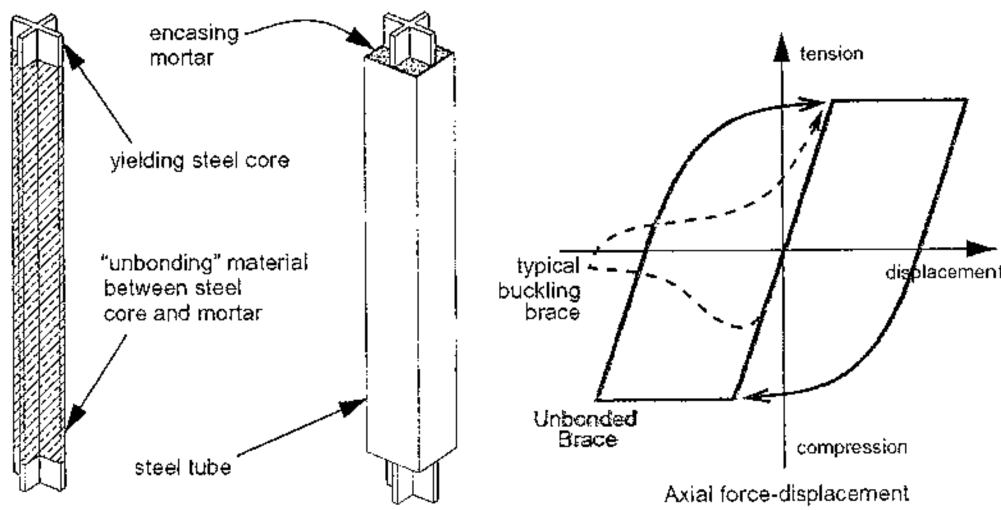

Unbonded Brace concept and typical hysteretic behavior

Tests of Unbonded Braces conducted at the University of California, Berkeley, and extensive testing in Japan, have shown the braces to produce repeatable symmetric behavior in tension and compression, up to post-yield ductilities in the range of 15-20. The symmetric behavior has particular design advantages for chevron or V configurations, and the well-defined elastic-plastic bilinear characteristic allows for rational capacity design methods for the connections, surrounding structural elements and foundations.

Job. No.	VICTOR O. GRAY & COMPANY	Client	Sheet
By ___ Date ___	CONSULTING ENGINEERS	Project	/
Chk. ___ Date ___	SEATTLE. WASH.	Subject	

ALASKAN WAY VIADUCT

ELEVATION - 3 SPAN UNIT

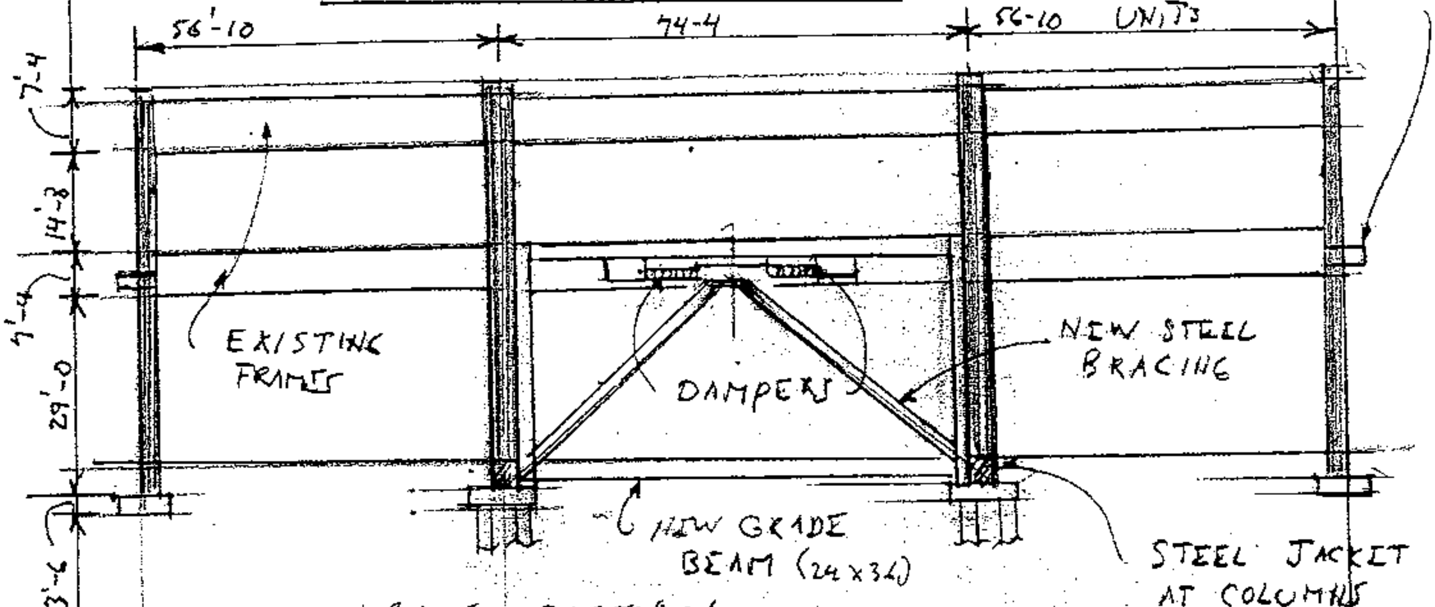

CROSS SECTION

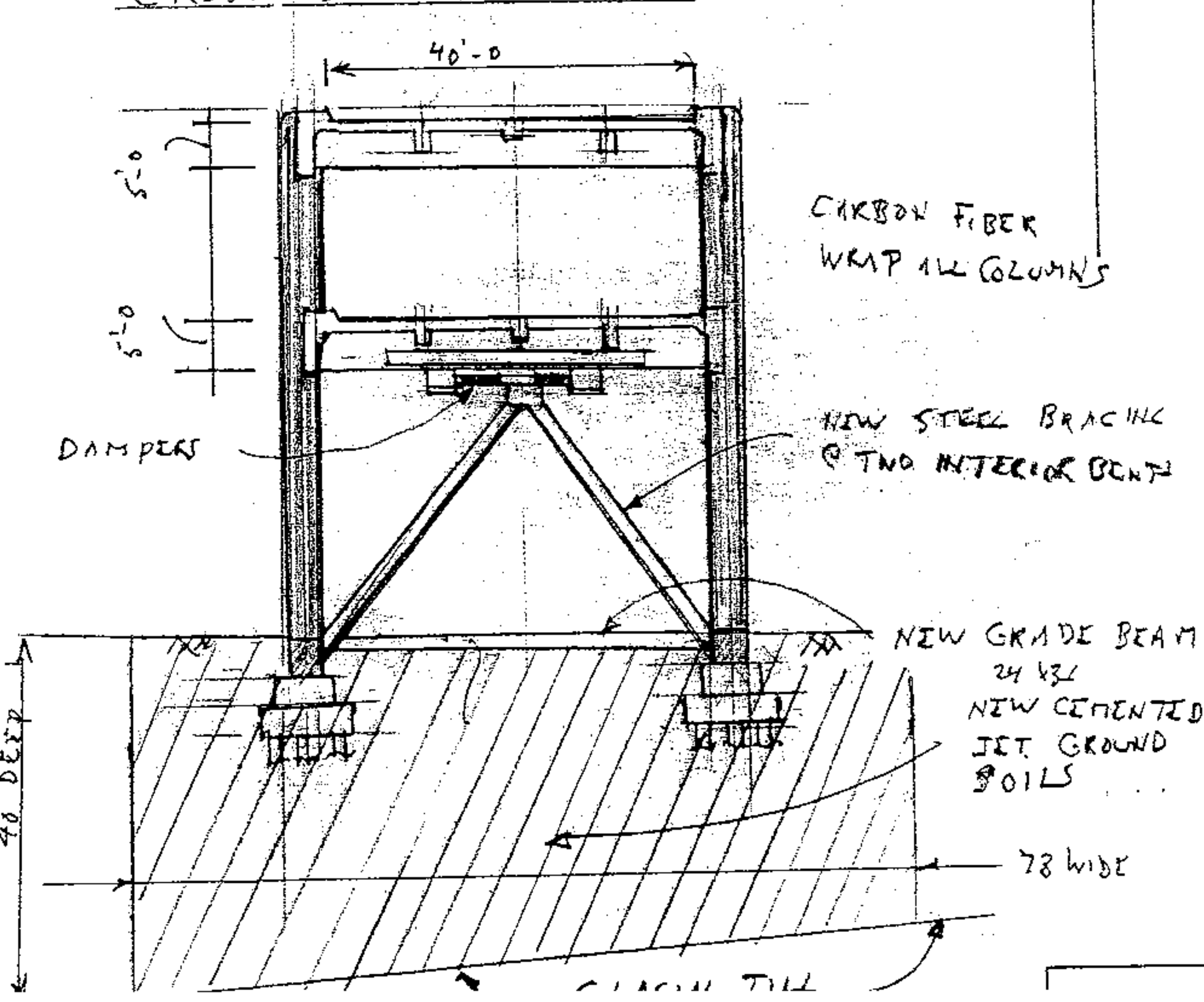

ALASKAN WAY VIADUCT

SECTION @ RELIEVING PLATFORM (NEAR SENECA) BENT 75

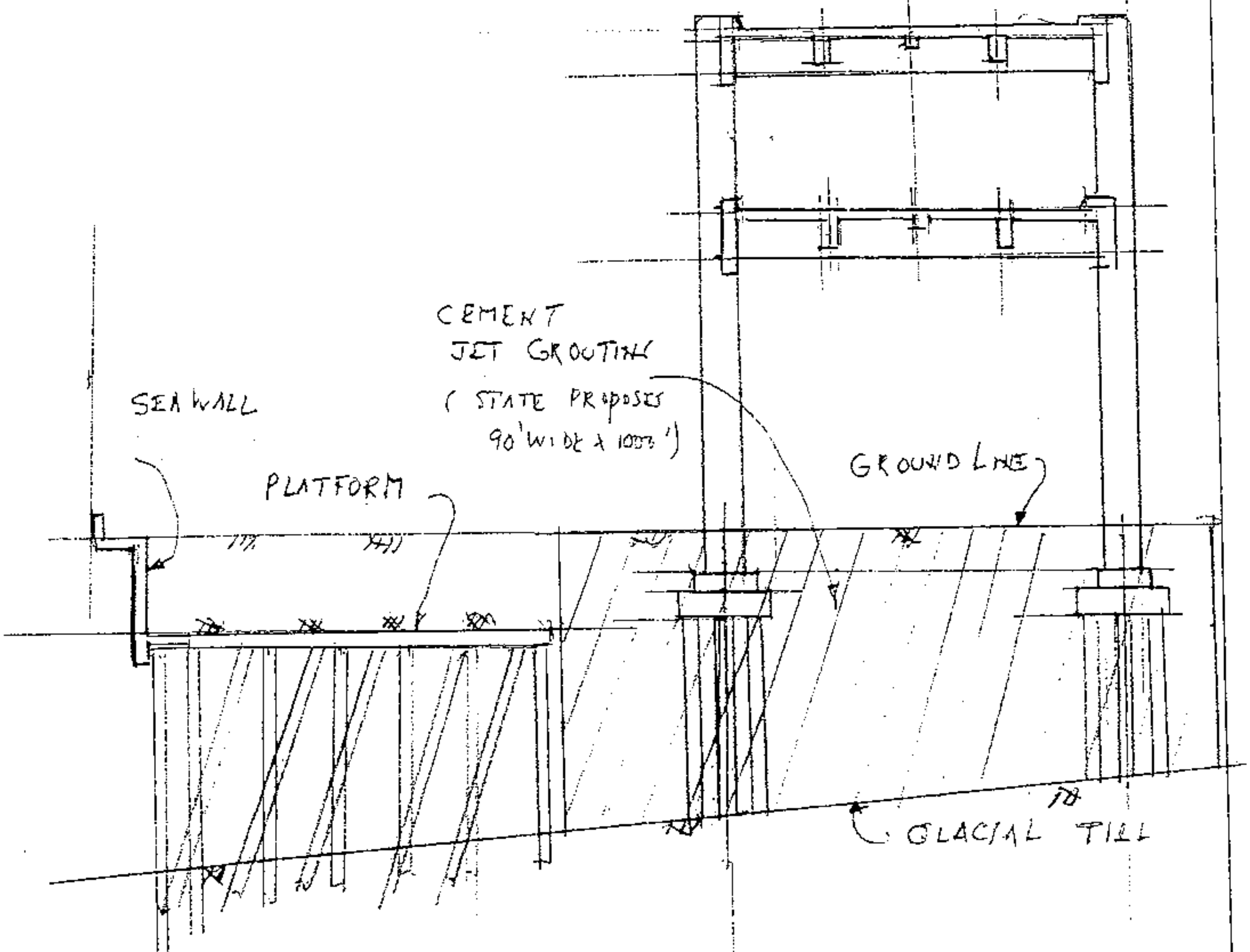

SECTION @ GRAVITY SEA WALL (NEAR YESLER) BENT 96

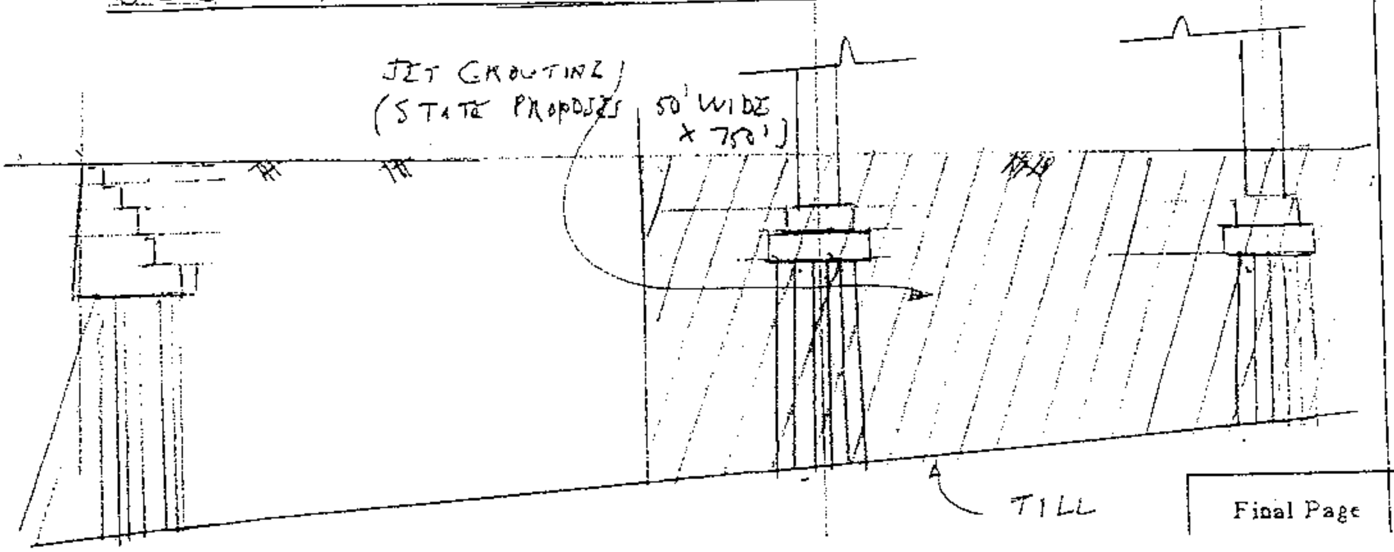

Final Page

CROSS SECTION @ SINGLE DECKS @ BENT 36

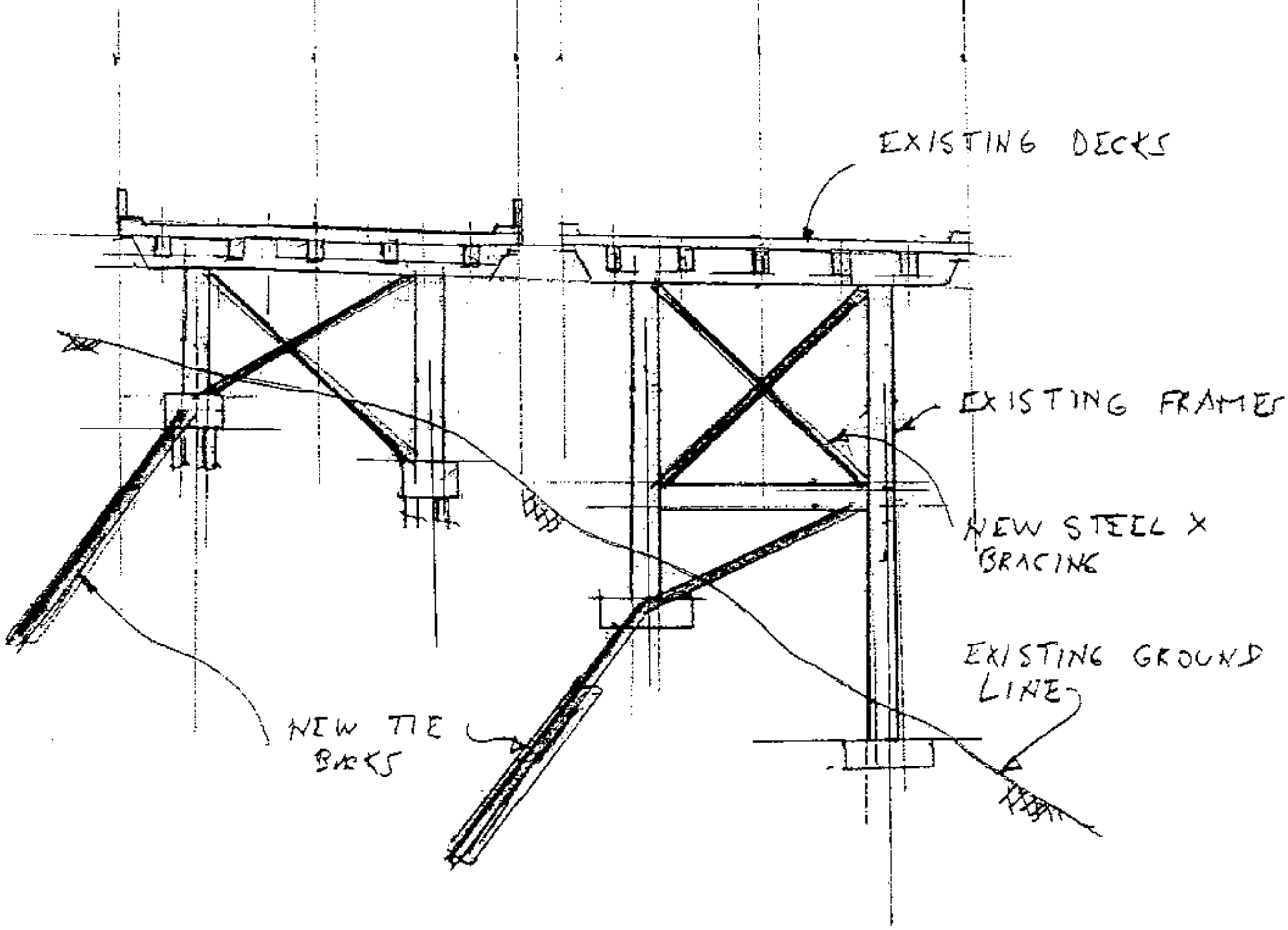

BENT 36

APPENDIX D

EVALUATION OF MODIFIED PROPOSAL BY MIYAMOTO

INTRODUCTION

Miyamoto International of Sacramento, California has proposed retrofitting the Alaskan Way Viaduct (shown in Figure D.1.) with fluid viscous dampers at the request of Victor Gray, et al. This review for the Washington State Department of Transportation (WSDOT) summarizes the results of an independent evaluation of the effectiveness of Miyamoto's proposal.

The viaduct consists of independent structural units comprising three bays each. A typical unit consists of four transverse frames that support longitudinal edge girders and stringers on two levels. Transverse sub-floorbeams connect the girders and the stringers on each level. The reinforced concrete deck is monolithic with all these members, on each level. With respect to earthquakes, the viaduct has several critical structural deficiencies [D.2]:

- The reinforcing bar splices in the lower-level columns may fail in flexure.
- Both the upper and lower-level joints are vulnerable to degradation from high diagonal tensile stresses; they may fail before the adjacent members hinge. Reinforcing details in these regions also are brittle, and subject to sudden failure after cracking of the concrete.
- The shear strength of the lower-level columns is marginal; they might fail in shear before reaching their flexural capacity.
- Both the upper and lower-level columns have inadequate confining reinforcement.
- The footings could fail if the columns do not.

Miyamoto's proposal includes the following retrofit measures [D.5]:

- "Add fluid viscous dampers to interior bays of viaduct frames.
- Add shock-transmission units between the frames in longitudinal direction.
- Increase shear capacity, confinement, and reinforcement splice length of existing columns by wrapping the columns in ductile fiber wraps.
- Increase the shear capacity of joints by either added cap concrete bolsters and drill-and-bond reinforcement or by prestressing (Optional)."

The arrangement of fluid viscous dampers proposed by Miyamoto is illustrated in Figure D.2.

This review of Miyamoto's proposal is brief; additional detail regarding the existing structure, the seismic hazard, and our evaluation methodology may be found in the main body of the report.

EVALUATION CRITERIA

Like Gray's proposal, Miyamoto's proposal was analyzed for three levels of seismic hazard. These are listed in Table D.1, along with the corresponding performance criteria.

Table D.1, Seismic Hazard and Performance Criteria		
Seismic Hazard		Damage Allowed
Event	Return Period, years	
Expected	108	Minimal
Design	500	Repairable
Rare	2500	Significant

The seismic hazard was established by Shannon & Wilson for the Alaskan Way Viaduct and Seawall Replacement Project [D.8], except that the design event was established specifically for the evaluation of Gray's proposal. Acceleration spectra for the expected and rare events are shown in Figure D.3a; acceleration spectra for the design event are shown in Figure D.3b. The spectra are for two generic soil profiles that represent the varying soil conditions along the alignment of the structure.

The rational for the performance criteria for the different events are given in the main body of the report. Significant damage is allowed in the rare event, but the risk of collapse should be minimal. Technical criteria (allowable material strains, etc.) corresponding to the three damage states are given in the main body of the report. The methods used for evaluation are generally those established by Priestly, et al. [D.7].

MODELING AND ANALYSIS

The evaluation was based on time history analysis of a three-dimensional model of Bents 151-154 of the viaduct (a typical WSDOT unit). The model used is shown in Figure D.2, including both the viaduct and the dampers. The model was constructed using the ADINA [D.1] general-purpose finite element program. The model was constructed from scratch from Drawings 7, 43, 44, & 45 (of 136) of Contract Number 5262 of the project.

The columns, floorbeams, and edge girders were all modeled with inelastic moment-curvature elements. The moment-curvature response of sections was computed using the computer program XTRACT [D.3]. Moment-curvature calculations were performed for all variations in reinforcement of the members and the various relationships were applied to different elements with due consideration of bar cut-offs and development lengths.

The membrane stiffness of the upper and lower decks was modeled with elastic shell elements. The tee and knee joints at the juncture of the columns, floorbeams, and edge girders were modeled with elastic beam elements between the geometric center of the joints and the faces of the respective members. The piles supporting the structure were modeled with individual truss elements. Because the piles are not connected to the footings to resist tensile forces, truss elements with gaps were used to allow separation of the footings from the piles.

Miyamoto doesn't give the parameters of the fluid viscous dampers that are the basis of his proposal. For our evaluation we assumed that all of the dampers (both longitudinally and transversely) were defined by the following force-velocity relationship:

$$F = 700 \frac{kip \cdot \sec^{0.1}}{ft^{0.1}} \cdot V^{0.1} , \tag{5}$$

The damper coefficient was obtained by iteration so as to obtain peak damper forces of the same order of magnitude as those reported by Miyamoto. The damper exponent was chosen to try to reproduce the small damper displacements reported by Miyamoto.

The dead and modal properties of the model are summarized in the main body of the report. Our evaluation of Miyamoto's proposal was based on time history analysis for a suite of ground motions. Three ground motions were used corresponding to each of Zones A and B, for each seismic hazard level [D.8]. The results presented below are the controlling results over the six ground motions, for the design and rare seismic hazard levels.

RESULTS

Structure Drift

For the rare earthquake, the peak transverse drifts of the *existing* structure are summarized in Table D.2.[9]

Table D.2, Transverse Drift, Existing Structure, feet

Bent	Level		
	Lower	**Upper**	**Total**
End	1.66	1.02	2.78
Middle	1.63	0.97	2.72

The table shows the peak relative displacement of the lower level of the structure with respect to the foundation, the peak relative displacement of the upper level of the structure with respect to the lower level, and the peak relative displacement of the upper level of the structure with respect to the foundation.

For the rare earthquake, the drift of the retrofitted structure is shown in Figure D.4.[10] The peak *transverse* drifts are summarized in Table D.3; the reductions in drift from the existing structure are shown in parentheses.

Table D.3, Transverse Drift, Retrofitted Structure, feet

Bent	Level		
	Lower	**Upper**	**Total**
End	0.59 (65%)	0.34 (67%)	0.95 (66%)
Middle	0.56 (66%)	0.34 (65%)	0.92 (66%)

All of these demands are significantly larger than those reported by Miyamoto [D.5]. The reason for this is not known; it may be related to that fact that Miyamoto's model was linear, whereas the model used for the present evaluation is both materially and geometrically nonlinear. The reduction in demand with the

---

[9] Run existing.06

[10] Run miyamoto.08

addition of dampers is also less than reported by Miyamoto. The reduction in demand in Table D.3 is about 65% whereas Miyamoto reports a reduction in demand of 78%.

The demands summarized in Table D.3 may be compared with the results of pushover analyses performed using the computer program CAPP [D.4]. Pushover analyses were performed for a typical end bent and a typical middle bent. The columns and floorbeams were modeled with concentrated hinges at their ends. The model also included inelastic elements modeling jacketed sections of the lower level columns, and the columns splices immediately above the lower deck. (The pushover analysis assumed retrofit following Gray's proposal—see the main body of the report.) A degrading moment-rotation relationship was used for the splice elements. The results of the pushover analyses are summarized in Table D.4:

Table D.4, Pushover Analysis Results, Displacement Capacities -Transverse Direction

Bent	Level	Capacity, feet	Failure	Note
End	Upper	0.38	Splice	Push @ lower; restraint @ upper
		0.49	U. floorbeam	Push @ upper; restraint @ lower
	Total	1.32	L. floorbeam	Force split 60/40 @ upper/lower levels
Middle	Upper	0.33	Splice	Push @ lower; restraint @ upper
		0.38	U. floorbeam	Push @ upper; restraint @ lower
	Total	0.85	L. floorbeam	Force split 60/40 @ upper/lower levels

There is no definite result for the displacement capacity of the upper level of the structure (relative to the lower level) from the pushover analysis. This is because there are multiple ways in which to perform the pushover. Nevertheless, the results are indicative of the magnitude of the displacement capacity and possible failure modes.

Comparing the drift demands for the rare earthquake with the calculated displacement capacity of the structure, it may be seen that the total demand exceeds the capacity of the middle bents; the demand capacity ratio is 0.92/0.85=1.08. This indicates that the lower floorbeams will fail during a rare event.

The pushover analysis described in this section has some limitations. As mentioned already, there is no definitive way to perform the pushover of a two level structure. Also, the pushover analysis assumed that the axial forces in the columns were constant, and equal to the dead load axial forces. These are significant limitations. The time history analysis results presented in subsequent sections do not suffer from these limitations.

For the design earthquake, the drift of the retrofitted structure is shown in Figure D.5.

Columns

For the rare earthquake, the curvature ductility demands on the columns are summarized in Figure D.6. The plots show that plastic hinges form in the tops and bottoms of the columns, in both levels of the structure and in both directions. In the upper level columns of the end bents, the hinges don't form at the very tops of the columns because there is additional main reinforcement at this location. The hinges form at a weaker section a few feet from the tops of the columns.

To evaluate the ratio of demand to capacity of the columns it is more meaningful to refer to Figures D.7 and D.8, however. For the end and middle bents, respectively, these are plots of simultaneous curvature and axial force demands versus capacity curves. Plots are shown for each variation of reinforcing occurring in each type of bent, and for each direction of motion. The designation "Columns.End.B.16," for instance, refers to section B on the drawings, with 16 main reinforcing bars. As shown in Figures D.7 and

D.8 the curvature capacity of a section is a function of the axial force acting on it. The capacity decreases with increasing axial force because the controlling failure criterion is the ultimate concrete strain.

Figure D.8 shows that the flexural demands on the middle columns slightly exceed the capacity in the longitudinal direction, for the section designated “Columns.Middle” (the typical section). (In design, one would insist of a significant margin between the calculated demands and the capacity, to compensate for uncertainty in either analysis or capacity evaluation.) Figures D.7 and D.8 compare the demands to the capacity of the *existing* structure. Miyamoto’s proposal does include improvement of the flexural and shear capacity of the columns by wrapping them with ductile fiber wraps. The results presented herein indicate that some such retrofit is required. We have not evaluated the effectiveness of retrofit with fiber wrap, however.

For the design earthquake, the curvature ductility demands on the columns are summarized in Figure D.9. These demands are consistent with repairable damage. Some degradation of the reinforcing bar splices in the upper columns may be expected unless the columns are retrofitted, say with fiber wrap.

Floorbeams

For the rare earthquake, the curvature ductility demands on the floorbeams are summarized in Figure D.10. There are separate plots for the upper and lower level floorbeams, and positive ($\cup$) and negative ($\cap$) demands are plotted separately. The plots show that plastic hinges form at the faces of the columns.

Plots of simultaneous curvature and axial force demands on the floorbeams are shown in Figure D.11; there are separate plots for the upper and lower level floorbeams. The capacity curves are represented by clusters of points along the curvature axes (for axial forces of zero). This is because the capacities of the various floorbeams sections are nearly the same, and because the capacity was only calculated for an axial force of zero (because the axial forces in the floorbeams are modest).

Figure D.11 indicates that the floorbeams will fail in flexure—in negative bending near one of the columns. This same failure was predicted by the pushover analysis described previously. A demand/capacity ratio of 1.08 was obtained for the middle bents from that analysis. A similar ratio may be inferred from Figure D.11b.

For the design earthquake, the curvature ductility demands on the floorbeams are summarized in Figure D.12. The largest demands are large enough to cause significant cracking and yielding of reinforcement, but within the limits for repairable damage provided that there is not major degradation in development of reinforcing details.

Knee Joints

In the transverse direction, principal tensile stresses in the (upper level) knee joints were computed from the peak moments in the floorbeams. The computed values of principal tensile stress are summarized in Table D.5, where they have been normalized by $\sqrt{f_c'}$ (psi units).

Table D.5, Knee Joint Principal Tensile Stresses, Normalized			
Event	**Bent**	**Direction**	**Normalized Stress**
Rare	End	Longitudinal	
		Transverse	5.2
	Middle	Longitudinal	
		Transverse	4.5
Design	End	Longitudinal	
		Transverse	3.7
	Middle	Longitudinal	
		Transverse	3.5

For the rare earthquake, the principal tensile stresses may be compared with $5.0\sqrt{f_c^{'}}$ (psi units), above which degradation of the joints may be expected. The calculated stresses are marginally acceptable.[11] For the design earthquake, the principal tensile stresses are all about $3.5\sqrt{f_c^{'}}$ (psi units), so joint damage may be repairable, in WSDOT design units. Any existing cracks are likely to be widened. In SED designed units, the noted marginal reinforcing details (welded rebar laps) can be expected to fail at the design demand level.

Miyamoto's proposal does (optionally) include the addition of either concrete bolsters and drill-and-bond reinforcement or prestressing to increase the shear capacity of the joints [D.5]. This would appear to be warranted, especially for the SED designed units.

Piles

There is little information available regarding the capacity of the piles supporting the structure. As described in [8] the piles were assumed to have a capacity of 120 kips for the purpose of tabulating demand/capacity ratios. The peak compressive forces in the piles are summarized in Table D.6. The tensile forces were zero since the structure was allowed to uplift from the piles, which aren't anchored to the footings.

---

[11] In the structures designed by the Seattle Engineering Department the top reinforcing bars in the upper level floorbeams are bent down within the knee joints and welded to the column bars. These bars are all 1-½ inch square bars. This detail is particularly vulnerable to joint shear stress, as evidenced by the fracture of some of these bars and welds at Bent 100 during the Nisqually earthquake. At the stress levels reported in Table D.5 for the rare earthquake, splice failure is likely, with consequent degradation of joint strength and stiffness. This detail is a worrisome feature of the SED portion of the viaduct, even for the expected event.

Table D.6, Pile Compressive Forces and D/C Ratios			
Event	**Bent**	**Force, kip**	**D/C**
Rare	End	310	2.6
	Middle	540	4.5
Design	End	210	1.7
	Middle	270	2.3

The demands on the end bents are less meaningful than the demands on the middle bents because the analysis was of a single unit only. Although the dead load of the adjacent units was included on the end footings, the dynamic effect of the adjacent units was missing in the analysis.

For the rare event, the computed demands are suggestive of severe damage to the foundations of the viaduct. This is damage exceeding the acceptable limits for significant damage, and possibly leading to collapse of the structure. The computed demands for the design event exceed the acceptable limits for repairable damage to the structure.

The lateral capacity of the foundations was estimated to be about 300 kips for the end bents and about 500 kips for the middle bents. For the middle bents only, the peak lateral forces on the foundations are summarized in Table D.7.

Table D.7, Foundation Lateral and Demand/Capacity Ratios			
Event	**Direction**	**Force, kip**	**D/C**
Rare	Longitudinal	660	1.3
	Transverse	660	1.3
Design	Longitudinal	540	1.1
	Transverse	570	1.1

Footings

The middle footings of the structure were evaluated for shear, flexure, column bar anchorage, and joint shear using the pile forces reported in the previous section.

For the rare earthquake, the computed demand/capacity ratio for beam shear was 4.0. The computed demand/capacity ratio for flexure of the footings was 2.2. The column bars are adequately anchored if the footing remains intact. But, because significant footing damage is indicated, the anchorage of the bars was evaluated using the splitting strength methodology of Priestley [D.6]. The computed demand/capacity ratio was then 1.3. The peak principal tensile stress induced in the column/footing joints by flexure of the columns was estimated to be $2.9\sqrt{f_c^{'}}$ (psi units). In aggregate, these demand/capacity ratios indicate that the footings would be severely damaged in a rare earthquake, in excess of limits for significant damage.

For the design earthquake, the computed demand/capacity ratio for beam shear was 2.8. The computed demand/capacity ratio for flexure of the footings was 1.5. The peak principal tensile stress induced in the column/footing joints by flexure of the columns was estimated to be $2.1\sqrt{f_c^{'}}$ (psi units). In aggregate, these demand/capacity ratios imply severe damage to the footings in a design earthquake, in excess of the limits for repairable damage. Foundation retrofit would, therefore, be required.

Dampers

For the rare and design events the computed damper demands are shown in Table D.8.

Table D.8, Damper Forces and Strokes[12]			
Event	**Direction**	**Force, kip**	**Stroke, in**
Rare	Longitudinal	770	4.8
	Transverse	740	3.6
Design	Longitudinal	700	1.2
	Transverse	700	1.6

For the rare event, the peak damper forces are similar to those reported by Miyamoto [5]. However, the peak strokes are significantly larger (2-2½ times) than those reported by Miyamoto. This same phenomenon was observed for the drift of the structure. The difference may be related to that fact that Miyamoto's model was linear, whereas the model used for the present evaluation is both materially and geometrically nonlinear.

The peak damper forces for the design event are not much less than those for the rare event. This is due to the nature of the dampers, which have a low exponent. Very little velocity (and displacement) is needed to produce a large force in the dampers. The computed forces imply a physically large damper, with a diameter of approximately 21 inches.

SUMMARY

1. Analytical review of Miyamoto's proposal [D.5] using nonlinear time history analysis indicates that performance of the system will be less effective than indicated in Miyamoto's report.
2. Miyamoto supplements his damper retrofit with a variety of significant additional retrofit items for a comprehensive retrofit, including:
   a. Wrapping columns with ductile fiber wraps.
   b. Adding cap concrete bolsters and drill-in joint reinforcement.
   c. Add geotechnical evaluation, and presumably general ground improvement (or related foundation retrofit).
3. Miyamoto's evaluation does not include foundation elements, which omits review of a major vulnerability of the structure. There is no consideration of soil liquefaction, pile connections, potential uplift, or the potential effects of ground improvement (Gray's proposal) on the effective ground motion.
4. There is also no consideration of the additional elements of foundation work in Miyamoto's proposal, which include utilities and the sea wall.
5. Miyamoto's evaluation is based on an inadequate performance standard, which is stated in the report to be simply achieving the response of the structure to the Nisqually event. That performance does not meet any codified design standard, and there is no assurance that subsequent exposure to an earthquake like the Nisqually event will not result in far greater accumulated damage to the Viaduct.
6. Miyamoto's evaluation states that the review does not consider remaining service life, adequacy of the level of service, maintenance costs, or any underlying cost-benefit of retrofit vs. replacement. No judgment can be made without these issues included.

[12] The damper strokes tabulated are in a single direction (plus or minus), the total strokes are twice the tabulated values.

7. Damper-Viaduct member connection details are not provided in Miyamoto's proposal, but their performance and details are essential to both the feasibility and/or effectiveness of the proposal and to any cost estimate. Additional strengthening of existing members may be necessary in order to support the damper system.
8. Seismic retrofit strategies of major multi-span bridges with the use of response modification devices such as the fluid viscous dampers utilized in Miyamoto's proposal are usually only economically viable if the need for retrofit of structural members is minimized or completely eliminated. According to the Miyamoto's own conclusions, this is not the case for the Viaduct, as it will likely need the following:
   a. Joints and members need additional reinforcement and confinement since new load paths are introduced.
   b. Potential brittle mechanisms, such as those caused by joint shear failure, need to be identified. This is particularly important for major double deck concrete viaducts.

REFERENCES

D.1. ADINA R&D, Inc., ADINA Theory and Modeling Guide, www.adina.com.

D.2. Eberhard, M.O., De la Colina, J., & Ryter, S., "Seismic Vulnerability of the Alaskan Way Viaduct: WSDOT Typical Unit, Washington State Transportation Center, June, 1995.

D.3. Imbsen & Associates, cross-sectional X sTRuctural Analysis of ComponenTs (XTRACT), www.imbsen.com/xtract.htm.

D.4. Imbsen & Associates, Capacity Analysis Pushover Program (CAPP), www.imbsen.com/capp.htm.

D.5. Miyamoto International, Inc., "Proposed Retrofit of Alaskan Way Viaduct Using Fluid Viscous Dampers: Preliminary Phase," July 5, 2006.

D.6. Priestley, M.J.N., Seible, F. & Chai, Y.H., Design Guidelines for Assessment, Retrofit and Repair of Bridges for Seismic Performance," Report No. SSRP-92/01, Department of Applied Mechanics and Engineering Sciences. University of California, San Diego, August, 1992.

D.7. Priestley, M.J.N., Seible, F. & Calvi, G.M., Seismic Design and Retrofit of Bridges, John Wiley & Sons, 1996.

D.8. Shannon & Wilson, "Alaskan Way Viaduct and Seawall Replacement Project, Ground Motion Study Report," October, 2004.

LIST OF FIGURES

List of Figures

FIGURES

Figure D.1 Alaskan Way Viaduct

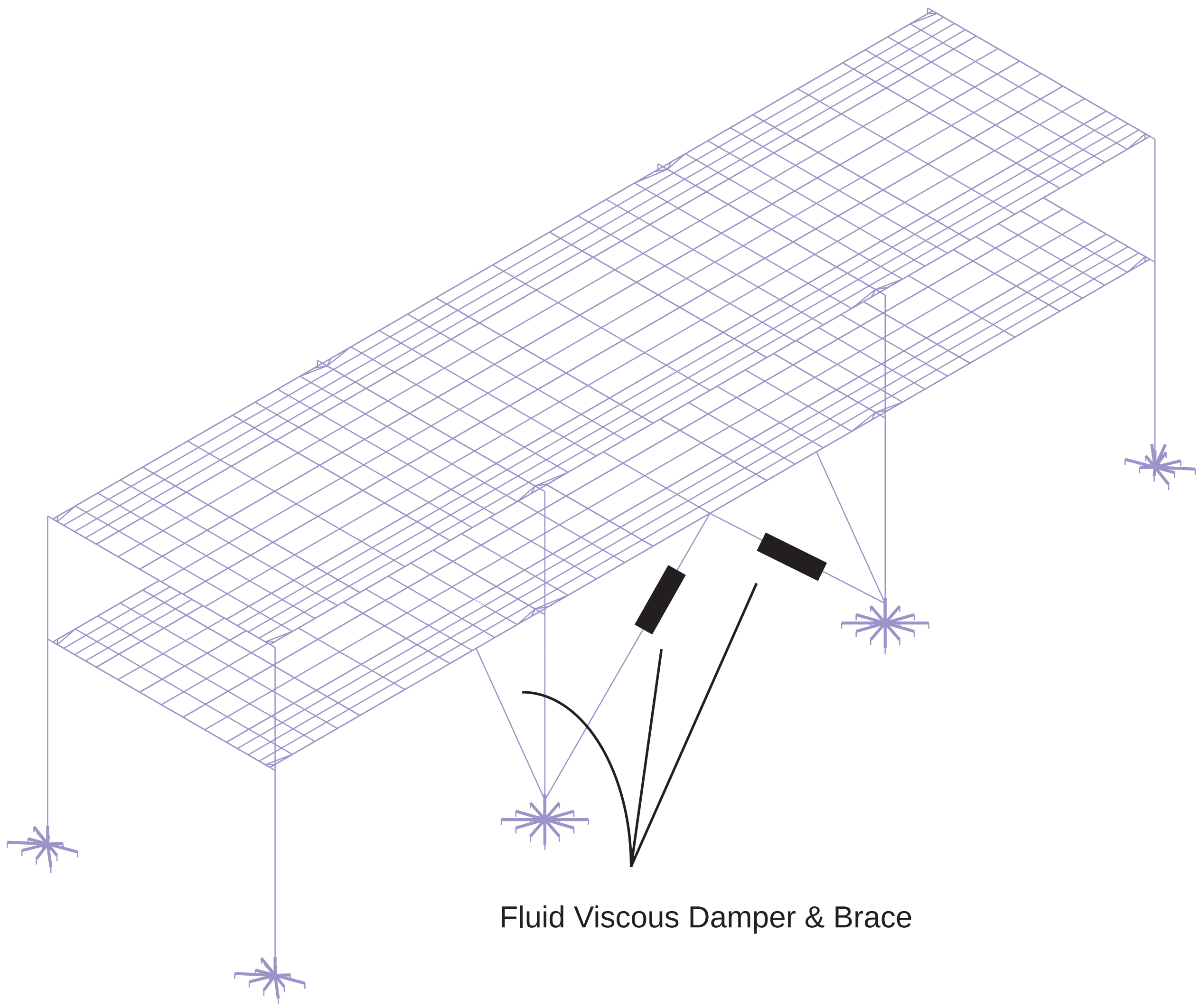

Figure D.2, Retrofit using fluid viscous dampers according to Miyamoto's proposal

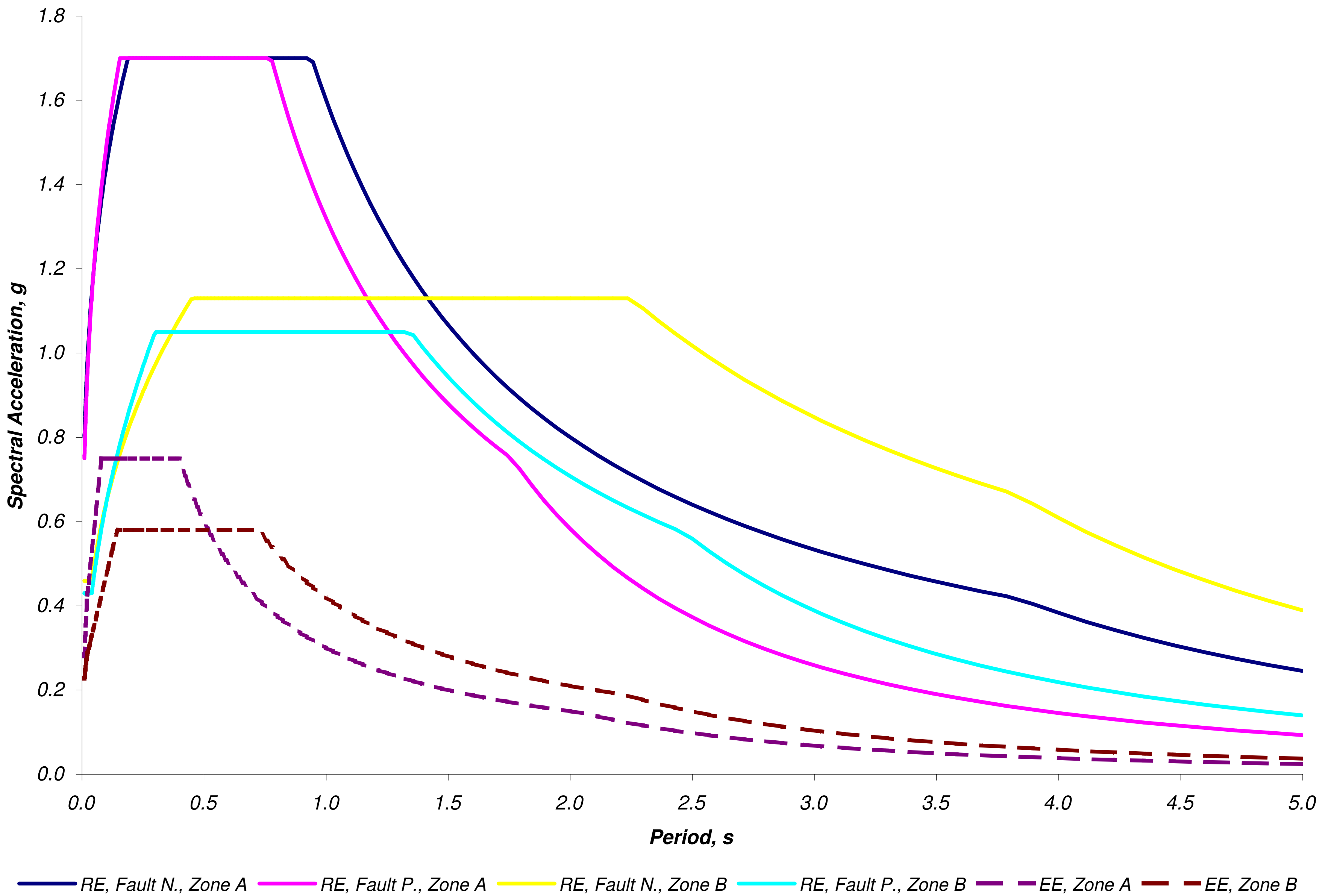

Figure D.3a, Acceleration spectra for horizontal motions, rare and expected earthquakes

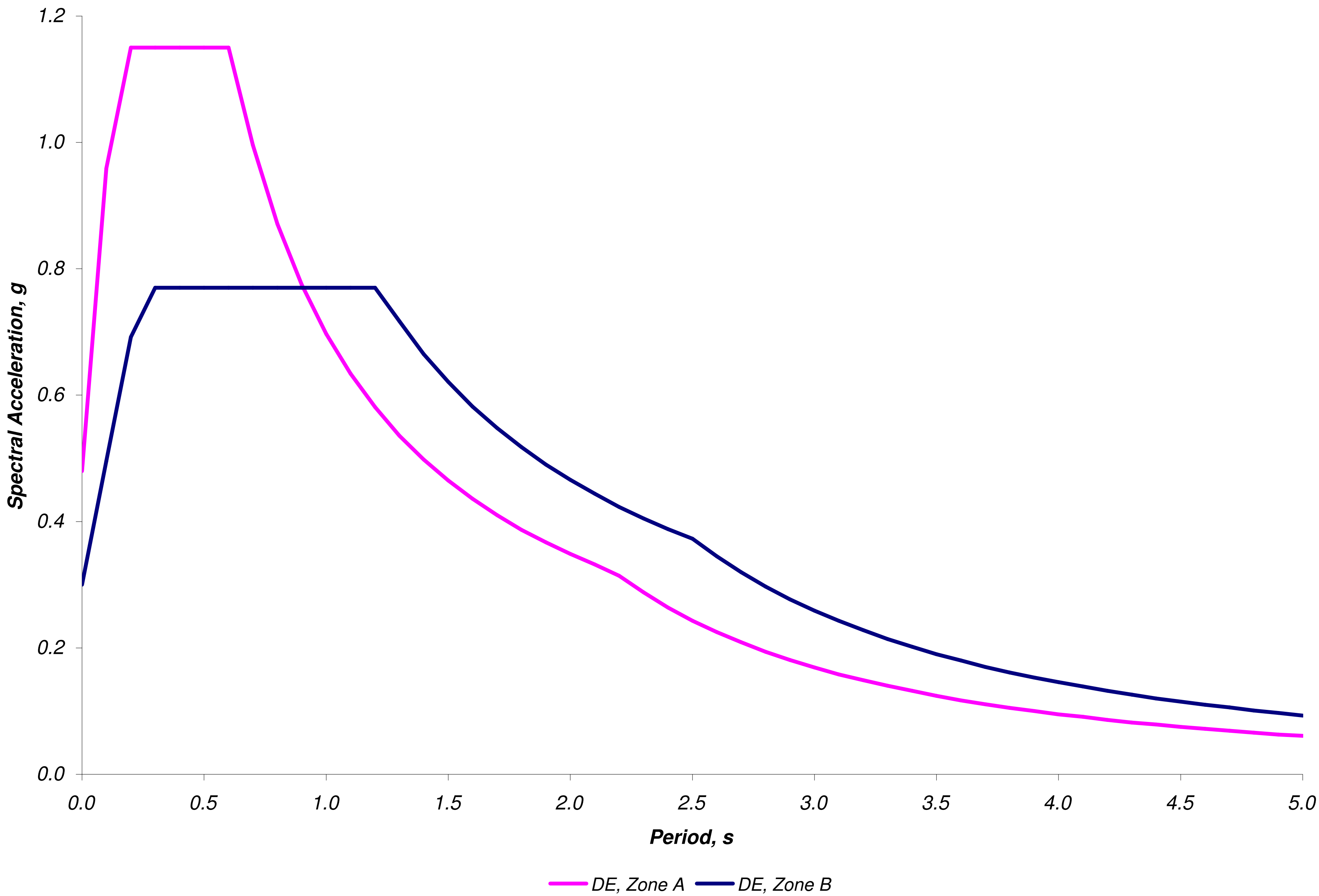

Figure D.3b, Acceleration spectra for horizontal motions, design earthquake

Model Name:	miyamoto.08	**Absolute Drifts**
Model Description:	Alaska Way Viaduct, Evaluation of Miyamotos Proposal	
Model Variation:	rare earthquake	31 Jul 06 10:46 AM

Longitudinal

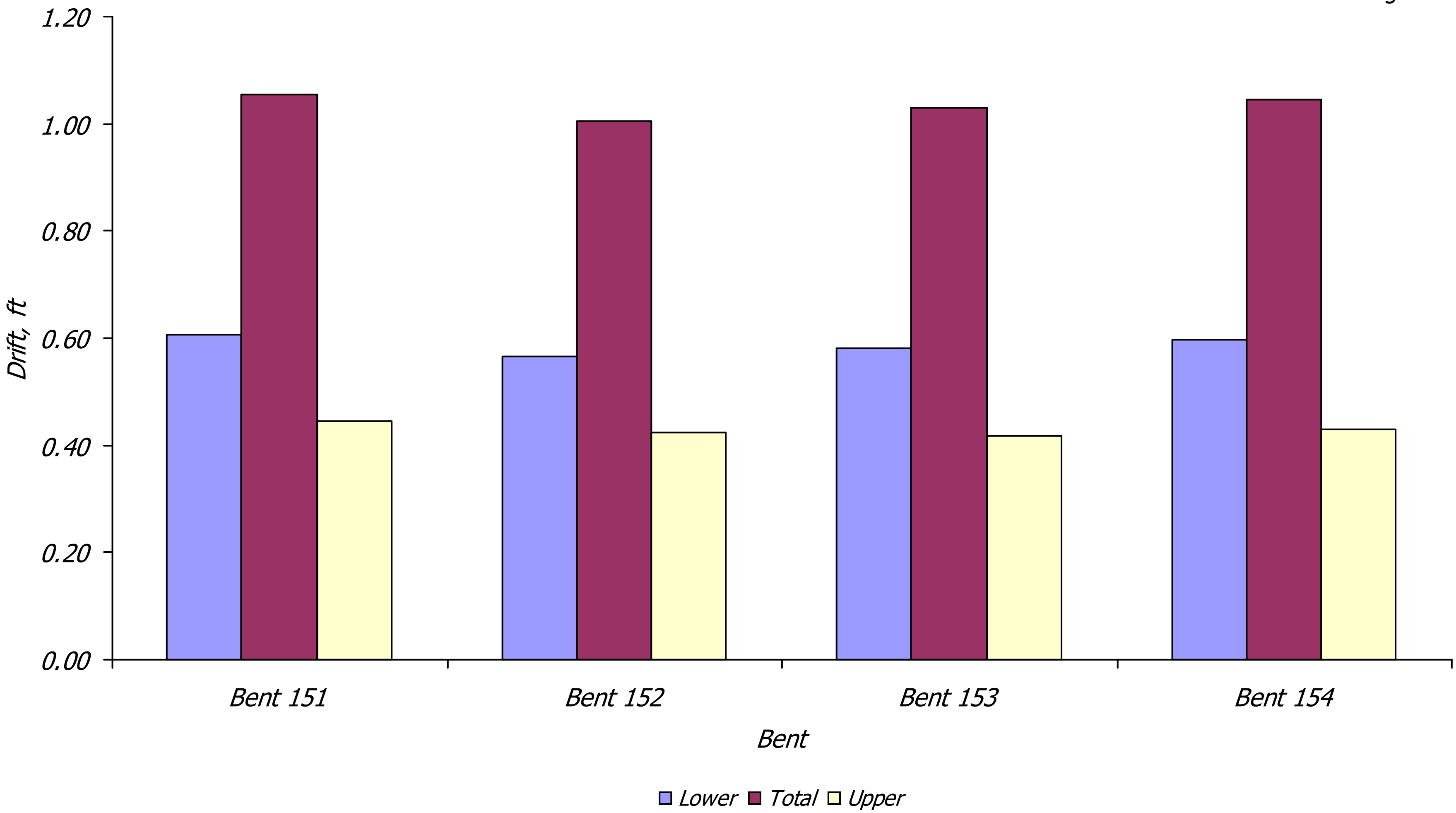

Figure D.4a Drift of retrofitted structure, rare earthquake, longitudinal direction

Model Name:	miyamoto.08	**Absolute Drifts**
Model Description:	Alaska Way Viaduct, Evaluation of Miyamotos Proposal	
Model Variation:	rare earthquake	31 Jul 06 10:46 AM

Transverse

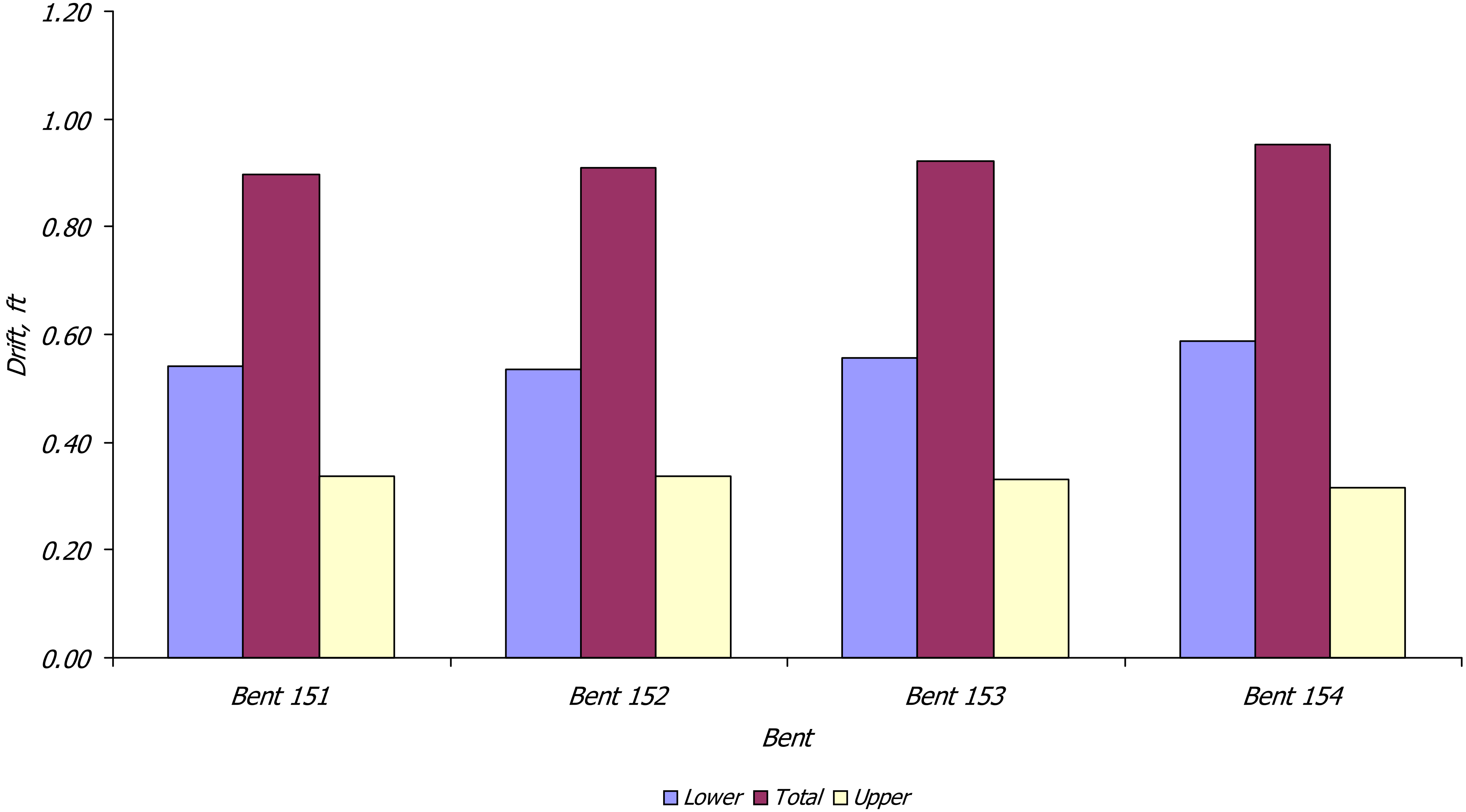

Figure D.4b Drift of retrofitted structure, rare earthquake, transverse direction

Model Name:	miyamoto.08	**Absolute Drifts**
Model Description:	Alaska Way Viaduct, Evaluation of Miyamotos Proposal	
Model Variation:	design earthquake	31 Jul 06 10:45 AM

Longitudinal

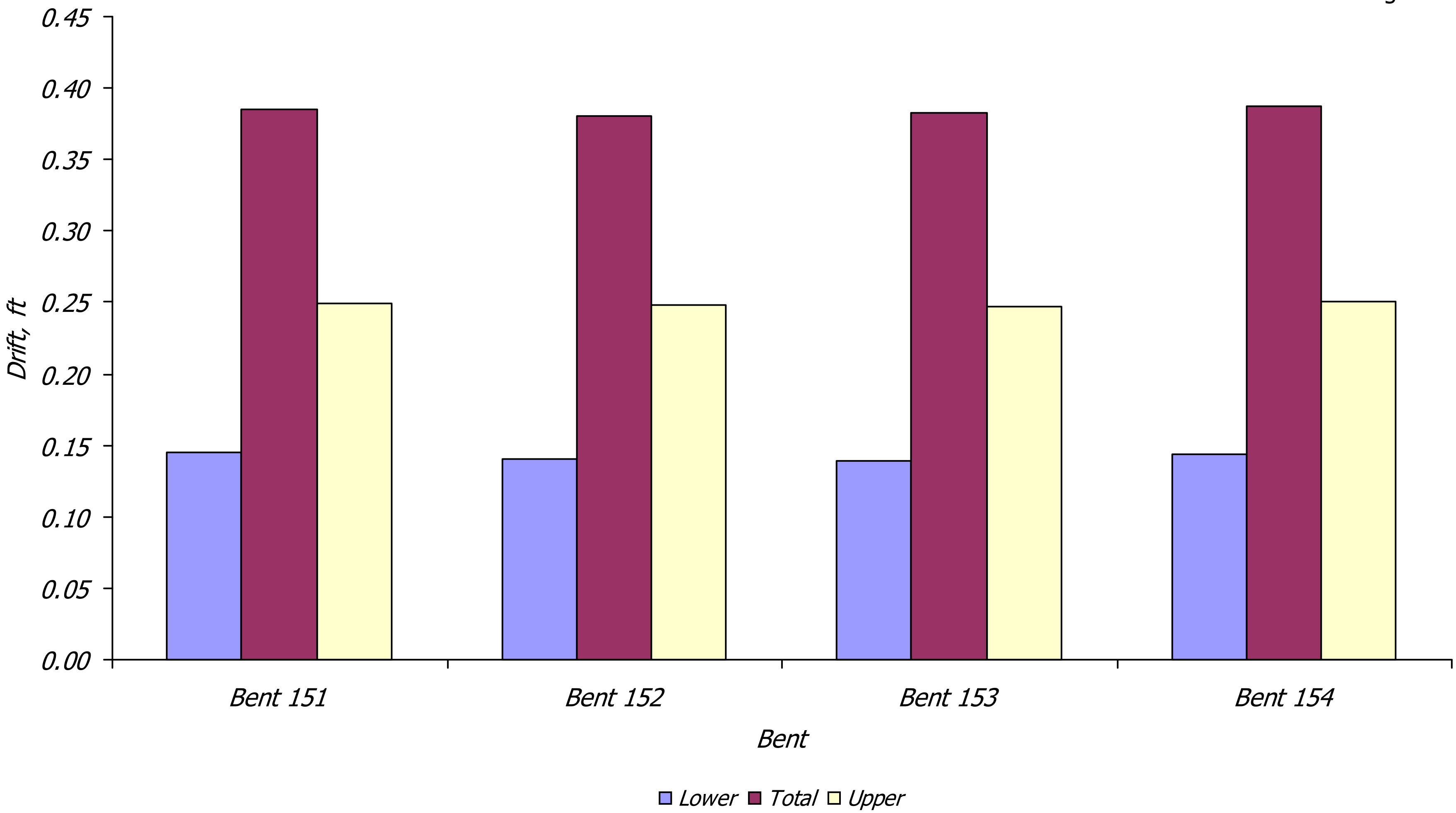

Figure D.5a Drift of retrofitted structure, design earthquake, longitudinal direction

Model Name: miyamoto.08

Absolute Drifts

Model Description: Alaska Way Viaduct, Evaluation of Miyamotos Proposal

Model Variation: design earthquake

31 Jul 06 10:45 AM

Transverse

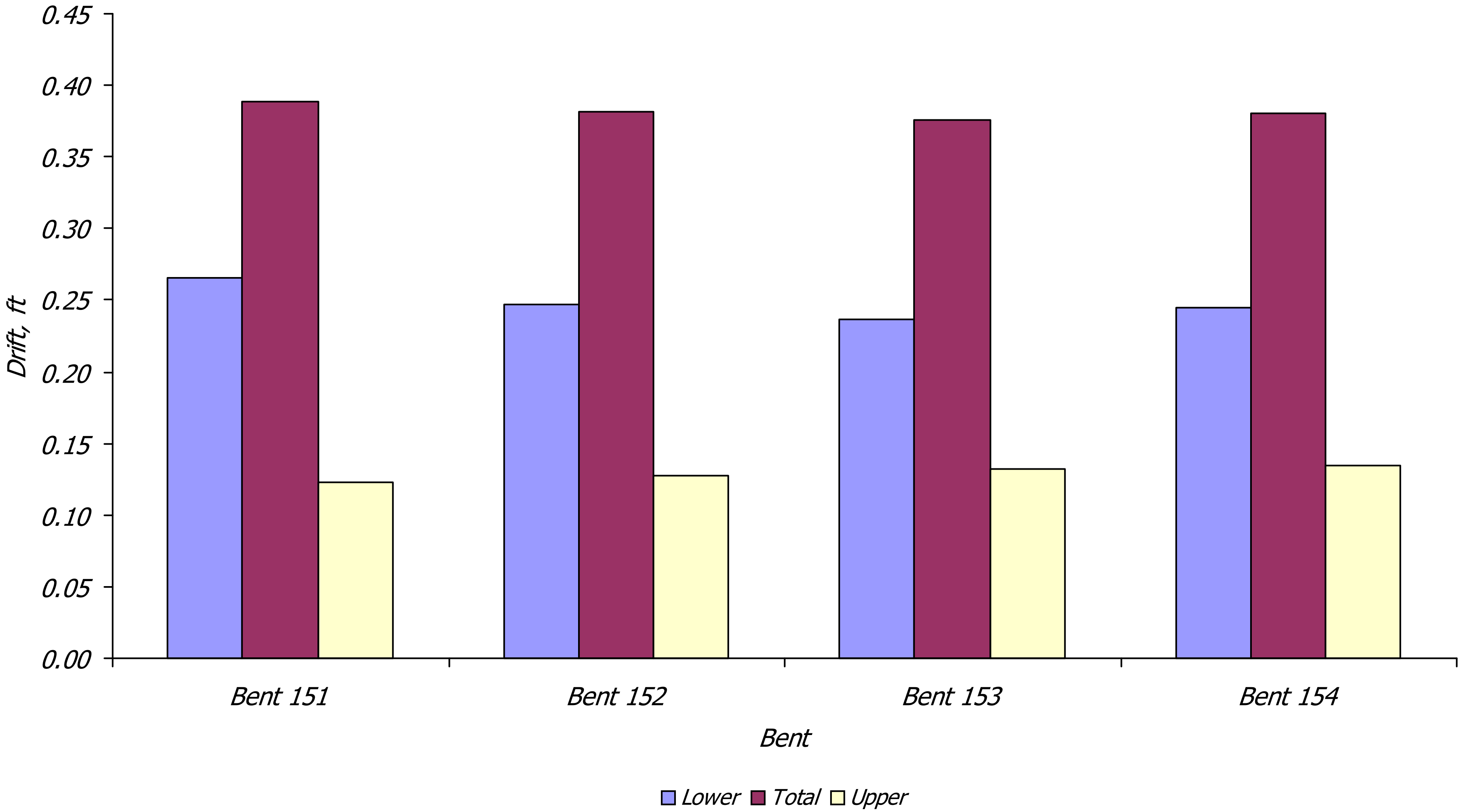

Figure D.5b Drift of retrofitted structure, design earthquake, transverse direction

Model Name: miyamoto.08

Column Curvature Ductility Demand

Model Description: Alaska Way Viaduct, Evaluation of Miyamotos Proposal

Model Variation: rare earthquake

31 Jul 06 10:48 AM

Longitudinal Direction

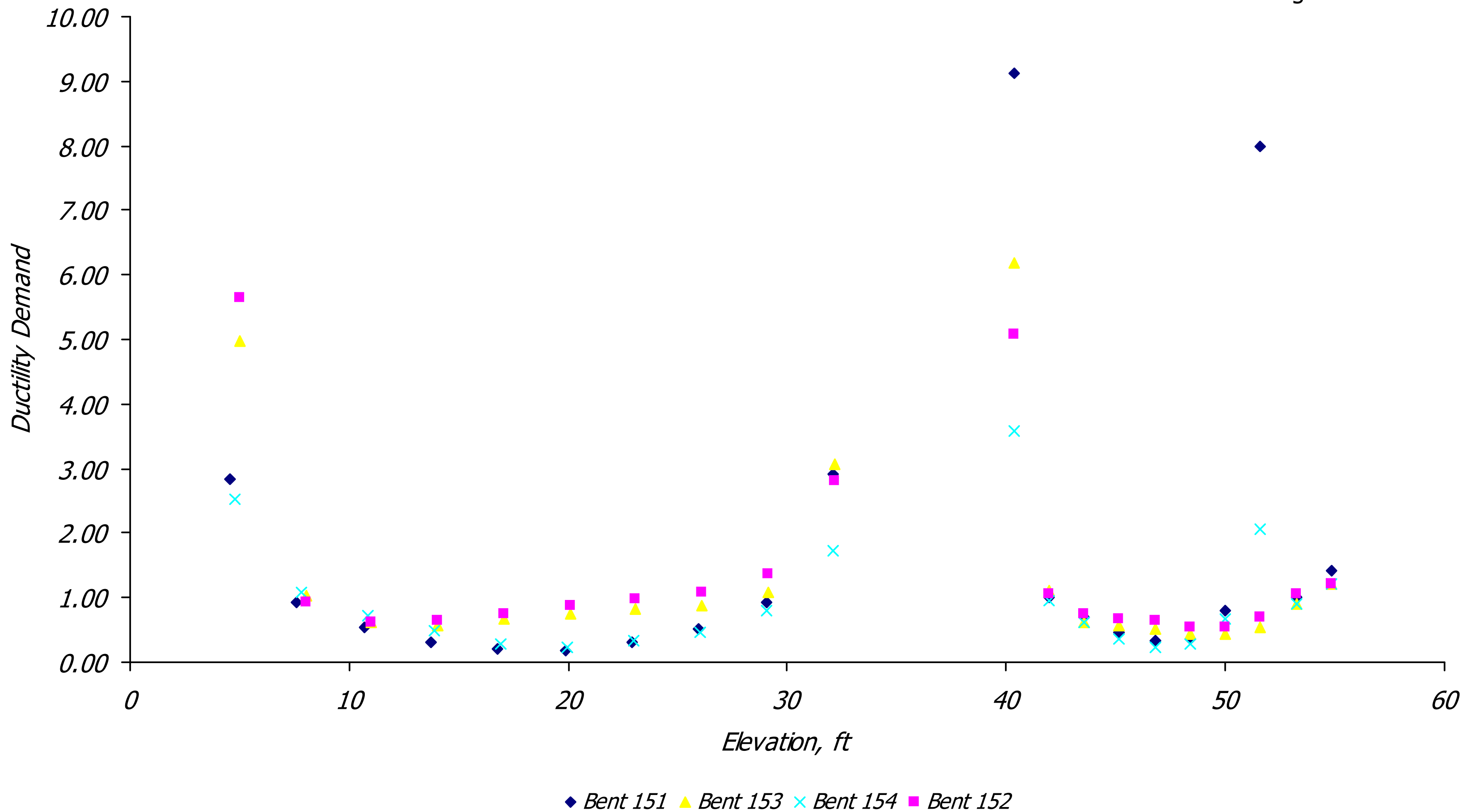

Figure D.6a Column curvature ductility demand, retrofitted structure, rare earthquake, longitudinal direction

Model Name: miyamoto.08

Column Curvature Ductility Demand

Model Description: Alaska Way Viaduct, Evaluation of Miyamotos Proposal

Model Variation: rare earthquake

31 Jul 06 10:48 AM

Transverse Direction

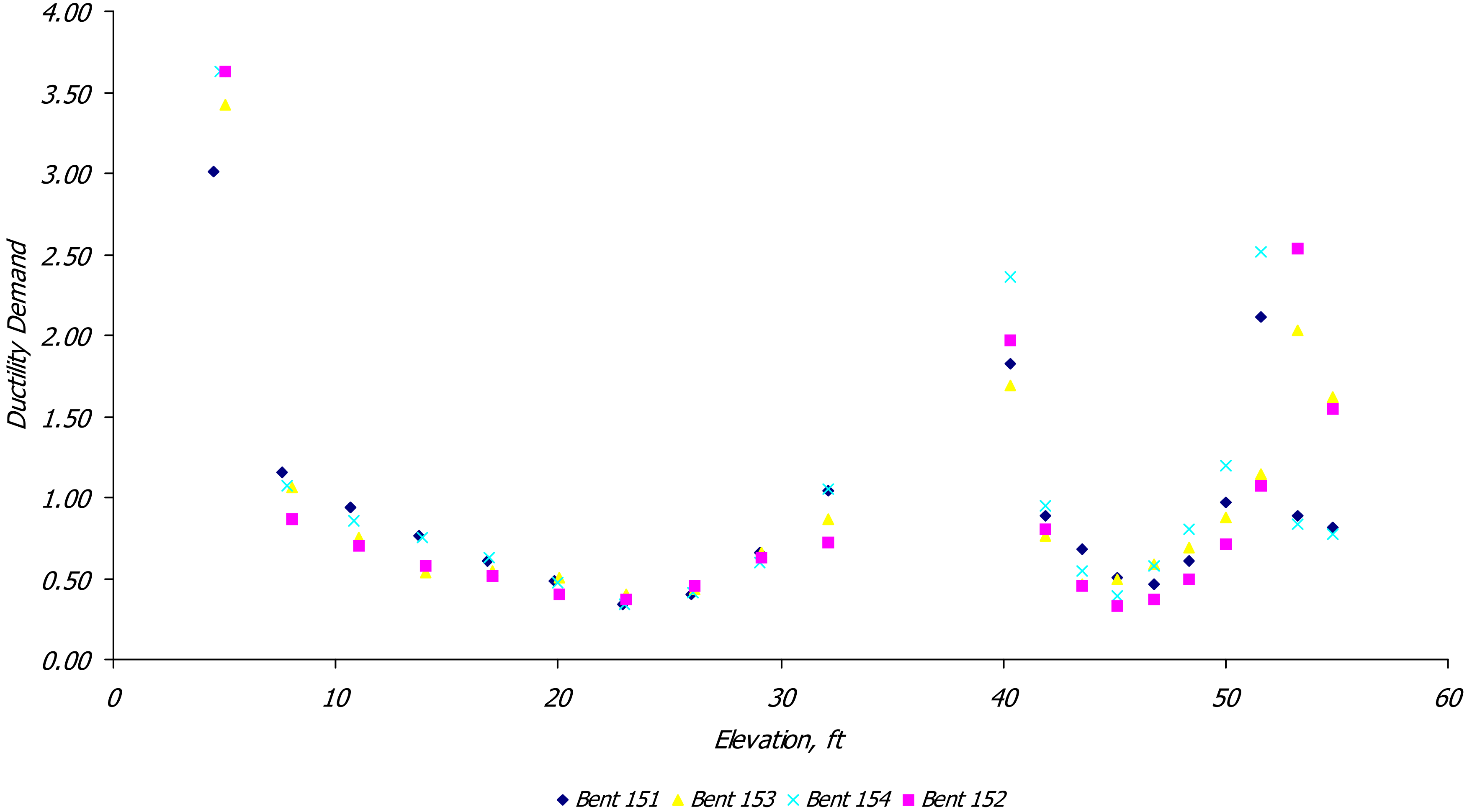

Figure D.6b Column curvature ductility demand, retrofitted structure, rare earthquake, transverse direction

Model Name: miyamoto.08

End Column Curvature

Model Description: Alaska Way Viaduct, Evaluation of Miyamotos Proposal

Model Variation: rare earthquake

31 Jul 06 10:48 AM

Section: Columns.End

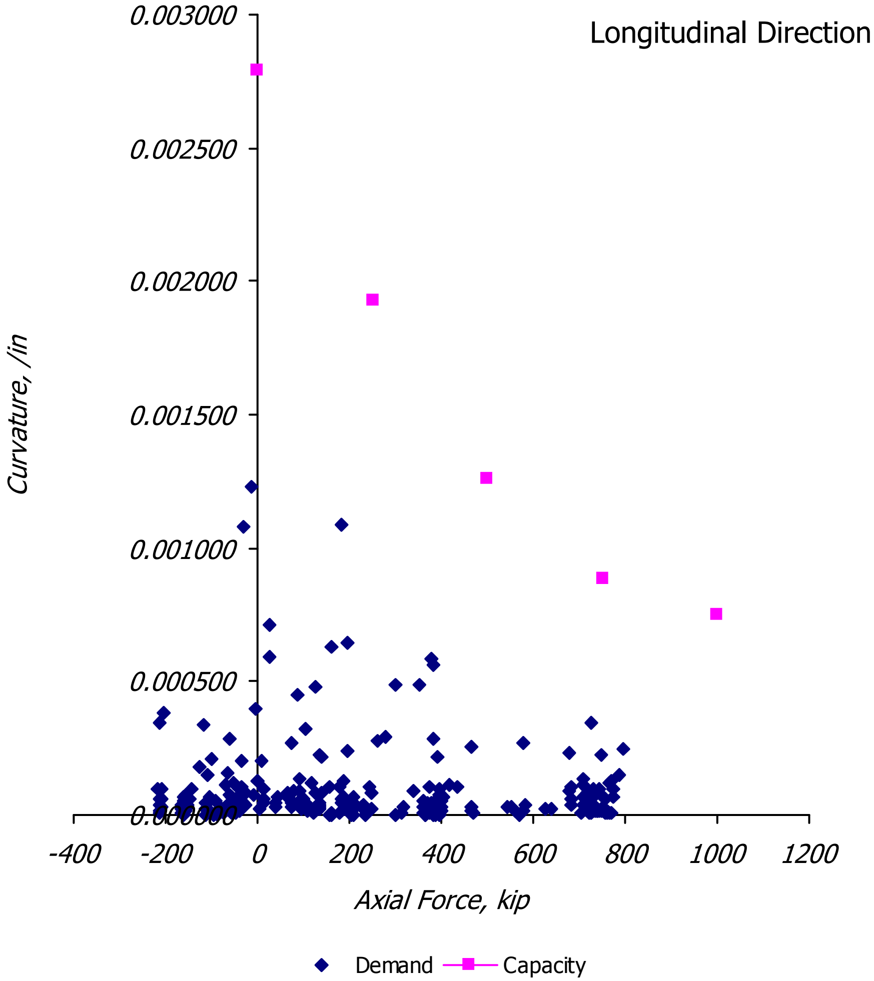

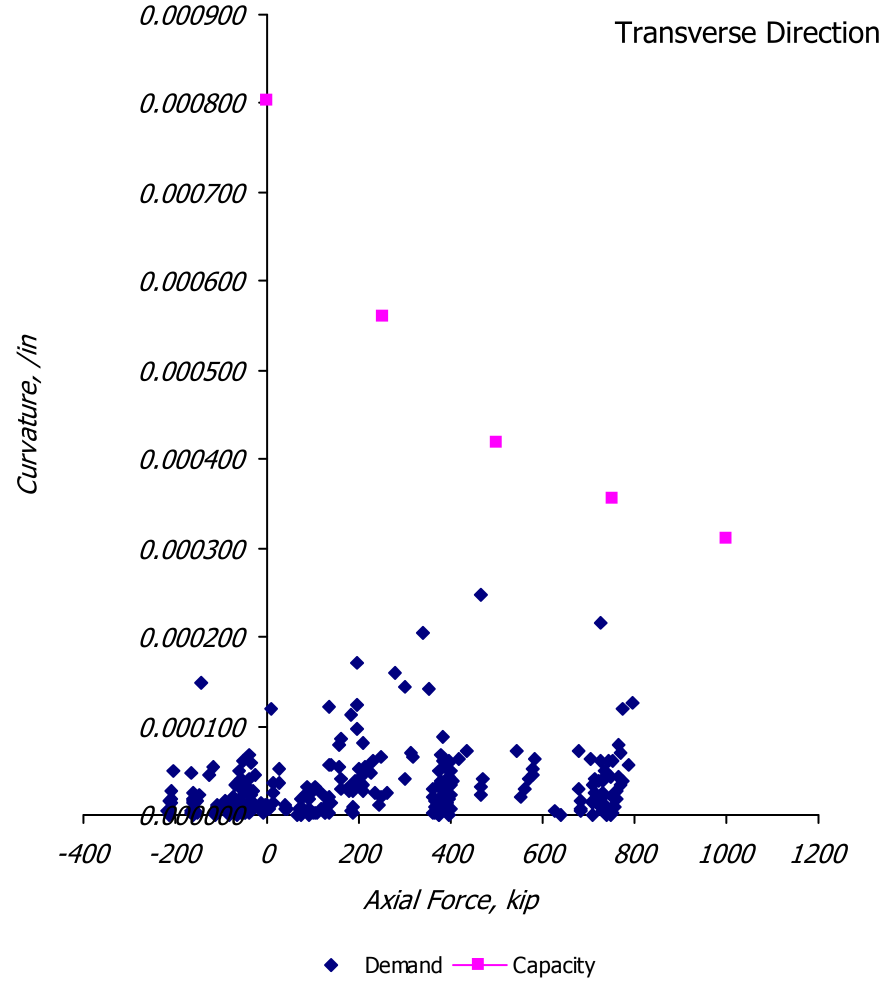

Figure D.7 Column curvature versus axial force, retrofitted structure, rare earthquake, end bents

Model Name: miyamoto.08

Model Description: Alaska Way Viaduct, Evaluation of Miyamotos Proposal

Model Variation: rare earthquake

End Column Curvature

31 Jul 06 10:48 AM

Section: Columns.End.B.16

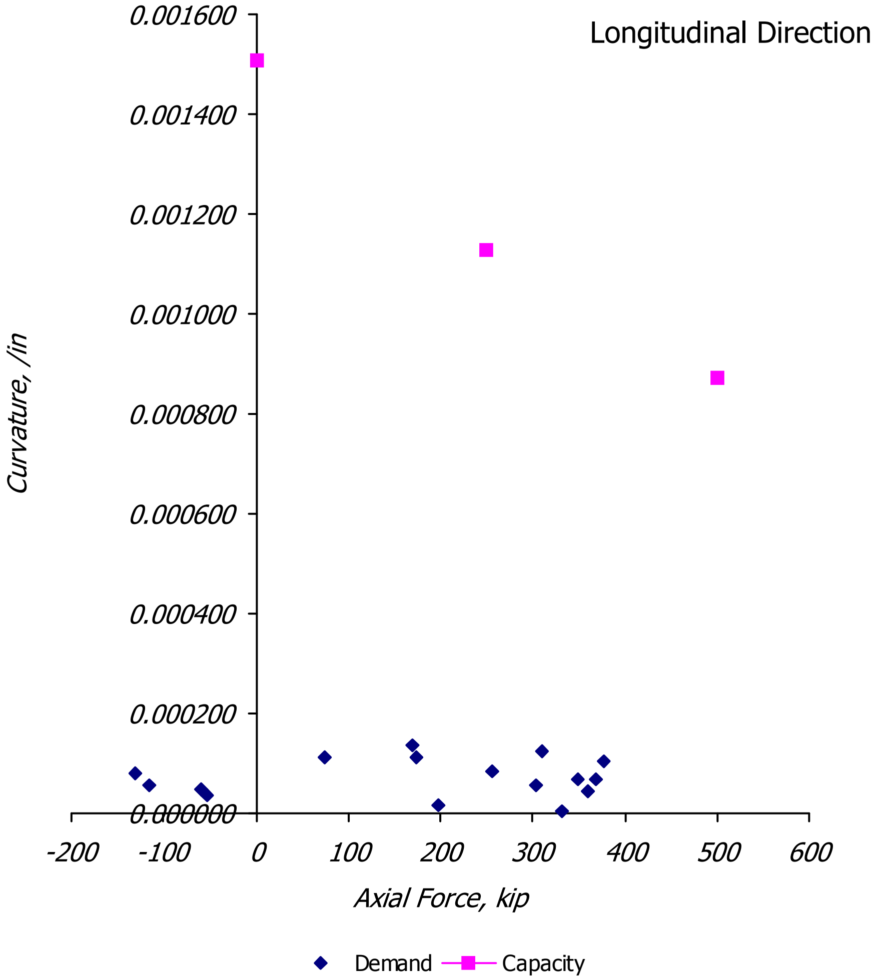

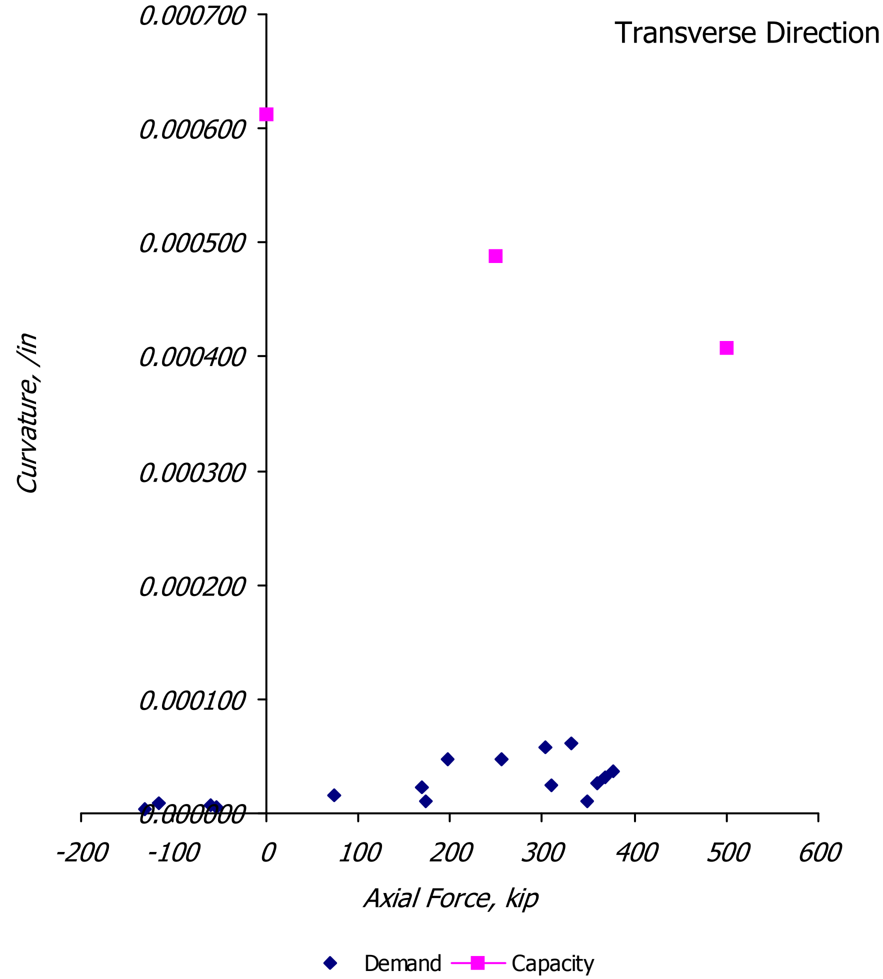

Figure D.7 (cont.) Column curvature versus axial force, retrofitted structure, rare earthquake, end bents

Model Name: miyamoto.08

End Column Curvature

Model Description: Alaska Way Viaduct, Evaluation of Miyamotos Proposal

Model Variation: rare earthquake

31 Jul 06 10:48 AM

Section: Columns.End.B.20

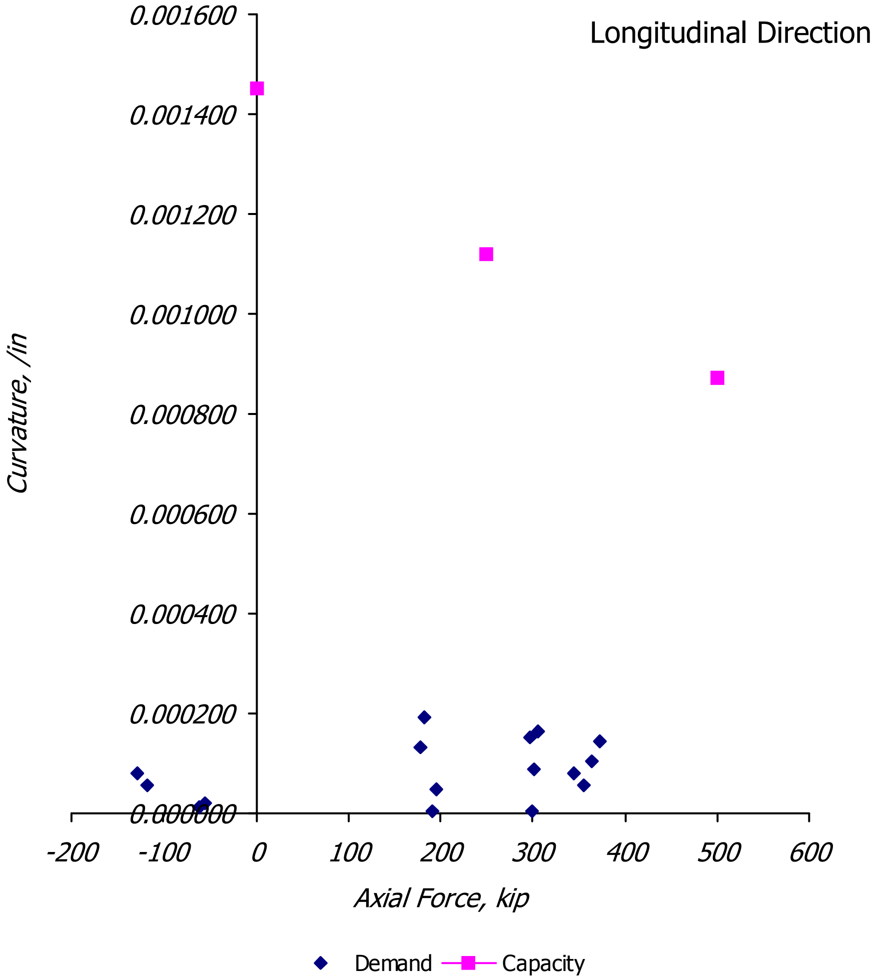

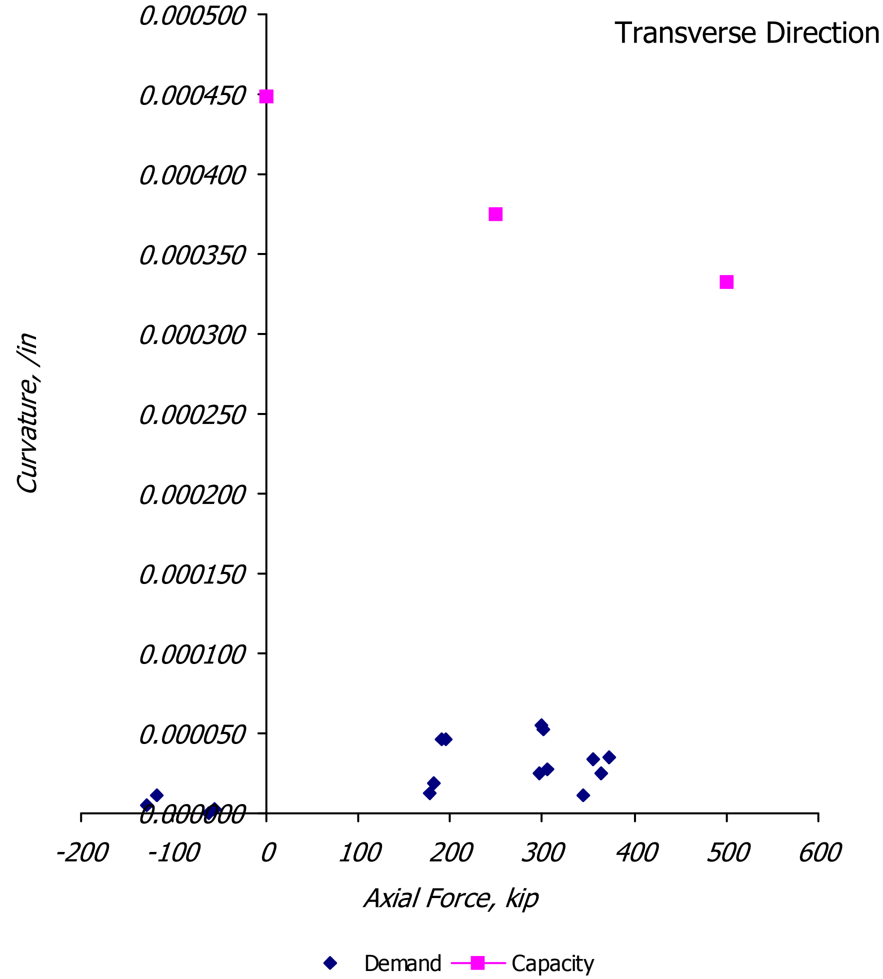

Figure D.7 (cont.) Column curvature versus axial force, retrofitted structure, rare earthquake, end bents

Model Name: miyamoto.08

Middle Column Curvature

Model Description: Alaska Way Viaduct, Evaluation of Miyamotos Proposal

Model Variation: rare earthquake

31 Jul 06 10:49 AM

Section: Columns.Middle

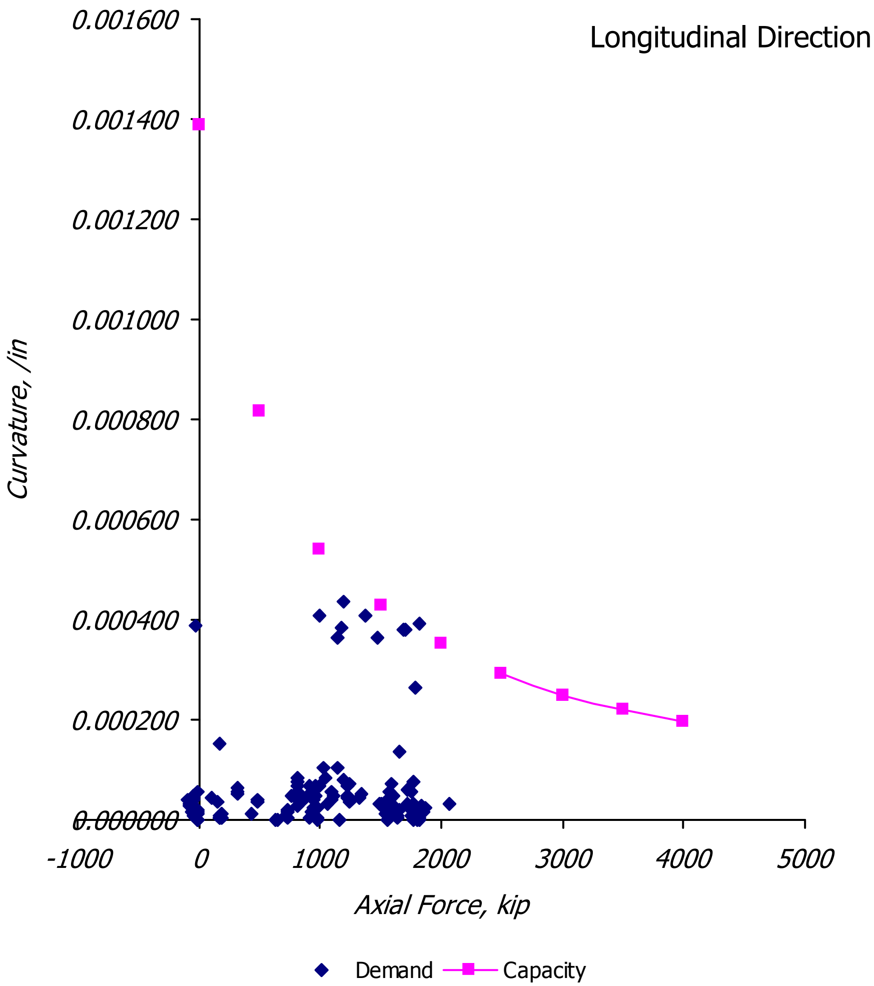

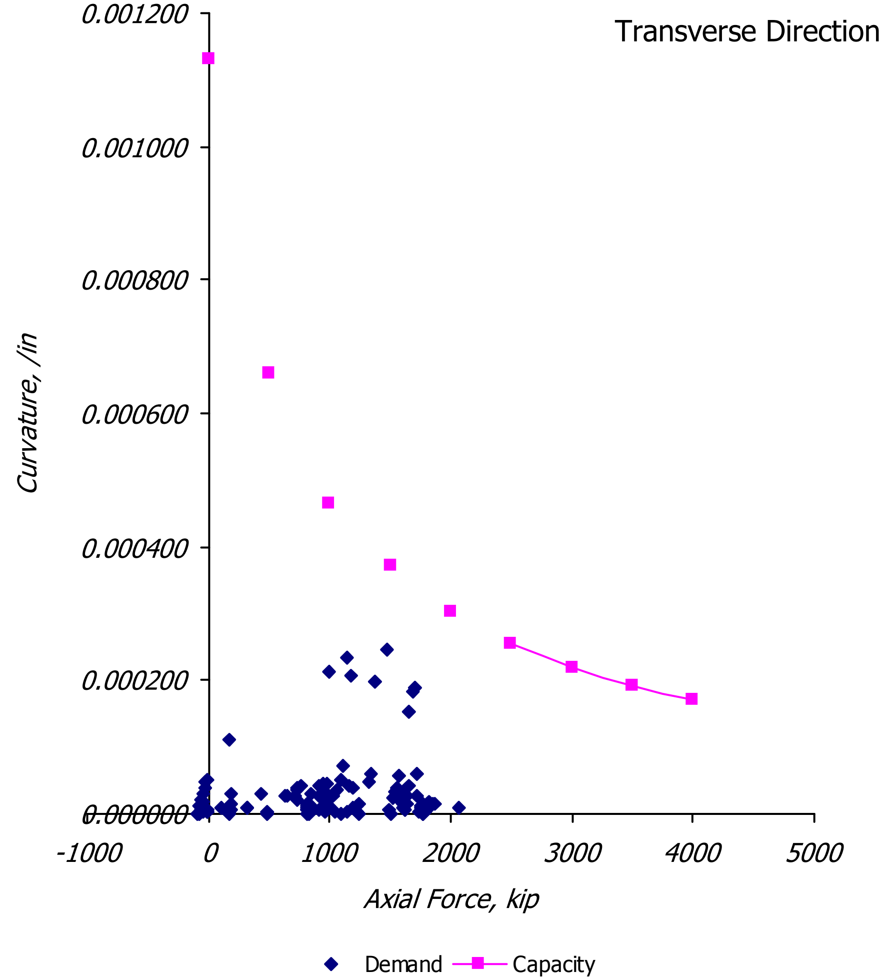

Figure D.8 Column curvature versus axial force, retrofitted structure, rare earthquake, middle bents

Model Name:	miyamoto.08	**Middle Column Curvature**
Model Description:	Alaska Way Viaduct, Evaluation of Miyamotos Proposal	
Model Variation:	rare earthquake	31 Jul 06 10:49 AM

Section: Columns.Middle.A

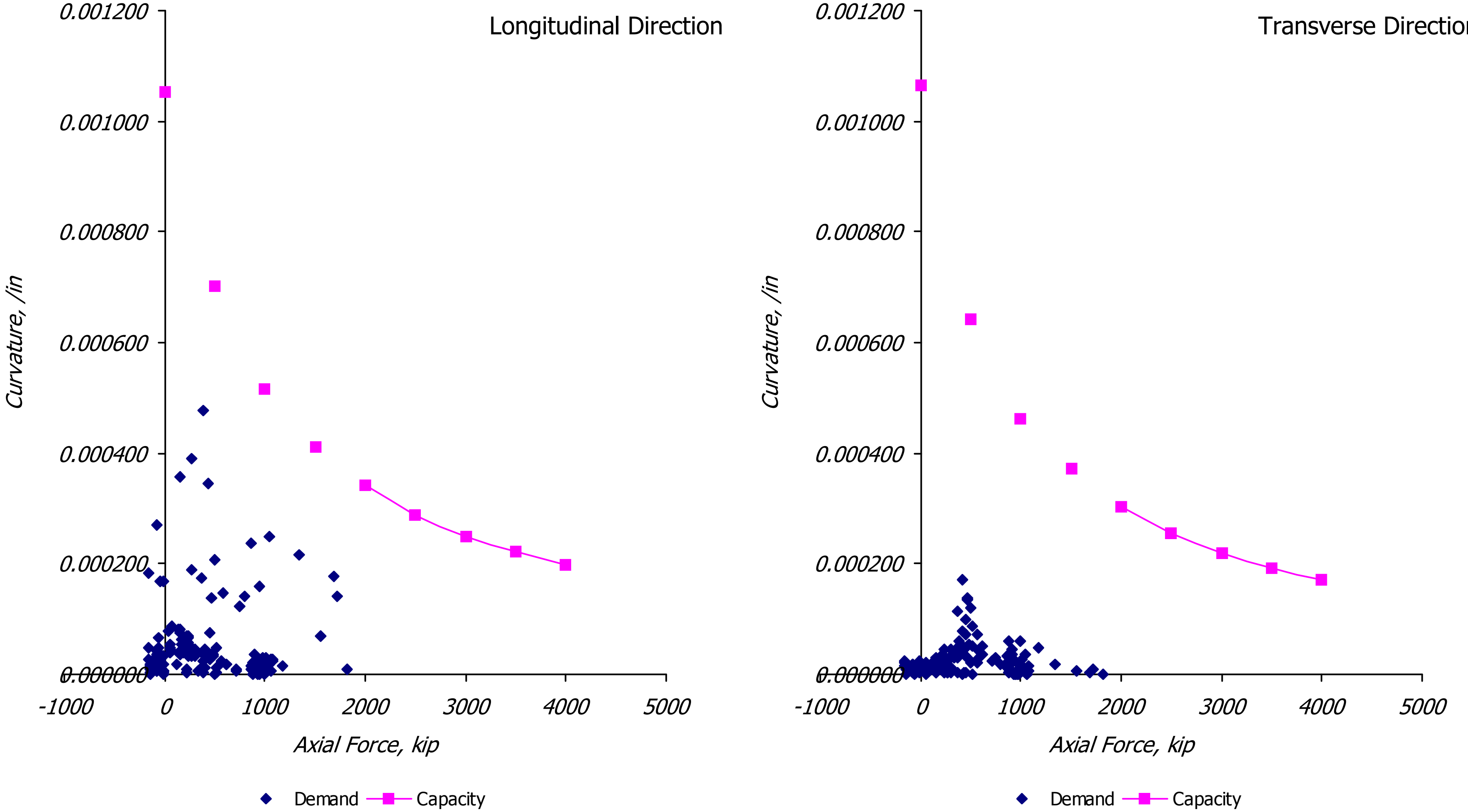

Figure D.8 (cont.) Column curvature versus axial force, retrofitted structure, rare earthquake, middle bents

Model Name:	miyamoto.08	**Middle Column Curvature**
Model Description:	Alaska Way Viaduct, Evaluation of Miyamotos Proposal	
Model Variation:	rare earthquake	31 Jul 06 10:49 AM

Section: Columns.Middle.F

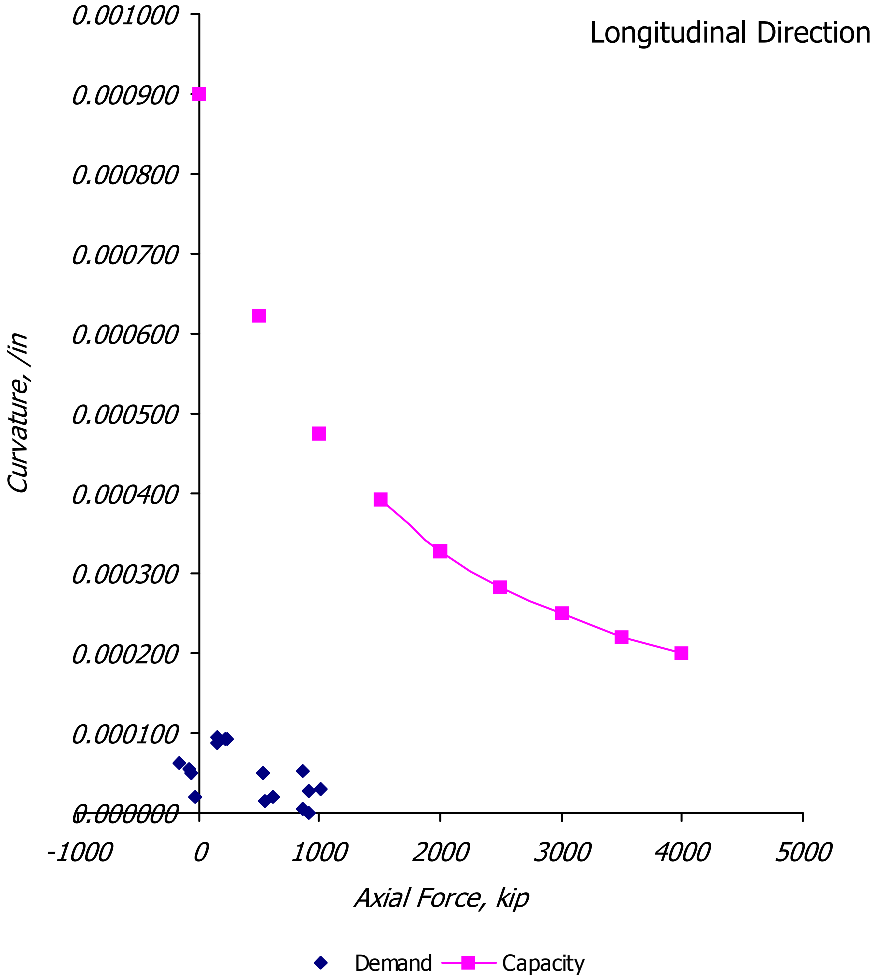

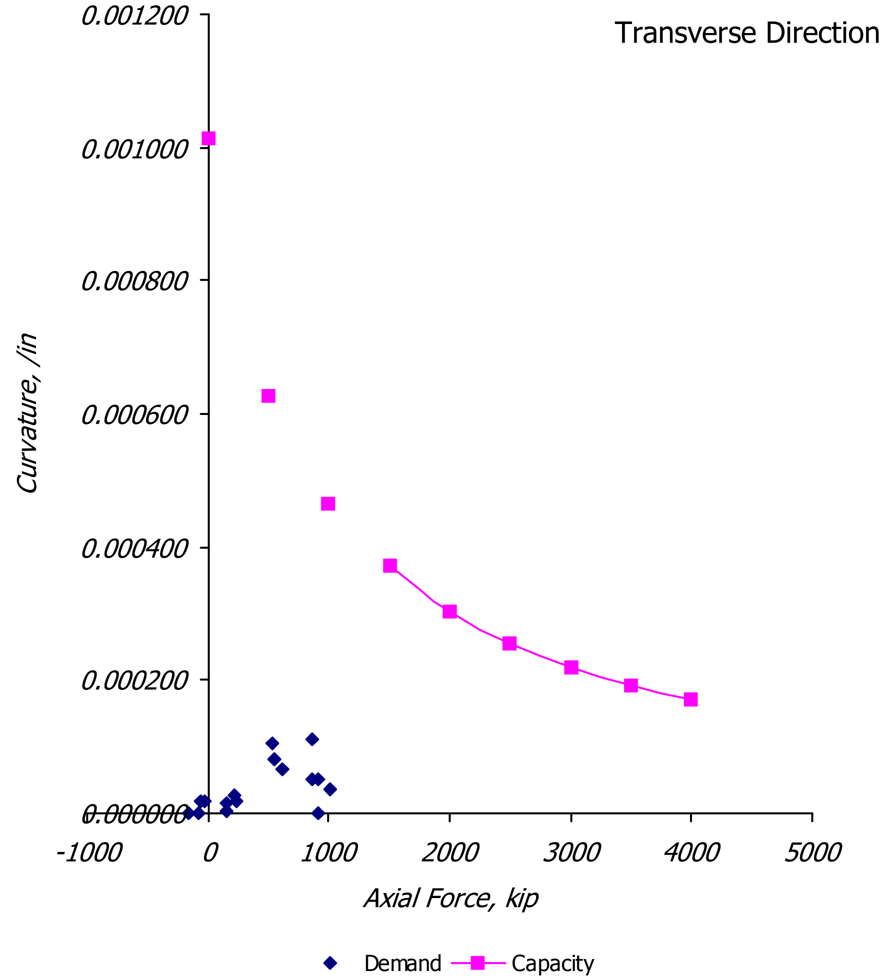

Figure D.8 (cont.) Column curvature versus axial force, retrofitted structure, rare earthquake, middle bents

Model Name: miyamoto.08

Column Curvature Ductility Demand

Model Description: Alaska Way Viaduct, Evaluation of Miyamotos Proposal

Model Variation: design earthquake

31 Jul 06 10:50 AM

Longitudinal Direction

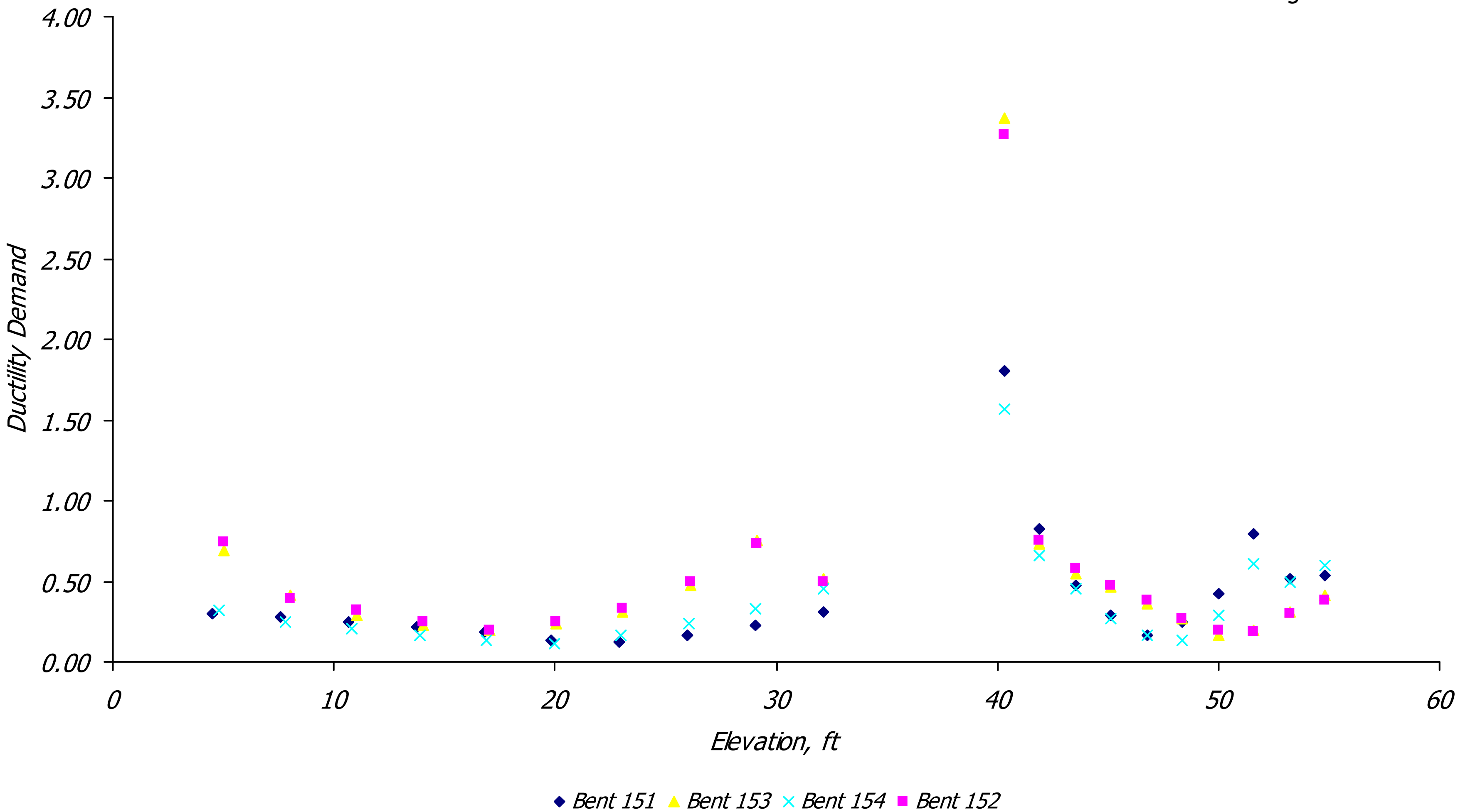

Figure D.9a Column curvature ductility demand, retrofitted structure, design earthquake, longitudinal direction

Model Name:	miyamoto.08	**Column Curvature Ductility Demand**
Model Description:	Alaska Way Viaduct, Evaluation of Miyamotos Proposal	
Model Variation:	design earthquake	31 Jul 06 10:50 AM

Transverse Direction

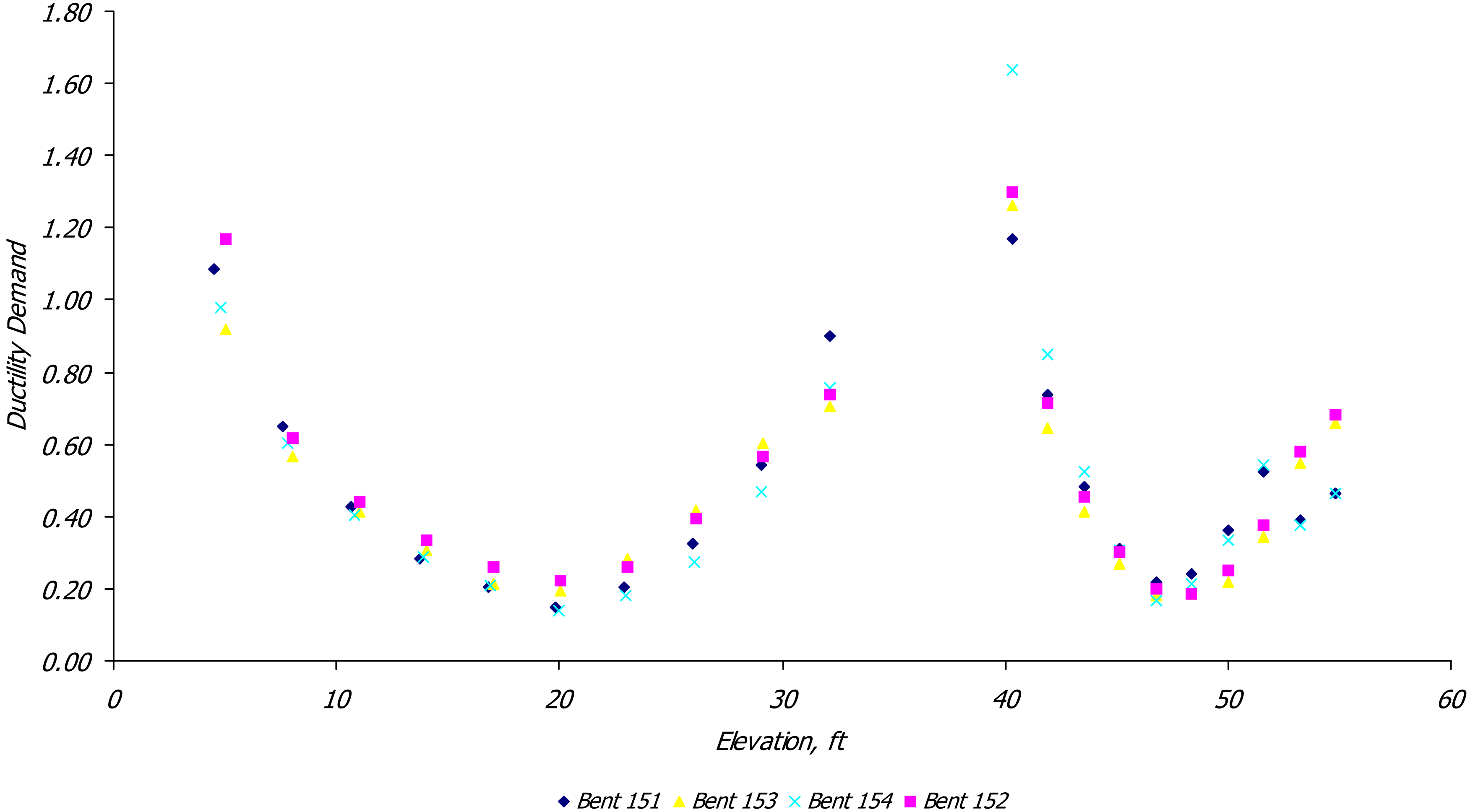

Figure D.9b Column curvature ductility demand, retrofitted structure, design earthquake, transverse direction

Model Name: miyamoto.08

Floorbeam Curvature Ductility Demand

Model Description: Alaska Way Viaduct, Evaluation of Miyamotos Proposal

Model Variation: rare earthquake

31 Jul 06 10:52 AM

Upper Level

Positive Curvature

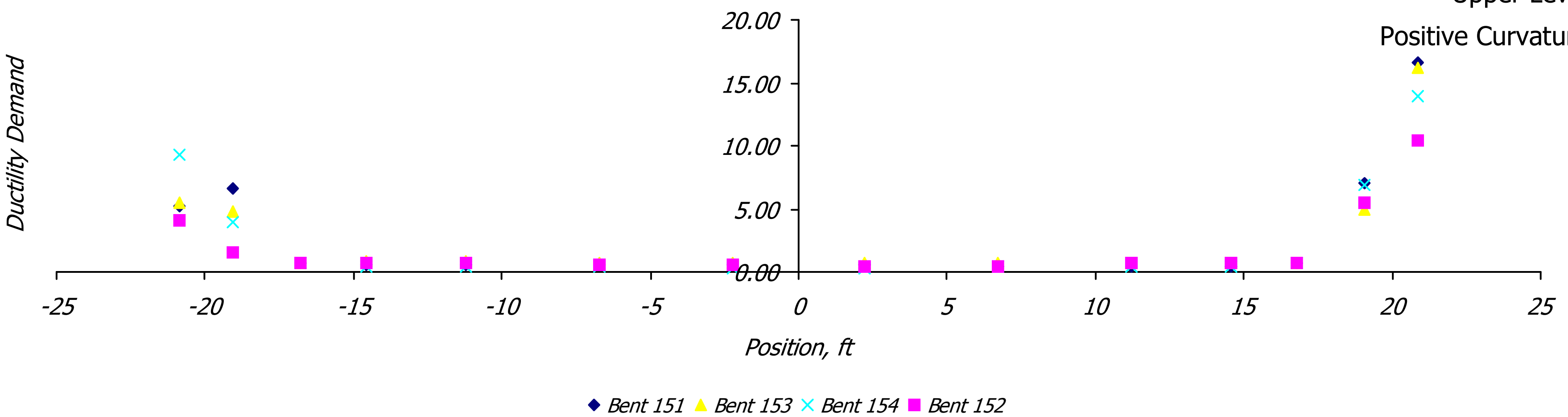

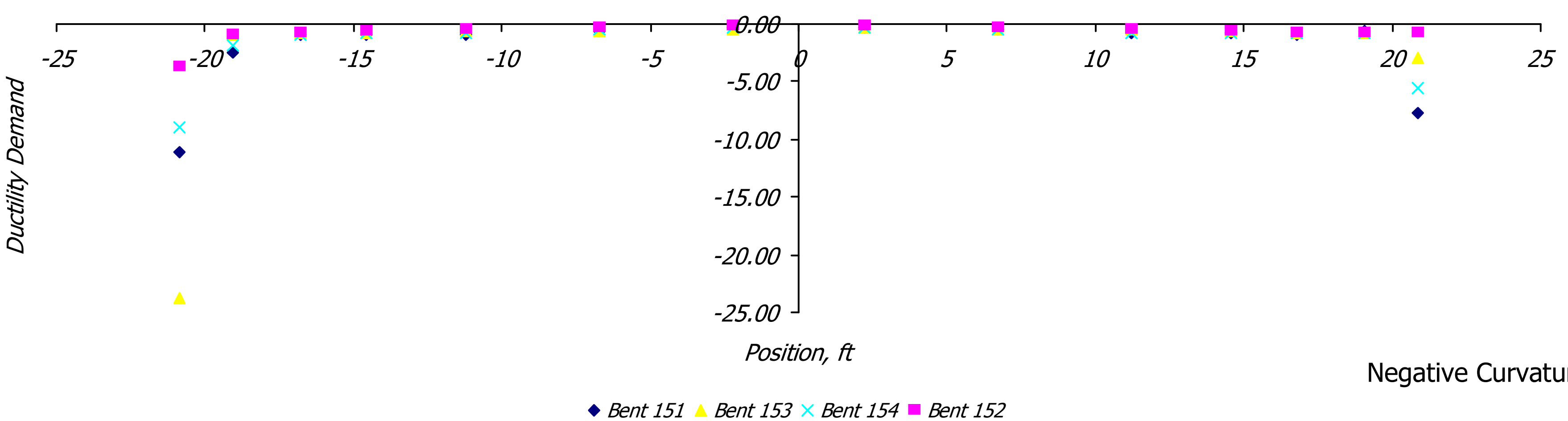

Negative Curvature

Figure D.10a Floorbeam curvature ductility demand, retrofitted structure, rare earthquake, upper level

Model Name: miyamoto.08

Model Description: Alaska Way Viaduct, Evaluation of Miyamotos Proposal

Model Variation: rare earthquake

Floorbeam Curvature Ductility Demand

31 Jul 06 10:52 AM

Lower Level

Positive Curvature

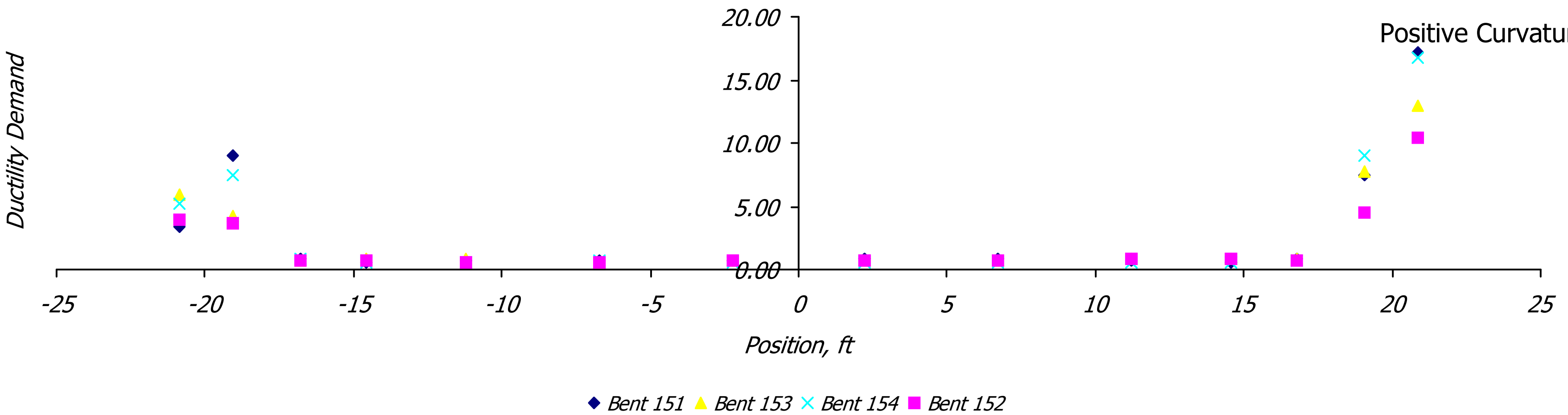

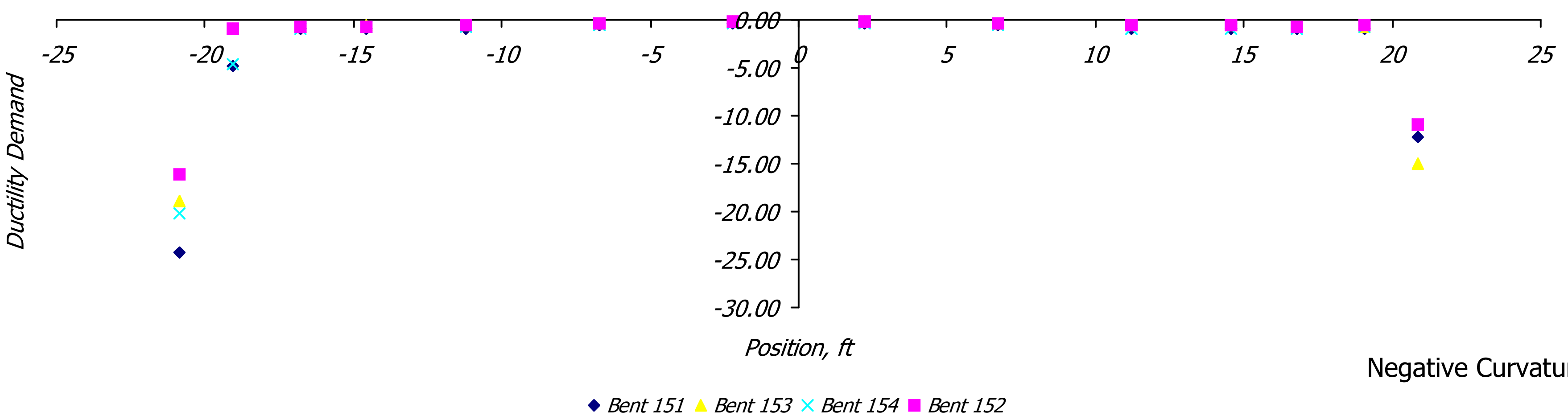

Negative Curvature

Figure D.10b Floorbeam curvature ductility demand, retrofitted structure, rare earthquake, lower level

Model Name: miyamoto.08

Floorbeam Curvature

Model Description: Alaska Way Viaduct, Evaluation of Miyamotos Proposal

Model Variation: rare earthquake

31 Jul 06 10:52 AM

Upper Level

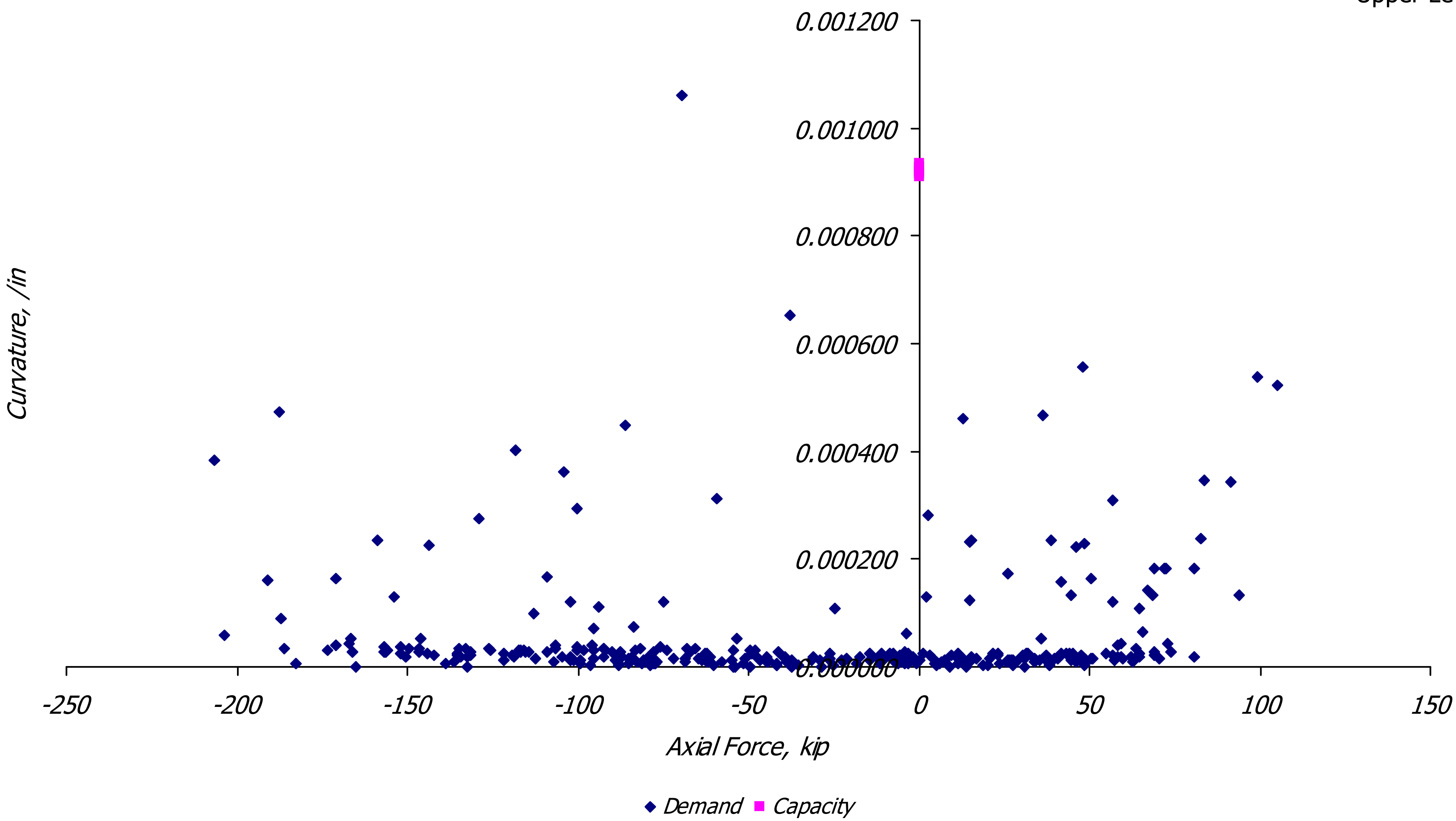

Figure D.11a Floorbeam curvature versus axial force, retrofitted structure, rare earthquake, upper level

Model Name: miyamoto.08

Floorbeam Curvature

Model Description: Alaska Way Viaduct, Evaluation of Miyamotos Proposal

Model Variation: rare earthquake

31 Jul 06 10:52 AM

Lower Level

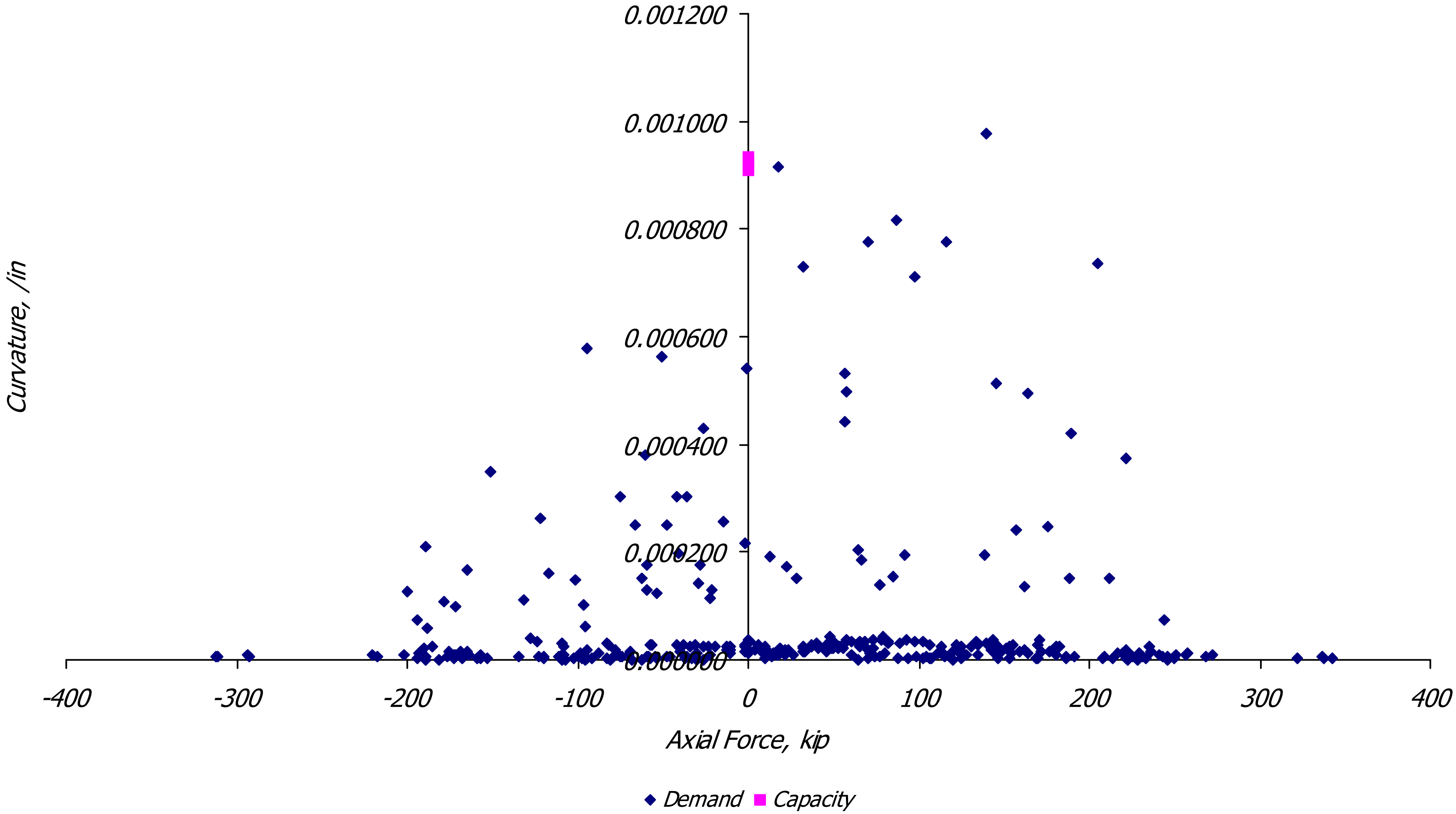

Figure D.11b Floorbeam curvature versus axial force, retrofitted structure, rare earthquake, lower level

Model Name: miyamoto.08

Floorbeam Curvature Ductility Demand

Model Description: Alaska Way Viaduct, Evaluation of Miyamotos Proposal

Model Variation: design earthquake

31 Jul 06 10:53 AM

Upper Level

Positive Curvature

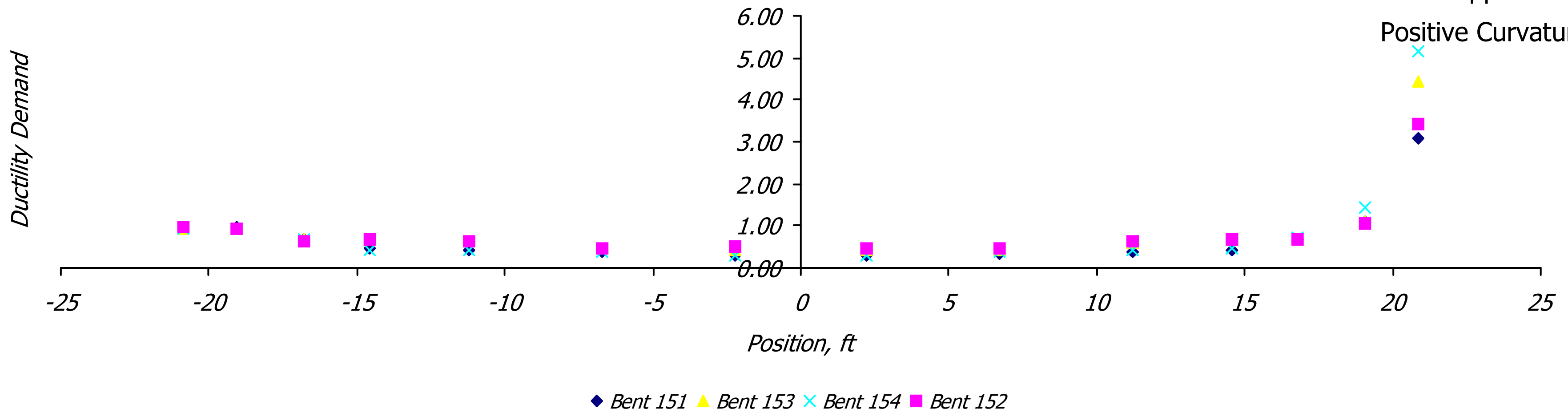

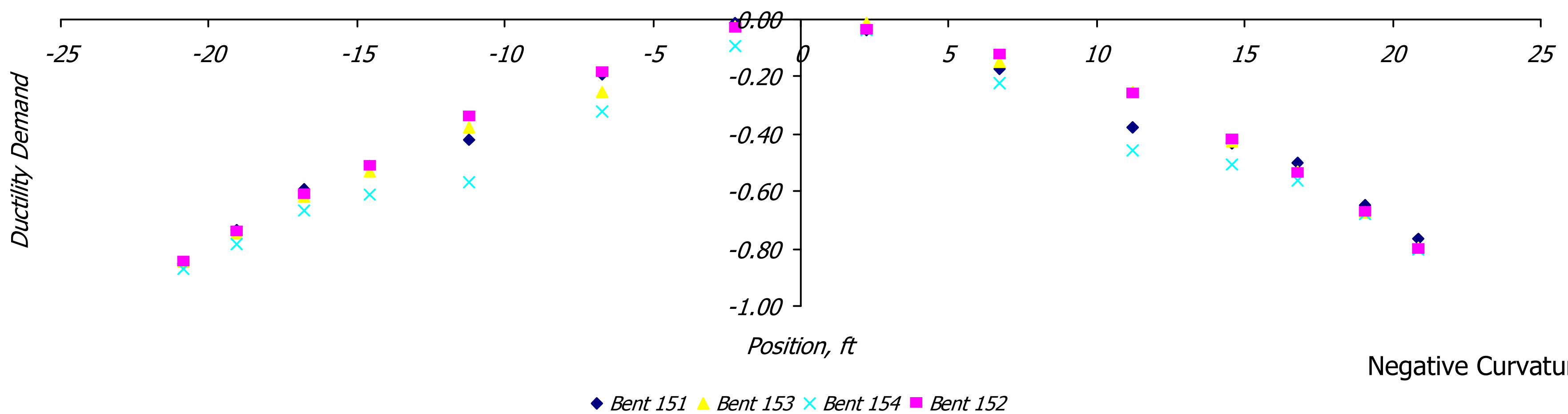

Negative Curvature

Figure D.12a Floorbeam curvature ductility demand, retrofitted structure, design earthquake, upper level

Model Name: miyamoto.08

Floorbeam Curvature Ductility Demand

Model Description: Alaska Way Viaduct, Evaluation of Miyamotos Proposal

Model Variation: design earthquake

31 Jul 06 10:53 AM

Lower Level

Positive Curvature

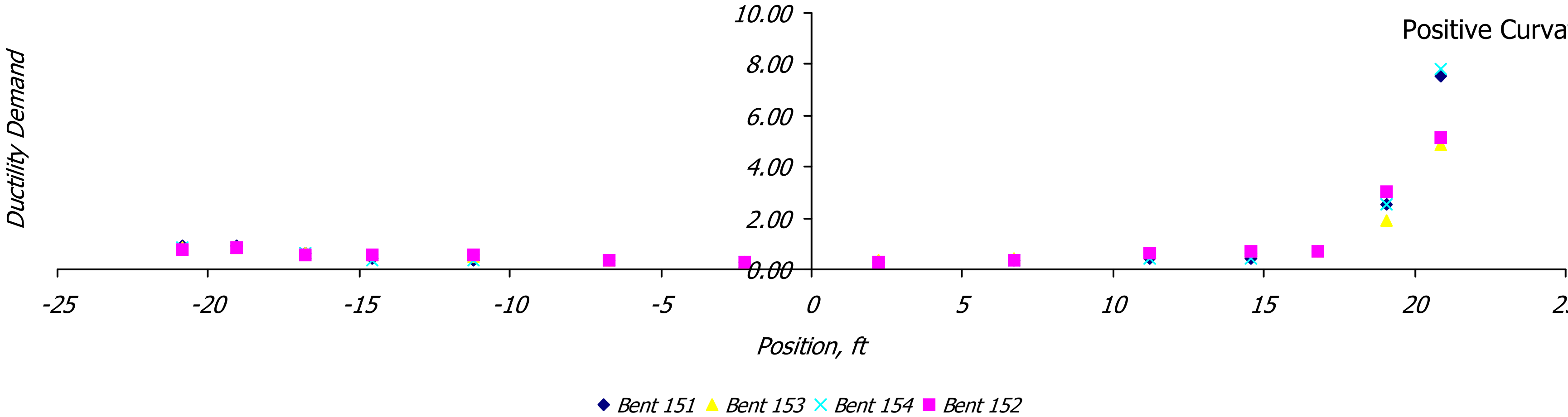

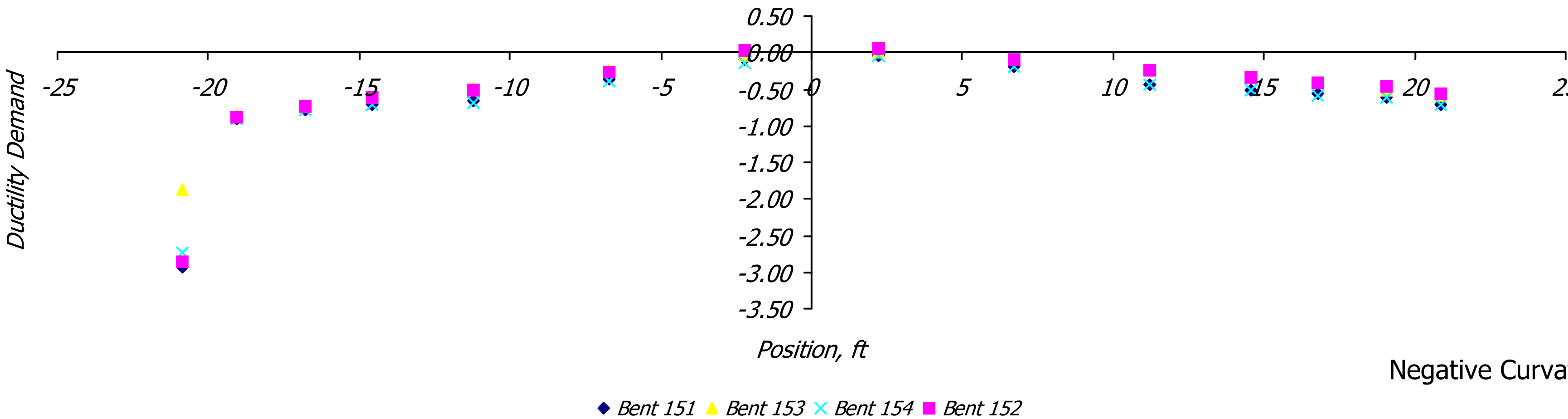

Negative Curvature

Figure D.12b Floorbeam curvature ductility demand, retrofitted structure, design earthquake, lower level

Proposed Retrofit of Alaskan Way Viaduct Using Fluid Viscous Dampers: Preliminary Phase

Miyamoto International, Inc.
Structural and Earthquake Engineers

1450 Halyard Drive
West Sacramento, CA 95691

5 July 2006

Contents

1 Overview

Preliminary time history analysis of a typical three-span frame of the Alaskan Way Viaduct was conducted. The scope of the work was to investigate the response of the superstructure in the existing configuration and after the retrofit with fluid viscous dampers.

The analysis was limited in scope to one of the frame types and it relied heavily on the findings of previous researchers to determine the capacity of the frame and its failure modes. For assessment, the design criteria and level of seismic input developed by others was used.

2 Description of the structure

The Alaskan Way Viaduct, hereafter referred to as the Viaduct, is a 2.1-mile long two-level elevated structure located along the Seattle seashore. The viaduct, also known as State Route 99 or SR 99, was designed and constructed in the 1950s. Figure 1 presents photographs of the viaduct.

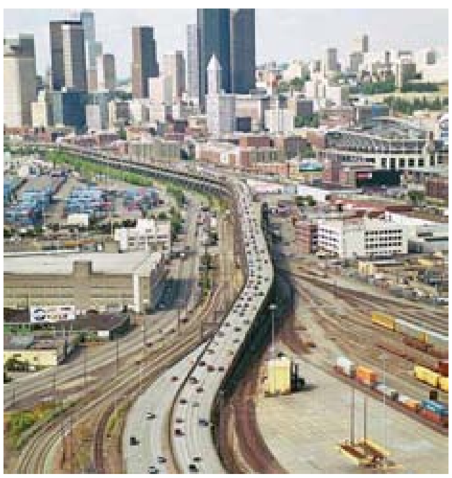

a. Panoramic view

b. Double-deck elevation

Figure 1. Alaskan Way Viaduct (From WSDOT web site)

The viaduct is comprised of a suite of different units, including outrigger frames, frames with steel framing. A great portion of the structure is made of three-span reinforced concrete double-deck frames. Frames measure 182 ft long, are 47 ft wide and the deck elevations are 36.5 and 58.5 ft above the top of footing fore the lower and upper decks, respectively. The exterior spans are 56-ft long and the interior span is 70 ft long. To allow for thermal movements, a 1.5-in. wide longitudinal gap is provided between adjacent frames. Typical frames weigh approximately 5,000 kips. All columns are supported on pile supported footings.

Two types of framing were used in construction. The Southern segment was designed by the Seattle Engineering Department (SED), whereas the Northern frames were designed by the Washington State DOT (WSDOT). The two frame types are similar in geometry. The main difference is the load path for the gravity loading from the decks to the columns. SED units use smaller transverse beams and large longitudinal girders to transfer the load to cap beams, whereas, the WSDOT frames utilize longitudinal stringers and large transverse beams to transfer the load to edge girders. Table 1 summarizes the member sizes for the frames, and Figure 2 shows the gravity framing.

	SED	WSDOT
Exterior columns	48x24	48x24
Interior columns	48x48	48x42
Exterior caps	75x16.5	60x18
Interior caps	75x29	60x18
Edge girder	75x16	88x18
Interior longitudinal beams	Two 38.5-64.5 (haunched)x29 One 19x17 centerline	Four 28.5x13.5
Internal transverse beams	19x20 (three end spans, four mid span)	63.5x15 (three each span)
Deck	6.5 in.	6.5 in.
Gravity framing	Deck transverse stringers longitudinal girders cap beams columns	Deck longitudinal stringers transverse beams exterior girders columns

Table 1. WSDOT and SED framing

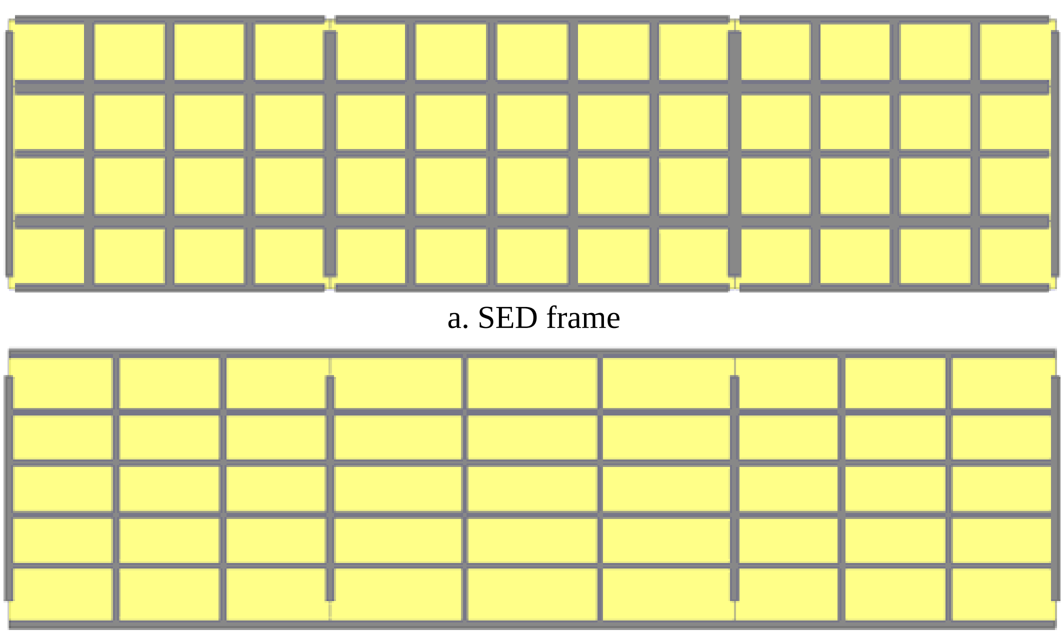

a. SED frame

b. WSDOT frame

Figure 2. SED and WSDOT frames

The two types of frames have similar elastic and dynamic properties. However, the reinforcement, structural detailing (splice, connections) differs between the two frames. As such, the expected seismic performance of the frames in the inelastic range and possible modes of failure would also vary between the frames. Since the scope of the analysis in this report is to limit the extent of nonlinear behavior by adding supplementary damping to the system, it would suffice to perform analysis on one of the frame types. As such, for the remainder of this report, the discussion is limited to typical SED frames. Figure 3 present a photograph of a SED framing.

Figure 3. Photograph of typical SED frames

3 Previous research

After the collapse of the double-deck Cyprus viaduct during the Loma Prieta earthquake in Oakland, CA, in 1989, WSDOT conducted a comprehensive investigation of the viaduct structure. Both geotechnical and structural evaluations were conducted. Following the Mw 6.8 Nisqually earthquake, WSDOT conducted field investigations, sponsored further analysis and developed design criteria for retrofit/replacement structure. The findings are summarized here.

3.1 Eberhard 1995-a and 1995-b

Eberhard conducted three-dimensional linear dynamic (modal and response spectrum) and two-dimensional nonlinear static analysis of typical SED and WSDOT frames and their longitudinal and transverse bents.

Dynamic analysis showed that for the fixed based frames, the fundamental periods of 0.8 to 0.9 sec. For pinned based frames, the fundamental periods were 1.6 to 2.0 sec. WSDOT and SED frames had similar modal properties. For all cases, the first mode response dominated and had mass participation of close to 100% of total seismic mass. Response spectrum analysis showed that for either fixed or pinned based models, most deformation was considered for the lower level. The drifts at the lower level were three to ten times that of the upper level. As such, soft-story type of response was prominent.

Pushover analysis was conducted to evaluate the capacity of frames. Only ductile flexural hinges were included in the model. Figure 4 presents the normalized pushover curves. The Eberhard 1995a and 1995b data were converted from base shear to base shear coefficient, BSC, (dividing by weight of the frame of 5,200 kips). The pushover curves are shown in Figure 4. Results for SED and WSDOT units in longitudinal and transverse directions are shown in Figure 4. For the SED unit only pinned base condition was evaluated; for WSDOT unit both support conditions were investigated. Since the frames respond primarily in the first mode, the pushover curves can also been considered as spectral displacement-spectral acceleration capacity curves.

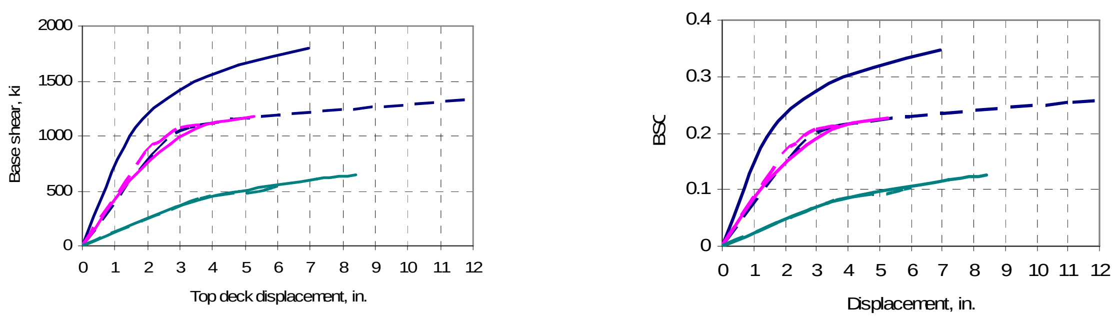

a. Base shear-deck displacement curve

b. Normalized capacity curve

SED transverse fixed	SED longitudinal fixed	WSDOT transverse fixed	WSDOT longitudinal fixed	WSDOT transverse pinned	WSDOT longitudinal pinned

Figure 4. Pushover curves, Eberhard 1995a and 1995b

The response is essentially elastic up to a BSC of 0.2g for the fixed support case. The pinned models exhibit elastic response up to approximately 0.1g. Minimal yielding is expected up to a displacement of approximately 2 in. for the fixed based frames and 3 in. for the pinned based frames.

The pushover analysis did not explicitly account for the potential brittle modes of failure. Eberhard 1995a and 1995b conducted determined that the frames would not be able to develop their full flexural capacity because each type of frame was susceptible to some of the following inadequacies: joint shear, column shear, bar pull out, reinforcement splice, or plastic hinge ductility. Eberhart tabulated the likelihood of each type of failure and produced a priority table for the areas of concern.

3.2 TY Lin 2001

After the February 28, 2001, Nisqually Earthquake (Mw 6.8) about 35 miles south of Seattle, WSDOT engineers noted that a structural unit had experienced significant damage. The rest of the viaduct did not experience major structural damage. Immediate repairs were undertaken and WSDOT initiated a committee for the long-term evaluation of the viaduct.

TY Lin 2001 evaluated the complied previous research, and developed retrofit/replacement design guidelines. The governing seismic level was selected as having a 10% probability of exceedance in 50 years (15% in 75 years or 500-year event) and the target performance was selected as collapse prevention at this seismic level. TY Lin 2001 concluded that:

- ❖ Nisqually (PGA of approximately 0.19g for stations within 1,000 ft of the viaduct) had a return period of 150 years.
- ❖ Estimated the earthquake that would cause collapse of a major portion of the viaduct at the 210-year event.
- ❖ Computed a threshold spectral acceleration of 0.26g, for frames with a period of 1.5 sec. This threshold was based on the pushover analysis of a unit 97-100 frame for which the column supports as springs to account for support flexibility.
- ❖ Stated that the level of earthquake loading in the design of the WSDOT frames was 0.1g.
- ❖ Compared the viaduct and the Cyprus Viaduct and stated that the frame hinges and girder expansion joints in the Cyprus Viaduct contributed to its collapse during the Loma Prieta earthquake..
- ❖ Developed response spectrum using USGS maps for the 500-year event and for the 1949 Puget Sound event with a return period of 200 years.
- ❖ Given the maintenance issues and that the viaduct's relatively advanced age, recommended replacement.

3.3 PBQD 2002

Parsons Brinckerhoff Quade & Douglas (PBQD 2002) assessed the seismic performance of the viaduct and looked at retrofit and replacement options. They conducted a pushover analysis of a specific frame. The pushover curve is shown in Figure 5. PBQD 2002 does not provide specifics of their analysis. However, from their pushover curve it appears that strain hardening, loss of strength in hinges were included in the model. From the level of BSC, it seems that their model used spring supports—and a period of 1.5 sec—similar to a value used by TY Lin 2001.

Figure 5. Capacity pushover curve for Bent #152, PBQD 2002

PBQD 2002 stated that

- ❖ Viaduct response to be evaluated using two levels of earthquake, one with PGA of 0.13g and peak spectral acceleration of 0.33g, and one with PGA of 0.65g and peak spectral acceleration of 1.61g. Although not stated, these values appear to be for site class B (Fa and Fv equal to unity). The first spectrum is used for functionality (immediate use) and the second for life safety (collapse prevention).

- ❖ Viaduct joints can experience brittle failure and there is no method of repairing the knee joints.
- ❖ SED frames would sustain damage at spectral acceleration of 0.13g, and structural limit would be reached at 0.25 to 0.30g.
- ❖ WSDOT frames would sustain damage at spectral acceleration of 0.10g, and structural limit would be reached at 0.25 to 0.30g.
- ❖ Rebar slip starts at a column moment of 5,000 k-ft. At the same time the joint has also reached its principal stress limit of $5\sqrt{f'_c}$. This corresponds to a BSC of 0.24g.
- ❖ Initial joint cracking (principal stress of $3.5\sqrt{f'_c}$) starts at BSC level of 0.18g.
- ❖ Retrofit/rebuild option must have seismic resilience and energy dissipation capabilities.

3.4 PBQD 2005

Structural design criteria for the viaduct were developed in PBQD 2005. The preliminary design criteria identify two target performance points for the viaduct: 1) immediate functionality for the Expected Earthquake or EE (50% in 75 years or return period of 108 years), and 2) collapse prevention for the Rare Earthquake or RE (3% in 75 years or return period of 2500 years). The seismic hazards have the following characteristics shown in Table 2.

Level	PGA, g	SS, g	S1, g
EE	0.14	0.34	0.14
RE	0.55	1.37	0.66

Table 2. Design response spectra for viaduct

Note that the design response spectra parameters different by what was used by both TY Lin 2001 (10% in 50 years) and from PBQD 2002 (different Ss and PGA for RE event).

4 Nisqually earthquake

The Mw 6.8 Nisqually earthquake of February 28, 2001, provides a great opportunity to investigate the response of the viaduct to a seismic event. Figure 6 shows a map of the viaduct and the surrounding area. Three stations recorded the strong motion data near the viaduct; see Figure 6 (red dots) and Table 3. (The viaduct coordinates are approximately 47.60 and -122.34 degrees.) Figures 7 and 8 depict a 40-second window of recorded accelerations and the corresponding acceleration response spectrum for the EW and NS components of records at these stations, respectively. Note that the accelerations had strong motion duration of 10 to 20 sec, and the response spectrum was rich in frequency content.

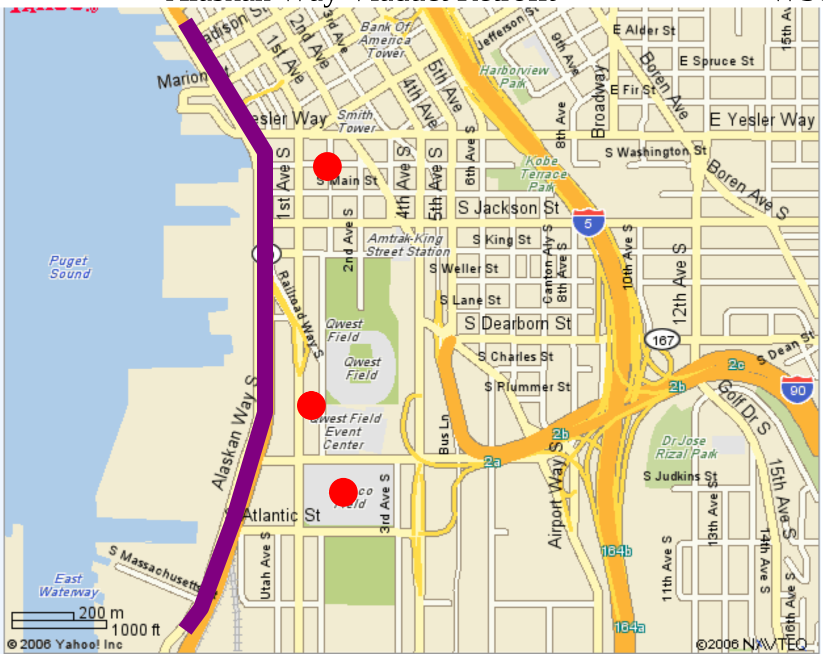

Figure 6. Map of viaduct and recording stations
(redmark indicates location of recording stations)

Station	Latitude	Longitude	PGA NS	PGA EW
NOR	47.6007	-122.3320	0.2	0.22
KDK	47.5951	-122.3336	0.19	0.15
HAR	47.5837	-122.3501	0.21	0.18

Table 3. Strong motion data station and recorded PGAs

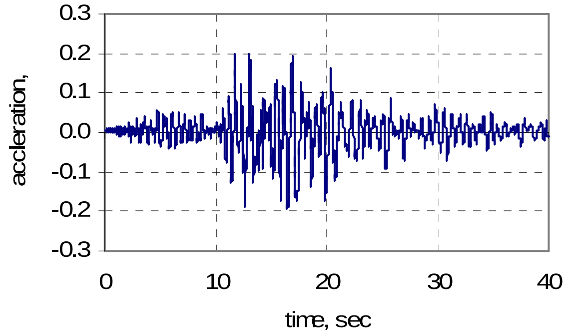

a. Station NOR, zero-degree component

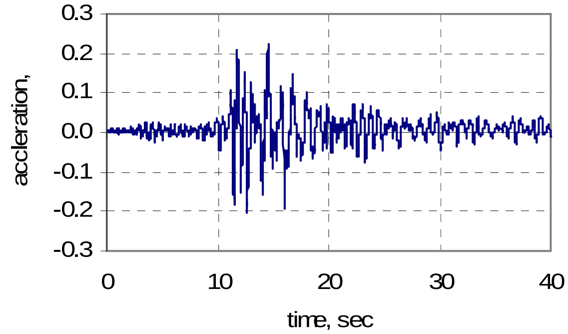

b. Station NOR, ninety-degree component

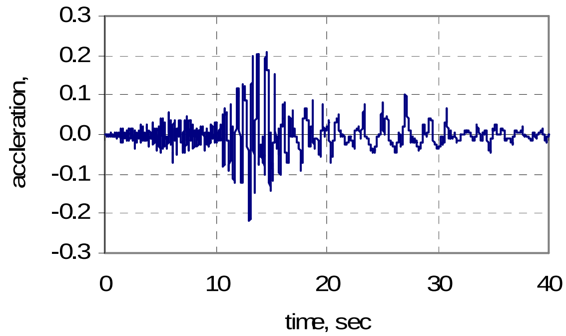

a. Station HAR, zero-degree component

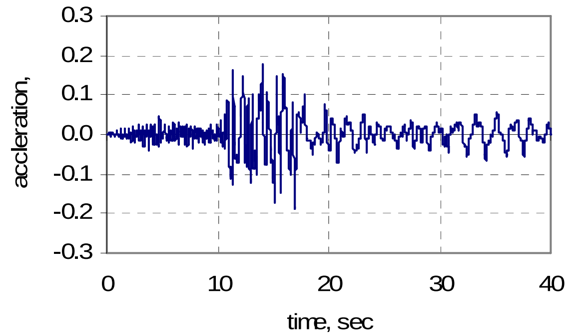

b. Station HAR, ninety-degree component

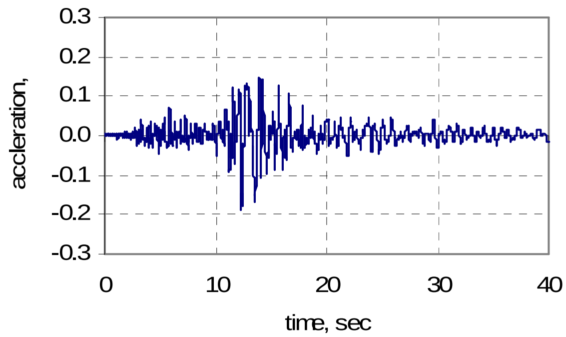

a. Station KDK, zero-degree component

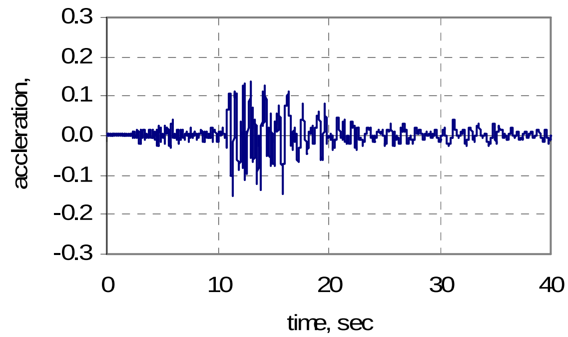

b. Station KDK, ninety-degree component

Figure 7. Acceleration records

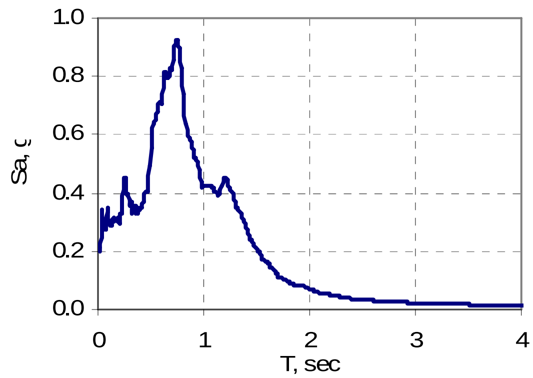

a. Station NOR, zero-degree component

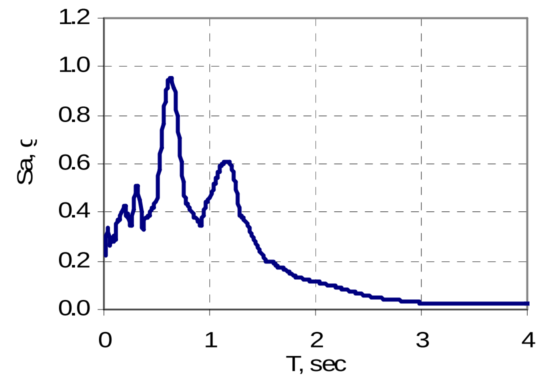

b. Station NOR, ninety-degree component

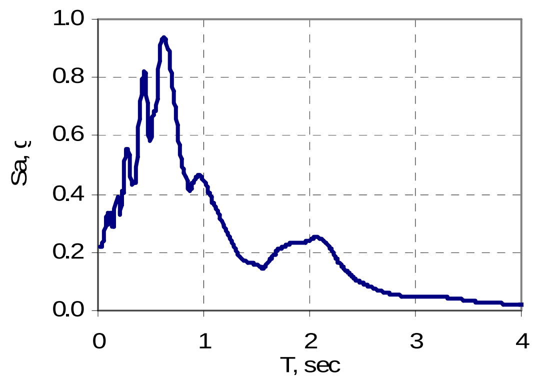

a. Station HAR, zero-degree component

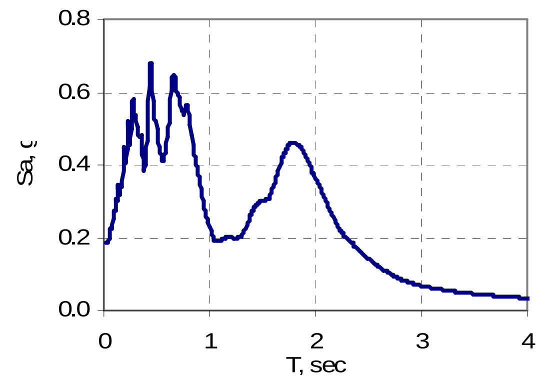

b. Station HAR, ninety-degree component

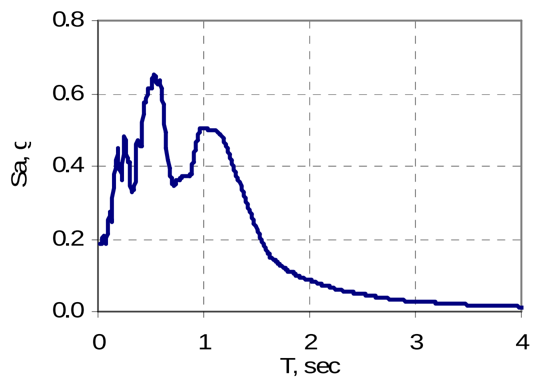

a. Station KDK, zero-degree component

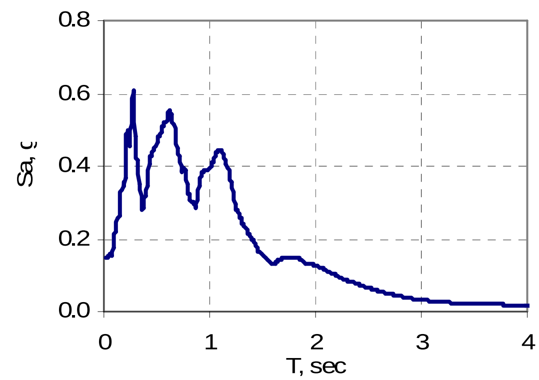

b. Station KDK, ninety-degree component

Figure 8. Response spectra, 5% damped

Figure 9 presents the average and maximum of spectral accelerations for these six records. Also shown in the figure are the 5%-damped EE response spectum and three lines indicating three periods of 0.8 sec (fixed), 1.8 sec (pinned), and 1.5 sec (spring supported) for a typical frame.

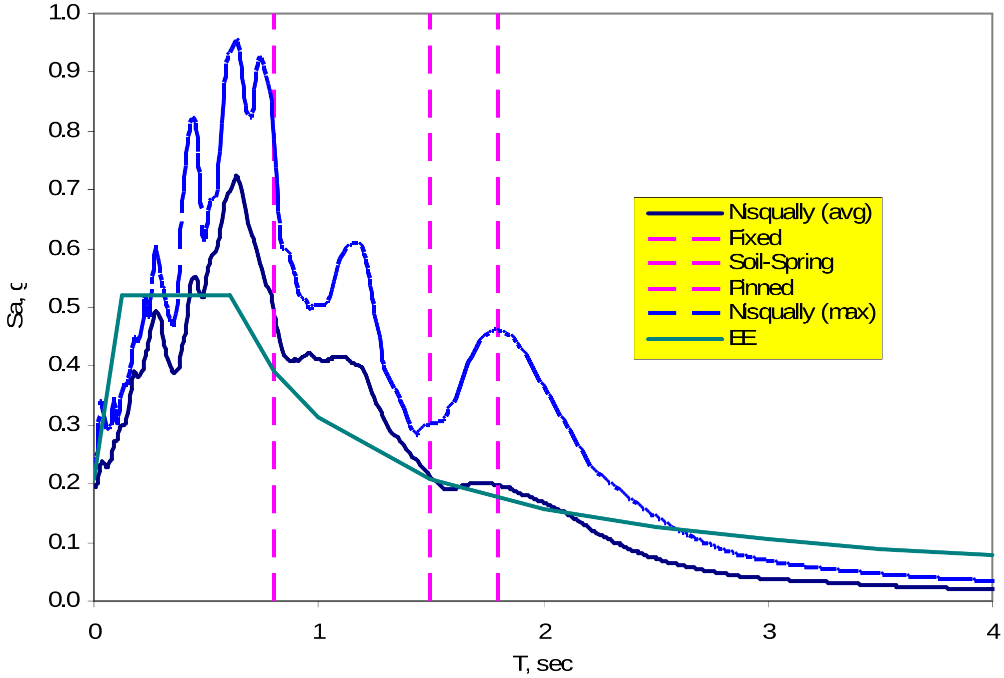

Figure 9. Nisqually and EE spectra

Note the following:

- ❖ The average spectrum approximates or exceeds the EE spectrum and the maximum spectrum greatly exceeds the EE spectrum. Thus, it appears that the Nisqually earthquake was a more severe test than the EE event.
- ❖ The recorded spectral amplitudes for the periods of interest are listed in Table 4

	T, sec	EE	Nisqually Average	Nisqually Maximum
SED/WSDOT fixed	0.8	0.39	0.49	0.79
Spring-supported	1.5	0.21	0.21	0.30
WSDOT pinned (avg)	1.8	0.16	0.20	0.46

Table 4. Spectral accelerations at target periods

Previous studies (TY Lin 2001 and PBQD 2002) had stated that the viaduct frames—with a period of 1.5—would experience yielding at Sa of 0.1 to 0.13g, would reach their capacity at 0.25-0.3g, and experience bar pull out and joint failure at 0.24g. Entries of Table 4 show that the viaduct did reach most of these target values. However, the structural damage to the viaduct was limited. This is noted by TY Lin 2001. This better-than-expected performance of the viaduct during the Nisqually earthquake points to the conservatism inherent in the above-mentioned studies.

5 Objective of current study

5.1 General

The objective of the analysis was to assess whether fluid viscous dampers can be used to retrofit the viaduct and meet its performance objectives as defined in PBQD 2006. Figure 10 presents the 5%- and supplementary-damped target response spectra for EE, DBE, and RE events.

Note that if this level of high damping was achieved, the response of the viaduct would then meet the seismic objectives, because the RE acceleration would then equal to or be less than the spectral ordinates computed from the accelerations causing maximum response at that period from the three recording stations during the Nisqually ground motion. The effectiveness of added damping was also noted by PBQD 2002 when they discussed energy dissipation capacity. The only difference being that PBQD 2002 discussed energy dissipated provided by new designed and detailed ductile concrete members.

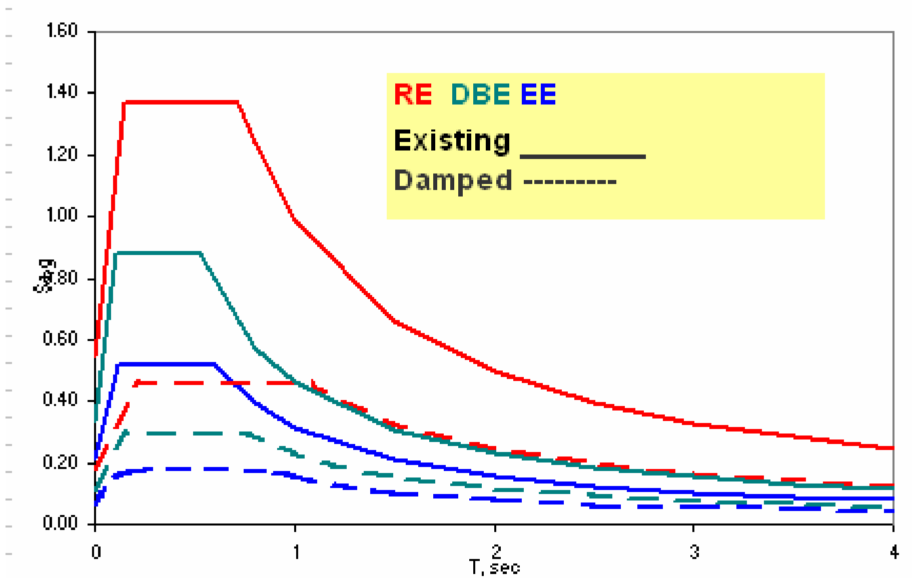

Figure 10. Original and damped response spectra

5.2 Analysis procedure

Limited nonlinear time history analysis was used for evaluation. Nonlinearity is limited to discrete FVD elements. Since the periods of the structure are large enough, the concept of equal displacement is used. This principal implies that the elastic and inelastic structures would have equal displacements, although, the level of force in the yielding structure is smaller; see Figure 11.

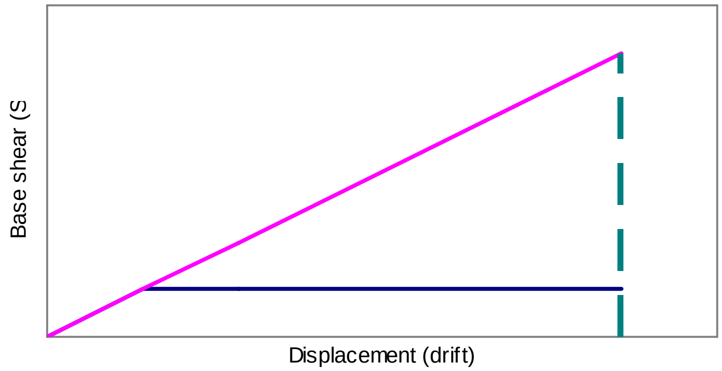

Figure 11. Principal of equal displacement

5.3 Evaluation procedure

Using the concept of equal displacement assumption, the data computed in previous analysis from nonlinear pushover analysis can be used for comparison. All the members were modeled using elastic beam-column elements. However, the nonlinear behavior can be compared accurately using the limited nonlinear dynamic analysis presented herein. Dampers were sized to meet the following performance targets:

- EE level
    a. Elastic response
    b. BSC below average Nisqually

- RE level
    a. Upper deck displacement similar to Nisqually
    b. Joint shear to $5\sqrt{f'_c}$ or lower level column moment of 5,000 k-ft
    c. Lower level column shear

6 Mathematical model of the building

Program SAP2000 (CSI 2006) was used to prepare mathematical models for the building. A typical three-span frame designed by SED was modeled and shown in Figure 12. The member sizes and frame geometry were selected per structural plans.

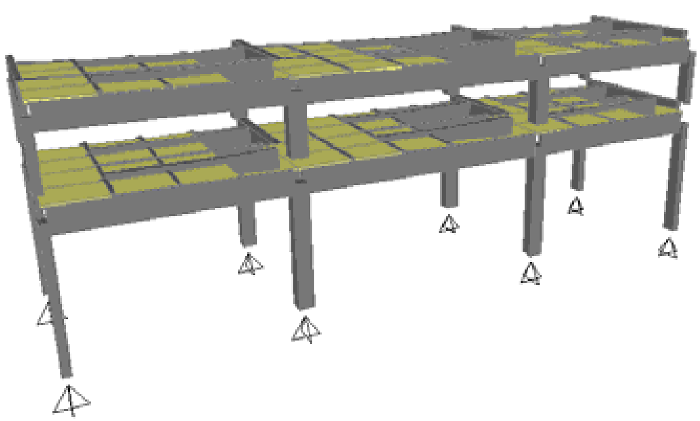

Figure 12. Three-dimensional model of the building

Member centerline dimensions were used in analysis. The joints were modeled as rigid and had dimensions equaling to member sizes framed by beams. Beams and columns were modeled using beam-column elements and decks were modeled using shell elements including both flexural and membrane action. P-Δ was included in analysis. To account for cracking in concrete, Icr/Ig was selected at 0.5 for beams and columns—same value as previous studies.

7 Analysis results

7.1 *Dynamic properties*

Table 5 presents a comparison of the current and the Eberhard 1995a model. Since the two models have similar mass, stiffness, and dynamic properties, they are dynamically equivalent.

		Eberhard 1995a	Model
	Base	Fixed	Fixed
	W, kips	5180	5160
Longitudinal	T, sec	0.86	0.81
	Participating mass, %	96	98
Transverse	T, sec	0.77	0.74
	Participating mass, %	96	98

Table 5. Properties of the analysis model and Eberhard 1995

The analysis conducted by TY Lin 2001 and PBDQ 2002 had a fundamental period of 1.5 sec in the transverse direction. For the current analysis, the bases of the columns were restrained against translation and rotational springs were placed at the base to simulate the boundary condition of columns. The fundamental periods of this model were 1.67 and 1.52 sec in longitudinal and transverse directions, respectively. As such, it is expected that the behavior of this frame would simulate the previous analysis and the SED frames in the field.

7.2 *Seismic loading*

Self-weight gravity and seismic loading were applied to the models. Six pairs of two-component accelerations were used in analysis. For each pair, two analyses were conducted. One with the first and second components aligned with the frame's longitudinal and transverse axis, respectively. The other analysis was conducted, with the acceleration components rotated by ninety degrees. The acceleration records used in analysis were comprised of the following.

- Three uncorrected Nisqually acceleration records of three stations—located within 1,000 ft of the viaduct—of Table 3. (The acceleration history and response spectra of the records are shown in Figures 8, and 9, respectively.)
- Three records from accelerations whose spectrum approximately matched the 5%-damped EE, DBE, and RE events, where EE and DBE and RE stand for Rare-, Design Basis-, and Rare - Earthquakes. The definition of these events is presented in Table 6. PBDQ 2005 guidelines were used to obtain the spectral values for EE and RE events, whereas, USGS web site was used to determine spectral ordinates of DBE events. Site Class D was used to compute modified response spectra ordinates. The acceleration response spectra for EE, DBE, and RE for Site Class D are presented in Figure 13.

Performance level	Probability of occurrence in 75 years	Return interval, years	PGA, g	Ss, g	S1, g
EE	50%	100	0.14	0.52	0.31
DBE	15%	500	0.33	0.88	0.46
RE (MCE)	3%	2,500	0.55	1.37	1.0

Table 6. Seismic design performance levels

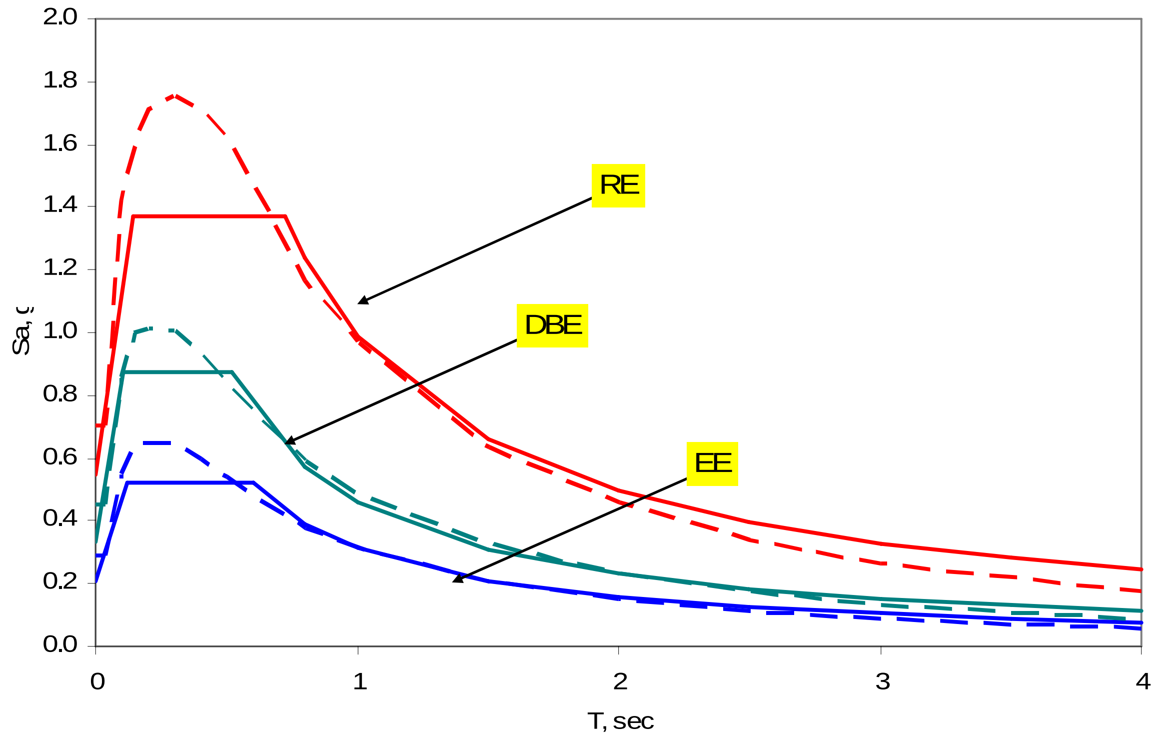

Figure 13. Target and analysis spectra

7.3 Response of the existing SED frame

Table 7 summarizes the maximum computed displacement at the upper deck level of the existing frame for each of the records. The computed response from the Nisqually records is similar to the EE level. As such:

- ❖ It is expected that the viaduct will experience minimal damage during the EE event, based on the 2001 Nisqually earthquake.
- ❖ The response of existing frame is not satisfactory for the RE event.
- ❖ If the viaduct displacement at the RE level is reduced to the levels experienced during the Nisqually event, then the structural damage will be limited during the rare event. This reduction in viaduct response—for example, from 15 in. to 4 in. in upper deck displacement—will be archived by adding supplementary FVDs to the frames to reach the target spectra of Figure 10.

Record	x-component, in. (longitudinal)	y-component, in. (transverse)
EE	4.6	4.4
DBE	7.3	7.0
RE	14.9	14.1
NOR	4.2	4.4
HAR	4.4	3.2
KDK	3.8	4.6

1. Maximum of two-component analysis
2. Response from one of the HAR component was large and discarded (possibly due to a peak in spectra matching frame period)

Table 7. Maximum computed upper deck displacement, existing frame

7.4 Fluid Viscous Dampers

Although there are several methods to add supplementary damping to the viaduct, Fluid Viscous Dampers (FVDs) are selected. The supplementary damping would serve to reduce the seismic demand on the viaduct to the target level. FVDs are selected because the force in them is mainly proportional to velocity. As such, they do not stiffen the structure (and add more seismic load) or increase load on the connecting frames or foundation by a significant amount. FVDs were initially developed for the defense and aerospace industry. They are reliable, efficient, and robust. FVDs have been extensively and successfully used for hundreds of seismic retrofit of buildings and bridges worldwide. Figure 14a present the application of FVDs for seismic of Immunex Central Utility Plant located in Seattle waterfront north of Alaskan Way Viaduct. Figure 14b depicts the FVD installed as part of the seismic retrofit of the SF-Oakland Bay Bridge.

a. Immunex Central Utility Plant

b. SF-Oakland Bay Bridge

Figure 14. Application of FVDs for seismic retrofit

7.5 Seismic retrofit

The mathematical model of the typical SED frame was modified by adding FVDs. Since the drifts are largest at the lower level—nearly 90% of component of displacement occurs here, resulting in soft-story behavior—dampers need only be added at this level. Two dampers were added in each direction; see Figure 16. In the longitudinal directions, FVDs were placed along the interior spans, whereas, in the transverse direction, FVDs were placed along the interior bents. Limited nonlinear analysis was then conducted.

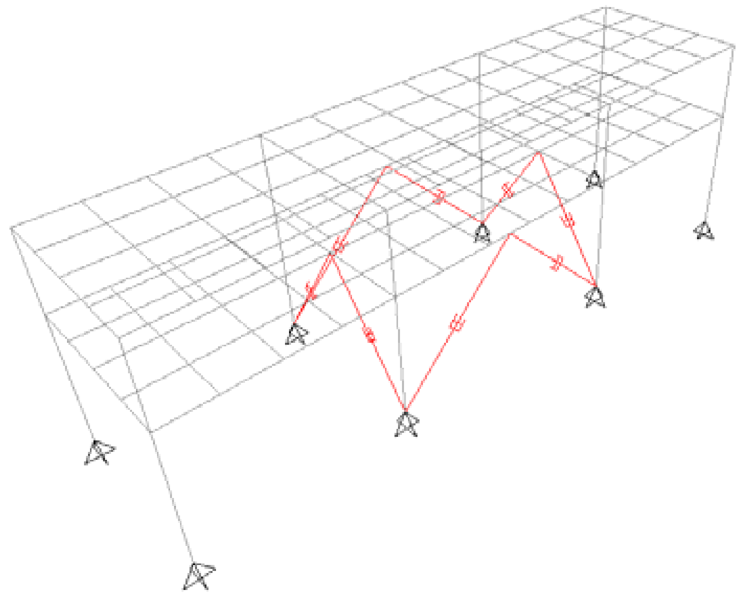

Figure 15. Isometric view of the viaduct frame with FVDs

7.6 Response of retrofitted SED frame

Table 8 presents the computed upper deck displacements for the retrofitted SED frame. Note that the maximum displacement for the RE level is now similar or less that the values that would not cause major structural damage or collapse of the frame. A comparison of upper deck displacement at performance seismic events is presented in Table 9. The addition of dampers has reduced the deck displacement from over 14 in. to less than 4 in. The entries of this table were obtained by averaging the x- (longitudinal) and y- (transverse) components of response at each performance level. The addition of the dampers has reduced the response by approximately 80%.

Record	x-component, in.	y-component, in.
EE	0.8	1.3
DBE	1.3	1.9
RE	2.6	3.9

Table 8. Maximum computed upper deck displacement, retrofitted frame

Record	Existing, in.	Damped, in.	% reduction
EE	4.5	1.0	78
DBE	7.2	1.6	
RE	14.5	3.3	

Table 9. Maximum computed upper deck displacement, retrofitted frame

Note that when FVDs are added to the viaduct, the upper deck displacements are limited to:

- EE level to 1.3 in. Previous research by TY Lin 2001 and PBQD 2002 shows that the viaduct frames would remain essentially elastic at this displacement. As such, the retrofitted viaduct would meet the first design objective of PBQD 2005.
- RE to 3.9 in. The viaduct experienced the Nisqually earthquake in 2001 under similar or larger displacements without major structural damage. As such, the retrofitted viaduct would meet the second design objective of PBQD 2005.

In the longitudinal direction, there is a nominal 1.5-in. wide gap between adjacent frames. To mitigate pounding problem, shock-transmission units, such as the one shown in Figure 16 can be used to limit the differential movement between the viaduct frames.

Figure 16. Shock transmission unit (Taiwan High Speed Rail viaduct)

Figure 17 presents the computed x- and y- components of the top deck displacement for the existing and damped frames. The results are shown for the 100-year, 500-year, and 250-year events. The addition of dampers has reduced the computed displacements significantly. To achieve such reduction, the seismic energy must be dissipated. Figure 18 presents the hysteresis response of dampers during the RE event. Note the dissipated energy for the dampers.

In new construction, state DOTs design and detail concrete members to behavior in a ductile fashion during seismic events. This entails the yielding of members. Such yielding (typically in columns) dissipates the input seismic energy. In the analysis presented here, similar effect was accomplished by resisting the seismic energy via the nonlinear response of the dampers. Figure 19 shows the component of input seismic energy for the RE level excitation. Dampers disperse almost the entirety of the seismic energy.

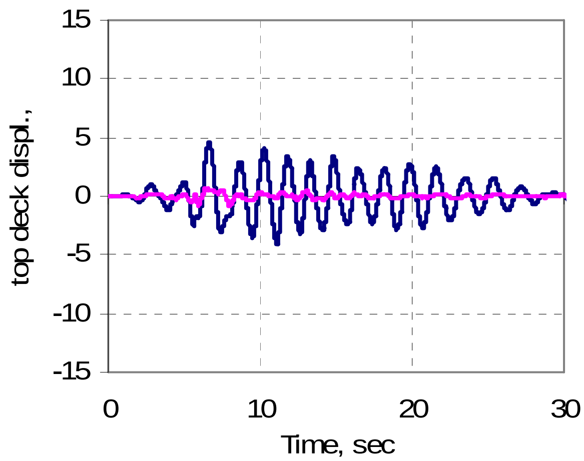

a. 100-year event, x-direction

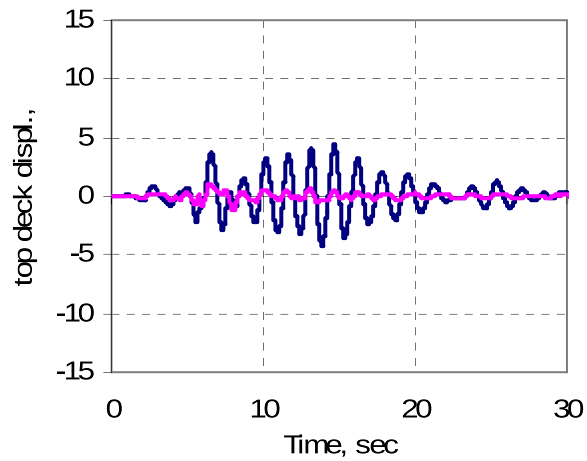

b. 100-year event, y-direction

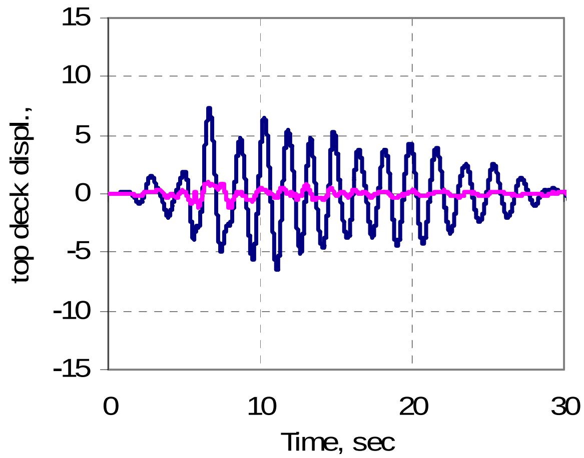

c. 500-year event, x-direction

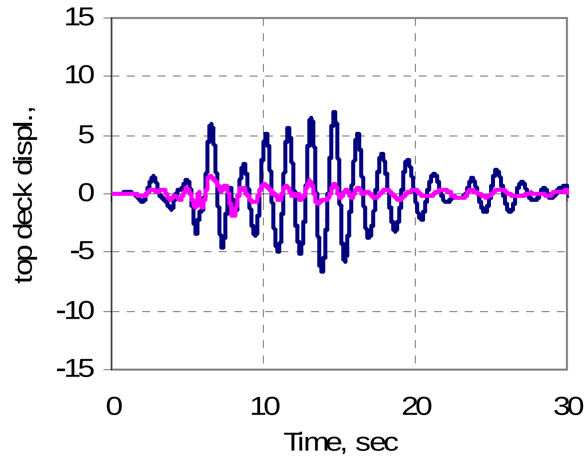

d. 500-year event, y-direction

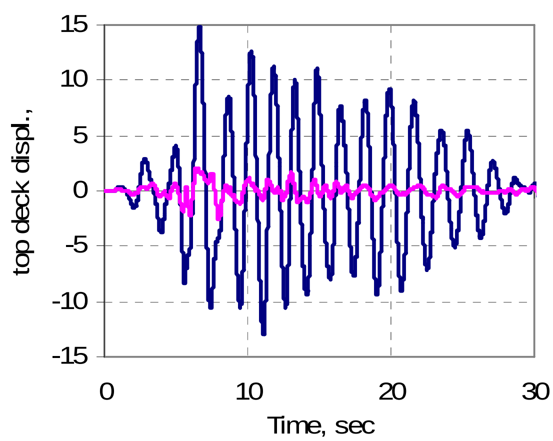

e. 2500-year event, x-direction

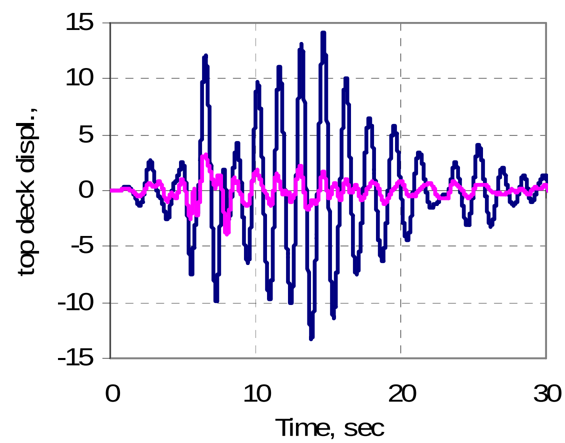

f. 2500-year event, y-direction

Figure 17. Upper deck displacement history (Existing ______ Damped ______)

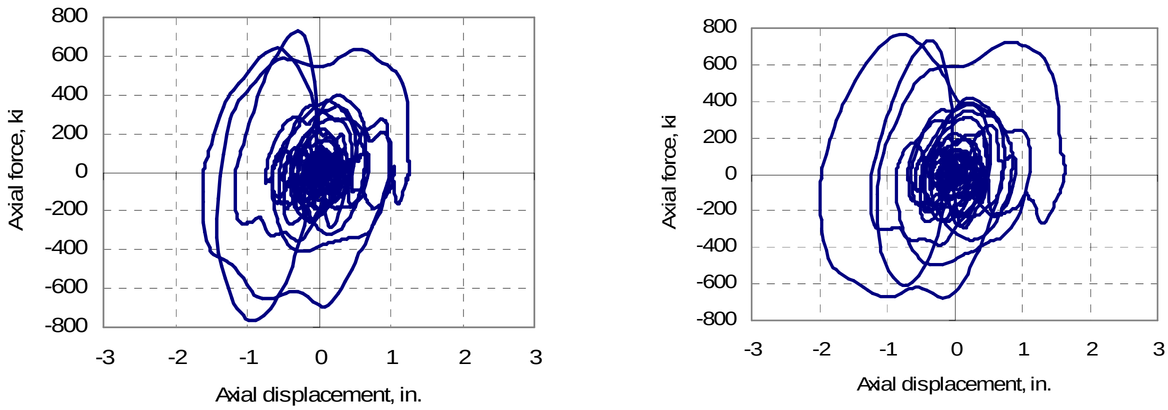

a. FVD in x-direction b. FVD in y-direction

Figure 18. Damper hysteretic response, RE level

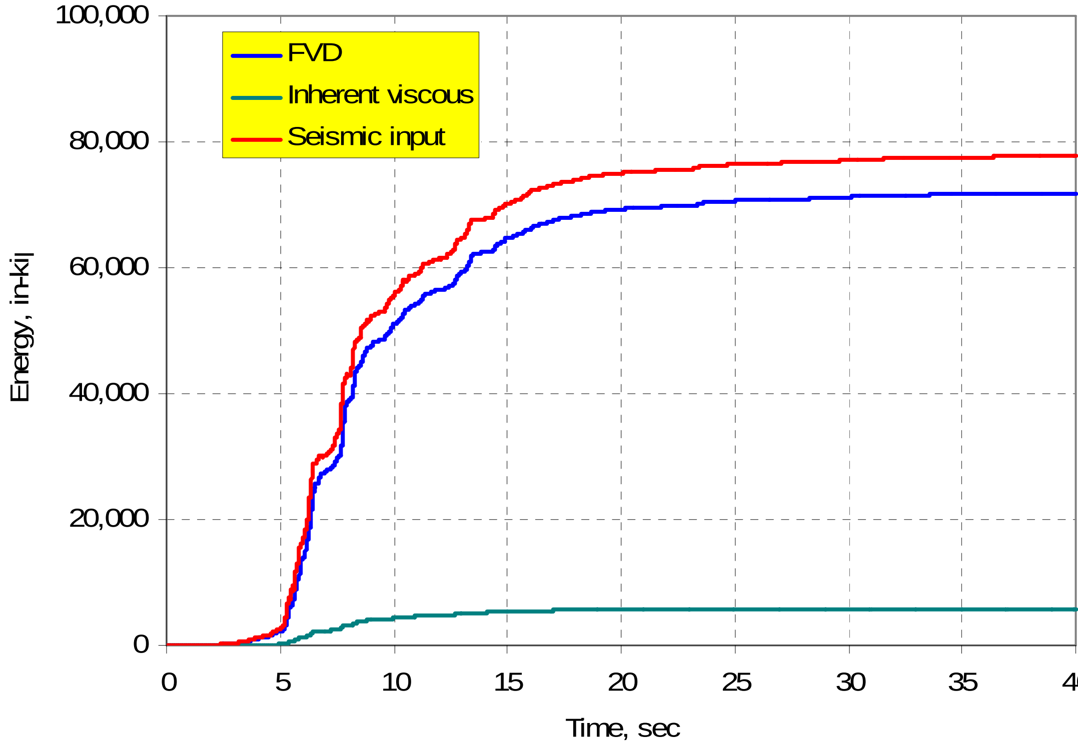

Figure 19. Components of input seismic energy, RE level

The maximum computed lower-level column bending moment and shear are approximately 4,600 k-ft and 150 kips, respectively. (The computed values for the exterior frames are smaller.) TY Lin 2001 and PBQD 2002 wrote that if reinforcement slip and joint principal limit state are reached at column bending moment of 5,000 k-ft.

To enhance seismic performance of the viaduct columns and joints, additional measures are recommended. In particular, jacketing of the columns would increase confinement, shear capacity, and alleviate reinforcement development problem due to the inadequate lap splices.

8 Summary and conclusions

Three dimensional time-history analysis of a typical SED frame in the Alaskan Way Viaduct was conducted to assess the efficacy of retrofitting the frames with dampers. Only the response of the superstructure was evaluated. The design guidelines developed by PBQD 2005 and WSDOT were used in this study. The analysis showed that the dampers materially improved the seismic response of the frame. The level of deck displacement was reduced such that the retrofitted frame would meet both of the requirements (functionality at EE level and collapse prevention at RE event) proposed for retrofit/replacement. Limited evaluation was also conducted to ascertain whether brittle failure would be expected and it was found not to be the case.

Based on the above findings, a retrofit measure that meets the Department's requirement consist of:

- ❖ Add Fluid Viscous Dampers to interior bays of viaduct frames.
- ❖ Add shock-transmission units between the frames in longitudinal direction.
- ❖ Increase shear capacity, confinement, and reinforcement splice length of existing columns by wrapping the columns in ductile fiber wraps.
- ❖ Increase the shear capacity of joints by either added cap concrete bolsters and drill-and-bond reinforcement or by prestressing (Priestley 1996) (Optional)

9 Future investigations

The analysis reported herein, was limited in scope. The objective of the investigation was to assess whether FVDs can be used to limit the superstructure displacements to meet the design criteria's performance objectives. Geotechnical evaluation as related to the foundations and condition of underlying soil was beyond the scope of the work presented here. The evaluation was limited to structural assessment. No attempt was made to evaluate the remaining service life, local traffic and population forecast and adequacy of the number of lanes for the future development plans. No analysis of maintenance costs was performed. Benefit-to-cost analysis to determine the merits of replacement vs. retrofit was not conducted.

The results presented here are conceptual and preliminary. It is suggested that the following steps be considered prior to implementation:

- ❖ Include the geotechnical data for the frame foundation. Assess substructure condition and investigate soil improvements.
- ❖ Investigate the response of a typical WSDOT frame.
- ❖ Perform material testing to determine the in-situ concrete and reinforcement properties.
- ❖ Conduct independent nonlinear static analysis to determine the response of a typical two-dimensional bay. Include flexural, shear, foundation, and joint nonlinear limit states.
- ❖ Refined nonlinear behavior: Develop three two-component site specific acceleration histories to be used for analysis, incorporate soil-structure interaction.
- ❖ Verification studies: Conduct comprehensive nonlinear time history analysis incorporating material and damper nonlinearity.

- Proof of concept testing: Construct a scaled model test frame and seismically conduct tests of existing and retrofitted frames at EE and RE levels.

10 References

Eberhard 1995a — Knaebel, P., Eberhard, M., Colina, J. *Seismic vulnerability of the Alaskan Way Viaduct: SED typical unit,* Report to Washington Department of Transportation

Eberhard 1995b — Knaebel, P., Eberhard, M., Colina, J. *Seismic vulnerability of the Alaskan Way Viaduct: WSDOT typical unit*, Report to Washington Department of Transportation

TY Lin 2001 — TY in International, Alaskan way viaduct report of the structural sufficiency review committee

PBQD 2002 — Parsons Brinckerhoff Quade & Douglas, Inc. SR 99: Alaskan Way Viaduct project; rebuild/retrofit alternative report

PBQD 2005 — Parsons Brinckerhoff Quade & Douglas, Inc. SR 99: Alaskan Way Viaduct & Seawall replacement project; Preliminary engineering design criteria

Priestley 1996 — Prriestley, M.J.N., Seible, F., and Calvi, G.M., Seismic design and retrofitted of bridges, John Wiley and sons Inc. NY, NY.

CSI 2006 — Computers and Structures Inc., SAP 2000 version 10: Structural Analysis Program, Berkeley, CA